

# HYPERSONIC AIRPLANE SPACE TETHER ORBITAL LAUNCH (HASTOL) ARCHITECTURE STUDY

## PHASE II: FINAL REPORT

Report submitted by:



**The Boeing Company**  
Phantom Works Advanced Space and Communications

Subcontract support provided by:



**Tethers Unlimited, Inc.**  
19011 36th Avenue West, Suite F, Lynnwood WA 98036-5752  
Phone: 425-744-0400; Fax: -0407; Email: TU@tethers.com  
*www.tethers.com*

on

NASA Institute of Advanced Concepts Subcontract No. 07600-040

under

Universities Space Research Association Contract No. NAS5-98051

Period of Performance:  
1 April, 2000 through 31 October, 2001

Report Date:

31 OCTOBER, 2001



# **HYPERSONIC AIRPLANE SPACE TETHER ORBITAL LAUNCH (HASTOL)**

## **TABLE OF CONTENTS**

Chapter 1.	HASTOL Program Overview	Page 1
Chapter 2.	Market Assessment and Mission Requirements	Page 13
Chapter 3.	Architecture Sizing Studies, Trades, & Simulations	Page 29
Chapter 4.	Airplane Trade Studies	Page 41
Chapter 5.	Tether Boost Facility Concept	Page 49
Chapter 6.	Conclusions and Recommendations	Page 57
Appendices		Page 67



### ACKNOWLEDGEMENTS

The Hypersonic Airplane Space Tether Orbital Launch (HASTOL) Phase II study has included contributions of many persons. Boeing has a broad base of expertise across the country that was called upon to support this program as needed. Core Boeing team members and their roles are the following:

John Grant	Program Manager
Kim Harris	Contracts Specialist
Jim Martin	Advanced RLV Performance
Dan Nowlan	Guidance, Navigation and Control
Karl Oittinen	Rendezvous and Capture Simulation
Mike Bangham	Boost Facility Concept Definition
Brian Tillotson	Market Definition, Mission and System Requirements

Other personnel who supported this activity included Don Johnson, Steve Hollowell, Beth Fleming, John Blumer, and Ben Donahue from Boeing. Tethers Unlimited, Inc. (TUI) personnel who supported this included Dr. Rob Hoyt and Dr. Robert Forward. Dr. Robert Cassanova, represented the NASA Institute for Advanced Concepts, in overseeing this activity. Mark Henley filled in as Program Manager for the conclusion of this activity, while John Grant was unavailable. Preparation of this final report for Boeing includes contributions from many of the team members, however special recognition is expressed here for the efforts of Rob Hoyt, Mike Bangham, Ronnie Lajoie, John Blumer, Beth Fleming and Brian Tillotson.



## CHAPTER 1: HASTOL PROGRAM OVERVIEW

### INTRODUCTION

The following pages document work performed by The Boeing Company for the NASA Institute of Advanced Concepts (NIAC), funded by NASA via the Universities Space Research Association. Tethers Unlimited, Inc. (TUI) supported this activity under subcontract to Boeing for tasks related to the design, operation, and performance analyses of the Tether Boost Facility portion of the HASTOL concept.

### CONCEPT OVERVIEW

Figure 1-1 depicts the sequence of events that occur as a payload is carried aloft by a hypersonic aircraft and then captured by a space tether and boosted into orbit. Starting at the left of this figure, a tether boost facility (i.e., a massive orbiting station, tether, and grapple assembly) is rotating in an elliptical orbit around the Earth. A hypersonic aircraft carries its payload in a sub-orbital trajectory, to a predetermined, high altitude, rendezvous point. When the aircraft reaches a high (exoatmospheric) altitude, its cargo doors open, exposing its payload. The aircraft's inertial velocity is significantly less than that of the orbiting facility's center of mass, however the rotational velocity at the tip of the long tether is sufficient to match the speed of the aircraft at the rendezvous point. A grapple assembly, located at the tether tip, meets the aircraft in a near vertical relative motion, to capture the payload at the moment of rendezvous. A grapple assembly, located at the tether tip, meets the aircraft in a near vertical relative motion, to capture the payload at the moment of rendezvous. The tether then rotates and tosses the payload into a higher orbit.

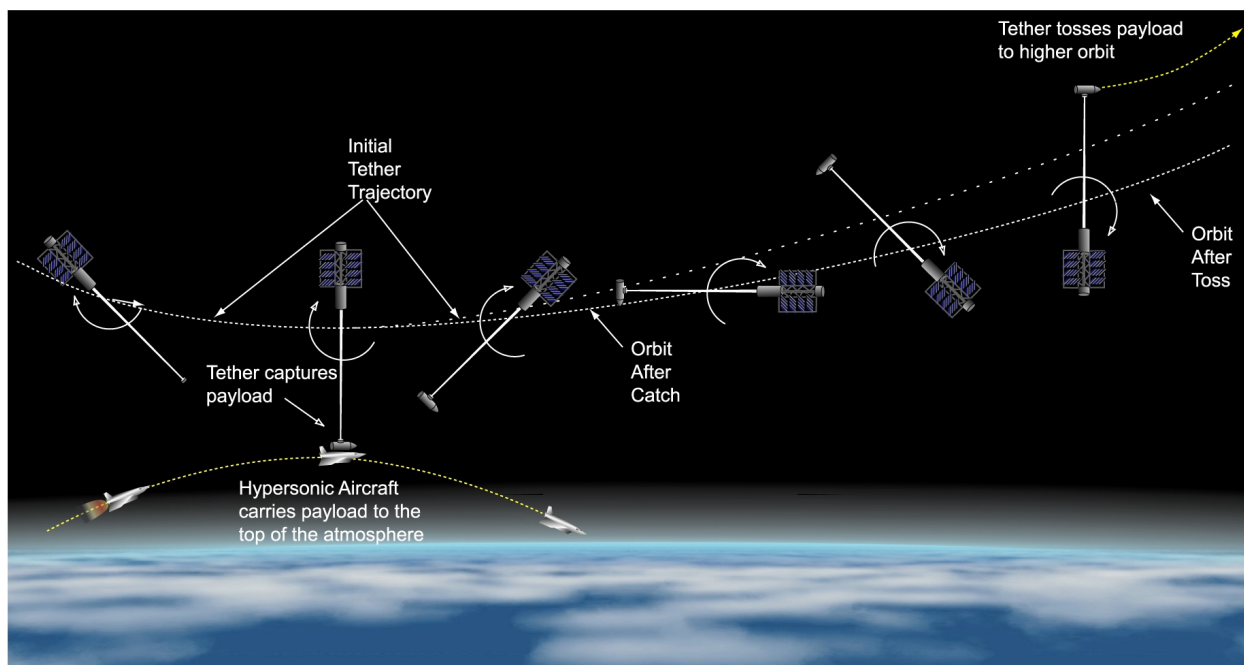


*Figure 1-1. The HASTOL concept would capture a hypersonic aircraft's payload by a tether facility in orbit, and send the payload on into space.*

After payload capture, the tether and grapple assembly lift the payload away from the aircraft and continue their rotation around the boost facility center of mass, which is now in a more circular orbit. The grapple and payload continue to rotate to their highest altitude, at which point, the payload is released into space. The payload's inertial velocity has now increased by approximately two times the difference between the orbiting facility's average velocity and the aircraft's inertial velocity. The result is that the payload is "boosted" to a much higher elliptical orbit (or to an escape trajectory).

## Background

The Hypersonic Airplane Space Tether Orbital Launch (HASTOL) concept was originally suggested by Dr. Robert L. Forward in the book, *FUTURE MAGIC* (Avon Books, New York, 1988). A "Rotovator", was described in this reference, as an 8,500-kilometer-long tether, in a 4,250 km altitude orbit, designed to reach down into the upper atmosphere three times per orbit and match its grapple tip velocity with a Mach 3 airplane carrying a passenger capsule. With recent improvements in tether materials (such as Spectra™ a high specific strength polymer) and continuing research in high velocity aircraft, the HASTOL concept may become technically feasible: a higher speed on the hypersonic airplane would allow a lower tip speed and a lighter tether. Boeing, Tethers Unlimited, and the University of Maryland proposed an initial study of such a HASTOL system to NASA Institute for Advanced Concepts (NIAC) in 1998. The resulting studies have shown that there is a range of credible hypersonic aircraft velocities and tether tip velocities where the HASTOL concept may become technically feasible.

The HASTOL Phase I study investigated an operational concept that considered a rendezvous point at 100 kilometers altitude and an aircraft velocity of Mach 12. The architecture utilized a modification of an existing hypersonic aircraft concept developed by Boeing for NASA Langley Research Center, called the DF-9. The aircraft trajectory, boost facility orbit, and tether plane of rotation were all assumed to be in the earth's equatorial plane, with the aircraft heading eastward.

One primary objective of Phase I was to validate that the DF-9 could fly off-nominal trajectories to achieve altitudes and velocities that are high enough to enter an envelope of acceptable tether tip positions for rendezvous. Tether and tether tip configurations trades were influenced by aerodynamic drag and aerothermodynamic heating considerations, as the tether passes through the upper atmosphere during operations.

Figure 1-2 illustrates some of the design parameters that influence hypersonic aircraft capabilities in conjunction with the HASTOL concept. Various combinations of rendezvous speed and altitude are shown in the lower left panel of this figure. Two primary constraints were considered as these points were investigated: 1) the maximum normal acceleration is 2.5 g, and 2) the maximum dynamic pressure is 2,000 lb./sq. ft. Both of these constraints need to be satisfied for acceptable rendezvous conditions. Examples of acceptable and unacceptable cases are shown in the two right hand panels. An interesting point for the highest altitude cases examined is that the aircraft was able to reach an altitude of 120 km for the speeds shown, but the constraints defined above were exceeded during descent.



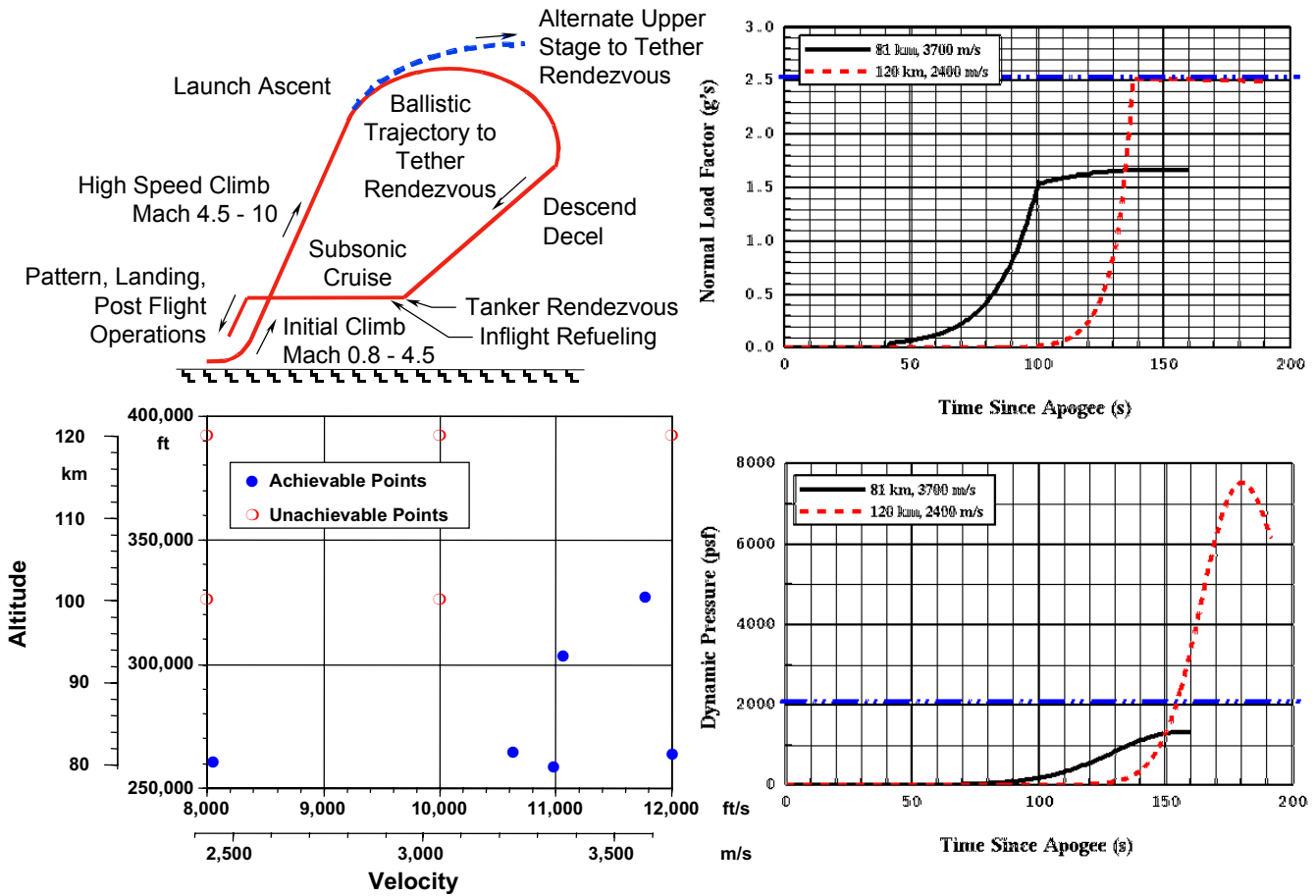


Figure 1-2. HASTOL aircraft are assumed to be limited to a normal acceleration of 2.5 g, and a maximum dynamic pressure of 2,000 lb/sq ft.

TUI’s concept for a High-Strength Electrodynamics Force Tether (HEFT) facility (Figure 1-3) was selected as the baseline boost facility during the initial HASTOL study activity. Primary features of the HEFT facility are a rotating tether using momentum exchange to boost payloads, and a conducting tether element to react with the earth’s magnetic field to re-boost the tether facility. Several HEFT grapple assembly concepts were considered, and a relatively simple concept was selected as a baseline. It became readily apparent that rendezvous and capture are key technical issues, and detailed simulations of the grapple and payload engagement are required to further define the system requirements. The HEFT Facility is comprised of the following elements:

Control Station, with a mass of ~1,650,000 kg

“HoyTether”, 600 km long, rotating with a mass of ~1,360,000 kg

Grapple Assembly at the end of the rotating tether, with a mass of ~650 kg

Conducting Tether Element for restoring boost facility momentum, via an electrodynamic force generated as the conducting element passes through Earth’s magnetic field.

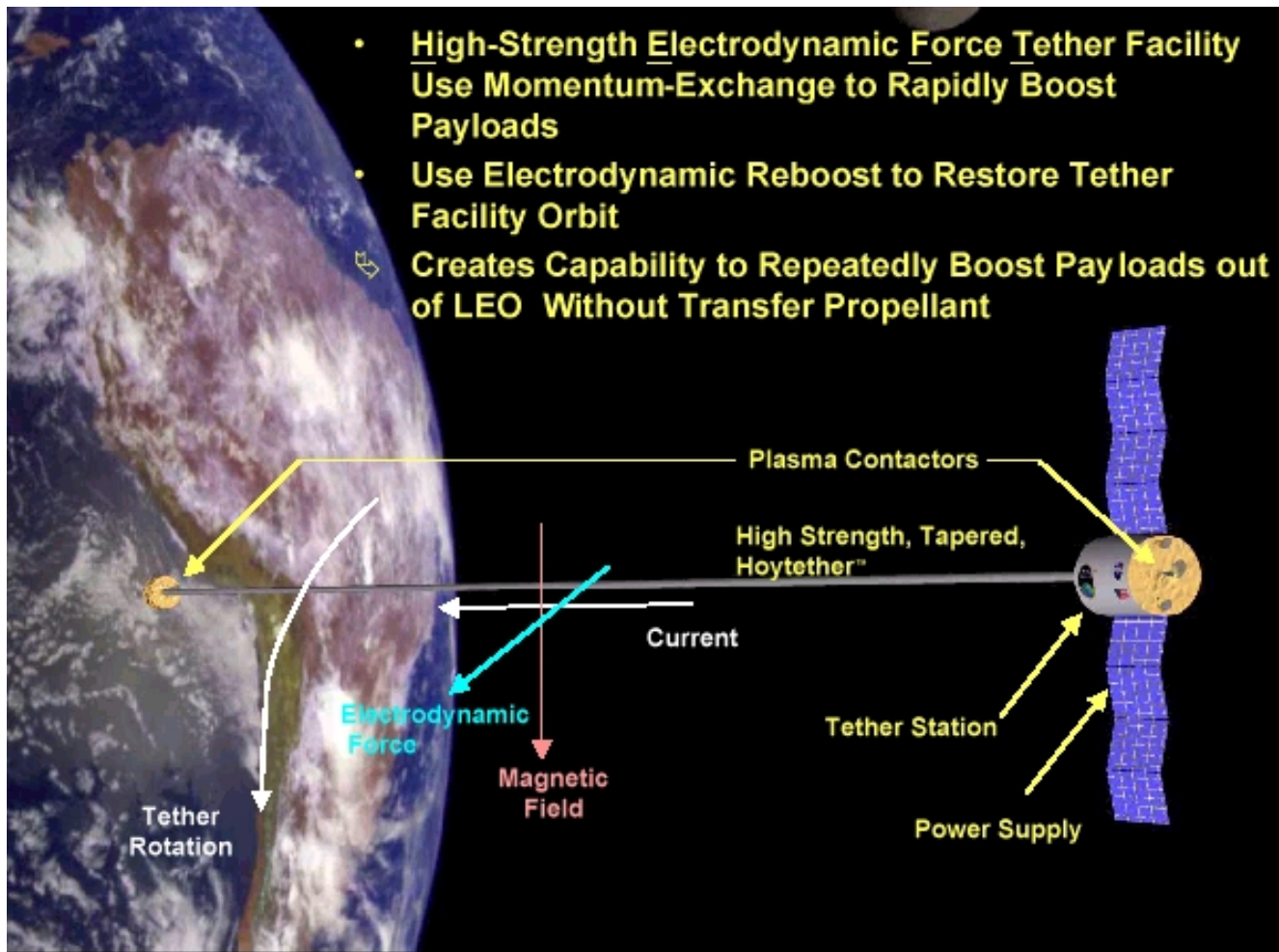


Figure 1-3. The HEFT facility concept uses a tether for both momentum exchange and electrodynamic propulsion.

The boost facility is in a slightly elliptical orbit around the earth prior to payload capture. During Phase I, boost facility operation was defined with the following characteristics:

- 700 km apogee, 610 km perigee orbit
- Center of mass is 90 km from the Control Station
- Tether tip velocity, when facility center of mass is at perigee, is 3.5 km/sec relative to the center of mass velocity. This is 4.1 km/sec inertial velocity, which is identical to the hypersonic aircraft velocity.

Total mass of the boost facility is approximately 3,000,000 kg, or about 200 times the mass of the maximum payload mass to be boosted to higher orbit. This very high mass stands out as a significant system cost driver, not only because of the mass itself, but also because of the number of missions that would be required to assemble the facility in orbit. We have attempted to reduce this mass ratio during Phase II.

Key features of the tether boost facility are illustrated in Figure 1-4. A “HoyTether” design is featured for the momentum exchange tether. This multi-strand design provides improved survivability in the micrometeoroid and debris environment of low Earth orbit. For extension of the rendezvous and capture time, we are postulating a “winch”- type subsystem at the tether tip. This system would reel out a length of tether, allowing the grapple to move along the path of the aircraft for an extended period during the capture maneuver. The grapple configuration shown is a “simplified” design, and grapple requirements are not fully understood. Grapple-payload rendezvous and capture simulations and analyses were used in definition of grapple subsystem and component requirements. Further facility design considerations are detailed in Chapter 5 of this report, while the rendezvous and capture simulation process is discussed in Chapter 3.

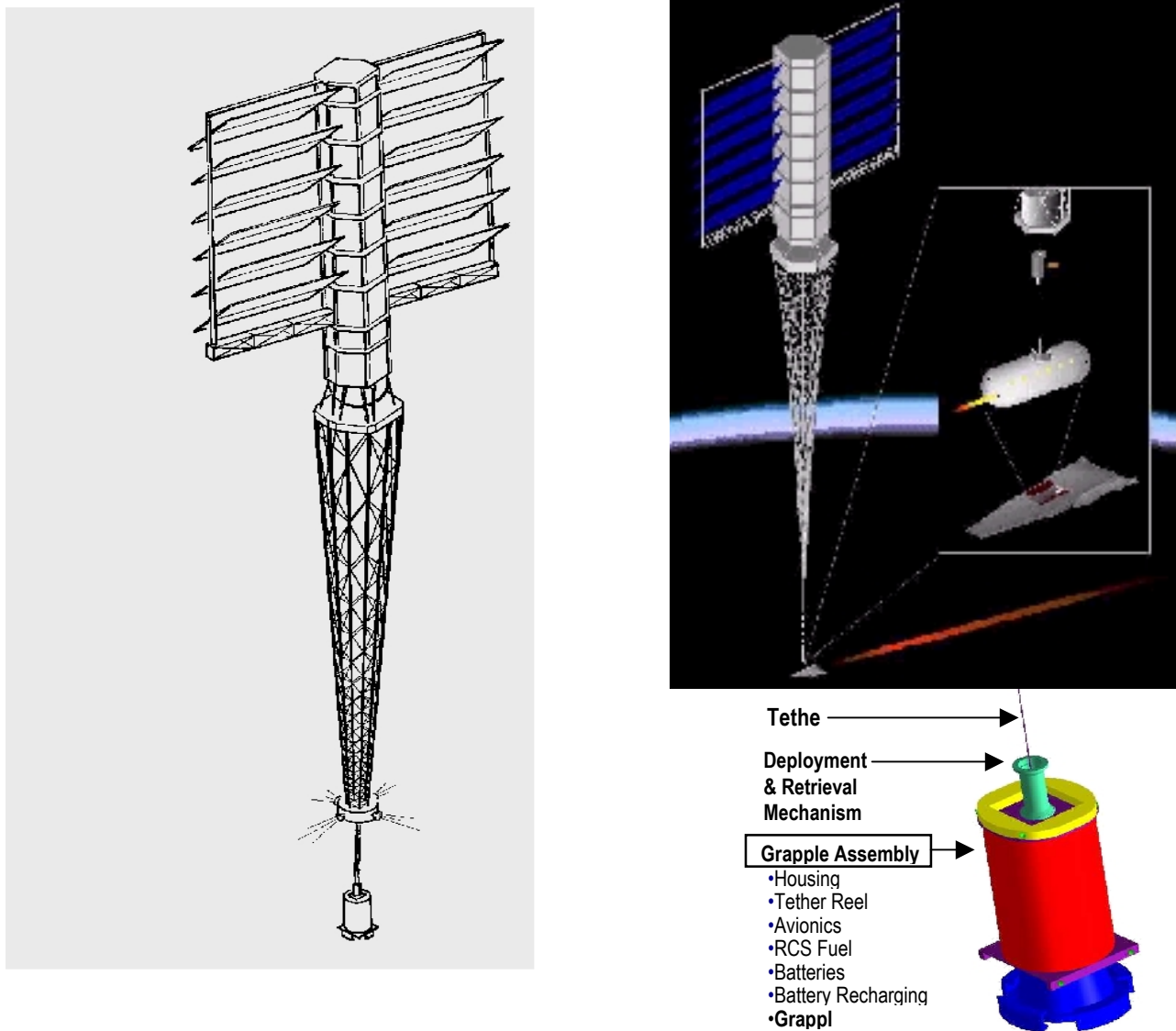


Figure 1-4. Key features of the HEFT facility include a multi-strand “HoyTether” and a deployable grapple actuator.

One of the primary concerns and trade parameters during HASTOL Phase I was tether tip temperature as the tether reaches its lowest altitude, in the upper atmosphere. Figure 1-5 shows altitude vs. time as the tether tip swings through the upper atmosphere, along with the corresponding tether tip temperature rise. When the tether tip dips down to an altitude of 100 km, its temperature rises from an ambient 40 degrees Centigrade to 80 degrees Centigrade. This 40 degree temperature rise is well within the thermal properties of either Spectra, the material selected for the HoyTether, or of Zylon (PBO), the material selected for the grapple tether. For comparison purposes, consider that, if the tether were to dip down to an altitude of 80 km, the tether tip temperature would rise to 1600 degrees Centigrade, and material properties would be compromised. Conditions shown here represent a rendezvous condition of an altitude of 100 km and an aircraft velocity of Mach 12. During this HASTOL Phase II study, we have modified the approach, with rendezvous at 150 km altitude and an aircraft velocity of Mach 15 to Mach 17. Tether tip temperature variations are much less significant for this rendezvous condition.

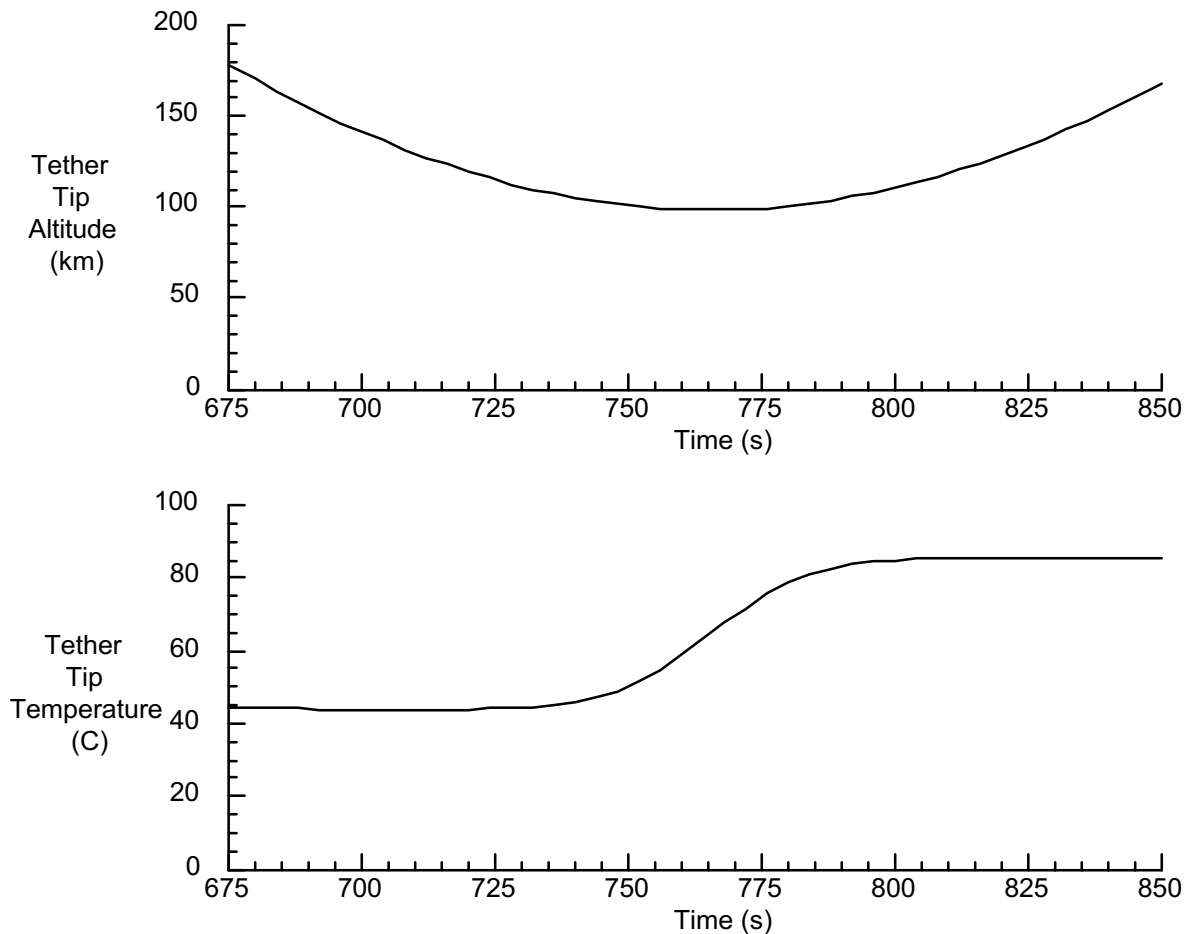


Figure 1-5. Tether tip temperatures may rise significantly, depending on altitude and velocity.

The relative position of the grapple and the aircraft / payload around the time of rendezvous is illustrated in Figure 1-6. [Note that the vertical distance scale is approximately 10 times that of the horizontal scale]. The relative horizontal and vertical distance between the grapple and aircraft is shown here from 60 seconds before to 60 seconds after the rendezvous event. The data

displayed here is based on an ideal rendezvous of the grapple and the aircraft. (The tether tip path and the aircraft trajectory meet at a single point in space, and zero relative velocity between the grapple and aircraft at the moment of rendezvous). Prior to rendezvous, the grapple approaches the aircraft from above and behind; it drops nearly vertically down to the aircraft at the moment of rendezvous, and rises nearly vertically from the aircraft immediately after rendezvous.

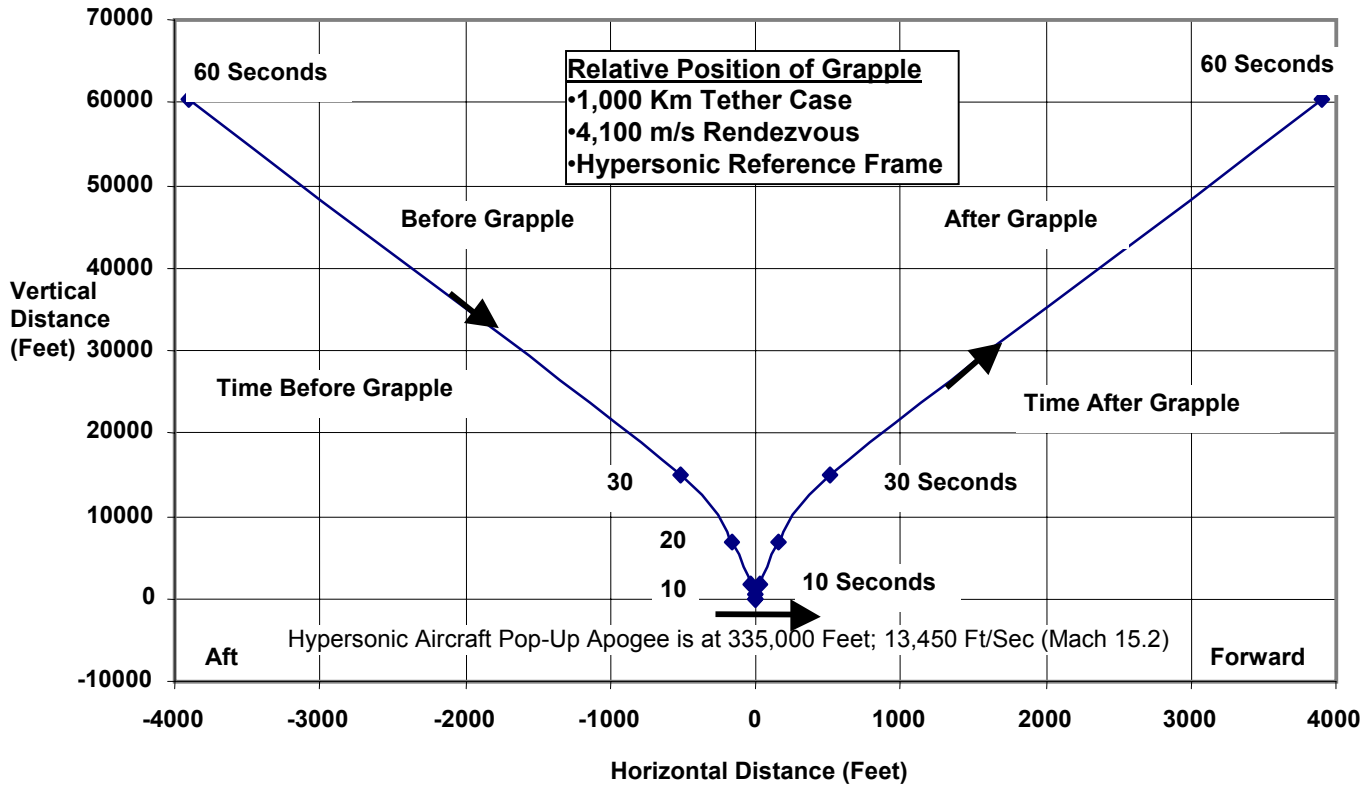


Figure 1-6. Precision timing and positioning of the aircraft trajectory is required to meet the tether as it rapidly descends to the rendezvous point, then moves onward and upward.

The next chart, Figure 1-7, portrays the same rendezvous condition, with the scale of the two axes forced to the same. The relative position of the grapple and the aircraft and payload is shown vs. time in the immediate vicinity of the rendezvous point, with the horizontal and vertical distances at the same scale, from about 10 seconds before to 10 seconds after the rendezvous event. It is very apparent that the grapple drops virtually vertically down to the aircraft during rendezvous, then rises vertically from the aircraft and proceeds forward of the aircraft. The relative motion is effectively one-dimensional – along a relatively straight (vertical) line, provided that the aircraft can 1) align itself with its flight path in the plane of the rotating tether, and 2) manage its velocity, to arrive at the rendezvous point at the same time as the tether tip. Provided these conditions can be met, the rendezvous and capture scenario is much less dynamic than may be imagined.

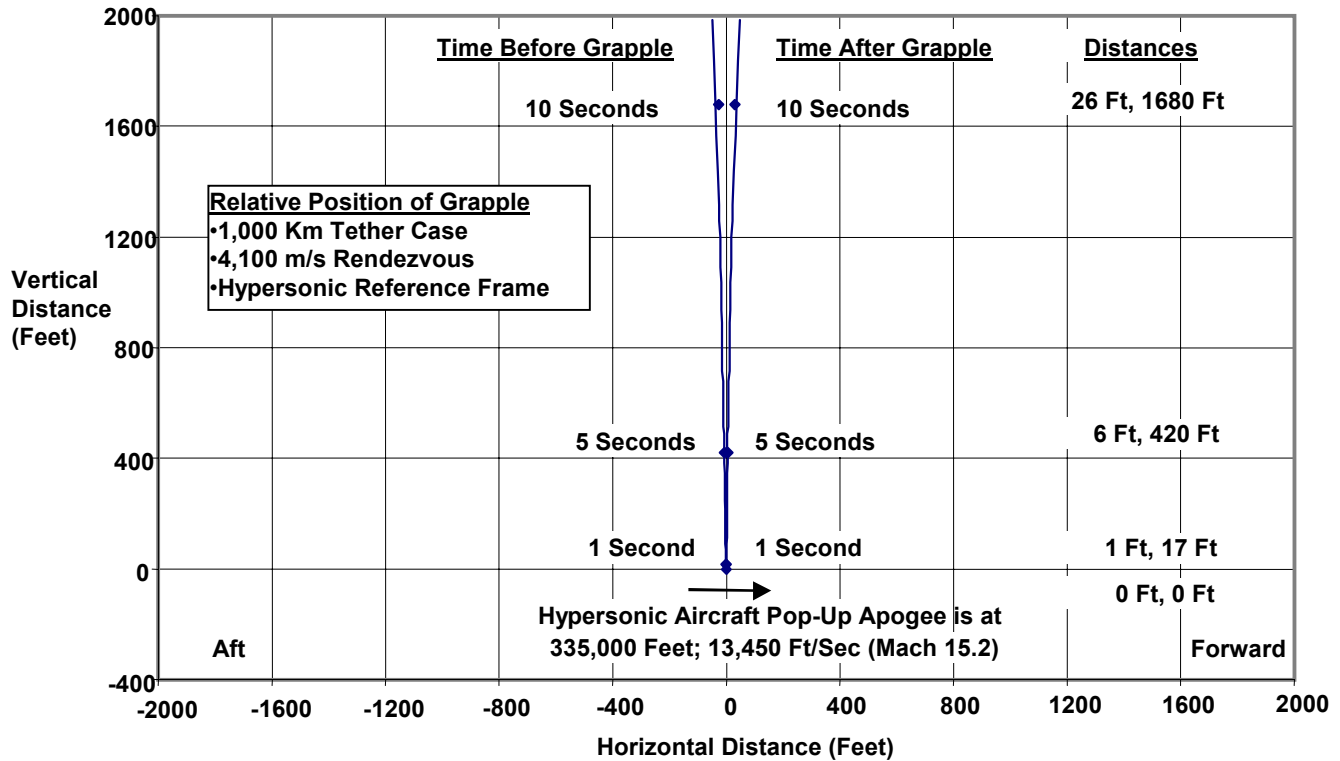


Figure 1-7. Relative motion of the tether tip can be approximately one-dimensional (solely in the vertical direction) for a few seconds around the moment of rendezvous.

The previous two charts portray an ideal rendezvous condition, where the grapple and aircraft meet at the same point in space at the same time -- the path of the grapple, or tether tip is tangent to the nominal ballistic path of the un-powered hypersonic aircraft at the rendezvous point. This is an ideal scenario, and even if the two bodies followed ideal paths, a finite amount of time will be required to accomplish payload capture. An approach to extend the total time for complete rendezvous and capture is illustrated in Figure 1-8 and described as follows:

- The aircraft is maneuvered precisely to the predicted rendezvous point using instrumentation for “midcourse guidance”, enhanced by communication with the grapple assembly.
- The grapple assembly is inactive as it descends to the aircraft, until it reaches the predicted rendezvous point. At this point it is released from the tether tip and goes into a free fall (retained, but not restrained, by a free-spooling secondary tether), resulting in the grapple following the same ballistic path as the aircraft.
- Terminal closing of distance errors between the grapple and aircraft are accomplished via aircraft maneuvers, grapple maneuvers, or both.

Simulation of the rendezvous and capture geometry is being used to analyze the rendezvous and capture scenario and to define the requirements for aircraft and grapple maneuvers, instrumentation, and subsystems.

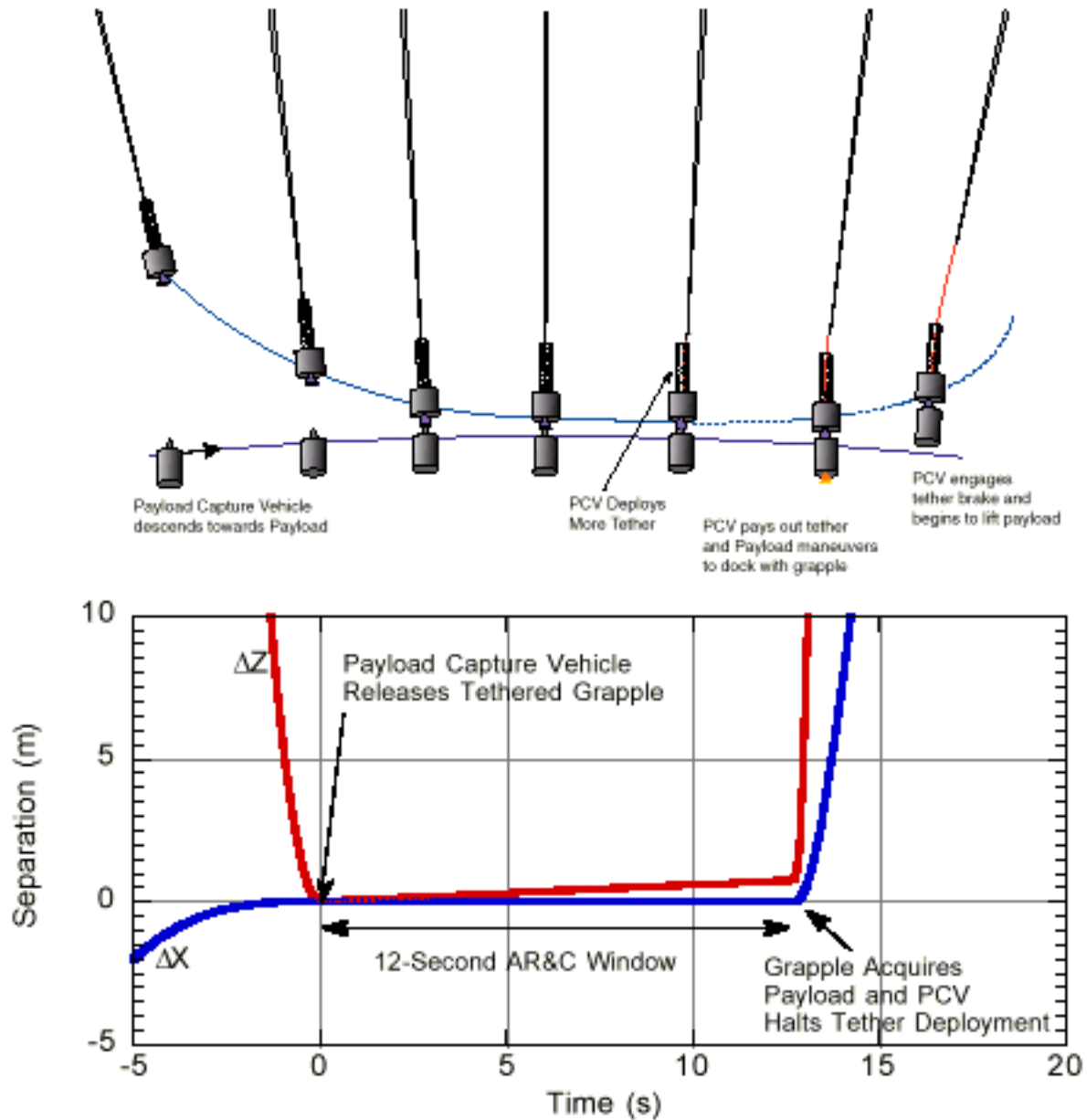


Figure 1-8. The automated rendezvous and capture window may be extended significantly if a “payload capture vehicle” at the tether tip can release a separately tethered grapple actuator.

One attractive feature of the HASTOL concept is the leverage of on-going hypersonic aircraft development programs. We expect that hypersonic vehicles will be developed and operated in the future, with development funded via other avenues, so economics of the HASTOL system would include operation, but not development of the aircraft. Several prototype aircraft technology development and demonstration programs are underway, and billions of dollars are being invested in relevant technologies:

- X-43, or Hyper-X, with a maximum speed expected to reach Mach 10.



- X-33 and X-34, prototype development programs to demonstrate advanced technologies for hypersonic vehicles.
- X-37, a technology demonstration test bed that will be taken to orbit aboard the Space Shuttle and flown back for a horizontal landing on earth.
- The Space Launch Initiative to develop and demonstrate related technologies.

## PUBLICATIONS

Our work on HASTOL for NIAC has resulted in many related publications, listed below in chronological order. The first eight publications are all numbered technical publications presented at international meetings, which are available at most technical libraries. Paper copies of these technical publications can be purchased from the American Institute for Aeronautics and Astronautics through their web site <<http://www.aiaa.org/>>. The final two publications, which have yet to be presented and published, are included as Appendices H and I to this Final Report.

1. Robert L. Forward, Thomas J. Bogar, Michal E. Bangham, and Mark J. Lewis, "Hypersonic Airplane Space Tether Orbital Launch (HASTOL) System: Initial Study Results", Paper IAF-99-S.6.05, 50th International Astronautical Congress, Amsterdam, The Netherlands, 4-8 October 1999.
2. Thomas J. Bogar, Michal E. Bangham, Robert L. Forward, and Mark J. Lewis, "Hypersonic Airplane Space Tether Orbital Launch (HASTOL) System: Interim Study Results", Paper AIAA-99-4802, 9th International Space Planes and Hypersonic Systems and Technologies Conference, Norfolk, Virginia, 1-5 November 1999.
3. Robert P. Hoyt, "Design and Simulation of Tether Facilities for the HASTOL Architecture Study", Paper AIAA-2000-3615, 36th AIAA/ASME/SAE/ASEE Joint Propulsion Conference and Exhibit, Huntsville, Alabama, 17-19 July 2000.
4. Robert P. Hoyt, "Commercial Development of a Tether Transport System", Paper AIAA-2000-3842, 36th AIAA/ASME/SAE/ASEE Joint Propulsion Conference and Exhibit, Huntsville, Alabama, 16-19 July 2000.
5. John E. Grant, Harvey J. Willenberg, Brian J. Tillotson, Joseph N. Stemler, Michal E. Bangham and Robert L. Forward, "Hypersonic Airplane Space Tether Orbital Launch - HASTOL: A Two-Stage Commercial Launch System to Any Orbit", Paper AIAA-2000-3841, 36th AIAA/ASME/SAE/ASEE Joint Propulsion Conference and Exhibit, Huntsville, Alabama, 16-19 July 2000. [Essentially the same as Publication 6 - AIAA-2000-5353.]
6. John E. Grant, Harvey J. Willenberg, Brian J. Tillotson, Joseph N. Stemler, Michal E. Bangham and Robert L. Forward, "Hypersonic Airplane Space Tether Orbital Launch - HASTOL: A Two-Stage Commercial Launch System", Paper AIAA-2000-5353, AIAA Space 2000 Conference and Exposition, Long Beach, California, 19-21 September 2001. [Essentially the same as Publication 5 - AIAA-2000-3841.]
7. James A. Martin and Steve Hollowell, "Vehicle Evaluations for Tether-Assisted Launch to Orbit", Paper AIAA-2001-1897, AIAA/NAL-NASDA-ISAS 10th International Space Planes and Hypersonic Systems and Technologies Conference, Kyoto, Japan, 24-27 April 2001.
8. John E. Grant, James A. Martin, Daniel R. Nowlan, Brian J. Tillotson, and Robert P. Hoyt, "HASTOL Tether System Applied to Commercial Launch", Paper AIAA-2001-3966, 37th AIAA/ASME/SAE/ASEE Joint Propulsion Conference and Exhibit, Salt Lake City, Utah, 8-11 July 2001.



9. Robert L. Forward, "Estimate of Avoidance Maneuver Rate for HASTOL Boost Facility", submitted to Space Technology and Applications International Forum (STAIF-2002), Albuquerque, New Mexico, 3-7 February 2002. [See Appendix H of this report.]
10. Robert L. Forward, "HASTOL Tether Module Replacement Rate Due to Space Impactor Cuts", submitted to 38th AIAA/ASME/SAE/ASEE Joint Propulsion Conference and Exhibit, Indianapolis, Indiana, 7-10 July 2002. [See Appendix I of this report.]



## **CHAPTER 2: MARKET ASSESSMENT AND MISSION REQUIREMENTS**

HASTOL requirements are derived from the needs and attributes of potential markets. The first part of this chapter defines the characteristics of an attractive market. The second part describes current and emerging markets and derives HASTOL mission requirement. The third part addresses possible future markets and the mission requirements for an advanced HASTOL system that addresses those markets.

### **ECONOMIC CHARACTERISTICS OF ATTRACTIVE MARKETS**

In seeking new markets to enter, corporate planners seek three primary characteristics: market size, growth, and stability. Size indicates the current annual value of the market. Capturing all of a small market offers less value than capturing a piece of a large market. Growth means both short-term annual growth rate and the ultimate market size as the market matures. High growth is attractive both because of increasing earnings potential and because high growth markets are often easier to enter. Stability indicates how well investors can predict market size from year to year or quarter to quarter. An unstable market may offer high median returns but unacceptable downside risk.

A combination of technical and economic factors make HASTOL a more attractive solution for some space transportation markets than for others. Four primary characteristics of an attractive market for HASTOL are small payloads, high flight rate, incremental growth paths, and balanced two-way traffic.

Small payloads (e.g. one to several tons) permit initial operation with a low-mass tether system, which reduces up-front investment in tether development and launch, and a small hypersonic aircraft, which reduces development cost. In addition, loss of a vehicle or payload is less damaging economically if both are small.

High flight rate offers a quicker return on investment. If each flight generates an operating profit of, say, 1% of the up-front investment, then a flight rate of 100 flights per year may provide a good return, while a rate of 10 flights per year may not.

An incremental growth path allows the system's capacity to be increased in small increments, with correspondingly small costs. This reduces financial risk and permits capacity to match demand, which maximizes profit and reduces opportunities for competitors to enter the market.

Balanced two-way traffic indicates a market in which the tether system transfers roughly the same mass of material down from orbit as it transfers up into orbit. If traffic only goes from Earth to orbit, then the tether must reboost frequently to regain momentum it transfers to payloads. Reboost is costly. If chemical or solar thermal propulsion is used for reboost, the cost of delivering propellant to orbit will be relatively high. If electric or electrodynamic propulsion is used, the cost may also be relatively high to build, launch, and maintain a power system that supports quick reboost. However, if every kilogram that the tether boosts into orbit is matched

by a kilogram that the tether deboosts from orbit, the change in the tether's momentum is small and little reboost is required. Thus, a market with balanced two-way traffic imposes lower costs.

**Candidate Markets**

We identified as many significant markets as possible, then scored each market against each of our market criteria using a scale of zero to three. The results of this exercise are shown below in Table 2-1. A score of three is best, with zero the worst (indicating markets that currently do not exist). Total scores for each market were produced by summing the scores for all criteria. Equal weights were assigned to all criteria in this evaluation.

Markets above the gray zone in Table 1 currently exist. Those within the gray zone currently do not exist. Existing markets include GEO communication satellites, LEO communication constellations, commercial remote sensing, civil payloads (e.g. NASA unmanned spacecraft, NOAA), and military. Solo tours (tourism for one or a few people at a time) is currently a very small area, but some recent activities fit within it so it is included as an emerging market. Future markets include mass tourism, LEO manufacturing, in-situ resource utilization (ISRU) for manufacturing, human planetary missions as part of NASA's Human Exploration and Development of Space (HEDS), and major new military systems.

Table 2-1. Attractiveness of space transportation markets for HASTOL.

		Small payloads	High flight rate	Balanced 2-way traffic	Incremental growth	Size Today	Growth	Stability	Total
Present	GEO Comm	2	2	1	3	2	1	3	14
	LEO Comm	3	2	1	3	1	1	2	13
	Rmt Sensing	2	1	1	3	1	1	3	12
	Civil	2	1	1	3	1	1	3	12
	Military	2?	1	1	2?	1	1	3	11
	Solo Tours	3	3	3	3	1	3	3	19
Future	Group Tours	1	2	3	2?	0	3	3	14
	Manufctrng	3	2?	3	3	0	2?	3	16
	New Military	2?	2?	1	2?	0?	1?	1?	9
	HEDS	1	1	1	1	0	1?	1	6
	SPS (ISRU)	1	3	2*	2?	0	2?	3?	13

\*1 without with lunar downmass

### CURRENT AND EMERGING MARKETS

In setting mission requirements for the initial HASTOL system, we addressed only current and emerging markets. The coarse scorecard suggests that LEO communications and remote sensing (commercial) would be good markets. However, both involve LEO orbits in moderate to high inclination, which is incompatible with the equatorial orbit we need to best serve the GEO market and the high-rate solo tour markets. Therefore, LEO communications and remote sensing markets are not likely to offer much revenue for HASTOL. Among the established markets, GEO and "Little LEO" commercial communication satellites appear to be the best matches for a HASTOL system.

Because deployment of a HASTOL system would occur after the year 2010, we projected each addressable market into the 2010 - 2020 period. Few projections are available beyond 2010, so we used available sources and our best judgment to develop projections of payload count by mass for each year from 2010 to 2020.

#### GEO Communication Satellites

Our projection of the GEO Communication Satellite market for the 2010-2020 period is illustrated in Figure 2-1. The Commercial Space Transportation Technical Advisory Committee (COMSTAC) forecasts satellite launches, but their forecast only extends until 2010). The vertical axis indicates the number of payloads launched per year. Each point in the plot shows the projected number of payloads for a given range of masses (in pounds) in a given year. There is some risk that GEO satellites will lose market share to optical fiber communications, but their advantage for broadcasting data should endure and give this market long-term value.

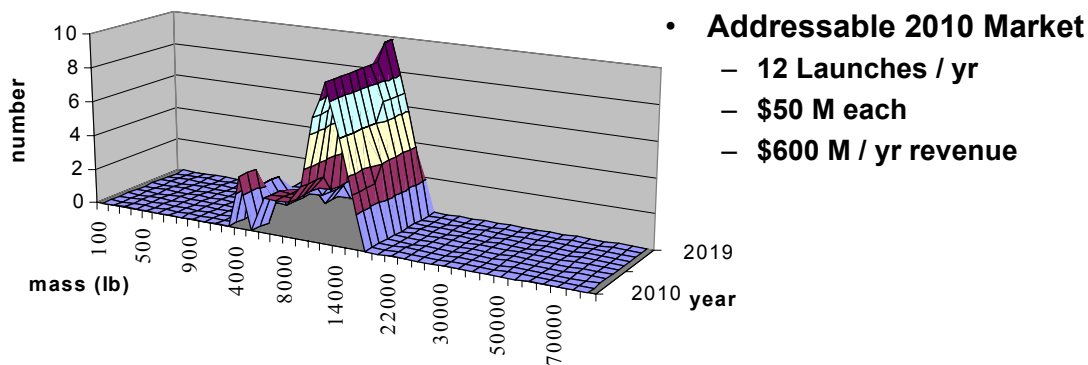


Figure 2-1. Projected launches of GEO communications satellites

Although we expect the current intense level of competition in the launch market for commercial GEO communications satellites to decrease as many current launch suppliers drop out, future competition will still be fierce. The current price for typical US launches into geosynchronous transfer orbit (GTO) is higher than \$50 M, but if HASTOL is to compete in the international commercial market the price offered must be aggressively low. Even with very low pricing,

HASTOL would not be likely to win 100% of the market, due to protectionist policies of many foreign customers.

Of all current markets assessed, this one has the best match to HASTOL’s capabilities. It also has the most well-defined payload mass and destination (~5500 kg to GTO in 2010), so this market drove the HASTOL sizing requirements.

**U.S. Civil Satellites**

United States civil satellites are a varied lot, encompassing weather, astronomy, research, technology demonstration, and other categories in a variety of sizes and orbits. This market is much smaller than the GEO communications satellite market. COMSTAC forecasts a steady market, and our projection through 2020 continues this trend (Figure 2-2). There will be a slow increase in average mass, but with no payload exceeding 5500 kg to LEO. These payloads have diverse destination orbits, so many of them are not well suited to HASTOL. Some will be a good match, however, and we expect to serve the market for those.

The launch market for these US government payloads is likely to exclude foreign competitors such as Long March. With less competition, launch pricing might typically cost a bit more per kilogram to orbit than would be experienced in open international competition.

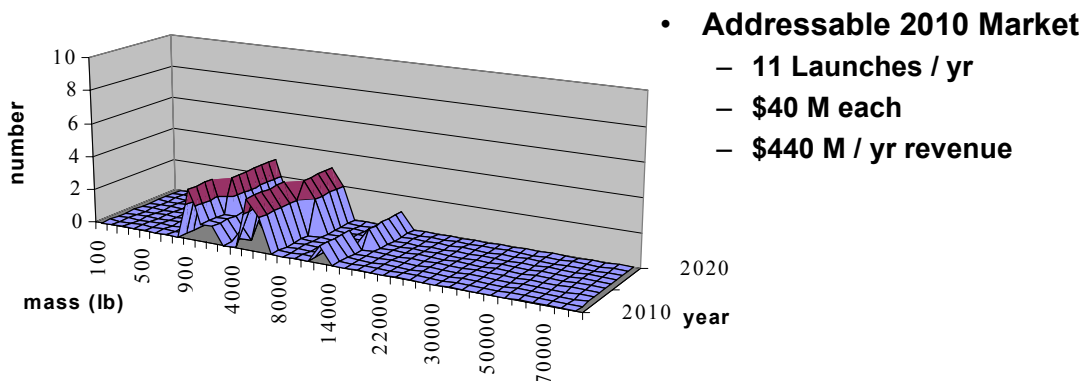


Figure 2-2. Projected launches of US Civil Satellites.

**Existing U.S. Military Satellites**

Like civil satellites, military satellites have diverse sizes and destination orbits, though they tend to be deployed as constellations, with several satellites of the same type in each constellation. Most of these satellites go to non-equatorial orbits, so a post-launch maneuver would be needed to transfer from the HASTOL release orbit to the destination orbit. Some of these payloads go to inclined high-altitude orbits; for these a lunar swingby from elliptical to inclined HEO might be cost-effective.

DOD systems were cataloged using Mark Wade's on-line Encyclopedia Astronautica (ref 3). Historically, there have been well-defined categories of military spacecraft. There has been an

historical trend toward increasing mass within each category. Our projection (Figure 2-3) includes this mass growth. However, there is very strong interest within the DOD R&D community in developing and using microsats, mostly for new missions such as space control. A set of quite small DOD payloads is projected based on this trend. Projecting from public information sources, we anticipate a steady launch rate with slow but steady growth in payload mass. The mass range goes as high as 7000 kg to GTO. There are no foreign launch competitors in this market, so pricing may not be as competitive as it is in international markets.

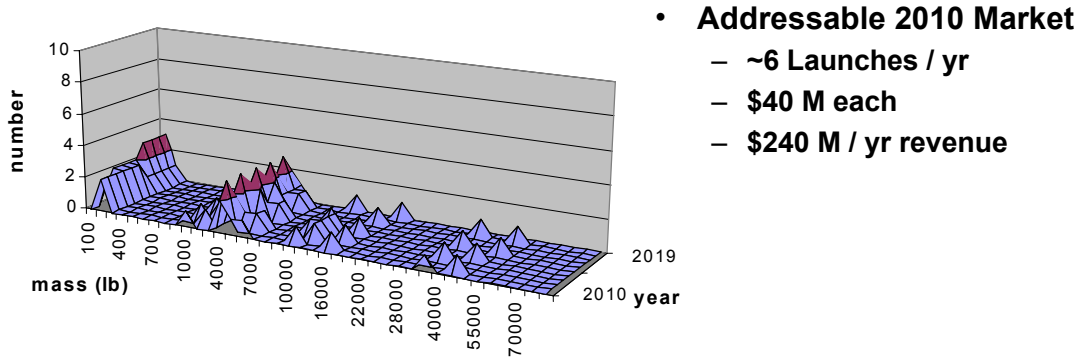


Figure 2-3. Projected launches of existing types of US military satellites.

**Total Existing Markets**

The combination of all existing markets is plotted below in Figure 2-4. The total shown includes LEO communication satellites and commercial remote sensing. These are markets for which HASTOL is poorly suited, which is why we estimate that HASTOL could capture no more than 50% of the total market.

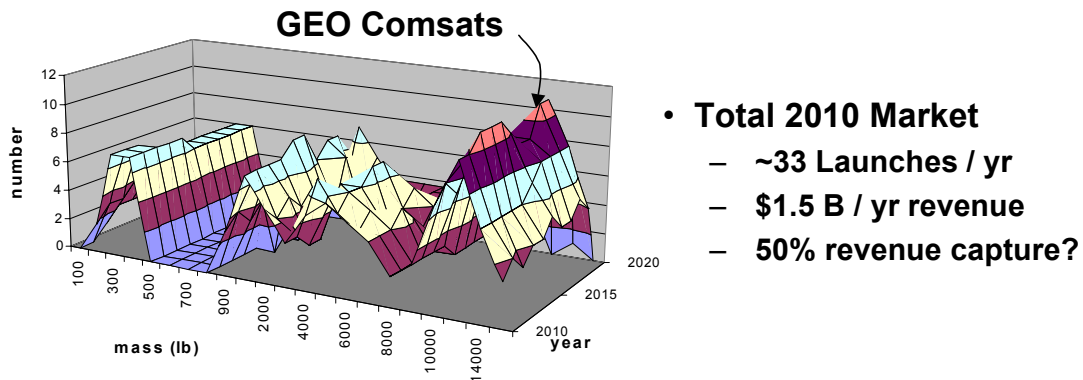


Figure 2-4. Projected total addressable launches.

The GEO communications satellite market provides the biggest, most stable peak in the total market and it matches the technical characteristics of HASTOL quite well. This stability and good match cause us to size HASTOL for that market. However, aggressive pricing will be required to compete in this oversupplied international market.

It is likely that a HASTOL system sized for the GEO communications satellite market would capture some payloads from other markets, e.g. civil, military, or remote sensing. Though not part of HASTOL's core business, these markets offer targets of opportunity that can provide extra revenue. For many of them, protection from non-US competition may allow HASTOL to charge higher prices.

### Space Tourism Market for Initial HASTOL System

Tourism - or more properly, “adventure travel” - is an emerging market that could match HASTOL’s capabilities very well. Two-way traffic allows a very high flight rate without a correspondingly high cost for reboost power. The requirements for a destination orbit are quite flexible: any orbit that gives a reasonably good view of any part of the Earth that isn’t entirely ocean. That gives a great deal of freedom to select altitude, inclination, and duration for maximum convenience. A comfortable g-level on the way to and from orbit (e.g. no more than three or four g) is easily provided with the long HASTOL tether. Increasing the number of passengers per year can be accomplished incrementally by increasing the flight rate, rather than by adding new vehicles or increasing the size of the tether. [We expect that the tether dimensions would grow, however, after several years of operation].

### Momentum Recycling

Momentum might be balanced (“re-cycled”) in a HASTOL system that transports passenger payloads. Figure 2-5 illustrates a simplified approach for HASTOL momentum recycling.

- 1 Single-seat passenger vehicle attaches to tether**
- 2 Tether throws vehicle into elliptical orbit & expends momentum**
- 3 Tether catches vehicle one vehicle orbit later**
- 4 Tether deposits vehicle in atmosphere & recovers momentum**
- 5 Vehicle lands**

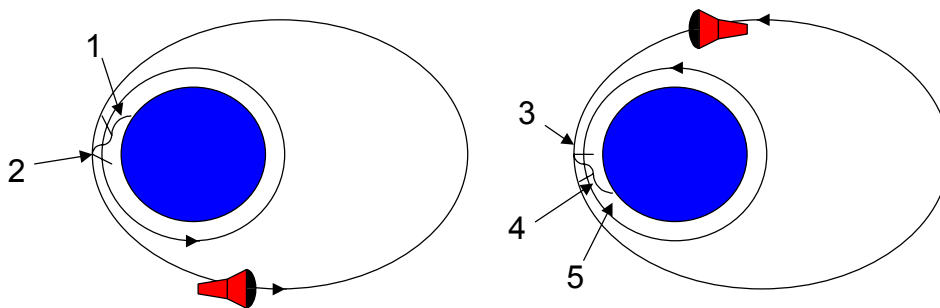


Figure 2-5. Ideal mission profile for passenger flight with momentum recovery.



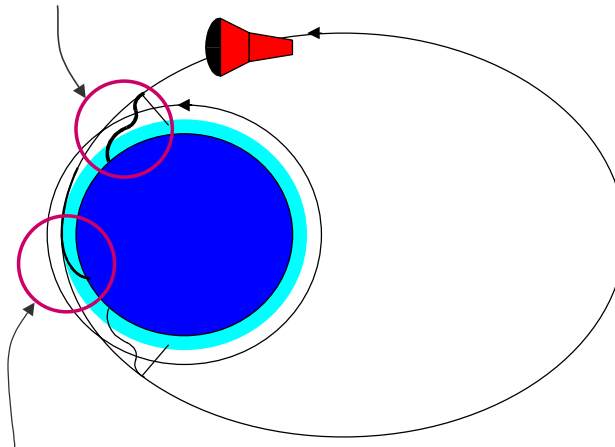
Key points of this scenario include the following:

- Passenger vehicles re-enter the atmosphere at sub-orbital speed, so entry heating is not severe.
- We do not propose that the tether catch a payload going up at the same time that it catches a payload coming down. Rather, it would handle these two functions on different orbits. We expect that after several years of operation we would be able to handle the two functions on adjacent orbits, so the maximum flight rate is one launch per two tether orbits. That limits the rate to about 2000 flights per year.
- The orbit period would be about 12 hours. That's a fairly long time to be tightly confined, but perhaps not too uncomfortable, given that the majority of the flight is in zero gravity. The duration is short enough that life support (oxygen, CO2 removal, food, and water) should not be major drivers in the passenger vehicle's mass.

### Missed Attachment Modes

Figure 2-5 illustrated a simplified concept. In reality, we would require that the passenger vehicle should be able to safely land in the event of a tether failure or a propulsion failure, as Figure 2-6 illustrates. Therefore, the tether should throw passengers into an orbit that will re-enter even if the tether fails to catch the payload when it returns to perigee. This would be a high-speed re-entry: in such a case, the heat shield would ablate, and re-entry might not be comfortable, but the landing would be survivable.

- **Tether throws vehicle into orbit w/ perigee in atmosphere**
  - **Tether-assisted entry (nominal) at low speed => heat shield reusable**



- **Assured re-entry & return if tether misses or propulsion fails**
- **Heat shield ablates for safe high-speed entry**

Figure 2-6. HASTOL mission profile for flight with assured safe abort modes.

During such a contingency re-entry, the module might land in an undeveloped region or in the ocean. It's probable that the HASTOL operating company would have to maintain a rescue team in the abort recovery area.

The abort scenario for failed handoff from the launch vehicle to the tether must also be addressed. This contingency is easy to handle. If the passenger module somehow fails to attach to the tether, yet detaches from the aircraft, it can safely re-enter and land. This would be within the parameters of a regular re-entry, so the vehicle should be reusable shortly after such a failed handoff.

Space Adventure Travel may provide a large “elastic” market for HASTOL. Market survey data for space adventure travel are plotted below in Figure 2-7. The plot shows how many passengers each year (x-axis) would pay how many dollars per person (y-axis) to travel in space. Each line in the plot shows the results of a different market estimate. This information was originally published by Ivan Bekey, who gathered it from a variety of sources.

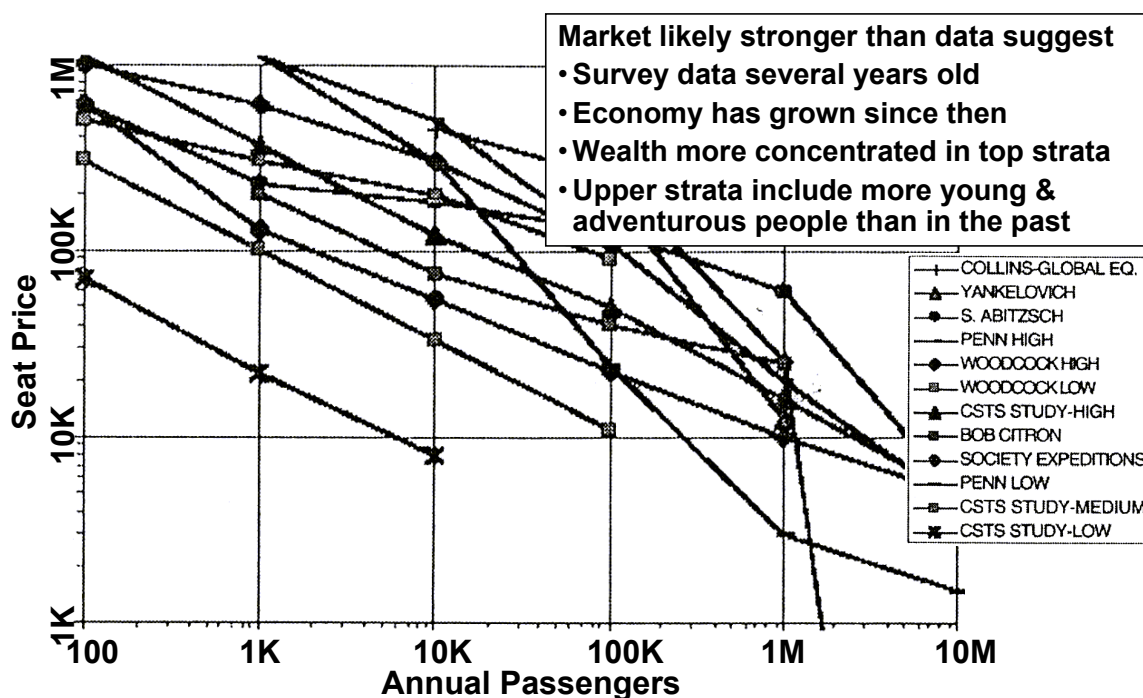


Figure 2-7. Market surveys for space adventure travel show a large elastic market.

Society Expeditions (the third line from bottom at 1K and 10K passengers per year) provides the most reliable estimate. Society Expeditions is a company that serves the adventure travel market, setting up tours of the South Pole or climbs of Mt. Everest. They did not simply guess or take a survey of their clients. Rather, they took cash deposits from existing customers. Because they serve the adventure travel market, they have a good sense for how deposits translate into ticket sales.

The Society Expeditions survey was made in the late 1980’s. The insert on the chart speculates on how the curves may have evolved since then. The most likely scenario is that the market today is substantially larger than these data suggest, and the market of 2010 should be even stronger.

**Market Entry: One- Or Two-Seat Vehicle**

A strategy for entering the adventure travel market is to minimize entry costs by starting with a small vehicle that can be developed at low cost. A vehicle that is an updated version of Mercury or Gemini may be ideal. Relatively little investment is needed - the vehicle designs already exist and are flight-proven, so little R&D is needed. A Mercury capsule masses about 1360 kg, while Gemini masses 3810 kg with its service module, small sizes that allow a relatively small tether and carrier vehicle. Indeed, these sizes are compatible with a HASTOL system sized for GTO communications satellites. The Mercury & Gemini capsules are legendary, so look-alike vehicles should have strong market appeal for adventure travelers. Many potential customers could picture themselves following the paths of Alan Shepard or John Glenn in Mercury or of Neil Armstrong and John Young in Gemini.

An important consideration is whether a proposed passenger vehicle could be certified for passenger travel by the FAA. The Mercury & Gemini capsules are quite robust. Either could easily meet the FAA's 90-second evacuation rule with one or two people. Both are aerodynamically stable during re-entry, even with a non-functional attitude control system. Both perform a parachute landing that is survivable essentially anywhere in the world. We have identified a mission profile that assures safe re-entry in the case of propulsion failure or attachment failure.

Our initial strategy for space adventure travel is to aim for a high-volume business using frequent flights of small numbers of passengers. At 180 flights per year (roughly one flight every two days), the projected revenue with a two-seat vehicle is about \$100M per year, based on the Society Expeditions market estimate, with no revision for recent economic growth. At 1000 flights per year, revenue doubles.

**Growth Paths for Space Adventure Travel**

There are several possible paths to increased revenue beyond the \$200M estimated above. One way to increase revenue is to carry more passengers per flight. Boeing has laid out a preliminary design for a Gemini-like vehicle that carries six persons for three 90-minute orbits. Its mass (with passengers) is 2541 kg. It is likely that HASTOL could carry at least six people in a module that meets the 5500 kg limit for GTO payloads; perhaps even as many as 12 people.

LEO gives a better view of Earth than GTO does, but would be more costly to access from HASTOL because momentum is not recycled. An aeromaneuver would probably be needed to get to LEO from the tether's release point. It's not clear that many customers would pay for this service.

An orbiting hotel would be supportable using HASTOL. This would permit much longer stays in orbit, which should permit higher prices. In an orbit that is conveniently accessible from HASTOL (essentially GTO), the hotel would require shielding against the Earth's trapped radiation belts.

Another interesting growth market is sending passengers on a free-return trajectory to the Moon and back. Because of limited opportunities to throw payloads to meet the Moon in its inclined

orbit, the maximum flight rate is much lower than for regular flights. However, the cost to provide each flight is not much greater than a regular GTO flight, so it should be possible to sell each seat at a very high markup. Ultimately it may be possible to support a hotel in an Earth-Moon cycling orbit. The hotel would be much more comfortable than an ETO capsule for these multi-day free-return trajectories.

Figure 2-8 summarizes the estimated number of flights per year vs. mass of the tether payload (i.e. vehicle plus passengers) by year from 2010 to 2020. Note that the vertical scale in this plot is logarithmic. The numerous passenger flights are scheduled around a much smaller number of high-revenue cargo flights. The maximum HASTOL launch rate is one launch per 2 tether orbits, so the maximum rate is about 2000 flights per year.

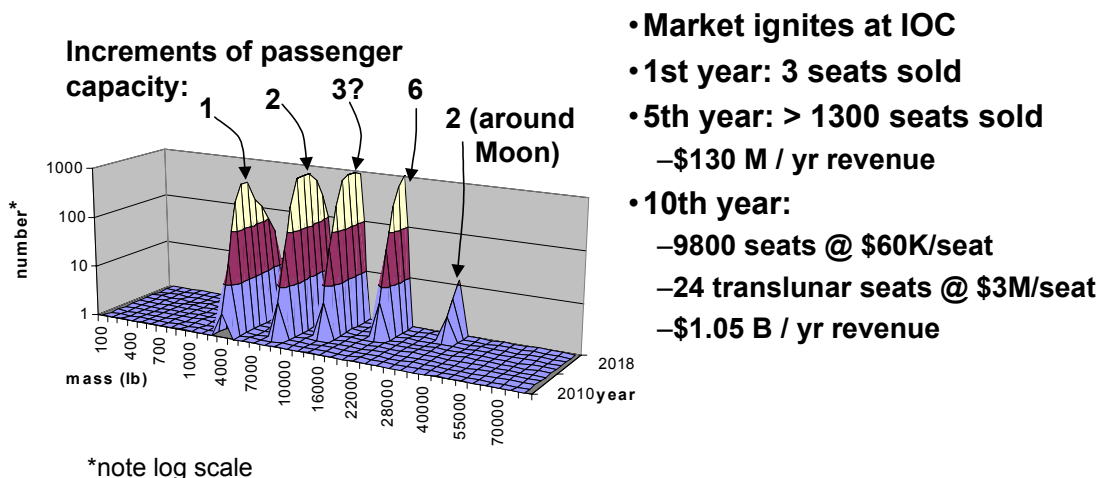


Figure 2-8. Projected market for space adventure travel.

It was assumed that we would offer passenger service using a family of vehicles where each new model seats more passengers than the previous one. Each model makes about three revenue flights in its first year of operation. The rate ramps up to about 1000 flights per year for a few years, then ramps down as a bigger model comes into service. This incremental approach should allow development of each model to be partially funded by revenues from previous models. A larger model is introduced roughly every two years. No space hotel is assumed.

The chart states that the tether thickness would be increased after about five years, but if Kendrick’s sizing of a six-person vehicle is correct, there may be no need to increase the tether size for at least ten years.

Revenues here are based on Society Expeditions market estimates. The circumlunar seat price is based on the Society Expeditions estimate for 24 seats per year to LEO; no price escalation has been applied for the close-up view of the Moon.

Though not relevant to the business case or to HASTOL requirements, it is interesting to note that by the 10th year of operation HASTOL would be sending almost 10,000 people into space

each year, 24 of whom would see the far side of the Moon. This is likely to cause a revolutionary shift in public attitudes toward space and space travel.

### IOC Mission Requirements

Table 2-2 below lists the mission requirements derived from current and emerging markets, driven by the GEO comsat market and the adventure travel market.

*Table 2-2. Mission Requirements at Initial Operational Capability*

<b>Payload mass</b>	<b>5500 kg</b>
<b>Release orbits</b>	<b>GTO + assured safe re-entry orbit</b>
<b>Orbit insertion error to GTO</b>	<b>&lt; Ariane 5 and Delta 4 error</b>
<b>Passenger orbit insert error</b>	<b>Within safe re-entry limits</b>
<b>Epoch</b>	<b>2015 to 2025</b>
<b>Mission reliability</b>	<b>98% for comsats, 99% for passengers</b>
<b>Mission safety</b>	<b>99% for comsats to be undamaged, 99.99% for passengers to survive</b>
<b>Orbital debris produced</b>	<b>Zero</b>
<b>Collision avoidance</b>	<b>Do not endanger operational spacecraft</b>

The requirement that GTO insertion error be less than the error of Ariane 5 and Delta 4 reflects the reality of a competitive market: if satellite vendors must redesign satellites to carry more propellant to compensate for HASTOL release errors, then HASTOL will have trouble competing. We assume the tether release will not meet the requirement, so the payload accommodation adapter will need propulsion to correct the release error.

Orbit insertion error for passenger flights poses little risk during the orbital phase of flight, but could cause problems during non-tether-assisted re-entry. If the entry angle is too shallow, the vehicle may fail to be captured by the atmosphere. If it is too steep, heating and g-loads may be non-survivable.

Thus the requirement for tether release error will be partly driven by characteristics of the vehicle:

- Lift-to-drag ratio determines the angle at which the vehicle can capture into the atmosphere.
- Heat shield robustness determines the survivable heating load.
- Seat design determines the survivable g-load.

Allocation of release error requirements to tether and performance requirements and to the passenger vehicle is part of the engineering to be done before the system can be fully designed.

## FUTURE MARKETS

This part of the report assesses space markets that do not yet exist: tourism for large groups of passengers, manufacturing of commercial products, large new military systems, NASA's enterprise called Human Exploration and Development of Space (HEDS), and solar power satellites (SPS) which would transmit power to Earth. Some proposals for SPS call for *in situ* resource utilization (ISRU), a possibility we included in our study.

As shown by question marks in the gray section of Table 1, none of the future markets are well defined. Though assessing an ill-defined market is difficult, we have made some assumptions - generally optimistic ones - to enable a coarse assessment. Markets for which we could generate plausible data are large-group tourism, HEDS, and SPS.

The potential match of HASTOL to a future business that manufactures a product in space using material from Earth is very strong. However, we could not identify any product that is likely to lead to such a manufacturing business. If such a product emerges, then HASTOL is likely to profit from sending payloads to and from the orbiting factory.

The only openly-discussed new military system that leads to a major increase in military Earth-to-orbit (ETO) traffic is Space-Based Laser. SBL would be in a highly inclined orbit. It is not at all certain to be built and deployed, and its parameters are currently too uncertain to allow a reasonable market estimate.

### Human Exploration Market

It is easy to imagine a NASA return to the Moon within the fiscally, politically, and technologically foreseeable future. A NASA Mars program would be much more ambitious and therefore much less likely to occur within a reasonable (to investors) number of years.

Current mission scenarios at NASA JSC involve use of a staging area at Earth-Moon L1 for both lunar and Martian exploration missions. We assume L1 would be the destination to which HASTOL would throw HEDS payloads. Other relevant characteristics of possible exploration launch markets are listed in the Table 2-3.

*Table 2-3. Characteristics of possible Human Exploration markets.*

Lunar missions	Mars missions
<b>Payloads ~32,000 kg to Earth-Moon L1</b>	<b>Payloads ~36,000 kg to Earth-Moon L1</b>
<b>4 payloads per year, may start in 2012</b>	<b>About 20 payloads every 26 months, may start in 2017, test unit possible in 2015</b>
<b>\$150 M per launch</b>	<b>\$200 M per launch</b>
<b>\$600M / yr revenue</b>	<b>\$2B / yr revenue</b>

Neither HASTOL at IOC nor any existing launcher can meet the launch needs of these programs. All recent NASA plans for human exploration start with a big new launch vehicle, an idea with a strong appeal to certain parts of NASA. To undercut the political constituency within NASA for building and using a big new rocket for HEDS, HASTOL would have to offer quite aggressive pricing with proven performance. An alternative is to allow NASA a major role in developing

HASTOL's tether, airplane, or both, i.e. NASA's long-sought big new vehicle is HASTOL. In that case, HASTOL would be a government program, not a commercial venture.

The HEDS market is very unattractive by ordinary investment criteria. There is only modest probability that a lunar exploration program will be funded in a reasonable number of years, and poor probability for a human Mars program. Even if one of these programs proceeds, the likely HASTOL launch revenue is quite small compared to the investment needed to launch such large payloads.

### **Solar Power Satellite Market**

NASA SPS supporters believe a major government-funded SPS program could possibly start in about 2019. For the type of program currently envisioned, the program would require about 1000 cargo launches per year, each of which would deliver a payload of about 35,000 kg to GTO. These would be one-way payloads (all up, none down), so momentum recycling would not be intrinsic to the market as it is with tourism. The result is that the electrodynamic (ED) reboost power a HASTOL tether would need to serve this market is greater than 50 MW.

It may not be possible to provide 50 MW of electrodynamic reboost power. The issue with ED reboost power is not that we can't provide 50 MW of electricity - especially if we're building solar power satellites. Rather, the issue is that we don't know whether any plasma contactor design could efficiently transfer the necessary amount of current to and from the Earth's ionosphere. If such a high-current plasma contactor cannot be designed, then HASTOL may not be a cost-effective way to deliver SPS components to GEO.

But what if we could find a way to reduce the reboost power needed? Figure 2-9 presents a possible solution to the ED reboost limit for SPS. We could simulate a balanced two-way traffic flow by sending material from the Moon down to Earth to balance the momentum of SPS payloads to GTO. (It would also balance many other possible ETO payloads.) The lunar material gets dropped from the bottom of the tether into uninhabited zones on the Earth's equator.

The figure implies a planar arrangement of Earth, Moon, and HASTOL. In fact, the Moon has a moderately inclined orbit. We would need to find a way to get lunar downmass from the Moon's orbit to an equatorial elliptical orbit. Some possible solutions are as follow:

- We may be able to sequence loads of downmass to arrive on alternate orbits of the tether by using long trajectories through the weak stability boundary.
- We may deliver larger, less frequent loads - but that requires a stronger, heavier tether.

We may launch SPS payloads at high rates during the part of the Moon's orbit that is close to the Earth's equator, and launch no SPS payloads during other parts of the Moon's orbit.

Further analysis is needed to see whether these or other approaches could enable HASTOL to rapidly restore its momentum after delivering a large payload to high-energy orbit. However, the possibility exists. This provides an alternative if ED power turns out to be a major limit on reboost. Having two technology paths (ED reboost and lunar downmass reboost) provides some assurance that HASTOL could serve a future SPS market.

- **Send packages of lunar regolith down to HASTOL's upper tip**
  - Provides momentum exchange for upward-bound payloads
  - High-power ED reboost not needed for one-way ETO

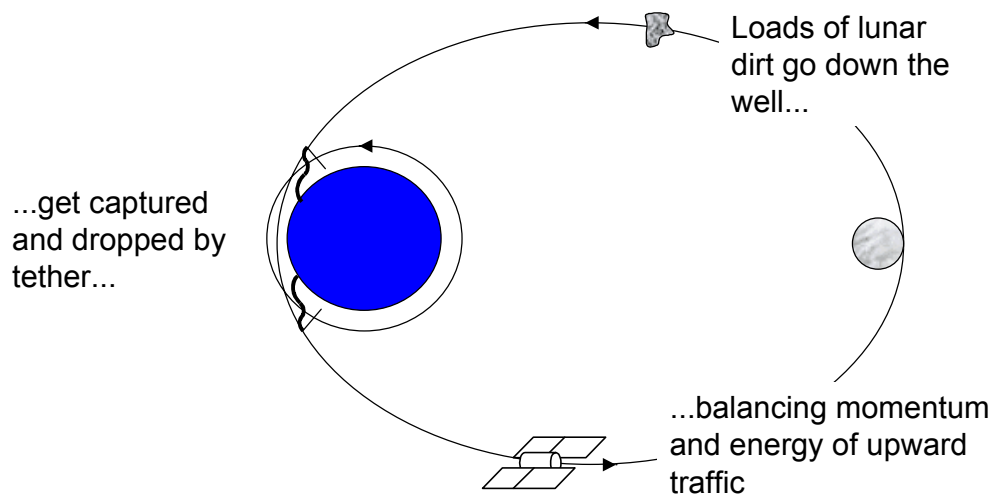


Figure 2-9. Lunar material might be used as downmass to restore tether's momentum.

### **Integrated HEDS, SPS, & Tourism Markets**

By considering lunar downmass for SPS, we can devise a scenario that exploits synergy among HEDS, group tourism, and SPS to form a plausibly attractive set of markets. The scenario begins with an enlarged HASTOL system that can support tourist flights with about 50 passengers per flight and can toss HEDS lunar payloads to the Moon about four times per year. These early HEDS missions at NASA expense could establish a lunar infrastructure that somehow throws lunar material toward Earth for use as tether downmass. That early, low-rate downmass capability permits relatively cheap launch of HEDS Mars payloads. As the lunar infrastructure grows, downmass capacity increases - perhaps using private investment. This increased capacity to supply downmass eventually allows HASTOL to support high launch rates for SPS payloads.

### **Summary of integrated market for HEDS, SPS, & Tourism**

Table 2-4 shows revenue projections for all three markets. (Current markets will presumably provide revenue as well, but those revenues are not included here.) We assume that SPS will only become viable if launch cost gets down to \$200/lb, a widely cited number in SPS literature. Therefore we assume a price of no more than \$200/lb for SPS launches. The overall business picture, though still quite speculative, is much more attractive than any of the markets considered alone.

As an aside, it is worth noting that \$200/lb to GTO makes large-scale space colonization a practical possibility. Likewise, an ETO cost near \$200/lb makes Mars exploration much more likely to occur than with current schemes.



Table 2-4. Revenue projections for integrated HEDS, SPS and Tourism market

- **Enlarged HASTOL supports NASA human missions to Moon**
- **Lunar missions deliver system to send downmass to HASTOL**
- **Enlarged HASTOL supports ~50-passenger tour flights**
  - 2000 flights per year before SPS
  - 1000 flights per year with SPS
  - Annual revenue is \$2 - 10 B
- **HASTOL + early lunar downmass support NASA Mars missions(?)**
  - ~20 flights every 2 years
  - Annual revenue is \$2B
- **HASTOL + mature lunar downmass support SPS delivery**
  - 1000 flights per year by 2025
  - @ \$200/lb, annual revenue is \$15B
  
- **Total annual revenue \$19 - 27 Billion**

**Extended Operational Capability Mission Requirements**

Table 2-5 shows the new mission requirements derived from the future markets we considered. These new mission requirements are driven by HEDS and SPS.

Table 2-5 Mission Requirements for extended operational capabilities.

Payload mass	36,000 kg
Release orbits	GTO + transfer orbit to Earth-Moon L1
Orbit insertion error	< Saturn V error
Rate	1000 SPS flights / yr, 15 HEDS flights / yr
Epoch	2020 to 2030
Mission reliability	98% for HEDS & SPS
Mission safety	99% chance that HEDS & SPS payloads will be undamaged
Orbital debris produced	zero (incl. lunar downmass)

The requirement that release orbit insertion error be less than the error of Saturn V is pure speculation. Lower precision may be tolerable. We assume tether release will not meet the requirement, so the payload accommodation adapter needs propulsion to correct the release error.

We have assumed that HEDS and SPS payloads are launched unmanned. Passenger flights add no requirements not already covered for current and emerging markets.

The requirement to generate zero orbital debris may be difficult to meet for lunar downmass. New concepts may need to be identified (e.g. propellant derived from lunar ice as downmass).

### CHAPTER 3: ARCHITECTURE SIZING STUDIES, TRADES, AND SIMULATIONS

The HASTOL team performed a number of trade studies and analyses, many of them supported by numerical simulations, to select system parameters, configurations, and technologies. This chapter summarizes each of these studies and analyses. Details of each are included as appendices to this report.

#### Variation with Rendezvous Velocity:

Using a HASTOL design worksheet, we explored the variations in the HASTOL Tether Boost Facility mass and orbital parameters as a function of the initial payload velocity at the time of rendezvous of the payload with the tip of the tether. We performed the analysis for two different tether safety factor (design tensile strength) values and two different initial payload altitudes. Results of these analyses are shown in Table 3-1.

Table 3-1. Tether Facility size, mass, and altitude for various rendezvous conditions.

#### Fixed Parameters

Tether length	600km
TCS Mass	150 Mg (10X payload mass)
Payload Mass	15 Mg
Tether Safety Factor	3.0 along entire length

Run	Rendezvous					Facility			Mass Ratio			Tip Altitude GTO		
	Velocity		Altitude		Accel	CM Peri	CM Apo	Tip Vel	TCS	Tether	Total	Perigee	Apogee	Apogee
	(Mach)	(m/s)	(km)	(n.mi.)	(gees)	(km)	(km)	(m/s)	(ratio)	(ratio)	(ratio)	(km)	(km)	(X Geo)
3111	19.0	5791	113	61	0.88	549	1314	1977	10	16	26	80	186	1.00
3007	18.0	5486	110	60	1.18	540	1012	2229	10	28	38	88	80	1.44
3010	17.0	5182	110	60	1.55	522	835	2502	10	51	61	97	80	2.76
3015	16.0	4877	110	60	1.96	512	701	2780	10	94	104	102	80	13.51
3032	15.0	4572	110	80	2.40	509	612	3064	10	175	185	106	80	-8.66
3031	14.0	4267	110	60	2.86	511	559	3353	10	331	341	108	80	-2.49
3030	13.0	3962	110	60	3.33	517	531	3645	10	638	648	109	80	-1.68
3027	12.0	3658	110	60	3.82	524	524	3941	10	1253	1263	109	85	-1.31
3029	11.0	3353	110	60	4.33	533	533	4241	10	2515	2525	110	97	-1.09
3028	10.0	3048	110	60	4.87	542	542	4541	10	5108	5118	110	103	-0.95

The HASTOL system baselined in the Phase I effort was "over-capable" in that it tended to release the payload into its final transfer orbit with too high a velocity. Most simulation runs ended up with the payload on an escape trajectory from Earth. This is a problem if the final payload apogee is GEO, but may be desirable for sending payloads to the Moon, Mars, and elsewhere. This final velocity "problem" can be solved in a number of different ways, which will be discussed later. It did NOT have a significant affect on these analyses, since the total mass of the Tether Boost Facility is dominated by the rendezvous parameters, not the toss parameters.

The total mass ratio of the Tether Boost Facility was found, as expected, to decrease as the tether material "design" tensile strength increased, and to decrease as the difference between the initial payload velocity and the initial perigee orbital velocity of the Boost Facility decreased. In general, we found that the total mass ratio of the Boost Facility was less than 100 times the payload mass when the initial payload velocity was above Mach 15. For velocities below Mach 15, the total mass ratio of the Boost Facility increased rapidly, becoming larger than 300 for Mach 12 and below. Increasing the initial payload altitude from 110 km to 185 km only decreased the total mass ratio numbers by about 10%. Accordingly, we determined that it is

more important for the hypersonic vehicle to operate at higher speed than at higher altitude, provided it is outside the atmosphere (>80 km) so that the tether doesn't overheat during the rendezvous and pickup. The major conclusion of these simulation runs, is that to end up with a HASTOL Architecture design with a reasonable total facility mass ratio (less than 100 times the payload mass), the HASTOL team needed to work on finding:

- Hypersonic vehicles with >Mach 12 velocity at >80 km altitude.
- Tether materials with higher ultimate tensile strength.
- Tether structure designs that allow the use of lower engineering safety factors.
- Phased tether rotations and orbits to insure the tether tip altitude is always >80 km.
- Methods of operating the Boost Facility to minimize tether stress.

### Total Facility Mass vs. Rendezvous Velocity

Tether Facility mass as a function of the airplane apogee velocity is plotted in Figure 3-1.

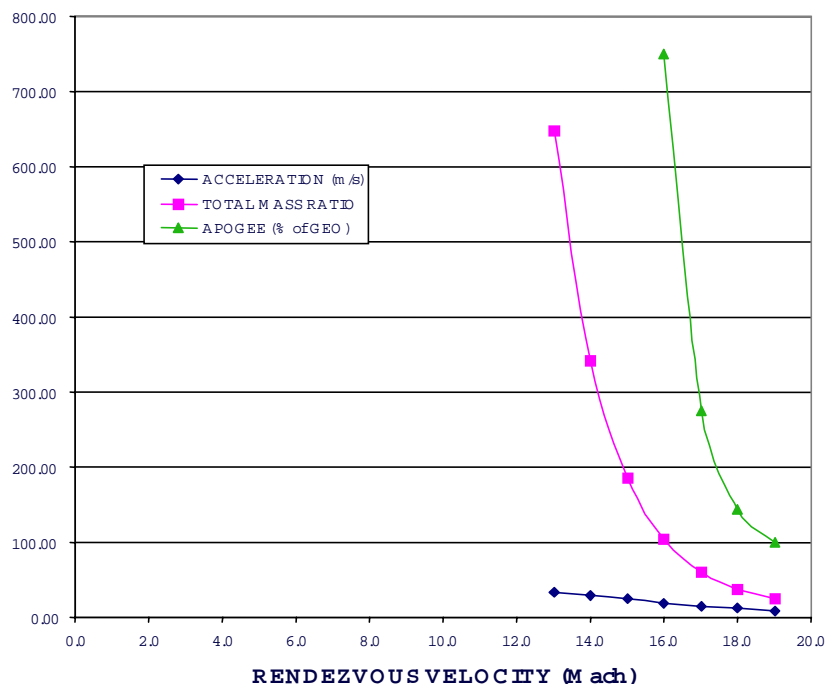


Figure 3-1. Acceleration, mass ratio, and release orbit apogee vs. rendezvous speed.

The results indicated that a rendezvous velocity of Mach 19 represents a “sweet spot” for the tether system design. This rendezvous velocity results in a tether velocity at the top of its swing such that the tether could release the payload exactly into a GTO trajectory. The Tether Facility's mass is 26 times that of the payload. (TCS 10 x payload mass, Tether 16 x payload mass, for a 3.0 Safety Factor). The tip acceleration at rendezvous is 0.9 g, well within the human comfort zone. At a Mach 19 rendezvous velocity, the airplane and tether would each be delivering half of the energy transfer necessary to place the payload into orbit.

Mach 17 rendezvous velocity is also reasonable. GTO can be achieved by early release, i.e. by releasing the payload before the tether reaches the top of its swing. In this case, the acceleration at rendezvous is 1.5 g and the total facility mass is 61 times as massive as the payload mass.

Rendezvous at lower Mach numbers is more difficult. The payload is thrown to Earth escape unless it is released very early. Very early release can leave the payload in an orbit that re-enters if the first GEO circularization burn must be postponed for some reason. Acceleration at rendezvous is 2 to 5 g and the total mass ratio exceeds 100.

### Variation with Tether Length

Using the HASTOL design worksheet, we also explored variations in the HASTOL Tether Boost Facility parameters as a function of the length of the tether. We considered a single point case where the Tether Boost Facility delivered the payload to GTO, under nearly ideal payload rendezvous conditions, without undue strain on the tether. Results are summarized in Table 3-2.

Table 3-2. Tether Facility mass for various lengths.

**Fixed Parameters**

Rendezvous Altitude 150 km (80 n.mi.)  
 Rendezvous Velocity 5791 m/s (Mach 19)  
 Payload GTO Apogee 35,786 km (1.00 GEO Altitude)  
 Payload Mass 15 Mg  
 TCS Mass 150 Mg (10X Payload)  
 Tether Safety Factor 3.0 along entire length

Run	Rendezvous			Facility			Mass Ratio			Tip Altitude		Tether Length (km)	GTO Apogee (X Geo)		
	Velocity		Altitude	Accel	CM Peri	CM Apo	Tip Vel	TCS	Tether	Total	Perigee			Apogee	
	(Mach)	(m/s)	(km)	(n.mi.)	(gees)	(km)	(km)	(m/s)	(ratio)	(ratio)	(ratio)			(km)	(km)
3121	19.0	5791	150	80	0.23	1183	1437	1530	10.0	49.0	59.0	116	83	1500	1.00
3122	19.0	5791	150	80	0.33	1006	1424	1657	10.0	29.7	39.7	108	100	1200	1.00
3123	19.0	5791	150	80	0.50	816	1417	1801	10.0	19.9	29.9	107	142	900	1.00
3124	19.0	5791	150	80	0.86	604	1390	1963	10.0	15.8	25.8	116	242	600	1.00
3125	19.0	5791	150	80	1.25	492	1362	2050	10.0	15.5	25.5	124	323	450	1.00
3126	19.0	5791	150	80	2.06	376	1324	2139	10.0	16.3	26.3	133	427	300	1.00

Tethers shorter than 450 km have high acceleration levels at payload pickup due to their short length and slightly larger tether masses due to higher tip speeds. Tethers longer than 1000 km increase rapidly in tether mass, due to the increased gravity gradient forces with a longer length. A length of about 600-900 km was found to be optimal, with longer lengths (lower pickup accelerations) preferred for "tourist" traffic. This optimum range is observable in Figure 3-2.

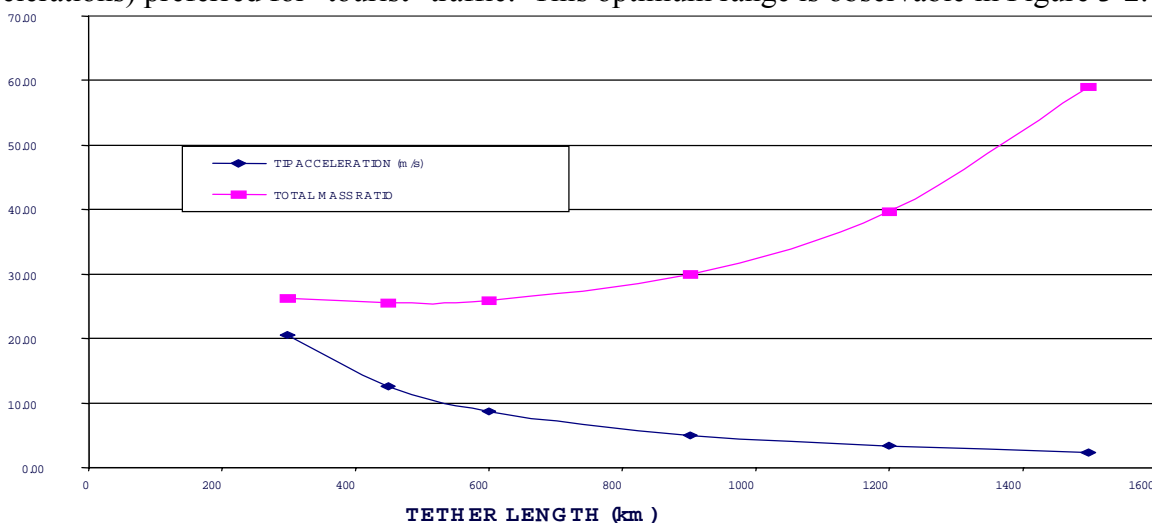


Figure 3-2. Tether mass and tip acceleration vs. tether length.

### Tether Facility Design

We developed a Tether Facility design based on the following requirements:

- Capability to capture a payload from a Mach 17 hypersonic airplane at 150 km apogee altitude.
- Operation in the Earth's equatorial plane (Mach 17 airplane inertial velocity is 5,110 m/s).
- Payload capacity of 5,500 kg.
- Capability to toss payload to a Geostationary Transfer Orbit (GTO)
- Orbit of tether after payload toss shall not allow the tether tip to drop below 80 km altitude.
- Nominal acceleration level on payload while attached to tether is 1.5 g.
- Peak acceleration level on payload is < 3 g.
- Capability to reboost facility to original orbit within 1 month.

The tether facility design was developed using the MX tether design Excel worksheet developed by TUI. This worksheet uses Keplerian orbital dynamics equations, a stepwise-tapered model of the tether mass, and an iterative solver to determine a tether facility design. The system masses just under 69 times the mass of the payload it is designed to boost. The tether itself masses 58.8 times the mass of the payload. Mass of the control facility is 10 times the payload mass. Total mass of the facility is driven mainly by the need to keep the facility and tether above the Earth's atmosphere after the payload toss. Orbital parameters and sizing are summarized, as follows:

#### Mass Ratios:

- |                                 |                    |
|---------------------------------|--------------------|
| • <b>Control Station</b>        | <b>10x payload</b> |
| • <b>Tether</b>                 | <b>58.8x</b>       |
| • <b>Grapple</b>                | <u><b>0.12</b></u> |
| • <b>TOTAL: &lt;69x payload</b> |                    |

**Tether Length: 630 km**

**Orbit: 582x805 km ->569x499**

More detailed data on the design of the Tether Facility and its orbit are shown in the Table 3-3. For the tether tip to be able to rendezvous with the hypersonic airplane, the tether must rotate with a tip velocity of 2.5 km/s. If the tether were to release the payload at the top of its rotation, it would give the payload an additional 2.5 km/s change in velocity, injecting it into a highly elliptical orbit with an apogee of 114,000 km. The system can, however, deliver the payload to other elliptical orbits by releasing the payload before the tether reaches its vertical orientation. To deliver the payload into a GTO, the tether would release the payload when the tether is 38.63 degrees from vertical. This will toss the payload into a 682 km x 35,790 km transfer orbit. At apogee, the payload will require a change in velocity of 1428 m/s to circularize into a GEO orbit.

Table 3-3. Tether Facility design and orbit details.

System Masses		Tether Characteristics	
Tether mass	323,311 kg	Tether Length	636,300 m
CS Active Mass	51,510 kg	Tether mass ratio	58.78
CS Ballast Mass	3490 kg	Tether tip velocity at catch	2,517 m/s
Grapple mass	650 kg	Tether tip velocity at toss	2,481 m/s
<b>Total Facility Mass</b>	<b>378,961 kg</b>	Tether angular rate	0.00583 rad/s
<b>Total Launch Mass</b>	<b>375,471 kg</b>	Gravity at Control Station	0.73 g
		Gravity at payload	1.48 g
		Rendezvous acceleration	1.50 g
<b>Payload Mass</b>	<b>5,500 kg</b>		

Positions & Velocities		Pre-Catch		Joined System	Post-Toss	
		Payload	Tether	Post-catch	Tether	Payload
resonance ratio		41	20		1	26.0
perigee altitude	km	-4603	582	576	569	1001
apogee altitude	km	150	805	650	499	107542
perigee radius	km	1775	6960	6954	6948	7379
apogee radius	km	6528	7183	7028	6877	113921
perigee velocity	m/s	18789	7627	7591	7555	10073
apogee velocity	m/s	5110	7390	7511	7632	652
CM dist. From Station	m		204469	210647	204469	
CM dist. To Grapple	m		431831	425653	431831	
$\Delta V$ to Reboost	m/s				72	
$\Delta V$ to Correct Apogee	m/s					-484
$\Delta V$ to Correct Precess.	m/s					416
$\Delta V$ To Circularize	m/s					1218

Basic Orbital Parameters		Pre-Catch		Joined System	Post-Toss	
semi-major axis	km	4152	7072	6991	6912	60650
eccentricity		0.6	0.016	0.005	-0.005	0.878
inclination	rad	0	0	0	0	0
semi-latus rectum	km	2792	7070	6991	6912	13861
sp. mech. energy	m <sup>2</sup> /s <sup>2</sup>	-4.80E+07	-2.82E+07	-2.85E+07	-2.88E+07	-3.29E+06
vis-viva energy	m <sup>2</sup> /s <sup>2</sup>	-9.60E+07	-5.64E+07	-5.70E+07	-5.77E+07	-6.57E+06
period	sec	2662	5918	5817	5720	148647
period	min	44.4	98.6	97.0	95.3	2477.5
station rotation period	sec		1077.8	1077.8	1077.8	
rotation ratio			5.5	5.4	5.3	

The tether tapering is shown in Figure 3-3. This tether taper was calculated using a safety factor of 3.0 for the entire tether.

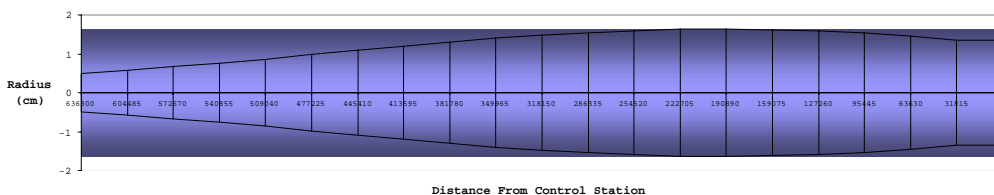


Figure 3-3. A tapered tether is designed to carry the load of its own mass, as well as its payload.

### Reboost Simulations and Analyses

When it captures and later tosses the payload, the tether facility transfers to the payload approximately 220 giga-joules (GJ) of energy. In order to restore the facility orbit within one month using electrodynamic tether boosting, the tether facility must perform thrusting at an orbital average rate of 76 kW. Using the average thrust efficiency of 40  $\mu\text{N/W}$  (calculated in previous simulations of the MMOSTT tether facility), and assuming that the tether facility

collects solar power during roughly 50% of its orbit, the tether facility will require a power supply capable of generating approximately 500 kW, when illuminated.

In this study effort, we have baselined the use of electrodynamic tether propulsion to restore the orbit of the tether. This propulsion method involves the use of onboard power supplies (solar arrays, solar concentrators, reactors, etc.) to drive current through a conductor contained in the tether. The tether current will interact with the Earth's magnetic field to produce a  $J \times B$  Lorentz force on the tether. By properly phasing the current with the rotation of the tether, the tether system can produce a net thrust force that will boost the orbit.

To evaluate the effectiveness of electrodynamic thrusting for reboost of the tether facility, we conducted a simulation using the TetherSim™ program in which the tether facility performed electrodynamic thrusting for a period of one day. In this simulation, we assumed that the tether control station has a solar power supply able to generate 167 kW of power during the sun-lit period of the orbit. To enable thrusting during periods when the tether is in eclipse, the station also contains a power storage system (batteries or flywheels) of 306.5 kW-hr. The Tether Facility mass in this case is 379,225 kg (69 times as massive as the payload).

In this simulation, we assumed that the conductor ran along 80% of the length of the tether, and that the system included hollow cathode devices at both ends of the conductive section capable of transmitting at least 5 amps of ion or electron current to the ionospheric plasma.

Because the tether catches and tosses the payload while the tether is at or near perigee, the primary change in its orbit is a large decrease in its apogee. The perigee drops slightly as well, but to a much lesser degree than the apogee. Thus, in order to restore the tether facility to its desired orbit, we must perform thrusting in such a way as to mainly boost its apogee. In this simulation, we performed thrusting only while the tether was in the 1/2 of its orbit near perigee.

Data in Figure 3-4 was produced by the simulation for tether current, battery charge level, orbital energy, and thrust efficiency. The results show that the system does indeed produce thrust and increase its orbital energy without exceeding the limits of the electrical conductor, the plasma contactors, or the batteries.

Data in Figure 3-5 was generated by the simulation for the orbital semi-major axis and eccentricity of the tether's orbit during the reboost operation, as well as the resultant apogee and perigee altitudes. (The high-frequency variations in the orbital elements are due to the fact that as the tether rotates, energy is exchanged between the "potential energy" of the tether in the gravity-gradient field, its orbital energy, and its rotational energy. When the tether is aligned along the local horizontal, it has more potential energy than when it is aligned along the local vertical, much like a pendulum in a terrestrial gravity field.)



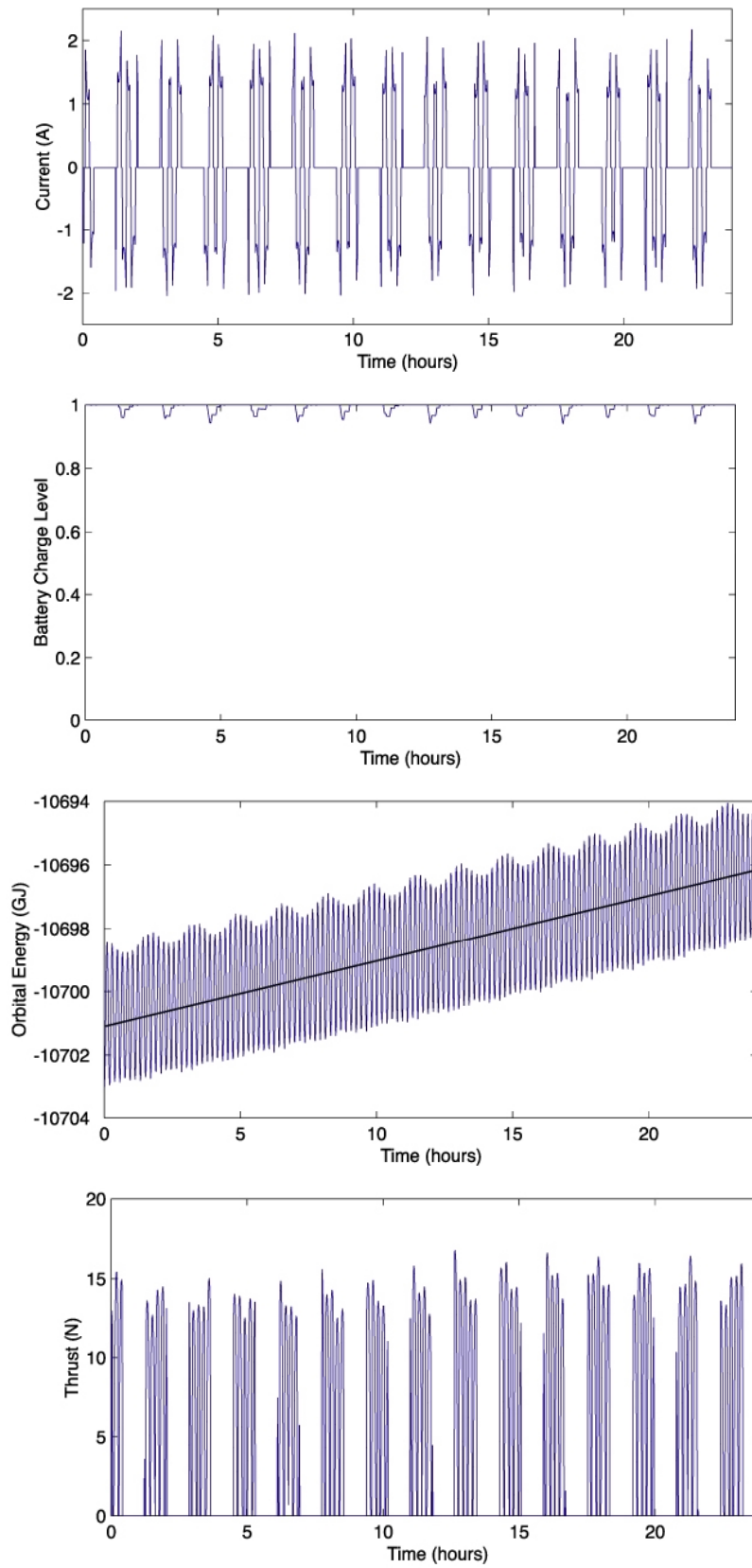


Figure 3-4. Simulated electrodynamic rebost over one day.

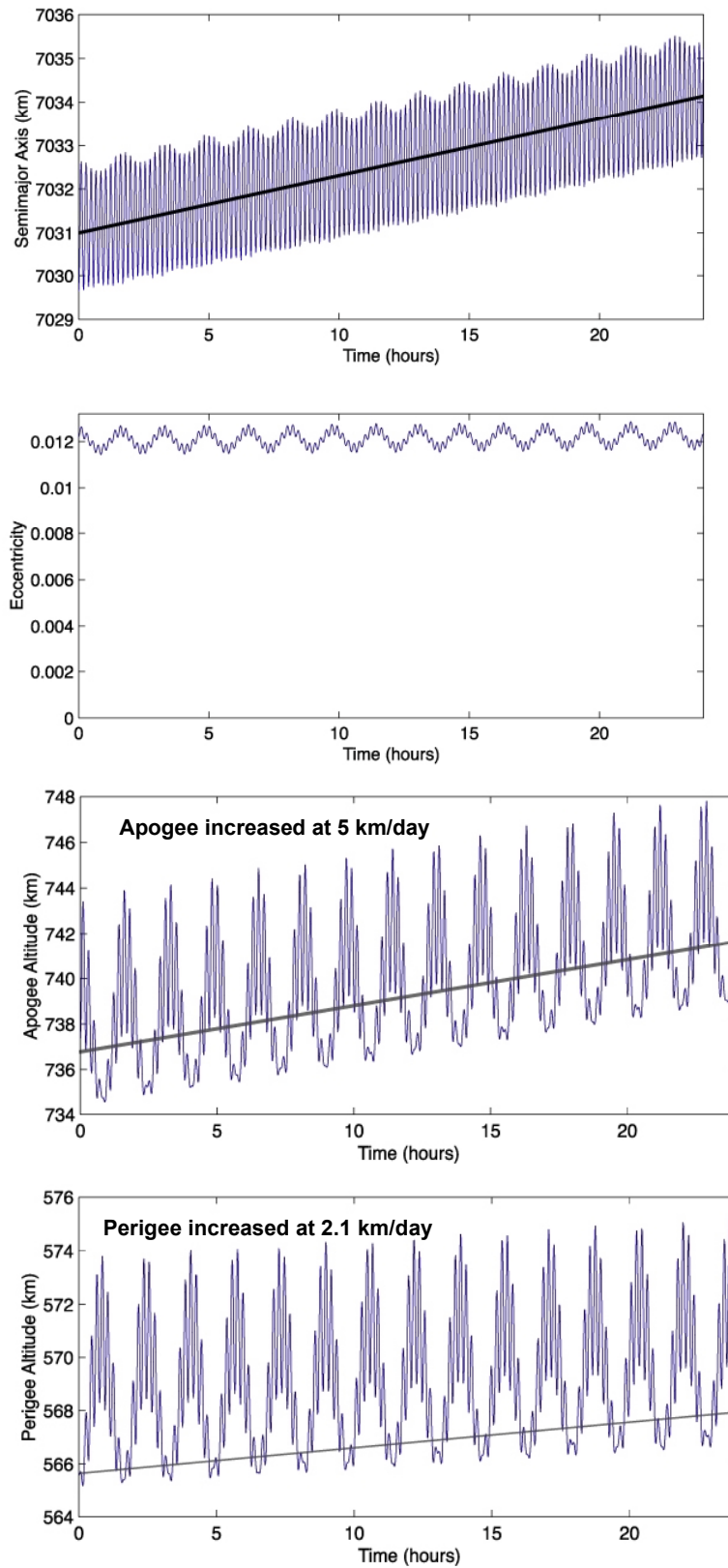


Figure 3-5. Orbital parameters during simulated electrodynamic reboost.

The reboost simulation data indicate that the thrust power of 150 kW used in this simulation was too low to restore the orbit of the facility within one month. In order to do so, the reboost rate would have to be increased to approximately 201 kW.

In addition, the rate at which the facility's perigee was boosted was too large when compared to the apogee increase rate. If this program of thrusting were continued, the resultant orbit would have an eccentricity too low to allow the tether to reach down to the 150 km payload rendezvous altitude. To manage this issue, the tether facility can use the thrust vectoring techniques developed in the MMOSTT effort, in which the current is modulated to increase the energy of an orbit more rapidly than the momentum of the orbit, thus increasing the eccentricity at a faster rate.

### **Rendezvous Simulation Development**

TUI continued to develop the capabilities of the TetherSim™ program by incorporating a model for the endmass (grapple) dynamics into the simulation code. This modification facilitated the study of the HASTOL architecture, and enabled Boeing and TUI to evaluate the tether-payload rendezvous scenario to determine requirements for the rendezvous and grappling systems. Furthermore, TUI has developed a modified version of the TetherSim™ code that can be utilized within MatLab computations. This TetherSim™ "MEX file" is meant to enable the HASTOL team to evaluate the impact of tether dynamic behavior on the rendezvous scenario.

The TetherSim™ model now includes:

- Orbital Mechanics (J8)
- Tether Dynamics
- Tether Deployment/Retrieval
- Tether Thermal Behavior
- Capture & Release Dynamics
- End-Mass Attitude Dynamics
- Atmospheric & Ionospheric Effects (IRI)
- Magnetic Field (IGRF)
- Visualization

The major challenge in accomplishing the tether-payload rendezvous will be ensuring that the trajectories of the airplane and the rotating tether can be predicted and controlled with sufficient accuracy that the final maneuvering and grappling can be accomplished with realistic requirements on the sensing, thrusting, and navigation systems. Future work on this effort should focus on identifying and characterizing the variations or dispersions in the position and velocity of the tether tip likely to be encountered during the rendezvous maneuver. A number of physical effects will contribute to these dispersions, including tether dynamics, short-term variations and uncertainties in the atmospheric density, thermal expansion of the tether as it moves from eclipse to sunlight and back, and the effects of the Earth's non-ideal gravitational field.

Strong initial steps toward characterizing these dispersions were carried out during the HASTOL Phase II effort. A simulation of the hypersonic airplane was developed to model the airplane's ability to match position, orientation, and velocity with the tether. The simulation includes a six

degree of freedom (6-DOF) airframe model, various models of sensors and actuators, and software to handle sensors, actuators, and guidance in flight. The simulation allows diverse scenarios to be specified so as to explore a range of rendezvous and capture conditions. It also produces animations of simulation runs.

We have identified several sensor configuration concepts to support the HASTOL rendezvous. These are listed in Table 3-4, along with corresponding operational and performance details.

*Table 3-4. Sensor concepts implemented in R&C simulation.*

<b><u>Concept</u></b>	<b><u>Considerations</u></b>
<b>HA - Active Ka band radar Grapple - Interactive radar beacon</b>	<ul style="list-style-type: none"> <li>• HA transmits interrogation waveforms</li> <li>• Grapple transmits response pulse train</li> <li>• Relative range/angles, range rates</li> <li>• Accuracy ~ 0.5 m</li> </ul>
<b>Grapple - Continuous radar beacon HA - Passive radar receiver</b>	<ul style="list-style-type: none"> <li>• Grapple transmits in R&amp;C timeframe</li> <li>• HA uses SBL/LBL interferometry</li> <li>• Derived relative position/rates</li> <li>• Angular accuracy ~ 0.05 deg</li> </ul>
<b>Grapple - GPS rcvr. comm. link HA - GPS rcvr. comm. link</b>	<ul style="list-style-type: none"> <li>• Grapple GPS P/V data sent to HA</li> <li>• HA GPS data provides its own P/V data</li> <li>• Satellite selection coordination possible</li> <li>• Can approach DGPS performance</li> <li>• Accuracy ~ 1.0 m</li> </ul>
<b>HA - P/L mechanism LRF</b>	<ul style="list-style-type: none"> <li>• Precise vertical separation</li> </ul>

The first concept has an active Ka band radar on the hypersonic airplane (HA) and interactive beacon on the space tether (ST) grapple assembly. The HA transmits interrogation wave-forms while the grapple beacon transmits a response pulse train after HA wave-form detection. Relative range, angle and rate information is obtained with an accuracy of approximately 0.5 meters.

A second concept has an ST grapple beacon providing a continuous signal during the R&C timeline. The HA has a passive radar receiver which performs short baseline (SBL) and long baseline (LBL) interferometry based on the received ST beacon signal. Relative range and rate information is derived with angular accuracy of approximately 0.5 degrees.

A GPS based concept is also identified. It includes GPS receivers and com links on both the ST grapple and HA. The ST grapple position and velocity (P/V) data is sent to the HA to perform the rendezvous guidance. The communications link also permits satellite selection coordination

between ST and HA GPS receivers to enhance relative performance and approach differential GPS (DGPS) accuracies ~ 1.0 m.

Rendezvous actuator concepts include equipment to move either the ST grapple assembly or the HA. Some options are identified in Table 3-5. The HA is serviceable and expendables can be readily replenished. This is not the case with the grapple assembly. Therefore the approach is to first see if HA linear articulation schemes can accomplish the rendezvous without grapple articulation. From an actuator sizing viewpoint the HA is relatively large compared with the ST grapple assembly and will require larger control authority to produce similar relative motion.

*Table 3-5. Actuator concepts implemented in rendezvous and capture simulation.*

<b><u>Concept</u></b>	<b><u>Considerations</u></b>
<b>HA linear articulation</b> <ul style="list-style-type: none"> <li>• Divert thrusters</li> <li>• Rocket/TVC</li> <li>• P/L rotation/elevation mechanism</li> </ul>	<ul style="list-style-type: none"> <li>• Relatively large (HA) mass to move</li> <li>• Readily serviceable/replenishable</li> </ul>
<b>Grapple linear articulation</b> <ul style="list-style-type: none"> <li>• Divert thrusters</li> <li>• Electric motor/plate</li> </ul>	<ul style="list-style-type: none"> <li>• Relatively small (grapple) mass to move</li> <li>• Thrusters require replenishment</li> </ul>

The HA model is a complete six degree-of-freedom model of the dynamics and control effects. It includes a thrust vector control (TVC) auto-pilot, a three-axis attitude control system (ACS) modeled after the Delta launch vehicle upper stage coast controller, a rendezvous guidance algorithm, linear divert thrusters, and discrete control events to initiate payload bay door opening and payload rotation.

The curves of Figure 3-6 provide some insight into the dynamics around rendezvous. The x-axis coordinate is essentially vertical at the rendezvous point. At 58 seconds the grapple assembly is released. The plots indicate that during the free-fall period, the ST and HA vertical velocities are very close. Once the grapple assembly tether reaches its maximum length, its free-fall ends. It is then effectively reattached to the ST main body.

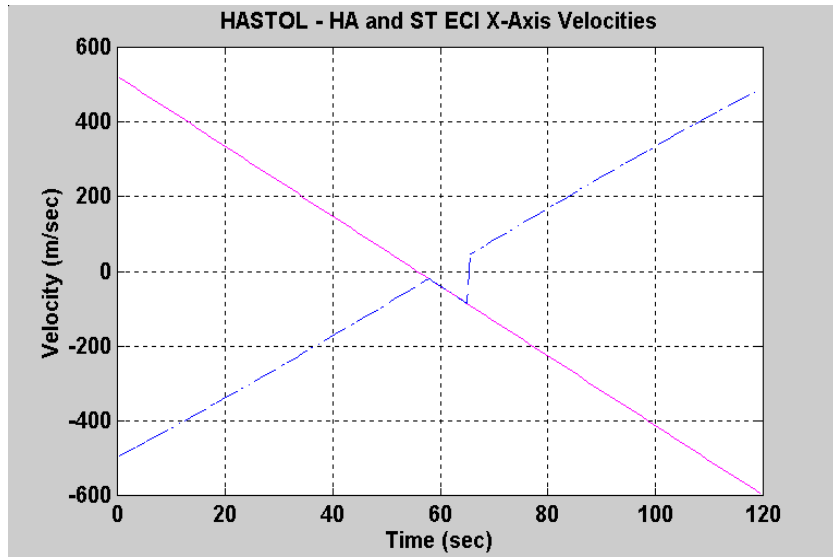


Figure 3-6. Airplane and tether tip x-axis velocities (Earth-Centered Inertial coordinates).

The data illustrated in Figure 3-7 represent an expansion of the previous plot around the rendezvous point. The x-axis (vertical) and z-axis (longitudinal to aircraft) relative velocities are essentially identical at 60 seconds. The y-axis (cross-track) relative velocity is within 0.6 m/sec in the two-second band around 60 seconds.

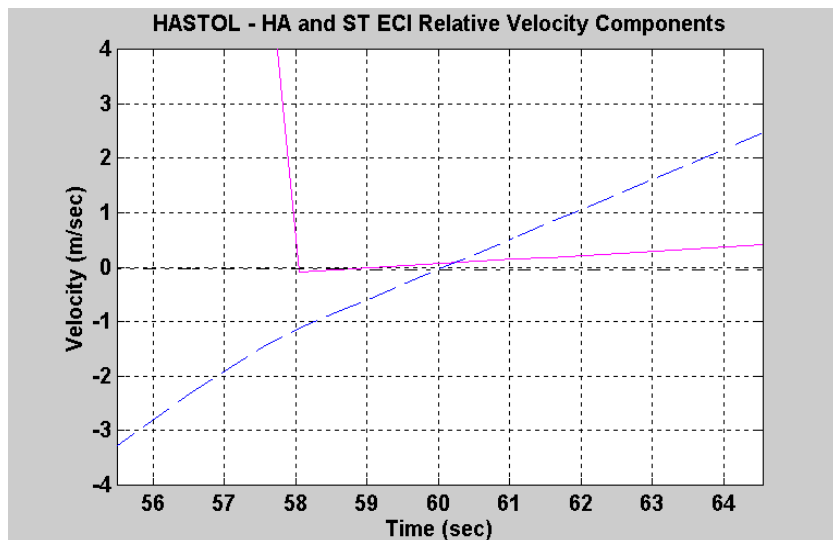


Figure 3-7. Airplane and tether tip velocities near rendezvous point.

From these analyses, it is clear that an effective rendezvous and capture can be executed for certain combinations of initial conditions. With appropriate sensors and actuators, the airplane and the grapple assembly in can meet requirements for mission safety and reliability.

Additional information about our HASTOL architecture sizing studies, trades, and simulations, is provided in Appendices A through I, attached at the end of this report.

## CHAPTER 4: HYPERSONIC AIRPLANE TRADE STUDIES

The hypersonic airplane from HASTOL Phase I design, based on the existing DF-9, had some difficulty reaching higher staging Mach numbers and altitudes. The Phase I solution required a massive tether (Mach 12, 100 km). Phase II efforts were based on a transfer at Mach 17 at 150 km, which can reduce the tether mass by a factor of about 3 compared to the Phase I results. This work was based on a payload mass of 6800 kg, payload length of 9.1 m, and payload diameter of 3.0 m. These values were a compromise between desired HASTOL values and values built into existing analyses. Changes in these values would not change the results of this effort significantly unless the payload is required to be much larger.

### LAUNCH VEHICLE TRADES

Eight launch vehicle concepts were considered in Phase II. The first concept considered was a rocket vehicle with vertical takeoff, included in the trades as a reference case. This Downrange Landing concept is shown in Figure 4.1. The thrust was reduced to allow the acceleration to continue to the rendezvous point so that the vehicle could be controlled with the main engines. The vehicle performed a gliding entry with the acceleration controlled to be less than 3g. The flight ended with a horizontal landing downrange from the launch site. The downrange landing concept is not considered an acceptable concept for operational reasons. The vehicle would have to be returned to the launch site, and the weather would have to be acceptable at both the launch site and the landing site.

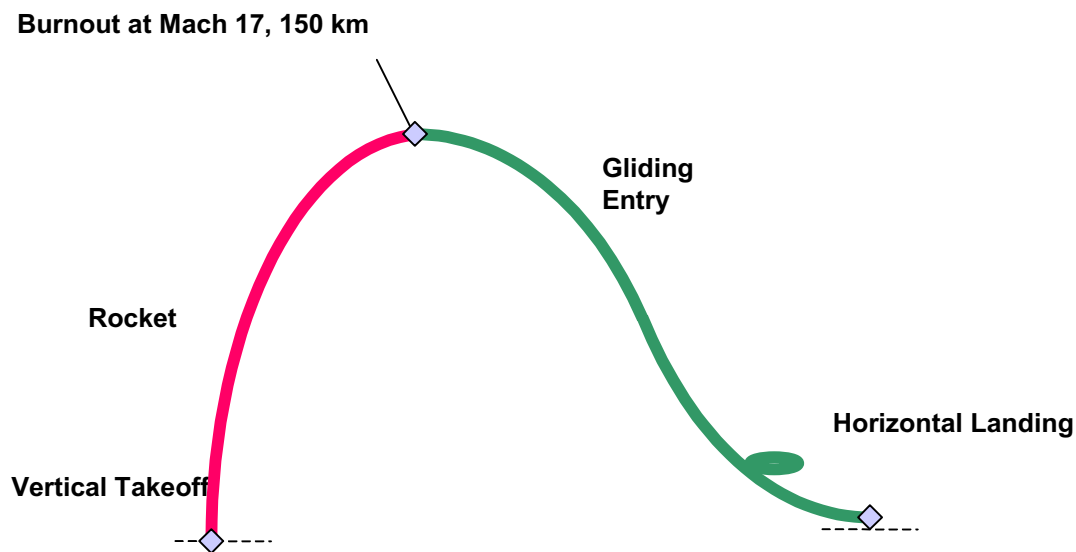


Figure 4-1 Reference Case: Vertical launch with down-range landing.

The second concept, Flyback Booster, was similar to the Downrange Landing, but turbofan engines were included on the vehicle to allow it to fly back to the launch site. The entry included a turn to minimize the flyback distance. With this addition, the concept was acceptable operationally, but adding the engines and fuel increased the size considerably.

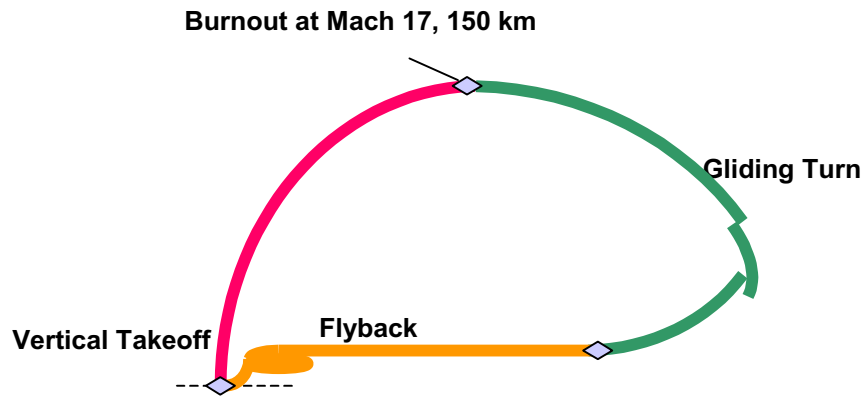


Figure 4-2 Flyback Booster/Gliding return

In an attempt to relieve the hypersonic vehicle of the need for flyback, an air-launched concept was considered in the third concept, “Air Launched Rocket”. A large subsonic airplane carried the hypersonic vehicle uprange about 1000 km, turned, launched the hypersonic vehicle, and flew back to the launch site. The hypersonic vehicle then used rocket propulsion to accelerate to the rendezvous point. After the entry, the hypersonic vehicle could glide to the launch site.

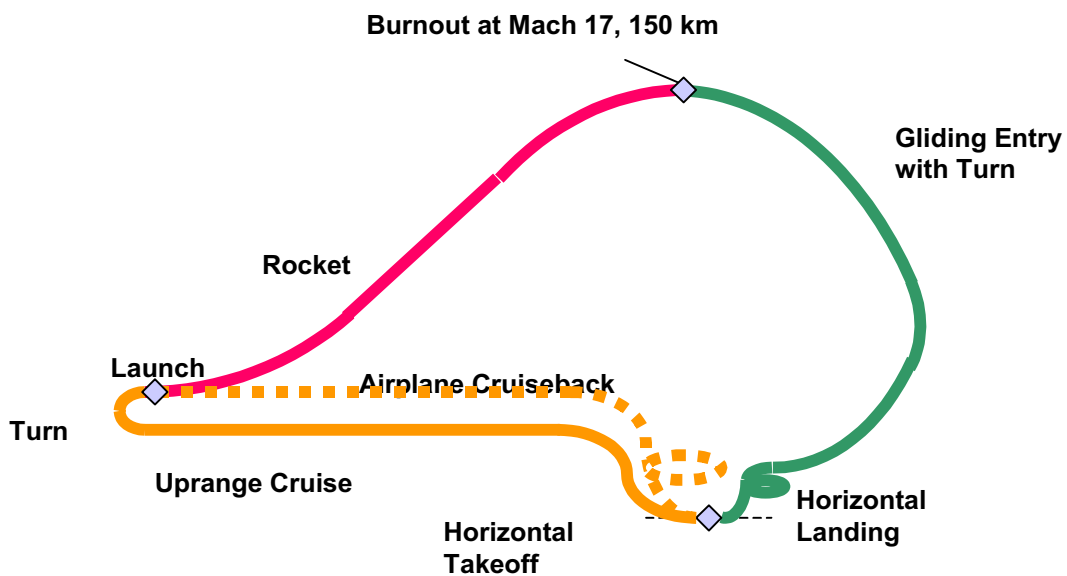


Figure 4-3 Airlaunch rocket with a cruising return



The fourth concept, “Air-turborocket” was similar to the air-launched rocket except that an air-turborocket engine was added to the hypersonic vehicle. This engine used kerosene and oxygen propellants with air to accelerate to Mach 6.

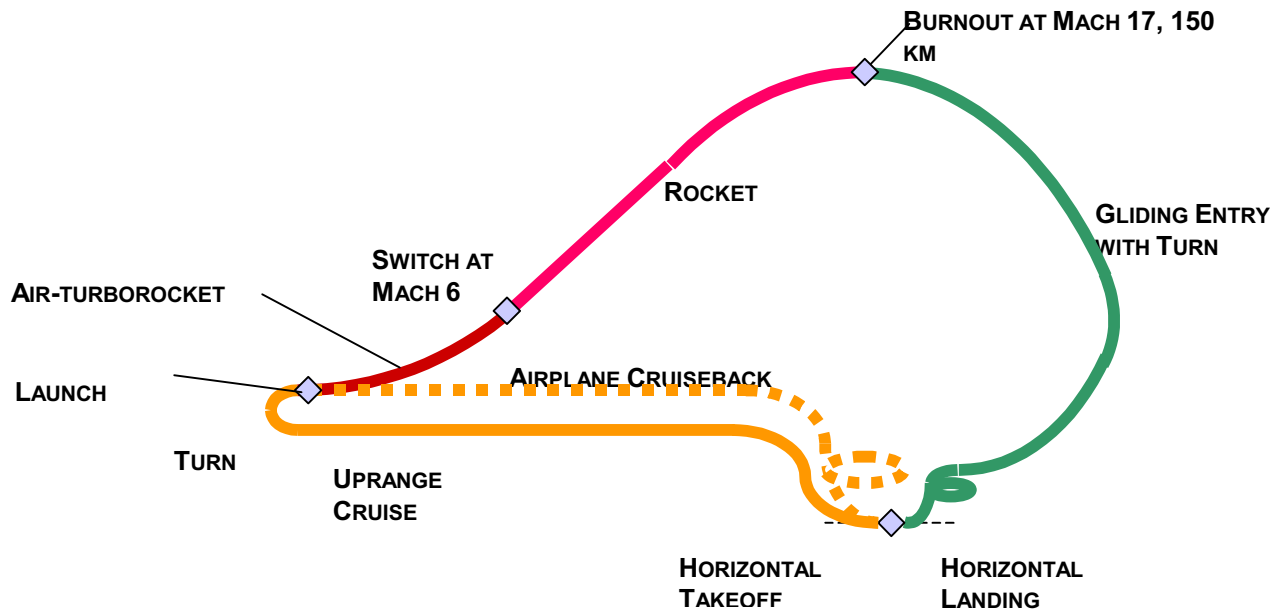


Figure 4-4: Air-turborocket Concept

A fifth concept, “Air Launched RBCC,” was considered using a rocket-based, combined-cycle (RBCC) engine on the hypersonic airplane and air launch. The RBCC uses ejector, ramjet, and scramjet operating modes to accelerate to Mach 10, where the ejector rocket is used for the final acceleration.

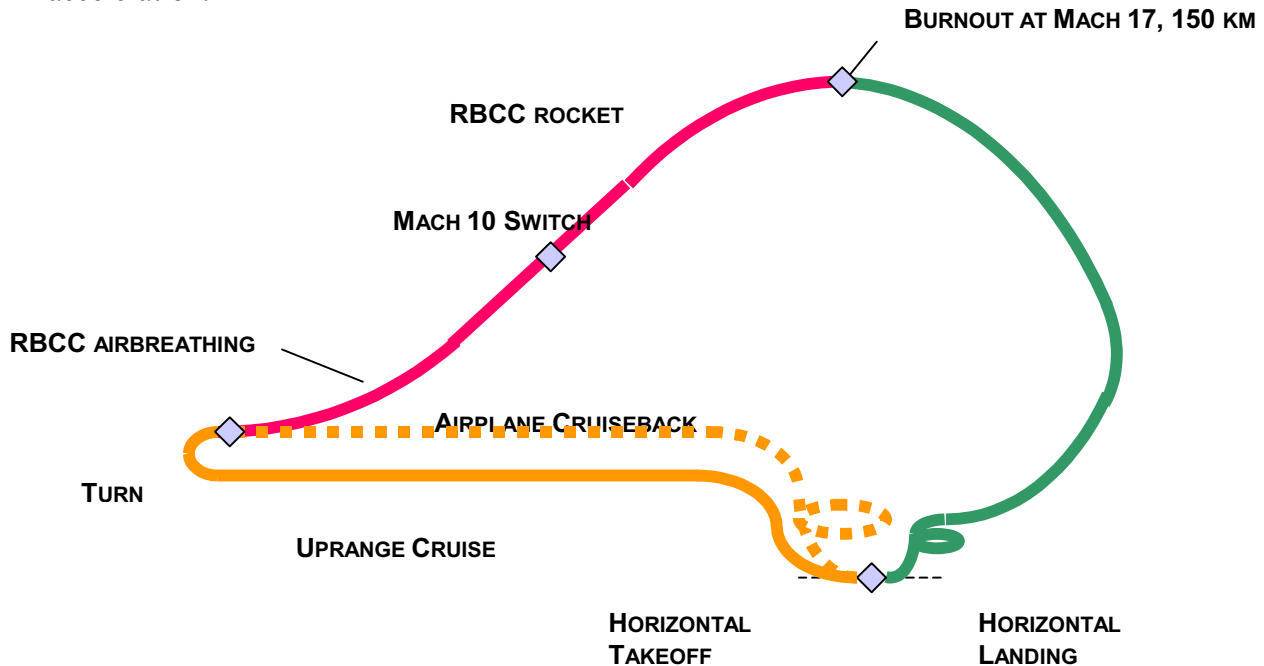


Figure 4-5: Air Launched RBCC

Two single-stage concepts were considered. The first, “Single-stage Airbreathers,” used a Hydrogen-oxygen RBCC engine with ejector, ramjet, scramjet, and rocket modes. The second, “Single-stage TRSR,” used over-and-under turboramjet, scramjet, and rocket (TRSR) separate engines. Both used a takeoff assist with some device such as a magnetic levitation (MAGLEV) sled. The flyback phase used the ramjet mode at Mach 4. To minimize the flyback distance, the initial acceleration was uprange, followed by a high-speed turn.

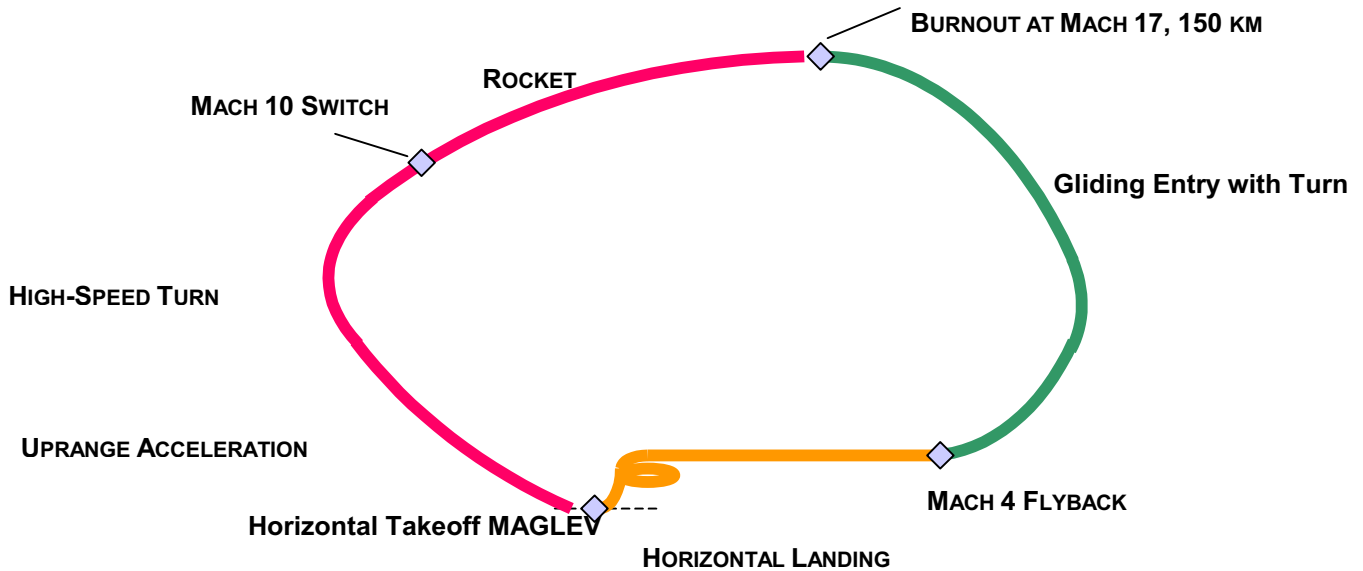


Figure 4-6: Single-stage Airbreathers

A two-stage concept, “Turboramjet Booster,” was considered with a booster powered by a turboramjet engine and a rocket second stage. The booster accelerated and cruised uprange before a high-speed turn and launch at Mach 4. Takeoff assist was assumed.

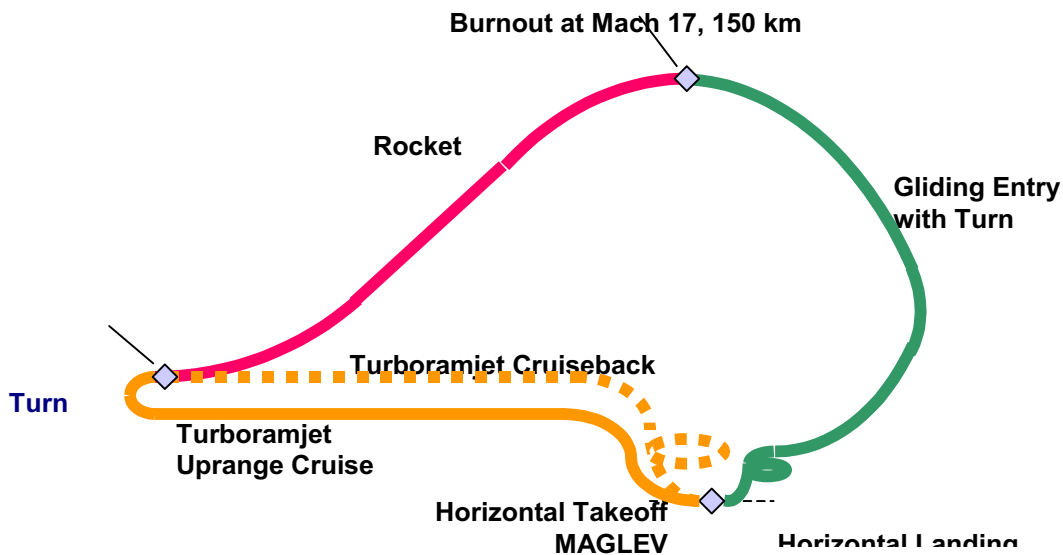


Figure 4-7: Turboramjet Boost

## LAUNCH VEHICLE ANALYSES

Our launch vehicle analysis used two methods. One was based on current Boeing analysis procedures being used in the studies of reusable launch vehicles (RLVs) that might replace the Space Shuttle in the near term. The second was based on a Design Sheet method being used for advanced vehicles, mostly airbreathing. The concepts analyzed by each method are shown in Table 4.1. The air-launched rocket concept was analyzed by both methods to show the differences in the methods.

**Table 4.1: Methods Used to Analyze Launch Vehicle Concepts**

<b>RLV Analyses</b>	<b>Design Sheet Analyses</b>
Downrange Landing	Air Launched Rocket
Flyback Booster	Air Launched RBCC
Air Launched Rocket	Single-stage Airbreathers (2)
Air-turborocket	Turboramjet Booster

### RLV Analysis

The RLV analysis used the well-known POST point mass trajectory program. The data included aerodynamic and rocket data used during the Rockwell X-33 studies. The mass-estimating equations and sizing analysis was based on current Boeing work with an Orbiter that has a payload bay external to the fuselage and four full-flow staged combustion engines designated RS-2100. The ascent was optimized to the Mach 17, 150 km altitude case and entry was controlled to 3g's. Air-turborocket data was provided by CFD Research Corp. The subsonic airplane used in air-launched concepts was not analyzed, assuming that an existing airplane would be modified for this purpose. Figure 4-8 is a computer-generated illustration of an RLV concept that portrays the general geometry built into the RLV sizing analysis and POST aerodynamics. (The external payload bay is not shown in this example).

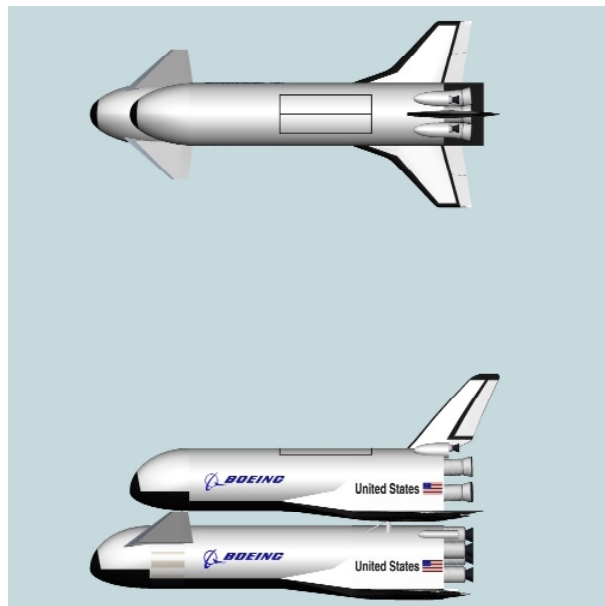


*Figure 4-8: Typical RLV*

### Design Sheet Analysis

Design-Sheet analysis uses a set of equations to optimize the entire design problem. Design Sheet optimizes total design, including trajectory and sizing. The equations can include curve-fit equations from detailed analyses of parts of the problem. The data built into the analysis used geometry from a slender vehicle, which would be appropriate for concepts using airbreathing propulsion. The takeoff assist was not analyzed, and the mass of the sled is not included in the results shown in this report.

The vehicle geometry shown in Figure 4.9 is typical of geometry used in Design-Sheet analysis.

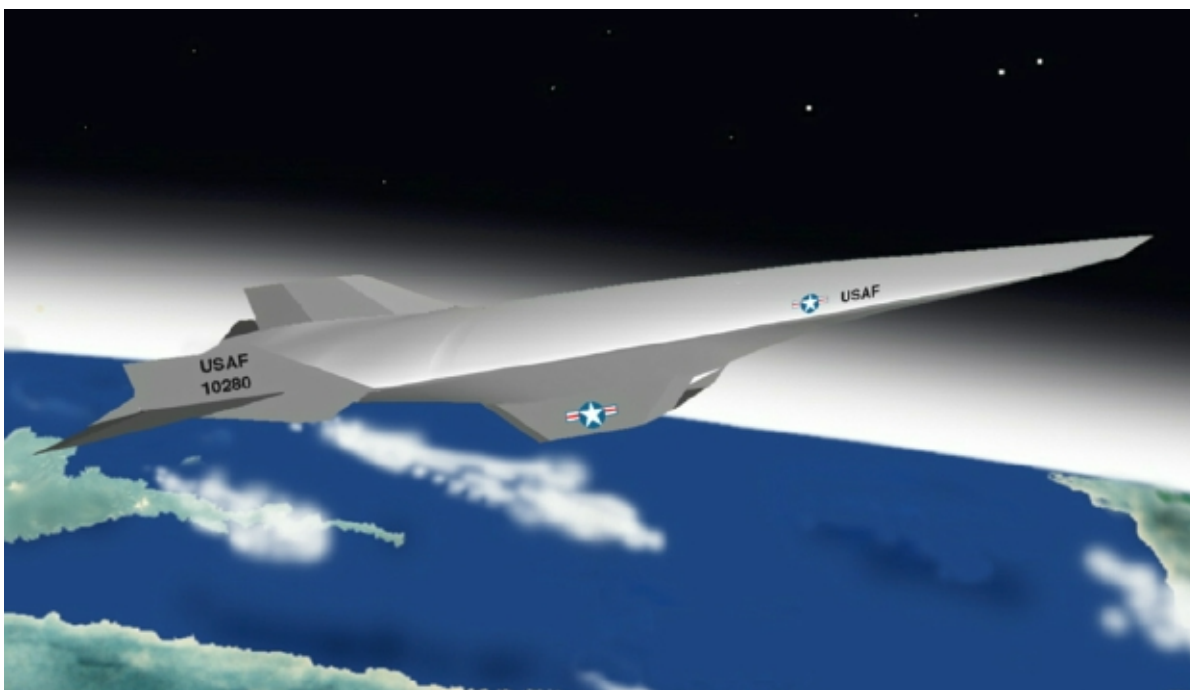


*Figure 4-9: Typical Slender Vehicle Geometry*

Results for the dry mass, gross mass, and lengths of the various concepts are shown in Figures 4.10 – 4.12. The downrange landing has relatively low dry mass but is not considered acceptable. The flyback rocket concept has a high dry mass and is not likely to be the most economical solution. The single-stage concepts and the turboramjet booster concept appear less attractive than the air-launch concepts.

One of the problems with the air-launch concepts is that the total mass of the hypersonic vehicle may exceed the capability of existing airplanes. The air-launch rocket concept is most likely to have this problem. The air-launch concept with RBCC or air-turbo-rocket propulsion would most likely be acceptable. The difference between the two analyses is not large for the air-launched rocket concept. The difference in the length results of the two analyses is evident and is expected from the different geometry each assumed.

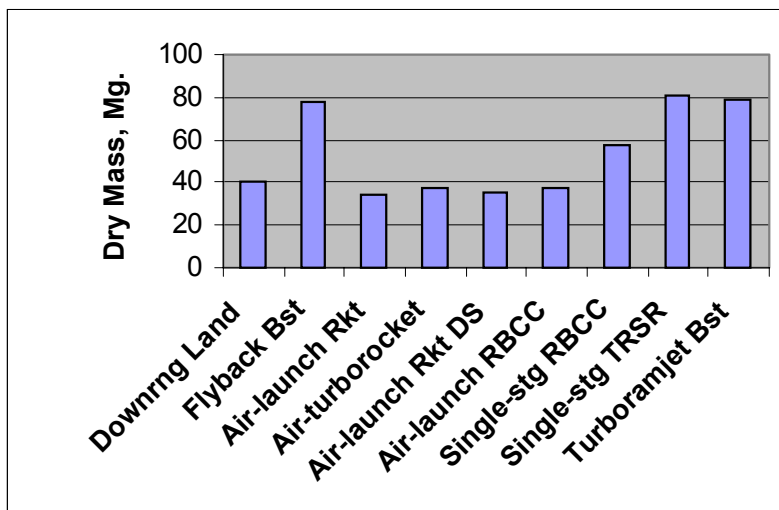


Figure 4-10: Dry Mass Comparison

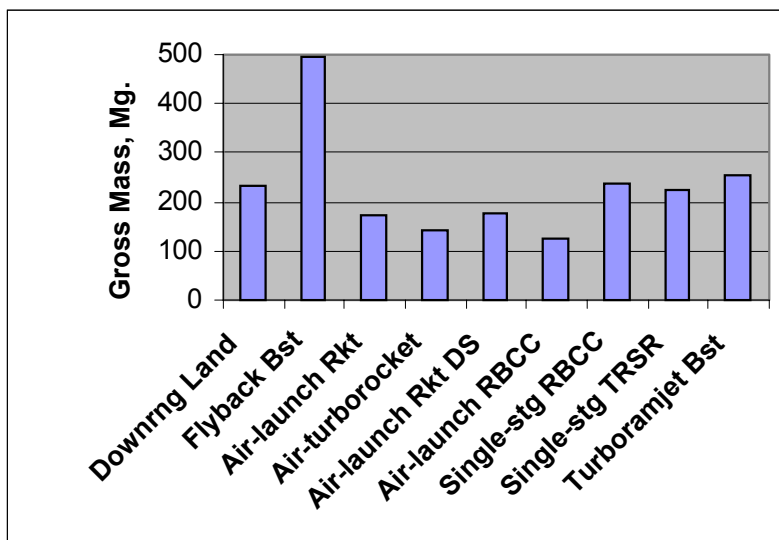


Figure 4-11: Gross Mass Comparison

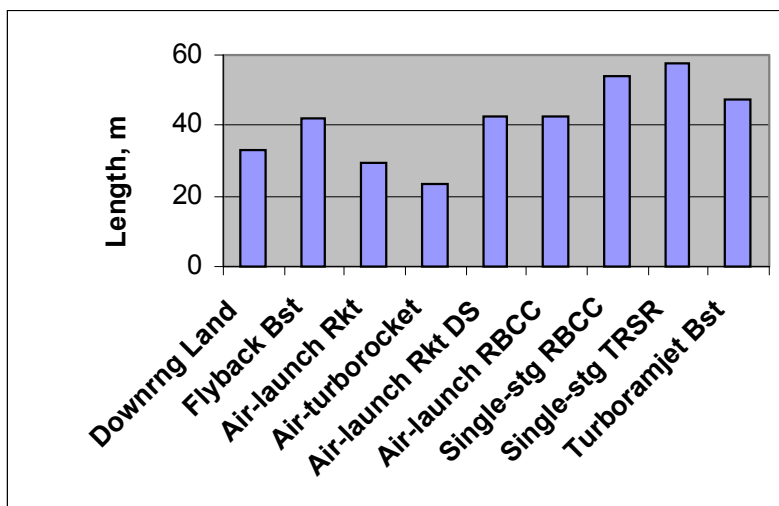


Figure 4-12: Length Comparison

### **Additional Effort on Air-Turborocket Concept**

After the initial work on several concepts, the air-turborocket concept was also evaluated using the Design-Sheet analysis. This additional analysis required more complete input for the air-turborocket, which was provided by Dr. John Bossard of CFD Research Corp., Huntsville, AL. The preliminary results indicated that the gross mass would be 151,000 kg, the dry mass would be 37,200 kg, and the length would be 38 metres. These results are comparable to the previous results and indicate that this concept is a reasonable choice.

### **Conclusions**

The most important conclusion of this effort is that rendezvous at Mach 17 and 150 km seems reasonable. Further work could show what rendezvous conditions optimize the launch vehicle and tether. Comparing the various concepts shows that air-launch with uprange cruise could be a good solution. Airbreathing propulsion on the hypersonic vehicle could be needed to keep the mass within the capability of existing airplanes. Comparing HASTOL to other launch concepts shows that HASTOL launch vehicles are much smaller than launch vehicles that must reach orbit. For the flight rates that would likely exist for HASTOL, fully-reusable launch vehicles would probably be the most economical solution.

## CHAPTER 5: TETHER BOOST FACILITY DESIGN

The following discussion describes an “operational” Tether Boost Facility that can successfully perform the following functions: housekeeping, ground communication, payload capture, payload toss, facility reboost, and communication (with a grapple assembly and/or the payload itself). The mass required for an operational Tether Boost Facility is too great to be launched within a single launch vehicle. Therefore, an operational Boost Facility will have to be designed for on-orbit assembly. The following discussion also describes a “Live” Facility that can perform the same functions as an operational Facility except for the payload capture and toss functions.

The suggested architecture is shown in Figure 5-1. This modular concept is based upon tether segment mass per unit length, tether segment taper, and tether segment diameters of the single tether design by TUI. Facility Mass Properties provide more details about the Facility mass breakout and estimated number of launches. A more precise estimate of tether segment lengths, their required taper, and resulting masses was calculated, and is detailed in Appendix G.

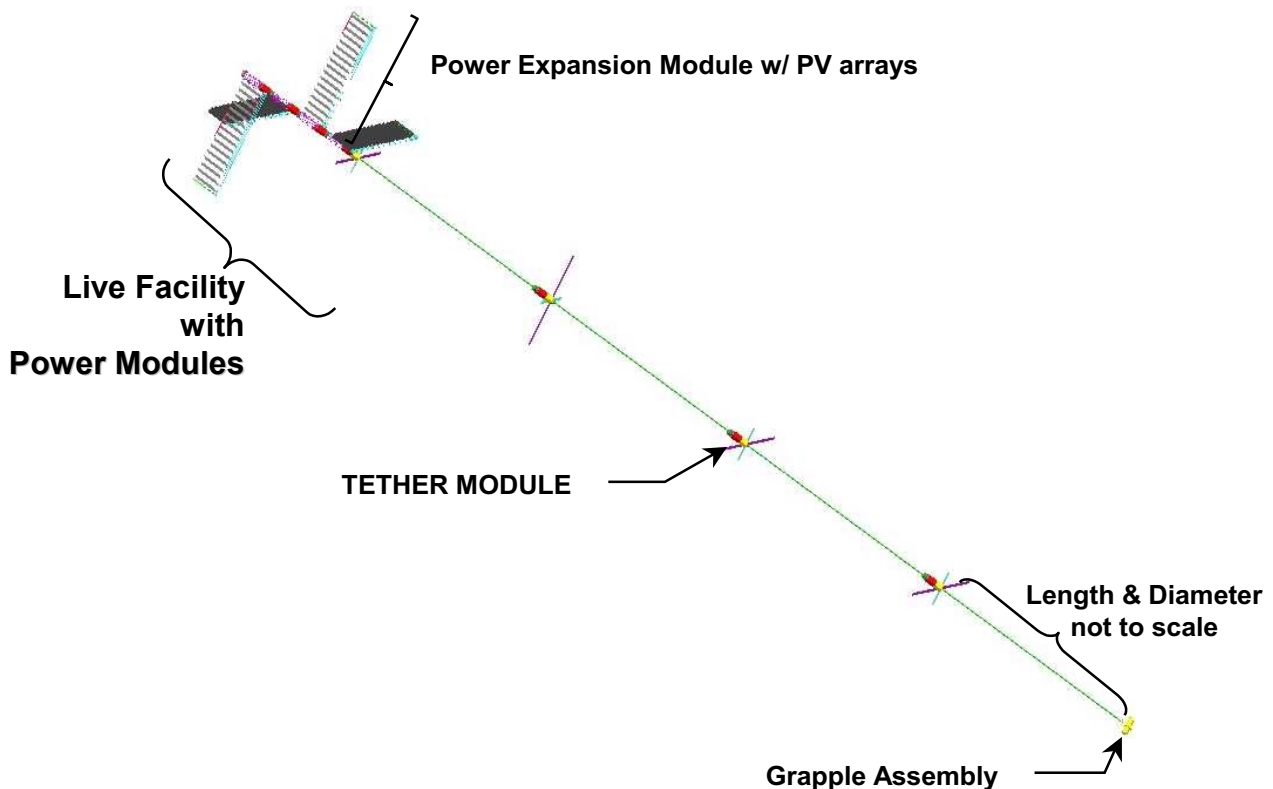


*Figure 5-1. Modular Boost Facility*

*Note: Tether diameter is shown grossly over scale and tether length between modules is shown under scale.*

In this modular concept, a “Live” Facility Module is launched first, with “Expansion Modules”, having common docking mechanisms, being launched at later dates. The initial Live Facility Module does not include a grapple assembly. The nadir end of the tether has one component of a docking assembly (a “node”). It does include on-board subsystems for Electrical Power (EPS), Guidance and Navigation (G&N), Command & Data Handling (C&DH), Attitude Determination & Control (ADCS), Communications (Comm), Tether Power (for Electrodynamic Reboost), and Tether Deployment/Control.

The subsequently launched Facility Expansion Assembly consists of two subassemblies: a Power Module and a Tether Module. After docking with the on-orbit Facility Module, the Tether Module separates from the Power Module subassembly. It then flies away to autonomously dock at the end of the Facility Module’s tether (which had a docking node at it’s end), and deploys it’s own Electrodynamic tether (which another docking node at it’s own end). Power/Tether Modules are added in this manner until the last Expansion Assembly is added. The last Expansion Assembly is launched with a grapple assembly on the end of it’s tether, to complete the fully operational Tether Boost Facility, with required mass and power generation capabilities.

The near term Delta IV Heavy launch vehicle was chosen as the maximum launch weight and size for facility components. Even though the Delta IV Heavy will provide higher launch weight than any launch vehicle readily available today, the HASTOL Facility will still need multiple flights to place the entire facility in orbit. The Delta IV payload weight and fairing dimensions were used as a sizing guide for HASTOL launches, to determine packaging and number of flights needed to place the complete facility in orbit.

### Facility Modularity

Figure 5-2 shows a close-up view of the initial “Live” Facility Module. The functions required for the first module include: housekeeping, ground communication, reboost, and communication with an automated docking system (common to all Expansion Modules). On-board satellite subsystems are housed in the Equipment Bay (illustrated in red). The Tether Subsystem Bay (in yellow) houses a separate tether power conversion unit, tether reel, boom actuator, and sensors.

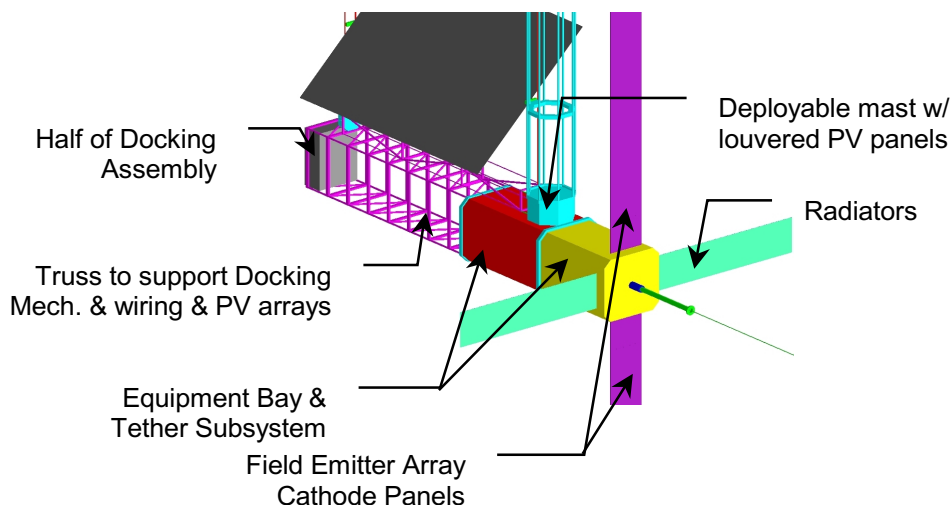


Figure 5-2. “Live” Facility Module



Plasma contactors are required because the tether is electrodynamic. The technology chosen for plasma contactors are the cathode panels of the field emitter array, which are lightweight and do not require any consumables for their operation. Deployed radiators are shown because the electrodynamic tether's power conversion unit is expected to produce a large amount of waste heat. The louvered solar panels will keep PV surface areas facing toward the sun as the Facility rotates. The truss provides adequate spacing between the on-orbit Module arrays and the arrays added on by later Power Modules. The truss also provides structure for mounting the docking node, as well as cable mounting surfaces and a stiff load path for Power Module docking.

### Power Expansion Module

The electrodynamic tether requires a significant amount of power to reboost the fully expanded Facility after a large payload has been tossed. The addition of Power Modules, as Figure 5-3 illustrates, increases the Facility Module's power generation capability.

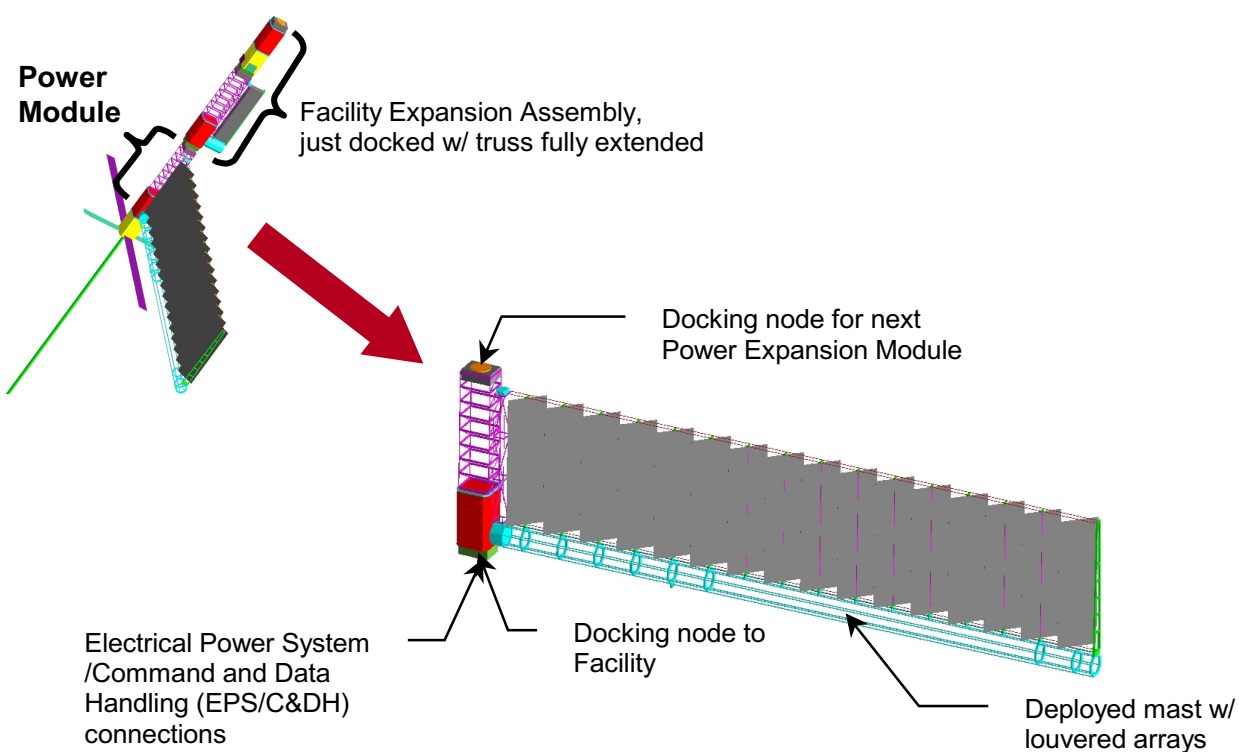


Figure 5-3. Power Expansion Module

Each Power Module consists of:

- An automated docking subsystem, with docking mechanisms, sensors, and related hardware, to attach itself to the Facility Module or a previously attached Power Module
- A deployable mast with louvered arrays
- An equipment bay, with EPS/C&DH connections to Facility Module EPS/C&DH subsystems
- A passive docking node, with EPS/C&DH connections for the next Power Module.

## Tether Module

The operational, electrodynamic Tether Module that the Facility requires is long and massive. Fifteen (15) Delta IV-H launches would be required to carry the wound tether mass (with reels) into orbit. Our current concept for sending this massive and very long tether into orbit is to assemble it on-orbit like the rest of the Facility (Figure 5-4). Each Tether Module consists of:

- A Reaction Control Subsystem, initially to transfer the Facility Expansion Assembly to its docking location, and then to transfer the Tether Module to its docking location
- A C&DH subsystem, to control the Facility Expansion Assembly flight and separation of the Tether Module from the Power Module, as well as other subsystem functions
- A docking subsystem to connect the Tether Module to the end of the Facility tether
- Tether deployment/control and tether power subsystems, to deploy an electrodynamic tether to extend the length of the main tether
- Radiators, plasma contactors (field emitter array cathode panels), and other materials to electrically isolate a clear path through the Module for electrodynamic tether operations
- Each Tether Module may carry equipment to relay its own position, and that of adjacent Tether Modules, to the Control Station at the end of the Facility, for large-scale control.

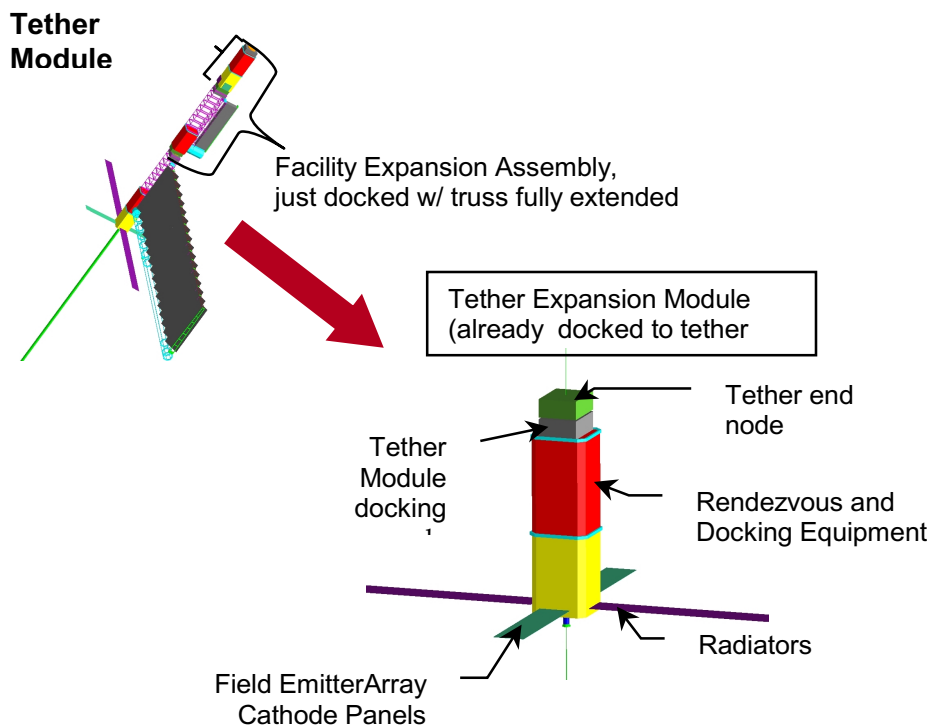


Figure 5-4. Tether Expansion Module

## Facility Mass Properties

The initial Live Facility mass is divided into allocations for subsystems in Table 5-1. Each Expansion Assembly will carry a large tether mass, but will have a similar percentage of its remaining mass in such subsystems. Table 5-2 shows that each of the modules can be launched with a single, eastward launch of a Delta IV-H expendable launch vehicle.

Table 5-1. Boost Facility Subsystem Mass Summary

Subsystems	% First Live Facility Mass
Thermal Control	10
Cabling/Harnesses	7
Structure	24
EPS and Tether Power	46
C&DH and Comm	1
G&N and ADCS	3
Tether Deployment and Control	7
Docking	2

Table 5-2. Modular Boost Facility Mass Properties

<b>DUE EAST LAUNCH, 350 KM CIRCULAR ORBIT AT 28-DEG INCLINATION</b>	<b>Mass (kg)</b>	<b>% Margin</b>
Delta IV-H Useful Load	23,768	
Delta IV Payload Adapter Fitting mass	386	
Delta IV-H Payload GLOW	23,382	
Expended Upper Stage Mass	3,467	
<b>First Launch Mass Estimate</b>		
1st Launch Mass (no growth margin):	16,290	
First tether section mass (5 km)	2,540	
Live Facility Mass (kg, No Margin)	13,750	
Available Launch Mass Margin	7,090	30%
On-Orbit Mass, 1st Launch, no margin	19,757	
<b>Next Launch Mass Estimate</b>		
Next Launch Mass (no growth margin):	17,770	
Next tether section mass (25 km)	12,700	
Tether Expansion Module Mass	5,070	
Available Launch Mass Margin	5,610	24%
<b>Last Launch Mass Estimate</b>		
Last Launch Mass (no growth margin):	19,850	
Next tether section mass (27 km)	13,720	
Grapple Mass	650	
Tether Expansion Module Mass	5,480	
Available Launch Mass Margin	3,530	26%
<b>Summary</b>		
Estimated # of Identical "Next" Launches between the 1st and Last Launch, not taking effects of margins into account	24	
Estimated Total # Launches	26	
Estimated total tether mass	323,244	
Estimated Final On-Orbit Mass (kg)	465,676	
Estimated mass impact of Tether Expansion Modules	138,315	

First Launch On-Orbit Mass = First Launch Estimated Launch Mass w/ Margin+ Expended Upper Stage  
 Available Launch Mass Margin = "Delta IV-H Payload GLOW" - "Launch Mass w/ Margin"

## Facility Subsystems

Several subsystems of the Tether Boost Facility require future advances in technology. The following subsystems are considered herein:

- Command and Data Handling (C&DH) and Telemetry
- Electrical Power Subsystem (EPS)
- Thermal Control
- Structure
- Interfaces
- Guidance Navigation and Control (GN&C) /Attitude Control

## Command and Data Handling / Telemetry Subsystems

The Command and Data Handling (C&DH) and Telemetry subsystems do not appear to be major design drivers at this time. Due to the vehicle rotation and long term reliability requirements, an active phased array antenna system may be needed for antenna pointing. Command and data handling is expected use new technology, with triple redundancy, for high reliability over 10 year mission. The Telemetry subsystem utilizes technology that will be available in the near-term.

## Electrical Power Subsystem

Electrical power is a key feature of the Control Station end of the Facility. Large power requirements infer large solar array panels and batteries. The Electrical Power Subsystem (EPS) has significant weight and lifetime issues, due to the large power requirements of the facility. Due to efficiency issues with the EPS system, thermal system maybe required to eliminate up to 40 kW of waste heat, which might require an active thermal control system for the batteries. Methods to recover the waste heat are being investigated, such as Stirling cycle engines.

The Electrical Power subsystem has several design drivers:

- High Voltage (20 kV at 10-20 Amps): This technology is needed for many space programs.
- Plasma Interaction: At 20 kV, plasma interaction is a significant concern.
- Inefficiencies: Loss & heat associated with DC/DC conversion losses and battery discharge
- Power switching systems: Even on the Earth, at 400kW, these are heavy and bulky.

## Power Generation

Highly efficiency concentrator arrays are necessary to minimize surface area and allow efficient radiation shielding A concentrator type solar array design was chosen; similar to the SCARLET design used on the Deep Space 1 mission. This design has several advantages, both economic and technical. Since the solar cells are only a small percentage of the solar array area (10-15% as opposed to ~95% for a normal planar array), thick radiation shielding becomes a viable option for the solar cells.

## Power Conversion

DC/DC conversion losses and battery discharge are a major issue for HASTOL Large conversion systems (e.g., Figure 5-5) tend to be heavy, and generate large amounts of waste heat. Even with efficiency of 96%, conversion losses result in significant thermal loads (e.g. 4% of 400 kW for an electrodynamic tether would be 16kW, which must be radiated as waste heat. Battery conversion losses are generally even higher, depending upon what type of energy storage system is utilized.

### **Power Storage**

Another other design driver is power storage. High-density lithium-ion batteries are the power storage baseline. The lithium ion chemistry is superior to present secondary battery storage technologies for the foreseeable future. To further reduce weight the Depth of Discharge was raised to 70%. Thus, to achieve the 10 year mission life an active thermal control system is required to maintain the batteries at approximately 20 degrees C. Flywheels hold promise for supplanting lithium ion batteries as the power storage baseline system. Dual, counter-rotating flywheels could also supplement or desaturate the flywheels/CMGs used for attitude control.

### **Thermal Control Subsystem**

Removing waste heat from the batteries and power conversion unit will be the main driver in thermal system sizing. This waste heat is expected to amount to 35 - 40 kW, in a fairly compact area. With current and near-term technologies, removal of this amount of heat from a limited area will require a fluid loop interfaced to a set of heat exchangers, interfaced to a set of radiators. As heat pipe technologies advance, they may offer a reasonable alternative in minimizing system complexity associated with the concentrated heat removal problem.

A further option under consideration is use of waste heat to drive a Stirling-cycle engine (secondary power generator). This alternative would reduce the amount of waste heat to be removed by radiators and would convert a large fraction of the waste heat into useful work to drive other subsystems. Stirling-cycle engines are currently being used in solar energy conversion projects, which should provide us with further insight into the reliability and life of the Stirling-cycle engine option.

### **Structure**

The Structural design does not appear to have any single large design drivers, although the sheer size, weight and rotational aspects may drive the use of more exotic design practices to meet the requirements without adding significant weight. In general, there are no major technology issues with rigid structures. The main configuration drivers are the Facility on-orbit expandability requirement, getting the required operational tether length on-orbit, and the yet-to-be explored configuration requirements of trying to electrically isolate a path between the ends of the electrodynamic tether being joined (with a Tether Module in between). Other configuration drivers are common to any spacecraft design and include finding acceptable launch configurations for assemblies to fit within the launch vehicle and CMG sizing. The tether itself may be considered to be a part of the structure, and in this context, the detailed structure and material properties of the "Hoytether" are areas where technology needs to be matured.

### **Interfaces**

The interfaces between adjacent Tether Boost Facility components are required for both the mechanical and electrical connections used in adding tether length in sections. Research in connection methods is a key requirement for future HASTOL development.

### GN&C/Attitude Control Subsystem

Current and future developments in GN&C sensors are expected to drive the size and mass of sensor units to extremely small values, thus the major driver in GN&C system sizing will be the reaction wheels or control moment gyros. The Guidance Navigation and Control (GN&C) /Attitude Control subsystem has a challenge in controlling such a large spinning platform, and a concern does exist about weight, control moment gyroscope (CMG) desaturation and control issues. Reaction wheels provide control torques by changing wheel speed, i.e., converting stored momentum into torque [ $T_j = d(h_j)/dt$ ]. Control moment gyros (CMGs, see Figure 5-5)) provide control torques by changing the direction of the wheel momentum vector (gyroscopic torque) and can provide more torque capability while requiring less power. Both reaction wheels and CMGs can provide large reservoirs of stored momentum, but the maximum reaction wheel torque available is severely limited by power considerations. An example:

$$\text{RW Power (@ 6000 rpm)} = 1300 \text{ watts @ 1 ft-lb or } 3900 \text{ watts @ 3 ft-lbs}$$

Typically, double-gimbal CMGs are used to control torque from 3 - 300 ft-lbs. Single-gimbal CMGs are used for applications requiring more than 300 ft-lbs. Skylab was designed to use two CMGs, each having a capability of +/- 160 ft-lbs. Skylab mass was 76,295 kg and design power with all solar panels working was 11 kW (average) for the entire system. Reaction wheels and CMGs usually require periodic desaturation, as system biases generally cause long-duration torque build up in one direction. Another source of control torque (e.g., RCS, or a secondary set of CMGs) might be needed to remedy this, or tether operations might be orchestrated to intentionally use gravity gradient torques to desaturate CMGs (for motions in the orbital plane).



Figure 5-5. Power conversion and control moment gyros are key technologies for HASTOL.

### Conclusions

The HASTOL facility is so massive that it could not to be launched in a single flight. Thus, the current design is modular, to add the tether and power generation equipment in sections. Many subsystem design issues need to be further characterized (mechanical and electrical connections in space, plasma interactions, etc.). HASTOL requires high power levels for electrodynamic tether reboost; even with future advancements in technology, this will result in a large, heavy power generation and storage subsystem.

## CHAPTER 6: CONCLUSIONS AND RECOMMENDATIONS

We have developed three primary conclusions as a result of our work:

1. HASTOL has large potential value to US government, industry, and citizens. HASTOL has the potential to substantially reduce future costs for launching government and commercial satellites into space. The surprising synergy of space tourism with momentum recycling means that HASTOL may make personal space travel a real, affordable proposition for many Americans. In the long term, a larger HASTOL system may greatly reduce the cost of human expansion into the solar system and may help build systems in space that send energy to Earth.
2. There are no fundamental technical show-stoppers for HASTOL. Several major technology challenges do, however, exist. The best currently available solutions to some of these challenges might fall short of the subsystem performance capabilities we have assumed here. Alternative approaches and technologies are possible, and we expect that workable solutions can be found in the future.
3. Substantial technology advancement is needed. HASTOL requires new or advanced technology in many areas. The years of technology development needed before HASTOL can be implemented imply that HASTOL is not currently a good target for private investment. Government investment is needed to develop the long-term value of HASTOL.

The remainder of this chapter describes the status of relevant technologies, the needs for technology development, and a recommended roadmap for meeting those needs.

### TECHNOLOGY READINESS LEVEL (TRL) ASSESSMENT

Technology readiness of each HASTOL subsystem was assessed using NASA's TRL scale, illustrated in Table 6-1. TRL scores were developed for today's technology and for two future dates: 2005, the earliest year in which HASTOL development might begin, and 2010, a more likely date for beginning of development (following a reasonably-paced technology development program). Tables 6-2 to 6-5 show the scores for subsystems of each HASTOL element. Where the TRL is predicted to increase over the 2001-2010 interval, the table includes a reference to the planned or ongoing activity that will raise the technology level. Table 6-7 shows TRL scores for some challenges that arise from integrating the elements into a single system.

*Table 1. Definitions of NASA Technology Readiness Levels*

<b>Technology Readiness Levels (TRL)</b>	
9	Actual system "flight proven" through successful mission operations.
8	Actual System completed and "flight qualified" through test and demonstration.
7	System prototype demonstration in an operational environment.
6	System/subsystem model or prototype demonstration in a relevant environment.
5	Component and/or breadboard validation in a relevant environment.
4	Component and/or breadboard validation in a laboratory environment.
3	Analytical and experimental critical function and/or characteristic proof-of-concept.
2	Technology concept and/or application formulated.
1	Basic principles observed and reported.

Table 6-2. TRL assessments for Control Station subsystems

<b>CONTROL STATION</b>	<b>TRL Today</b>	<b>TRL 2005</b>	<b>TRL 2010</b>	<b>Comments</b>
<b>Communications Subsystem (CS)</b>	<b>7</b>	<b>8</b>	<b>8</b>	
- Comm net Antenna, Transmitter, Receiver	7	8	8	
- Downlink Antenna, Tx, Rcvr	8	8	8	
<b>Attitude and Location Determination /Control Subsystem (ALDCS)</b>	<b>5</b>	<b>5</b>	<b>5</b>	
- GPS Antenna, Receiver	7	7	7	Today's TRL due to S/W
- Attitude Stabilization	6	6	6	Large CMGs needed. ISS size or bigger
- Software	5	5	5	Relevant algorithms used in flight
<b>Electrodyn. Tether Subsystem</b>	<b>4</b>	<b>5</b>	<b>6</b>	
- Power Converter (high voltage/high power), Power Controller	5	5	6	High power: ISS, high voltage: electric propulsion = Today's TRL, with growth
- Plasma Contactor (FEAC or similar needed)	4	5	6	Plasma contactor -ProSEDS/ISS in flight, FEAC unit in development
- Tether Dynamics Control System	4	7	8	ProSEDS/Terminator Tether/ $\mu$ PET/MIR for 2005 TRL; MIR for TRL 2010
<b>Mechanical Subsystem (MS)</b>	<b>7</b>	<b>7</b>	<b>7</b>	
- Facility Structures	7	7	7	No unusual structural challenges
- Erosion Protection	7	7	7	Similar to ISS
- Micrometeoroid Protection	7	7	7	Similar to ISS
<b>Thermal Control Subsystem (TCS)</b>	<b>6</b>	<b>6</b>	<b>6</b>	
- Temp Sensors	7	7	7	
- Heaters	7	7	7	
- MLI, Radiators	6	6	6	Higher power than previously done, but similar to ISS
<b>Electrical Power Subsystem (EPS)</b>	<b>5</b>	<b>6</b>	<b>6</b>	
- Solar Collectors/Drive Motors	6	6	6	SCARLET arrays = Today's TRL
- Sun Angle Sensor	8	8	8	
- Pwr Mgt Unit	5	6	6	More power than anything done to date. Other system on the drawing board such as SpaceBased Radar. Laser, Solar Power, etc.
- EPS Control Processor				
- Battery Charger				
- Power Regulator				
- Power Distributor				
- Batteries	6	8	8	Li Ion batteries in use today, higher end units needed should be ready by 2005
- Software	5	6	6	
<b>Cmd and Data Handling</b>	<b>6</b>	<b>6</b>	<b>7</b>	<b>Some autonomy with ground assist</b>
- Computer	7	8	8	
- TLM Mux/Demux	7	8	8	
- Software	6	6	7	
- Operating System				
- Applications	6	6	7	
- Orbital Mechanics				
- Equipment Control				
<b>Networks Subsystem (NS)</b>	<b>8</b>	<b>8</b>	<b>8</b>	
- Power Cables				
- Data Cables				
<b>Retrieval,Deployment and Spin Control</b>				
- Winch, winch motor, traction drive, motors and controller	6	6	6	TSS = Today's TRL
- Tether cutter	7	7	7	
- Tether deploy speed sensor	6	6	6	
- Tether deployed length sensor	6	6	6	
- Tether fully deployed sensor	6	6	6	
- Tether tension sensor	6	6	6	
- Tether impact detector	6	6	6	
- Separated tether detector	6	6	6	
- Tether departure angle sensor	6	6	6	
- Tether position sensor	6	6	6	



Table 6-3. TRL assessments for Grapple Assembly subsystems

	TRL Today	TRL 2005	TRL 2010	Comments
<b>GRAPPLE ASSEMBLY</b>	<b>2</b>	<b>3</b>	<b>3</b>	<b>Concept not fully defined</b>
<b>Communications Subsystem (CS)</b>				
- Comm net Antenna, Transmitter,	7	8	8	
<b>Attitude and Location Determination /Control Subsystem (ALDCS)</b>	<b>6</b>	<b>7</b>	<b>7</b>	<b>Similar to existing space flight vehicles</b>
- GPS Antenna, Receiver				
- Attitude Stabilization Software				
<b>Mechanical Subsystem (MS)</b>	<b>7</b>	<b>7</b>	<b>7</b>	<b>Similar to existing space flight vehicles</b>
- Facility Structures				
- Erosion Protection				
- Micrometeoroid Protection				
<b>Thermal Control Subsystem (TCS)</b>	<b>7</b>	<b>7</b>	<b>7</b>	<b>Similar to existing space flight vehicles</b>
- Temp Sensors				
- Heaters				
- MLI, Radiators				
<b>Electrical Power Subsystem (EPS)</b>	<b>5</b>	<b>8</b>	<b>8</b>	
- Solar Collectors	5	8		Current effort on quad-junction cells = 2005
- Sun Angle Sensor	8			
- Pwr Mgt Unit	7	8	8	
- EPS Control Processor				
- Battery Charger				
- Power Regulator				
- Power Distributor				
- Batteries	8	8	8	
- Software	6	8	8	
<b>Cmd and Data Handling</b>	<b>6</b>	<b>6</b>	<b>6</b>	
- Computer	7	8	8	
- TLM Mux/Demux	7	8	8	
- Software	6	6	6	Need to modify existing flight
- Operating System				
- Applications				
- Orbital Mechanics				
- Equipment Control				
<b>Networks Subsystem (NS)</b>	<b>8</b>	<b>8</b>	<b>8</b>	
- Power Cables				
- Data Cables				
<b>Proximity Sensing</b>	<b>4</b>	<b>7</b>	<b>7</b>	
LIDAR	4	7	7	STS demos = 2005
Radar	6	7	7	
<b>P/L Capture/Release Device</b>	<b>2</b>	<b>3</b>	<b>3</b>	HASTOL Phase II = 2005 TRL
<b>Differential GPS (Beacon)</b>	<b>4</b>	<b>7</b>	<b>7</b>	ProSEDS success = 2005 TRL

Table 6-4. TRL assessments for Payload Accommodation Assembly subsystems

<b>PAYLOAD ACCOMMODATION ASSEMBLY</b>				
	<b>TRL Today</b>	<b>TRL 2005</b>	<b>TRL 2010</b>	<b>Comments</b>
<b>Communications Subsystem (CS)</b>				
- Comm net Antenna, Transmitter, Receiver	7	8	8	
<b>Attitude and Location Determination /Control Subsystem (ALDCS)</b>				
- GPS Antenna, Receiver				
- Attitude Stabilization Software				
<b>Mechanical Subsystem (MS)</b>				
- Facility Structures				
- Erosion Protection				
- Micrometeoroid Protection				
<b>Thermal Control Subsystem (TCS)</b>	7	7	7	
- Temp Sensors				
- Heaters				
- MLI, Radiators				
<b>Electrical Power Subsystem (EPS)</b>	6	6	6	
- Sun Angle Sensor	8	8	8	
- Pwr Mgt Unit	7	8	8	
- EPS Control Processor				
- Power Regulator				
- Power Distributor				
- Batteries	8	8	8	
- Software	6	6	6	
<b>Cmd and Data Handling</b>	2	3	3	
- Computer	7	8	8	
- TLM Mux/Demux	7	8	8	
- Software	2	3	3	Develop new algorithms
- Operating System				
- Applications				
- Orbital Mechanics				
- Equipment Control				
<b>Networks Subsystem (NS)</b>	8	8	8	
- Power Cables				
- Data Cables				
<b>Proximity Sensing</b>				
LIDAR	4	7	7	STS demos = 2005 TRL
Radar	7	7	7	
<b>Passive Reflectors</b>	8	8	8	
<b>Docking Adapter</b>	2	3	3	HASTOL Phase II = 2005 TRL
<b>Differential GPS (Beacon)</b>	4	7	7	ProSEDS success = 2005 TRL

Table 6-5. TRL assessments for Tether subsystems

<b>TETHER</b>	<b>TRL Today</b>	<b>TRL 2005</b>	<b>TRL 2010</b>	<b>Comments</b>
<b>Mechanical Subsystem (MS)</b>				
- Survivable Tether Structure	4	5	5	Terminator Tether = 2005 TRL
- Tether Material(s)	7	7	7	TiPs/SEDS = Today's TRL
- Erosion Protection (AO & UV)	5	5	5	Tests at MSFC = Today's TRL
<b>Electrodynamic Tether</b>				
- Bare Wire Anode	5	7	7	ProSEDS = 2005 TRL
- High Voltage Insulation	4	4	4	

Table 6-6. TRL assessments Earth to Near LEO Payload Carrier

<b>Earth to near LEO payload carrier</b>	<b>TRL Today</b>	<b>TRL 2005</b>	<b>TRL 2010</b>	<b>Comments</b>
<b>Software - Algorithms</b>	3	5	6	SLI and rendezvous experiments in work
<b>Flight System</b>	2	2	2	Several X vehicles in development

Table 6-7. TRL assessments for HASTOL Integration technologies

<b>INTEGRATION</b>	<b>TRL Today</b>	<b>TRL 2005</b>	<b>TRL 2010</b>	<b>Comments</b>
<b>Software - Algorithms</b>	4	5	5	HASTOL Phase II = 2005 TRL
<b>System</b>	2	2	2	

Many HASTOL subsystems or components are easily within the reach of today's technology. Communications, computing hardware, most structures, and many of the sensors will require little or no improvement. TRLs for these subsystems range from 6 to 8. TRL 6 indicates that the technology is ready to be implemented in a component for the objective system. TRL 8 indicates that a working product exists that could be plugged directly into the objective system with no development effort.

Some HASTOL subsystems face requirements that are similar in quality but much greater in quantity than today's systems. Examples are electric power management, power conversion, and thermal control. Each of these must handle many hundreds of kilowatts of power - an order of magnitude increase above current technology. TRLs for these subsystems are typically 4 or 5.

The power conversion system for the electrodynamic tether faces the additional challenge of working with unusually high voltage as well as high power.

The flight control subsystems of various HASTOL elements face qualitatively different requirements than previous flight control systems. Previous spacecraft have not had to control their attitude or position while attached to a long, flexible tether that exerts considerable force and is as massive as the spacecraft. Orbital mechanics codes must contend with a spacecraft whose mass is so widely distributed that orbital speed varies appreciably as the system rotates. The magnitude and direction of electrodynamic thrust vary as the local magnetic field and plasma density change, so trajectory planning requires more flexibility than systems that use well-defined rocket firings. All of these challenges can be solved, but they have not been solved yet, or tested in flight. The TRL for flight control is 3.

Another area with qualitatively new requirements is erosion protection for the tether itself. The preferred tether structural material is Spectra 2000. Tests at MSFC suggest that Spectra is susceptible to rapid erosion by atomic oxygen (and, potentially, degradation by ultra-violet (UV) light). Coatings are currently used to protect surfaces on other spacecraft from atomic oxygen and UV, but unlike those surfaces, the tether will stretch and bend. It is unknown whether any existing coatings will adequately adhere to Spectra through many stretching cycles, and if so, how they might affect the overall strength to mass ratio of the tether system. Erosion protection for the high-voltage insulation around an electrodynamic tether faces similar issues and is similarly undefined. Erosion protection for both the tether structure and the current-carrying component are considered to have a TRL of 2.

Three HASTOL subsystems defined at the concept level currently rate a TRL of 2. These are the grapple mechanism, the collision avoidance subsystem, and the Earth to near LEO payload carrier. The HASTOL rendezvous and capture simulation has helped define requirements for a grapple system, and our analytical work bring us closer to a grapple TRL of 3. The collision avoidance subsystem covers ground elements as well as flight elements, but the key challenge is a flight issue: maneuvering the tether system to avoid a predicted collision or close approach. Current spacecraft have only one reasonable approach to collision avoidance: change the spacecraft's trajectory to provide a safe miss distance. In most cases, a tether can use at least four approaches: change trajectory, change rotation rate or phase, change tether attitude (e.g. change libration angle or phase), or change tether shape (e.g. induce a bending motion different from the bend due to ED thrust.) Beyond defining these options, no development has yet occurred in collision avoidance technology for tethers. The payload carrier concept is based on several X-plane concepts. Some, like X-37 are proceeding to a flight test stage, however it remains unclear if any of the present X-plane concepts can grow to meet our payload carrier requirements.

#### TECHNOLOGY NEEDS

Some of the technologies needed for HASTOL are likely to be developed for other space applications. High-power electrical systems and heat rejection systems are the subject of a new technology project sponsored by the Air Force Research Lab. Development of Field Emitter Array Cathodes, our preferred choice for plasma contact technology, is underway at JPL. It is unclear whether these efforts will succeed and whether they will be demonstrated in flight.

Areas where technology development must be planned specifically for a tether system include:

**Rendezvous and capture.** Simulation work in the HASTOL program has raised this technology to TRL 3. Hardware tests and demonstrations are needed for higher levels. A thorough flight test would include a variety of sensors, beacons, and thrust modes. This variety would allow several different rendezvous and capture techniques to be raised to TRL 5 or 6 and would provide data by which to compare their performance.

**Flight control.** This technology is especially needed for electrodynamic (ED) propulsion. A ED flight control system must contend with variations in the geomagnetic field and in plasma density, factors that make ED thrust much less predictable and less controllable than conventional propulsion. The ED thrust direction depends on the tether's orientation and curvature. Like conventional propulsion, ED thrust can modify the system's trajectory, change its rotation rate or phase, or influence its attitude. In addition, ED thrust will change the tether's shape - an issue not addressed at all by previous flight control methods.

To bring tether flight control to TRL 6 requires flight demonstration. The demonstration should use ED thrust and/or tether pumping to perform controlled changes in all orbital elements; in rotation rate and phase; in libration amplitude and phase; and in tether shape (fundamental mode amplitude and phase, at a minimum). It should demonstrate these in an orbit that is eccentric enough to take the tether from a strong thrust region to a zero-thrust region (e.g. 2000 km).

**Collision avoidance.** Collision avoidance is a demanding application of flight control. All the flight control capabilities listed above may be used. In addition, collision avoidance requires a timely flow of information from a satellite tracking system to a decision making system and then to the flight control system. Raising tether collision avoidance to TRL 6 could be accomplished without performing collision avoidance against real threats. Rather, the satellite tracking system would report realistic simulated threats to the decision-making system. The decision system prioritizes each threat, chooses an avoidance strategy, and sends appropriate commands to the flight control system of a real tether in flight. The tether's motion is then monitored to assess whether it would have avoided each threat, had the threat been real.

**Erosion protection.** A ground-based program is needed to identify and characterize coatings that adhere well to Spectra or to insulation while being stretched, bent, heated, cooled, and exposed to atomic oxygen and ultraviolet. This ground-based effort can reach TRL 4. When promising materials are identified, they would be tested on a pallet attached to Space Station or Shuttle. The pallet would provide bending and stretching forces and temperature control. This experiment would bring erosion protection to TRL 5. A subscale tether with samples returned to Earth for analysis would be needed to reach TRL 6. Such an experiment could be attached to Space Station, Shuttle, or some unmanned re-entry system.

**High-voltage, high power conversion.** Components of this technology may be separately developed and demonstrated before an integrated, operational high-voltage, high power system is demonstrated. A tether-oriented program might do a separate short-duration demo of high-voltage, high power conversion itself. This would run for only a few seconds at a time, demonstrating that the requisite voltage and power can be handled safely. The short run time would prevent heat from building up catastrophically. It would use stored energy, so PV arrays need not provide hundreds of kW. (The energy storage system would have to provide hundreds of kW for a few seconds.) Such a demo done in space could bring the conversion technology by itself to TRL 6. However, an integrated, continuously running system for power conversion

would only reach TRL 5 (component validation in a relevant environment). To reach TRL 6 would require flight demonstration of an integrated, continuously running system.

**High-power plasma contact with FEAC.** A technology demonstration program for FEACs must address two issues: high-power performance and lifetime. We can define a demo that addresses both issues economically. For high-power performance, the issue is how well the large FEAC array contacts the ionosphere. That can be measured with a run time of a few seconds. A brief test like this could use stored energy and could end quickly enough that heat buildup is not catastrophic. (Obviously this test would be synergistic with the brief power conversion demo outlined above.) To measure lifetime, the same hardware could run for months or years at low power with all the current going through a single FEAC rather than the large, high-power array. This test would use PV arrays for power and would provide modest cooling. The combination of the high-power test and the lifetime test would bring high-power FEAC technology to TRL 6.

**HASTOL ROAD MAP**

The road map in Figure 6-1 identifies the needed space flight experiments that have happened to date and the ones required to support a HASTOL development effort. In addition the space flight experiments, extensive ground-based simulation is needed via computers and test facilities, such as the MSFC Flight Robotics Laboratory. For example, it is anticipated the extensive models will be tested for simulated rendezvous and docking at the flat floor test facility, within the MSFC Flight Robotics Laboratory.

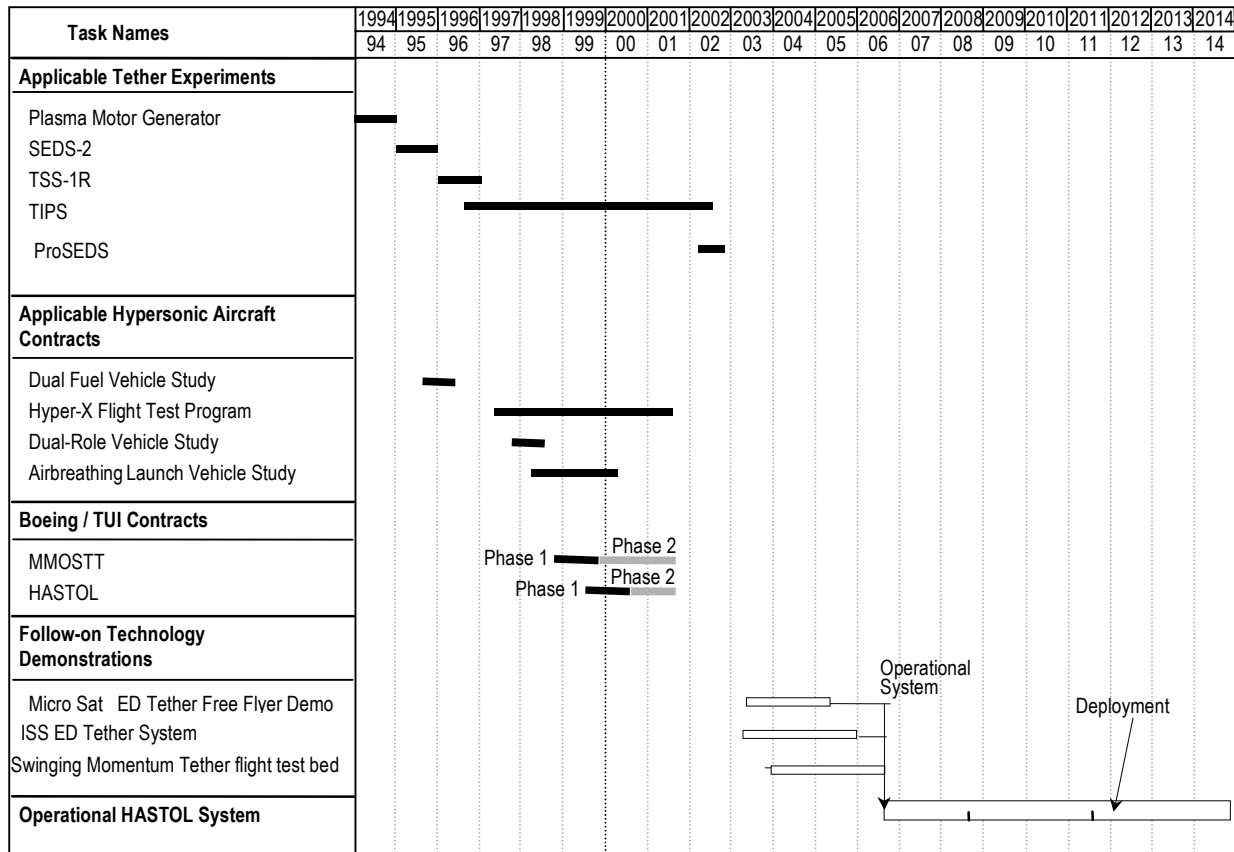


Figure 6-1. HASTOL technology roadmap.

A minimum of two flight demonstrations are required for a HASTOL proof of concept demonstrations. One flight demonstration would test electrodynamic propulsion, as well as the swinging, then spinning up, of tether rotation from an initial gravity gradient orientation. The second experiment tether platform would demonstrate capture and release of a payload. The first phase is a simple release of a payload launched with the tether platform. The second phase is to attempt capture and subsequent release, with the tether platform in a gravity gradient orientation. The third phase involves spinning up the tether platform and attempting capture and release using a spinning tether. If other space-based tether programs (i.e., the ISS electrodynamic tether effort) do not proceed, additional space flight experiments may be needed for HASTOL. As a minimum, the two planned space flight experiments will be necessary, to demonstrate long term operations and thus longevity of electrodynamic tethers in space for momentum exchange.





## APPENDICES

A number of separate analyses are documented in this Final Report as Appendices. The following section summarizes the analytical appendices that are attached in the following pages.

### **Appendix A: Rendezvous Speed Trade Study:**

TUI performed a trade study using calculations to examine the effect of increased apogee speed and altitude available from the Gryphon™ two-stage reusable launch vehicle concept, invented by the consortium of The Boeing Company and Andrews Space and Technology, Inc.. Gryphon™ would use a modified Boeing airplane as a first stage and an Andrews S&T liquid oxygen/liquid hydrogen rocket as the second stage, with the liquid oxygen being manufactured in mid-air from liquid hydrogen carried by the Boeing airplane. These analyses are documented in the attached Appendix A.

**Appendix B: Tether Boost Facility Mass vs. Tether Length:** We also explored the variations in the HASTOL Tether Boost Facility parameters as a function of the length of the tether, for a single point case where the Tether Boost Facility was able to deliver the payload into a Geosynchronous Transfer Orbit (GTO) with an apogee at the 35,786 km altitude of Geosynchronous Earth Orbit (GEO), under the nearly ideal rendezvous conditions of a velocity of Mach 19 and an altitude of 150 km. We found that tethers shorter than 450 km have high acceleration levels at payload pickup due to their short length, and slightly larger tether masses due to their higher tip speeds, while tethers longer than 1000 km begin to increase rapidly in tether mass due to the increased gravity gradient forces on the longer length. A tether length of about 600-900 km was found to be close to optimum, with the longer lengths and their lower pickup accelerations preferred for "tourist" traffic. The results of this study can be found in Appendix B.

**Appendix C: Tether Boost Facility Mass vs. Control Station Mass:** Variations in the HASTOL Tether Boost Facility total mass were assessed as a function of the mass of the Tether Central Station (TCS), including any ballast mass. We carried out a number of simulation runs at 110 km rendezvous altitude with both high (Mach 17) and low (Mach 12) rendezvous velocities, and high safety factor and low safety factor tethers, which produced total facility masses ranging from 28 to 338 times the payload mass. The total Tether Boost Facility mass was found to decrease slowly as the TCS mass decreased, with the minimum total mass occurring when the TCS mass was negligible. The tether tip acceleration level, however, increased as the TCS mass decreased, becoming significantly larger as the TCS mass dropped below 10 times the payload mass. The optimum TCS mass was determined to be the mass of all the useful equipment that would be needed in the TCS for a given operational scenario, with no additional ballast mass being used unless it cost nothing to install on the TCS. For the purposes of further HASTOL simulations, we usually assumed a TCS mass of 10 times the payload mass. The results of this study can be found in Appendix C.

**Appendix D: Tether System Mass vs. Payload Initial Velocity:** We also assessed variations in the HASTOL Tether Boost Facility mass and orbital parameters as a function of the initial payload velocity at the time of rendezvous of the payload with the tip of the tether. We did the

analysis for two different tether safety factors (design tensile strength) and two different initial payload altitudes. We first found that the HASTOL system is "over-capable", in that it nearly always throws the payload into its final transfer orbit with too high a velocity. Most simulation runs ended up with the payload on an escape trajectory from Earth. This is a "problem" if the final payload apogee is GEO, but is desirable for sending payloads to the Moon, Mars, and elsewhere. This final velocity "problem" can be solved in a number of different ways, which will be discussed in later simulations. It did NOT have a significant affect on these analyses, since the total mass of the Tether Boost Facility is predominantly determined by the rendezvous parameters, not the toss parameters. The total mass ratio of the Tether Boost Facility was found, as expected, to decrease as the tether material "design" tensile strength increased, and to decrease as the difference between the initial payload velocity and the initial perigee orbital velocity of the Boost Facility decreased. In general, we found that the total mass ratio of the Boost Facility was less than 100 times the payload mass when the initial payload velocity was above Mach 15. For velocities below Mach 15, the total mass ratio of the Boost Facility increased rapidly, becoming larger than 300 for Mach 12 and below.

Increasing the initial payload altitude from 110 km to 185 km only decreased the total mass ratio numbers by about 10%. Accordingly, we determined that it is more important for the hypersonic vehicle to operate at higher speed than at higher altitude, provided it is outside the atmosphere (>80 km) so that the tether doesn't overheat during the rendezvous and pickup.

These simulation runs have concluded that a HASTOL Architecture design with a reasonable total facility mass ratio (less than 100 times the payload mass) requires:

- (1) Hypersonic vehicles with >Mach 12 velocity at >80 km altitude.
- (2) Tether materials with higher ultimate tensile strength.
- (3) Tether structure designs that allow the use of lower engineering safety factors.
- (4) Phased tether rotations and orbits to insure the tether tip altitude is always >80 km.
- (5) Methods of operating the Tether Boost Facility to minimize tether stress.

The results of this study can be found in Appendix D.

**Appendix E: Rendezvous and Capture Simulations** A 6-DOF simulation of the hypersonic airplane was developed to test various methods for rendezvous with the tether facility and capture of the payload by the grapple assembly. The simulation includes modules for the airplane guidance algorithms and processor. These modules use data from modules that simulate the performance of several types of rendezvous sensors: active Ka band radar, passive radar receiver, GPS and DGPS receiver, and laser range finder. Some of the sensor modules interact with other modules representing beacons on the tether: interactive radar beacon, continuous radar beacon, GPS receiver and comm link, and laser reflector.

This simulation allows us to measure R&C performance under a variety of conditions: different aircraft actuators, algorithms, and sensor suites, together with variable atmospheric conditions. The dispersion of position, orientation, and velocity relative to the grapple assembly sets requirements for the grapple mechanism, e.g. if the dispersion in position is large, then the grapple mechanism must have a long reach.

**Appendix F: HASTOL Tether Boost Facility Sizing Spreadsheet Tool - Iteration 2:** As part of our initial HASTOL activities, Dr. Hoyt created a spreadsheet-based analysis tool for designing HASTOL tether facilities. This initial tool assumed that the mass of the payload was 15,000 kg, the payload capacity of the Boeing DF-9 Hypersonic Airplane concept. This spreadsheet tool was used to analyze the sizing of the Tether Boost Facility, and determine that it was technically feasible to build an orbiting rotating Tether Boost Facility whose grapple tip end could match speed and altitude with a Mach 18 Hypersonic Airplane at an altitude of 120 km. Our initial analyses estimated that Tether Boost Facility mass would be over 100 times the mass of the payload to be lifted by the Tether Boost Facility.

One of the first tasks undertaken in the Phase II contract was to carry out optimization analyses of the Tether Boost Facility, using the HASTOL Tether Boost Facility worksheet developed by Dr. Hoyt of Tethers Unlimited, Inc. These were done for a number of different scenarios, with the objective of minimizing the Tether Boost Facility total mass ratio with respect to the payload mass being boosted. The Excel spreadsheet tool for HASTOL Tether Boost Facility design was revised to fit the new requirements selected for the HASTOL tether facility:

- Payload mass of 5,500 kg.
- Trajectories of the hypersonic airplane and tether facility are in Earth's equatorial plane.
- Payload is picked up from a hypersonic airplane at 150 km altitude.
- Speed of hypersonic airplane is 5,110 km/s relative to inertial frame (Mach 16).
- Payload is tossed into a Geostationary Transfer Orbit (GTO).
- Tether Boost Facility orbit after payload toss does not drop below 80 km altitude.
- Nominal acceleration level on payload while attached to tether is ~1.5 g.
- Peak acceleration level on payload is 3 g.
- Facility is reboosted back to original orbit within 1 month.

An Excel spreadsheet tool for the HASTOL Tether Boost Facility design meeting the above requirements was developed using the momentum exchange electrodynamic reboost tether design Excel worksheet developed previously by TUI. This worksheet uses Keplerian orbital dynamics equations, a stepwise-tapered model of the tether mass, and an iterative solver to determine a tether facility design. Electronic copies of the Excel Worksheet may be obtained via email from Dr. Robert P. Hoyt of TUI at <hoyt@tethers.com>.

### **Appendix G: Modular Design of a Tether Boost Facility**

To minimize the development and deployment costs of a HASTOL tether facility, the system should be designed so that it can be constructed of a number of essentially identical components. In the May-June 2001 time period, we considered several approaches to modular construction of the tether system, including:

- Deploying an initial full-length but "thin" tether facility with a low load capacity, then launching identical full-length thin tether facilities, which are ganged together in parallel with the initial facility to increase the total load capacity of the combined facility;
- Deploying an initial launch facility, then attaching additional power modules to the control station and attaching additional lengths of tether in series and parallel;
- Deploying an initial launch facility, then launching multiple nearly-identical tether facilities and combining them in series with the initial launch facility to create a longer, more capable tether with power/control stations spaced along the tether.

After evaluating these options, we concluded that the third method would likely provide the best solution because it will minimize the complexity of assembling the components and because spacing the power stations along the length of the tether will reduce the maximum voltages that must be applied to the tether. Further details can be found in Appendix G, which describes a Tether Boost Facility concept which is designed to be built modularly. The first component deployed would be a 100-km-long, fully operational Tether Boost Facility capable of boosting to Geosynchronous Transfer Orbit (GTO) 2,500-kg payloads that are already in low Earth orbit. Subsequent modules would add tether length and power modules to increase the system capabilities so the facility can boost payloads up to 5,500-kg in mass from suborbital trajectories into various orbits. A total of 20 launches would create a 636-km-long Tether Boost Facility able to pick up 5,500-kg payloads from an Reusable Launch Vehicle (RLV) flying at Mach 17 at 150 km altitude, and either lift the payloads into Earth orbits or boost them to GTO.

#### **Appendix H: Estimate of Avoidance Maneuver Rate for HASTOL Tether Boost Facility**

The Hypersonic Airplane Space Tether Orbital Launch (HASTOL) Tether Boost Facility will have a length of 636 km. Its center of mass will be in a 604 km by 890 km equatorial orbit. It is estimated that by the time of the start of operations of the HASTOL boost facility in the year 2020, there will be 500 operational spacecraft using the same volume of space as the HASTOL facility. These operational spacecraft would likely be made inoperative by an impact with one of the lines in the multiline HASTOL Hoytether™ and should be avoided. There will also be non-operational spacecraft and large pieces of orbital debris with effective size greater than five meters in diameter that could cut a number of lines in the HASTOL Hoytether™, and should also be avoided.

In July 2001 we carried out a study of the number of times per year that the HASTOL Tether Boost Facility will need to take avoidance maneuvers in order to avoid these objects. It was estimated, using two different methods and combining them, that the HASTOL facility will need to make avoidance maneuvers about once every four days if the 500 operational spacecraft and large pieces of orbital debris greater than 5 m in diameter, were each protected by a 2 km diameter miss distance protection sphere. If by 2020, the ability to know the positions of operational spacecraft and large pieces of orbital debris improved to allow a 600 m diameter miss distance protection sphere around each object, then the number of HASTOL facility maneuvers needed drops to one every two weeks. This paper was submitted for presentation and publication in the Proceedings of Space Technology and Applications International Forum (STAIF 2002) to be held in Albuquerque, New Mexico from 3-7 February 2002, and can be found in this report at Appendix H.

#### **Appendix I: HASTOL Tether Boost Facility Module Replacement Rate Due to Space Impactor Cuts**

The baseline Hypersonic Airplane Space Tether Orbital Launch (HASTOL) Tether Boost Facility will likely be constructed in modular fashion, with each module containing a solar power module and a tether deployer containing a Hoytether™ with line diameters determined by the stress that needs to be handled by the tether at that position of the module on the Boost Facility, and with a length that allows the tether to fit inside the fixed 20 m<sup>3</sup> volume of the standardized tether deployer in the module. In August 2001 we carried out an analysis which calculates the long term effect of multiple cuts by small orbital debris and micrometeorite impactors of the line

segments in the failsafe Hoytether™ structure presently planned as part of the HASTOL Tether Boost Facility.

We find that with the present modular Hoytether™ design, using presently available tether materials, that of the 20 tether modules in the Hoytether™, 18 of them will never need replacement in the 30-year commercial operational lifetime of the facility. Of the two remaining portions, the longest, thinnest tether module at the grapple end of the facility will need replacement after 8.5 years, while the next longest, next thinnest tether module from the grapple end will need replacement after 15 years. These time-between-replacement rates could be increased to 100 years or more with improvements in the strength of tether materials or the use of a more complex "fractal" Hoytether™ design, where the lines in the main Hoytether™ are themselves mini-Hoytethers™. This analysis was extended into a technical paper and submitted to the 38th AIAA/ASME/SAE/ASEE Joint Propulsion Conference and Exhibit to be held in Indianapolis, Indiana from 7-10 July 2002. It is included as Appendix I in this report.

**Additional Simulations:** Some of our analytical software simulations are not available in the form of a printed document. The simulations discussed briefly below are not documented in separate appendices of this report.

#### **HASTOL Rendezvous Simulation:**

Boeing Phantom Works worked together with Tethers Unlimited, Inc. to combine the tether simulation program, TetherSim™, with the Boeing simulation programs for the DF-9 Hypersonic Airplane. This work produced a program that could simulate the rendezvous of the grapple (at the tip of the tether), with the payload (in the bay of the DF-9 Hypersonic Airplane).

**Grapple/Payload Attitude Dynamics Simulation:** TUI also developed a model for tether grapple/payload endmass dynamics. This model was used in the Boeing Rendezvous and Capture Simulation program. The model was developed and tested in MATLAB, and then coded in C++ for incorporation into the TetherSim™ tether dynamics simulation program. This simulation model was then used to perform detailed simulations of the tether grapple/payload rendezvous dynamics.

**Tether Boost Facility Simulation MatLab Plug-in:** Interface code was developed by TUI to enable the TetherSim™ tether simulation tool to be "plugged in" to the HASTOL Rendezvous and Capture Simulation under development at Boeing. The HASTOL Rendezvous and Capture Simulation used a combination of MATLAB and Satellite Tool Kit. TUI also modified the TetherSim "TrafficController" object class to remove Macintosh-GUI specific code, and created new C++ routines to permit the MatLab MEXFile routines to initialize the tether simulation, update the simulation over a specified time step, output tether data to a text data file, and terminate the simulation. TUI completed the modification to the TetherSim™ code to enable it to be run within Boeing's MatLab-based HASTOL simulation. TUI added routines for passing commands to the tether simulation, and returning data to the MatLab environment. TUI also developed a set of pre-generated input files to enable a HASTOL rendezvous scenario to be simulated.

## Appendix A

### The Gryphon™ as an Alternate for the HASTOL Hypersonic Airplane Component

Dr. Robert L. Forward  
Tethers Unlimited, Inc.

The Hypersonic Airplane Space Tether Orbital Launch (HASTOL) Architecture has, as one of its major components, a hypersonic airplane to take the payload from the surface of the Earth up to the top of the atmosphere. The task of the hypersonic airplane is to reach an altitude and an eastward velocity with respect to the air sufficient to match the altitude and velocity of the grapple at the lower tip of the rotating space tether component of the HASTOL architecture in its eastward equatorial elliptical orbit. In our HASTOL Phase I contract studies to date, we have determined that the Boeing DF-9 hypersonic airplane design has the capability to reach a eastward velocity of 3,650 m/s (12,000 ft/s ~ Mach 12) with respect to the air, at an altitude of 100 km. Adding in the ~470 m/s (~1540 ft/s) velocity of the air at 100 km altitude due to the eastward rotation of the Earth, this produces a velocity of the hypersonic airplane with respect to inertial space of ~4,100 m/s (13,500 ft/s). In our HASTOL Phase I contract studies, we have come up with a space tether design that can rotate fast enough and reach down low enough that it can match speeds with the hypersonic airplane and pick up the nominal payload of 14 Mg (~30,000 lb) and not drop too much in center-of-mass (COM) altitude, so that the grapple on the end of the tether never reaches below 80 km in altitude. The tether length in our design is a nominal 600 km and the tether rotation speed is a nominal 3,500 m/s (11,500 ft/s), which produces an acceleration at the tip of 2.1 gees. This tether rotational speed combined with the strength of the Spectra™ 2000 material that will be used, plus a safety factor of 2, requires that the tether mass at least 90 times the nominal payload of 15 Mg (33,000 lb), which is high, but feasible.

At the other end of the HASTOL facility from the grapple is the Tether Central Station, which contains the solar electric power supplies, winches, control electronics, etc., plus ballast mass. In the nominal design, the center-of-mass (COM) of the HASTOL facility is 90 km down the tether from the Tether Central Station or 510 km from the grapple end. The orbit selected is slightly elliptical with the COM varying from 700 km altitude at apogee, to 610 km at perigee, with the grapple at the tether tip at 100 km altitude. The orbital velocity at perigee is a nominal 7,600 m/s (25,000 ft/s) with respect to inertial space. The backward rotation of the tether tip at 3,500 m/s (11,500 ft/s) thus has the grapple moving at 4,100 m/s (13,500 ft/s) with respect to inertial space, matching speeds with the hypersonic airplane. After the payload is caught, the COM of the HASTOL facility plus payload drops in altitude, and the orbit becomes nearly circular. In order to avoid undue heating of the payload or grapple, a large amount of ballast must be added to the HASTOL facility to keep the tether tip from dipping below 80 km in altitude. This requires that the Tether Control Station, including ballast, mass 110 times the payload, making the mass of the entire HASTOL facility approximately 200 times the mass of the 15 Mg payload, or 3000 Mg (660,000 lb). A facility of this size and mass is engineeringly and economically feasible, especially since the HASTOL facility is completely reusable and will last for decades, but it would be desirable to lower the mass if possible.

If the rendezvous between the payload and grapple could take place at a slightly higher speed, then the mass of the tether would drop significantly, since the mass ratio of the tether goes as the exponential of the tip velocity *squared*. If the rendezvous could take place at a slightly higher altitude, then the amount of ballast mass needed could also be reduced, since the HASTOL facility could be allowed to drop further in altitude after pickup, without the tip dipping below the 80 km minimum altitude. Although the Boeing Phantom Works engineers will explore methods of obtaining higher rendezvous altitude and velocity out of the DF-9 design, and will look at alternate hypersonic airplane designs, it would be useful to consider other types of reusable launch systems for taking payloads from the surface of the Earth to the upper atmosphere.

One such system would be the Andrews Space & Technology Gryphon™ Reusable Launch Vehicle concept described in the figures in the following pages. Figure A-1 shows the basic concept. The Gryphon™ is a two-stage launch system consisting of a second stage Shuttle-Orbiter-like aerospace plane riding on top of a combined subsonic airplane and rocket launch vehicle. The subsonic airplane takes off using ordinary jet engines with a tank of JP-8 jet fuel, and large tank liquid hydrogen and an empty tank for liquid oxygen. It flies to a cruising altitude of 6 km (20,000 ft), where it uses a portion of the liquid hydrogen to extract and liquify oxygen out of the air using the Alchemist™ System shown in Figure A-2. Each pound of liquid hydrogen can extract 13 pounds of liquid oxygen. After the first stage subsonic airplane has filled its liquid oxygen tanks, then the subsonic airplane reverts to its liquid hydrogen/liquid oxygen rocket boost system, and the entire two-stage structure is boosted by the rocket to an altitude of 107 km (350,000 ft) and a speed of 8 Mach. The upper stage separates and continues on into orbit using its own internal rockets, while the second stage returns into the atmosphere and flies back to base. The second stage, with Orbiter-like reentry thermal protection tiles, returns in the same manner as the Space Shuttle Orbiter.

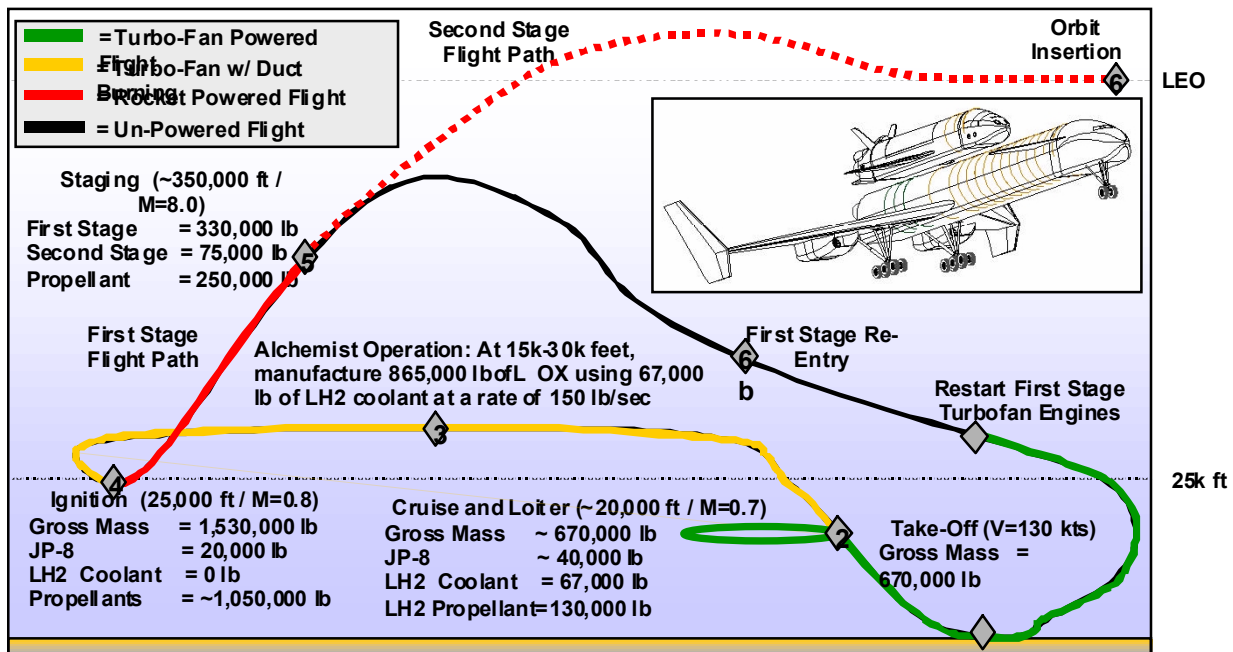


Figure A-1. The AST Gryphon™ concept.

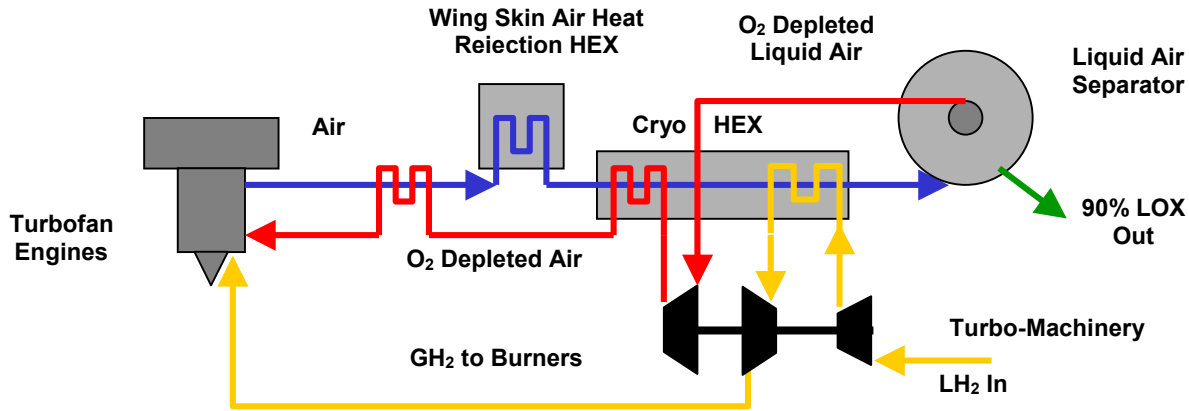


Figure A-2. The AST Alchemist™ oxygen liquefaction concept.

We have corresponded with Andrews Space & Technology about the possibility of using their system to bring payloads to a HASTOL Tether Facility. They have used their Gryphon™ simulation model to estimate the kinds of altitudes and velocities they can reach without overly stressing their system design. They have informed us that they can easily take a 14 Mg (30,000 lb) payload to a velocity of 4570 m/s (15,000 ft/s ~ Mach 15) at either 110~km (60 n.mi.) or 150 km (80 n.mi.), and to a velocity of 4420 m/s (14,500 ft/s ~ Mach 14.5) at 185 km (100 n.mi.). In these scenarios, because their first stage payload to be delivered to the HASTOL facility is only 30,000 lb instead of the 75,000 lb second stage vehicle assumed in Figure A-1, their Maximum Gross Take-Off Weight drops to approximately half the 670,000 lb shown in Figure A-1, and the first stage wing span, dry mass (and cost) drops proportionately.

We have made first cut estimates of the tether mass and the facility mass that would be needed in the HASTOL Tether Facility assuming that these speeds and altitudes could be attained by the Gryphon™ system. The tether mass was calculated using a simple tether mass spreadsheet program that took into account not only the tether tip rotation speed and its effect on the tether taper and mass ratio, but also the effect of the gravity gradient field of the Earth, which exerts a force along the tether proportional to the length of the tether and the altitude of the Facility COM. The results for the minimum total facility mass at representative altitudes and velocities with respect to the air are shown below in Table A-1. In the table, the masses are given as mass ratios of the mass of the tether, tether central facility, and total tether facility mass to the payload mass. Note that as the rendezvous altitude increases, the ballast mass needed in the Tether Central Station to keep the tether tip above 80 km altitude decreases, while as the rendezvous altitude increases, the mass ratio of the tether decreases because of the smaller tether tip velocity needed and therefore the smaller tether taper and diameter needed.



Table A-1

Parameter	Low Alt. & Speed	High Speed	High Altitude
Altitude (km)	110	150	185
Altitude (n.mi.)	60	80	100
Velocity (w.r.t. air)	4267	4572	4420
Velocity (Mach No.)	14	15	14.5
Station Mass Ratio	35	30	15
Tether Mass Ratio	33	18	29
<b>Total Mass Ratio</b>	<b>68</b>	<b>48</b>	<b>44</b>
Facility Perigee	656	713	683
Facility Apogee	1010	1197	1225

A number of other representative runs were made with different choices of tether tip speed (which determined the tether mass ratio) and facility altitude (which determined Tether Central Station mass ratio). These two were coupled through the assumption that the final Facility orbit had to be circular, with the tether tip never reaching below 80 km altitude. This meant that the initial Facility orbit had to be elliptical, and the more elliptical it was, the higher the perigee velocity was, and the faster the tether tip had to rotate with respect to the Facility COM to achieve the desired tether tip velocity with respect to the air. In general, in this region, it was difficult to get the total tether facility mass ratio down below 45 times the payload mass. This is still a considerable reduction from the mass ratio of 200 needed to reach the DF-9 Hypersonic Airplane at 100 km altitude and Mach 12.

The conclusion of this preliminary study is that we should consider the option of using the many emerging sub-orbital reusable rocket designs for the Earth-to-altitude boost portion of the HASTOL Architecture, rather than limiting the HASTOL study to Boeing Hypersonic Airplane designs. The Andrews Space & Technology Gryphon™ concept was jointly conceived with the Boeing Airplane group in Seattle and would use a Boeing airplane frame that would be built and paid for as a subsonic cargo carrier. Their concept should be one of those considered in the HASTOL study. It is recommended that Andrews Space & Technology get a \$20,000 subcontract from Boeing to do a detailed study on that option.

17 August 2000

## Appendix B

### HASTOL Tether Boost Facility Parameter Variations vs. Tether Length

Robert L. Forward, Tethers Unlimited

#### ABSTRACT

Using a HASTOL simulation worksheet developed by Dr. Robert P. Hoyt of Tethers Unlimited, Inc., we explored the variations in the HASTOL Tether Boost Facility parameters as a function of the length of the tether, for a single point case where the Tether Boost Facility was able to deliver the payload into a Geosynchronous Transfer Orbit (GTO) with an apogee at the 35,786 km altitude of Geosynchronous Earth Orbit (GEO), under nearly ideal payload rendezvous conditions that didn't put undue strain on the tether. We found that tethers shorter than 450 km have high acceleration levels at payload pickup due to their short length, and slightly larger tether masses due to their higher tip speeds, while tethers longer than 1000 km begin to increase rapidly in tether mass, most likely due to the increased gravity gradient forces on the longer length. A tether length of about 600-900 km was found to be close to optimum, with the longer lengths and their lower pickup accelerations preferred for "tourist" traffic.

#### ANALYSIS RESULTS

For the analysis of the effect of tether length on the HASTOL Tether Boost Facility parameters, we chose a case where, for each tether length studied, the Boost Facility was able to perform the mission of picking up a payload and delivering it into a GTO orbit with an apogee at GEO altitude (35,786 km). The rendezvous of the payload with the tether was assumed to occur at an altitude of 150 km and a velocity of 5791 m/s (Mach 19). This selected velocity is a much higher rendezvous velocity than would normally be considered for the HASTOL Architecture, which would like to arrange for pickup at velocities of Mach 10-15. The selected altitude is also somewhat high, and it would be desirable to arrange for pickup at an altitude of 110 km (60 n.mi.) or lower. We can arrange to have the Boost Facility pick up the payload at those low speeds and altitudes, but the resulting Boost Facility rotation speed and orbit, results in the payload being thrown into a transfer orbit with an apogee way beyond GEO and sometimes even to Earth escape. It would be difficult to do a valid comparison of various tether lengths if the final payload destination were not fixed, so we selected the given rendezvous parameters of 150 km altitude and 5791 m/s velocity, so that the payload was delivered to a GTO with an apogee of 35,786 km for each different length of tether. We also fixed the mass of the Tether Central Station (TCS) at 150 Mg or 10 times the payload mass of 15 Mg. The tether safety factor was chosen to be 3.0 along the entire length of the tether. If the safety factor is changed in the future, it should not have any effect on the optimum length that we found in this analysis.

We carried out 6 runs with tether lengths of 300, 450, 600, 900, 1200, and 1500 km. The Boost Facility initial perigee altitude was then varied until the payload was placed into a GTO with an apogee of 1.00 times the GEO altitude of 35,786 km. The results of the output of the HASTOL Boost Facility parameter worksheets are summarized in Table B-1 - "HASTOL Tether Boost Facility Parameter Variations with Tether Length Variations".

**TABLE B-1 - HASTOL Tether Boost Facility Parameter Variations with Tether Length Variations**  
 Robert L. Forward, Tethers Unlimited, Inc. - 19 Oct 2000

**Fixed Parameters**

Rendezvous Altitude 150 km (80 n.mi.)  
 Rendezvous Velocity 5791 m/s (Mach 19)  
 Payload GTO Apogee 35,786 km (1.00 GEO Altitude)  
 Payload Mass 15 Mg  
 TCS Mass 150 Mg (10X Payload)  
 Tether Safety Factor 3.0 along entire length

Run	Rendezvous					Facility			Mass Ratio			Tip Altitude		Tether	GTO
	Velocity		Altitude		Accel	CM Peri	CM Apo	Tip Vel	TCS	Tether	Total	Perigee	Apogee	Length	Apogee
	(Mach)	(m/s)	(km)	(n.mi.)	(gees)	(km)	(km)	(m/s)	(ratio)	(ratio)	(ratio)	(km)	(km)	(km)	(X Geo)
3121	19.0	5791	150	80	0.23	1183	1437	1530	10.0	49.0	59.0	116	83	1500	1.00
3122	19.0	5791	150	80	0.33	1006	1424	1657	10.0	29.7	39.7	108	100	1200	1.00
3123	19.0	5791	150	80	0.50	816	1417	1801	10.0	19.9	29.9	107	142	900	1.00
3124	19.0	5791	150	80	0.86	604	1390	1963	10.0	15.8	25.8	116	242	600	1.00
3125	19.0	5791	150	80	1.25	492	1362	2050	10.0	15.5	25.5	124	323	450	1.00
3126	19.0	5791	150	80	2.06	376	1324	2139	10.0	16.3	26.3	133	427	300	1.00

We find in all cases that the final apogee of the Tether Boost Facility is always greater than the perigee at all times during the pickup and toss process. (This is not always the case, since in some scenarios the loss of orbital energy and momentum by the Tether Boost Facility is such that the apogee before the payload transfer becomes the new perigee after the payload transfer.) Also, in all cases the apogee and perigees are always high enough that the tether tip would never get below 80 km altitude even if the facility rotation was not phased to avoid the tether pointing to the nadir during closest approach to Earth.

One major result of the 6 runs can be found in the column labeled Rendezvous Acceleration, where we can see the obvious advantage of using a longer tether for any given pickup and toss scenario. The longer the tether, the lower the acceleration load on the payload during pickup and during the 15-20 minutes the payload is riding on the rotating tether between pickup and toss. The acceleration level varies from a mild 0.23 gees for the 1500 km long tether, to a severe 2.06 gees for the 300 km long tether. Since this scenario has the rendezvous taking place at a very high rendezvous velocity of 5791 m/s (Mach 19), the tether is not being stressed very much, so the tip speed required of the tether is low and the acceleration level on the payload is low. When we get to much lower rendezvous velocities, the required tether tip speed is going to rise, and since the acceleration goes as the square of the tip speed, the acceleration on the shorter tethers is going to be very high, many gees, too high for tourist traffic and even stressful for commercial satellites. The use of longer tethers would keep these acceleration levels down.

The second major result of the 6 runs can be found in the columns labeled Mass Ratio, specifically the Total Mass Ratio, which is the ratio of the HASTOL Tether Boost Facility total mass to the Payload mass. We see that there is a shallow minimum in the Total Mass Ratio at a tether length of 450 km. The minimum extends from tether lengths of 300 km to 900 km, with the mass ratio of 29.9 at 900 km being 117% of the minimum mass ratio of 25.5 at 450 km. As we go to the longer tether lengths of 1200 km and 1500 km, the Total Mass Ratio starts to rise considerably, being 156% and 231% respectively of the minimum mass ratio at 450 km.

**CONCLUSIONS**

Based on these 6 simulation runs, we can conclude that the optimum length for the tether of a HASTOL Tether Boost Facility is between 600 km and 900 km, with the longer lengths being preferred when the level of acceleration on the payload is of concern.

## Appendix C

### HASTOL Tether Boost Facility Total Mass vs. Tether Control Station Mass

Robert L. Forward, Tethers Unlimited

#### ABSTRACT

Using a HASTOL simulation worksheet developed by Dr. Robert P. Hoyt of Tethers Unlimited, Inc., we explored the variations in the HASTOL Tether Boost Facility total mass as a function of the mass of the Tether Central Station (TCS), including any ballast mass. We carried out a number of simulation runs at 110 km rendezvous altitude with both high (Mach 17) and low (Mach 12) rendezvous velocities, and high safety factor and low safety factor tethers, which produced total facility masses ranging from 28 to 338 times the payload mass. The total Boost Facility mass was found to decrease slowly as the TCS mass decreased, with the minimum total mass occurring when the TCS mass was negligible. The tether tip acceleration level, however, increased as the TCS mass decreased, becoming significantly larger as the TCS mass dropped below 10 times the payload mass. The optimum TCS mass was determined to be the mass of all the useful equipment that would be needed in the TCS for a given operational scenario, with no additional ballast mass being used unless it cost nothing to install on the TCS. For the purposes of further HASTOL simulations, we should assume a TCS mass of 10 times the payload mass.

#### ANALYSIS OF RESULTS

For the analysis of the variations in the total mass of the HASTOL Tether Boost Facility as a function of the TCS mass, we carried out simulation runs of three scenarios. All three scenarios use a 600-km-long tether, a rendezvous altitude of 110 km (60 n.mi.), payload mass of 15 Mg, and a minimum tip altitude requirement of 80 km.

In the first scenario, shown in Table C-1 - "HASTOL Tether Boost Facility Total Mass Variation with TCS Mass Variations - Mach 17 - F3.0", we assumed a safety factor for the tether material of 3.0 along the entire length. This safety factor is used to "derate" the ultimate tensile strength of the material used in the tether to a safer "design tensile strength" value before it is used in calculating the tether mass. A high safety factor generally results in a heavier tether for any given stress level in the tether. To explore the region where the tether mass is comparable to the TCS mass, we chose a relatively high rendezvous velocity of 5182 m/s (Mach 17) for Table C-1. This would mean that the tether did not have to rotate at a high tip speed in order to match speeds with the payload at the rendezvous point. The stress on the tether would be low and therefore the tether mass would be low. We chose values for the TCS mass ranging from 2 to 100 times the payload mass. The simulation worksheet automatically calculates the center-of-mass (CM) of the Boost Facility, chooses a CM perigee that will result in a pickup at 110 km and Mach 17, and calculates the perigee and apogee after catch and after toss of the payload. The user then chooses different values for the initial CM apogee to get different results. Since a high initial CM apogee means a high velocity at perigee, which requires a higher tether tip velocity to achieve velocity match with the payload at rendezvous, which means a heavier tether, it is usually desirable to choose a low initial Facility CM apogee. If, however, the CM apogee is chosen too low, then the minimum tether tip altitude could drop below 80 km after tossing the payload, and the tether tip could become overheated by atmospheric drag. This was the case for this first scenario, and all

the simulations in Table C-1 were stopped when the 80 km limit was reached on the altitude of the tether tip when the CM of the tether was at its "apogee" after toss of the payload. (In reality, the loss of altitude by the CM of the tether was so severe after toss of the payload, that the CM apogee became less than the CM perigee - the two had switched places. With this tether tip altitude limit dominating, it was not possible to arrange to put the payload into a true Geosynchronous Transfer Orbit with an apogee at 35,786 km (1.00 GEO altitude). Instead, the payload was tossed higher than GEO altitude, with an apogee ranging from 2.64 to 2.82 times GEO altitude. As can be seen from the Total Mass Ratio column, as the TCS mass was decreased, the total mass of the Boost Facility decreased, but not as fast as the TCS mass was decreasing, since the required tether mass was increasing. The increase in tether mass occurs because the tether tip speed increases with decreasing total mass, and a higher tip speed requires a heavier tether to withstand the higher stresses. Note also that because of the higher tip speed, the acceleration felt by the payload also increases with decreasing TCS mass.

TABLE C-1 - HASTOL Tether Boost Facility Total Mass Variation with TCS Mass Variations - Mach 17 - F3.0  
Robert L. Forward, Tethers Unlimited, Inc. - 17 Oct 2000

Fixed Parameters

Tether Length 600 km  
 Rendezvous Altitude 110 km (60 n.m.i.)  
 Rendezvous Velocity 5182 m/s (Mach 17)  
 Payload Mass 15 Mg  
 Tether Safety Factor 3.0 along entire length  
 Minimum Tip Altitude 80 km

Run	Rendezvous					Facility			Mass Ratio			Tip Altitude		GTO
	Velocity		Altitude		Accel	CM Peri	CM Apo	Tip Vel	TCS	Tether	Total	Perigee	Apogee	Apogee
	(Mach)	(m/s)	(km)	(n.m.i.)	(gees)	(km)	(km)	(m/s)	(ratio)	(ratio)	(ratio)	(km)	(km)	(XGeo)
3301	17.0	5182	110	60	<b>1.80</b>	474	803	2534	2.0	55.4	57.4	98	80	2.64
3302	17.0	5182	110	60	<b>1.68</b>	495	819	2520	5.0	53.5	58.5	97	80	2.69
3303	17.0	5182	110	60	<b>1.55</b>	522	835	2502	10.0	50.8	60.8	97	80	2.76
3304	17.0	5182	110	60	1.46	543	842	2487	15.0	48.5	63.6	<b>97</b>	80	2.79
3305	17.0	5182	110	60	1.39	560	<b>845</b>	2474	20.0	46.6	66.7	<b>97</b>	80	2.81
3306	17.0	5182	110	60	1.33	574	844	2462	25.0	45.0	70.0	97	80	2.82
3307	17.0	5182	110	60	1.29	586	842	2452	30.0	43.7	73.7	97	80	<b>2.82</b>
3309	17.0	5182	110	60	1.22	605	833	2434	40.0	41.5	81.5	98	80	2.81
3311	17.0	5182	110	60	1.17	619	824	2420	50.0	39.9	89.9	99	80	2.80
3313	17.0	5182	110	60	1.14	630	814	2408	60.0	38.6	98.6	100	80	2.78
3315	17.0	5182	110	60	1.09	646	797	2391	80.0	36.9	116.9	101	80	2.75
3317	17.0	5182	110	60	1.05	657	782	2378	100.0	35.8	135.8	102	80	2.72

In the second scenario, shown in Table C-2 - "HASTOL Tether Boost Facility Total Mass Variation with TCS Mass Variations - Mach 17 - F2.0 - 4.10 GEO", we again use a rendezvous altitude of 110 km (60 n.m.i.) and velocity 5182 m/s (Mach 17), but we have changed the safety factor from 3.0 to 2.0 along the tether except for the tip section where the shock loads would be strongest. (Instead of lowering the safety factor, an equivalent result would have been obtained if the tensile strength of the tether material had been raised from 4.0 GPa to 6.0 GPa.) The required mass of the tether now drops by roughly a factor of two. This time, instead of stopping the simulation when the post-toss tether tip altitude dropped below 80 km, we instead adjusted the initial CM apogee so that the final apogee of the payload was the same for all cases - 4.10 times GEO altitude or 146,723 km. We again see that as the TCS mass decreases, the total facility mass decreases, while the tip acceleration increases.

**TABLE C-2 - Tether Boost Facility Total Mass Variation with TCS Mass Variations - Mach 17-F2.0-4.10 GEO**  
 Robert L. Forward, Tethers Unlimited, Inc. - 17 Oct 2000

**Fixed Parameters**

Tether Length 600 km  
 Rendezvous Altitude 110 km (60 n.mi.)  
 Rendezvous Velocity 5182 m/s (Mach 17)  
 Payload Mass 15 Mg  
 Tether Safety Factor 2.0 along entire length except 3.0 at tip  
 GTO Apogee 146,723 km (4.10 GEO)

Run	Rendezvous					Facility			Mass Ratio			Tip Altitude		GTO
	Velocity		Altitude		Accel	CM Peri	CM Apo	Tip Ve	TCS	Tether	Total	Perigee	Apogee	Apogee
	(Mach)	(m/s)	(km)	(n.mi.)	(gees)	(km)	(km)	(m/s)	(ratio)	(ratio)	(ratio)	(km)	(km)	(X Geo)
3501	17.0	5182	110	60	2.00	467	1244	2651	2.0	25.8	27.8	85	101	4.10
3502	17.0	5182	110	60	1.77	505	1249	2620	5.0	23.5	28.5	83	84	4.10
3503	17.0	5182	110	60	1.55	549	1235	2581	10.0	20.9	30.9	82	82	4.10
3504	17.0	5182	110	60	1.41	579	1212	2550	15.0	19.2	34.2	83	97	4.10
3505	17.0	5182	110	60	1.33	600	1187	2527	20.0	18.1	38.1	85	114	4.10
3506	17.0	5182	110	60	1.27	616	1164	2508	25.0	17.3	42.3	87	133	4.10
3507	17.0	5182	110	60	1.22	628	1144	2493	30.0	16.7	46.7	88	150	4.10

In the third scenario, shown in Table C-3 - "HASTOL Tether Boost Facility Total Mass Variation with TCS Mass Variations - Mach 12 - F2.0 - -1.29 GEO", we again use a rendezvous altitude of 110 km (60 n.mi.) and a safety factor of 2.0 except for the tip of the tether, but this time we use a rendezvous velocity of 3658 m/s (Mach 12). The slower rendezvous velocity means that the tether tip must be moving faster, which increases the stress on the tether and the tether mass needed to withstand that stress. The total mass is now around 300 times the mass of the payload, many times that of the TCS mass. In these runs, the simulations were stopped when the minimum tip altitude condition was reached. In all cases, the resulting apogee was a hyperbolic escape velocity trajectory with a negative "apogee" of -1.29 GEO "altitude". Even in this dramatically different scenario we see the same results. As the TCS mass decreases, the total facility mass decreases, while the tip acceleration increases.

**TABLE C-3 - HASTOL Tether Boost Facility Total Mass Variation with TCS Mass Variations - Mach 12 - F2.0**  
 Robert L. Forward, Tethers Unlimited, Inc. - 19 Oct 2000

**Fixed Parameters**

Tether length 600km  
 Rendezvous Altitude 110 km (60 n.mi.)  
 Rendezvous Velocity 3658 m/s (Mach 12)  
 Payload Mass 15 Mg  
 Tether Safety Factor 2.0 except 3.0 at tip  
 Minimum Tip Altitude 80 km  
 GTO Apogee Escape (-1.29 GEO)

Run	Rendezvous					Facility			Mass Ratio			Tip Altitude		GTO
	Velocity		Altitude		Accel	CM Peri	CM Apo	Tip Ve	TCS	Tether	Total	Perigee	Apogee	Apogee
	(Mach)	(m/s)	(km)	(n.mi.)	(gees)	(km)	(km)	(m/s)	(ratio)	(ratio)	(ratio)	(km)	(km)	(X Geo)
3701	12.0	3658	110	60	4.21	494	569	3979	2	292	294	107	80	-1.29
3702	12.0	3658	110	60	4.15	499	574	3976	5	290	295	107	80	-1.29
3703	12.0	3658	110	60	4.06	506	582	3972	10	286	296	107	80	-1.29
3704	12.0	3658	110	60	3.98	513	588	3968	15	283	298	107	80	-1.29
3705	12.0	3658	110	60	3.92	519	594	3964	20	279	299	107	80	-1.29
3706	12.0	3658	110	60	3.80	530	604	3958	30	273	303	107	80	-1.29
3707	12.0	3658	110	60	3.71	540	612	3953	40	267	307	107	80	-1.29
3708	12.0	3658	110	60	3.56	556	626	3943	60	256	326	107	80	-1.29
3709	12.0	3658	110	60	3.34	581	645	3927	100	238	338	107	80	-1.29

## CONCLUSIONS

In examination of the three scenarios, we find that there is no "minimum" in the total facility mass as a function of the TCS mass. The change in total mass with change in TCS mass is also small in the region below 20 times the payload mass, so it doesn't really matter much what the TCS mass is. Thus, the TCS mass should be chosen for other reasons than minimum total facility mass. The acceleration on the payload at the tip of the tether does increase significantly as the TCS mass decreases below 10 times the payload mass, so too small a TCS mass could cause payload problems. Since the TCS mass includes all the command, control, and power electronics, such as the solar power arrays, the power conditioning circuits, and the electrodynamic tether drive current circuits, the mass of the TCS should be selected to fit those electronic system mass requirements, with no additional ballast mass being used unless it costs nothing to install on the TCS. As can be seen from the columns labeled Tip Velocity, free ballast mass that increases the total TCS mass is useful in keeping the tether tip velocity and tether mass down. Launching ballast mass does not pay. It is better to launch more tether mass or more electronics mass instead. It is recommended that until we have calculated an actual TCS mass, that for HASTOL simulations in the near future, we should assume a TCS mass of 10 times the payload mass.

## Appendix D

### HASTOL Boost Facility Parameter Variations vs. Initial Payload Velocity

Robert L. Forward, Tethers Unlimited

#### ABSTRACT

Using a HASTOL simulation worksheet developed by Dr. Robert P. Hoyt of Tethers Unlimited, Inc., we explored the variations in the HASTOL Tether Boost Facility mass and orbital parameters as a function of the initial payload velocity at the time of rendezvous of the payload with the tip of the tether. We did the analysis for two different tether safety factor (design tensile strength) values and two different initial payload altitudes. We first found that the HASTOL system is "over-capable", in that it nearly always throws the payload into its final transfer orbit with too high a velocity. Most simulation runs ended up with the payload on an escape trajectory from Earth. This is a "problem" if the final payload apogee is GEO, but is desirable for sending payloads to the Moon, Mars, and elsewhere. This final velocity "problem" can be solved in a number of different ways, which will be discussed in later simulations. It did NOT have a significant affect on these analyses, since the total mass of the Tether Boost Facility is predominantly determined by the rendezvous parameters, not the toss parameters. The total mass ratio of the Tether Boost Facility was found, as expected, to decrease as the tether material "design" tensile strength increased, and to decrease as the difference between the initial payload velocity and the initial perigee orbital velocity of the Boost Facility decreased. In general, we found that the total mass ratio of the Boost Facility was less than 100 times the payload mass when the initial payload velocity was above Mach 15. For velocities below Mach 15, the total mass ratio of the Boost Facility increased rapidly, becoming larger than 300 for Mach 12 and below. Increasing the initial payload altitude from 110 km to 185 km only decreased the total mass ratio numbers by about 10%, so we determined that it is more important for the hypersonic vehicle to operate at higher speed than at higher altitude, provided it is outside the atmosphere (>80 km) so that the tether doesn't overheat during the rendezvous and pickup. The major conclusion of these simulation runs, is that to end up with a HASTOL Architecture design with a reasonable total facility mass ratio (less than 100 times the payload mass), we will need to find:

- (1) Hypersonic vehicles with >Mach 12 velocity at >80 km altitude.
- (2) Tether materials with higher ultimate tensile strength.
- (3) Tether structure designs that allow the use of lower engineering safety factors.
- (4) Phased tether rotations and orbits to insure the tether tip altitude is always >80 km.
- (5) Methods of operating the Boost Facility to minimize tether stress.

#### ANALYSIS OF RESULTS

For the analysis of the variations in the mass and orbital parameters of the HASTOL Tether Boost Facility as a function of the initial payload velocity at the time of rendezvous, we carried out simulation runs of three scenarios. All three scenarios use a 600 km long tether, a payload mass of 15 Mg, a Tether Control Station (TCS) mass of 150 Mg (10 times the payload mass), and a minimum tip altitude requirement of 80 km, where we assume there is no control of the phase of tether rotation to avoid the tether tip going below 80 km altitude at the point of closest approach of the Boost Facility to Earth at any time during the scenario.



In the first scenario, shown in Table D-1 - "Tether Boost Facility Parameter Variations with Initial Payload Velocity Variations - 110 km - F3.0", we assumed a safety factor for the tether material of 3.0 along the entire length. A high safety factor generally results in a heavier tether for any given stress level in the tether. For this scenario we chose a constant rendezvous altitude of 110 km (60 n.mi.) and varied the payload velocity at the rendezvous point from Mach 19 down to Mach 10. Given those initial parameters, the simulation calculates the center-of-mass (CM) of the Boost Facility and picks the CM perigee altitude needed for the tether to reach down to the rendezvous altitude. The user then adjusts the CM apogee altitude to obtain the desired final payload orbital parameters after toss of the payload at the next post-catch perigee. The simulation then iterates the mass distribution of the tether until the solution converges, and then calculates the final orbital parameters of the Boost Facility after the payload toss, and the minimum tip altitude for the Boost Facility apogee and perigee (typically, the post-toss "apogee" and "perigee" have switched places). If the final orbital parameters of the Boost Facility are such that the Boost Facility has "crashed", by having a negative apogee or perigee, or if any of the Boost Facility orbital parameters are such that the tether tip goes below 80 km, then that "solution" for the final payload apogee is unobtainable.

If we look at Table D-1, we notice in run 3111 at an initial payload velocity of 5791 m/s (Mach 19) and altitude of 110 km (60 n.mi.), it was possible to find a set of initial Boost Facility parameters where the final payload apogee was at the desired 1.00 times the GEO altitude of 35,786 km. However, the post-toss altitude of the Boost Facility CM was such that the tether tip could dip down to 77 km if the tether rotation phase were not controlled. First of all, the tether rotation phase can be controlled to prevent this. Second, the tether tip could probably survive the heating at 77 km if it could survive at 80 km. Third, by raising the initial payload rendezvous by 3 km to 113 km, the final Boost Facility orbit rises by a similar amount and the minimum tether tip altitude is a safe 80 km. Note that in this run only, the final Boost Facility apogee altitude is truly larger than the perigee altitude. The total mass of the Boost Facility in this run is only 26 times the payload mass, and the acceleration on the payload is only 0.88 gees.

TABLE D-1. Tether Boost Facility Parameter Variations with Initial Payload Velocity Variation-110 km-F3.0  
Robert L. Forward, Tethers Unlimited, Inc. - 19 Oct 2000

**Fixed Parameters**

Tether length 600km  
 Rendezvous Altitude 110 km (60 n.mi.)  
 TCS Mass 150 Mg (10X payload mass)  
 Payload Mass 15 Mg  
 Tether Safety Factor 3.0 along entire length  
 Minimum Tip Altitude 80 km

Run	Rendezvous					Facility			Mass Ratio			Tip Altitude		de GTO
	Velocity		Altitude		Accel	CM Peri	CM Apo	Tip Vel	TCS	Tether	Total	Perigee	Apogee	Apogee
	(Mach)	(m/s)	(km)	(n.mi.)	(gees)	(km)	(km)	(m/s)	(ratio)	(ratio)	(ratio)	(km)	(km)	(X Geo)
3111	19.0	5791	110	60	0.88	563	1308	1977	10	16	26	77	182	1.00
3007	18.0	5486	110	60	1.18	540	1012	2229	10	28	38	88	80	1.44
3010	17.0	5182	110	60	1.55	522	835	2502	10	51	61	97	80	2.76
3015	16.0	4877	110	60	1.96	512	701	2780	10	94	104	102	80	13.51
3032	15.0	4572	110	80	2.40	509	612	3064	10	175	185	106	80	-8.66
3031	14.0	4267	110	60	2.86	511	559	3353	10	331	341	108	80	-2.49
3030	13.0	3962	110	60	3.33	517	531	3645	10	638	648	109	80	-1.68
3027	12.0	3658	110	60	3.82	524	524	3941	10	1253	1263	109	85	-1.31
3029	11.0	3353	110	60	4.33	533	533	4241	10	2515	2525	110	97	-1.09
3028	10.0	3048	110	60	4.87	542	542	4541	10	5108	5118	110	103	-0.95

As we look at the other runs at different velocities from Mach 18 down to Mach 10, we find that the limit of 80 km on the minimum tether tip altitude prevents us from picking a payload toss velocity that is low enough to produce a payload apogee of 1.00 times GEO altitude. Instead, we are forced to throw the payload too high (Mach 18 to Mach 16) until at Mach 15 and below, the negative value for the "apogee" indicates that the payload has been thrown into a hyperbolic escape trajectory. The present simulation routine only picks up at perigee and throws at perigee. It should be possible to pick a different set of throw points and angles by selecting different points along the Tether Boost Facility orbit to throw the payload instead of just at the perigee point, and different rotation angles for the tether instead of just tossing just at the zenith angle. Additional options would include picking up the payload at different orbital positions than perigee and different tether rotational angles than nadir. We will explore expanding the simulation software to include those options so that the payload can be delivered to a GTO with an apogee of 1.00 GEO altitude no matter what the initial rendezvous conditions.

In evaluating the parameters in Table D-1, it should also be noted that for Mach 12 down to Mach 10, the attempt to decrease the initial Boost Facility apogee in order to decrease the mass ratio and the final payload velocity, encountered a condition where the initial Boost Facility CM apogee equaled the CM perigee (the initial Boost Facility orbit was circular). It is possible to enter into the simulation an initial "apogee" that is less than the "perigee", and lower the total facility mass and the final payload velocity without running into the 80 km minimum tether tip altitude requirement, but the simulation was not pushed past that point for the runs in Table D-1.

The major results from the simulation runs in Table D-1 can be found in the columns titled Rendezvous Acceleration and Total Mass Ratio. As the Rendezvous Velocity decreased from Mach 19 down to Mach 10, the Rendezvous Acceleration rose from a comfortable 0.88 gees at to a severe 4.87 gees, and the Total Mass Ratio rose from a reasonable 26 times the payload mass to a completely unreasonable 5118 times the payload mass. If we want to keep the Total Mass Ratio below 100 times the payload mass, using a tether safety factor of 3.0 for tether material with an ultimate tensile strength of 4.0 GPa and a density of 970 kg/m, then we will need to use a hypersonic vehicle with the capability of reaching greater a velocity of greater than Mach 16 (4877 m/s) at 110 km altitude.

In the second scenario, shown in Table D-2 - "Tether Boost Facility Parameter Variations with Initial Payload Velocity Variations - 110 km Altitude - F2.0", we again use a rendezvous altitude of 110 km (60 n.mi.), but we have changed the safety factor from 3.0 to 2.0 along the tether except for the tip section where the shock loads would be strongest. (Instead of lowering the safety factor, an equivalent result would have been obtained if the ultimate tensile strength of the tether material had been raised from 4.0 GPa to 6.0 GPa.) The required mass of the tether for each value of Rendezvous Velocity now drops significantly, especially at the lower values of Rendezvous Velocity, while the Rendezvous Acceleration does not change significantly. If we want to keep the Total Mass Ratio below 100 times the payload mass, using a tether safety factor of 2.0 for tether material with an ultimate tensile strength of 4.0 GPa and a density of 970 kg/m, then we will need to use a hypersonic vehicle with the capability of reaching greater a velocity of greater than Mach 14 (4267 m/s) at 110 km altitude. Also note that at Mach 18 and Mach 19 it was not possible to find a workable solution without the post-toss Boost Facility perigee being so low that the tether tip altitude fell below the minimum 80 km value. Basically, the Boost Facility

has so little total mass that it can't pick up the payload at the low altitude of 110 km without dropping too far after payload toss. The minimum pickup altitude is 133 km for a pickup velocity of Mach 19 and 113 km for Mach 18. The minimum pickup altitude for lower velocities can be less than 110 km if desired.

**TABLE D-2. Tether Boost Facility Parameter Variations with Initial Payload Velocity Variation-110 km-F2**  
Robert L. Forward, Tethers Unlimited, Inc. - 19 Oct 2000

**Fixed Parameters**

Tether length 600km  
 Rendezvous Altitude 110 km (60 n.mi.)  
 TCS Mass 150 Mg (10X payload mass)  
 Payload Mass 15 Mg  
 Tether Safety Factor 2.0 except 3.0 at tip  
 Minimum Tip Altitude 80 km

Run	Rendezvous					Facility			Mass Ratio			Tip Altitude GTO		
	Velocity		Altitude		Accel	CM Peri	CM Apo	Tip Vel	TCS	Tether	Total	Perigee	Apogee	Apogee
	(Mach)	(m/s)	(km)	(n.mi.)	(gees)	(km)	(km)	(m/s)	(ratio)	(ratio)	(ratio)	(km)	(km)	(X Geo)
3600	19.0	5791	110	60	0.85	600	1614	2019	10	8	18	57	80	1.09
3601	18.0	5486	110	60	1.17	554	1444	2306	10	13	23	77	80	1.84
3602	17.0	5182	110	60	1.55	549	1233	2580	10	21	31	82	80	4.08
3603	16.0	4877	110	60	1.98	529	1027	2850	10	35	45	92	80	-112.18
3604	15.0	4572	110	80	2.45	516	856	3123	10	59	69	98	80	-4.28
3605	14.0	4267	110	60	2.96	508	728	3401	10	99	109	102	80	-2.30
3606	13.0	3962	110	60	3.50	505	639	3684	10	168	178	106	80	-1.63
3607	12.0	3658	110	60	4.06	506	582	3972	10	286	296	107	80	-1.29
3608	11.0	3353	110	60	4.63	510	546	4264	10	493	503	108	80	-1.09
3609	10.0	3048	110	60	5.21	516	527	4558	10	859	869	109	80	-0.96

In the third scenario, shown in Table D-3 - "Tether Boost Facility Parameter Variations with Initial Payload Velocity Variations - 185 km Altitude - F2.0", we raised the initial payload pickup altitude from 110 km to 185 km to see what effect it would have on the total boost facility mass numbers. We knew it would allow the post-boost parameters to improve slightly, and at this altitude it is again possible to achieve a GTO trajectory with an apogee of 1.00 times GEO altitude with a Mach 19 (5791 m/s) Rendezvous Velocity and 185 km Rendezvous Altitude. At lower Rendezvous Velocities, however, the final payload velocity is still way more than is needed to serve the GTO market. With the higher Rendezvous Altitude of 185 km, the Rendezvous Accelerations remain essentially the same, while the Total Mass Ratio does drop slightly, about 10%, which is useful, but not a significant change considering the large change in Rendezvous Altitude.

**CONCLUSIONS**

In the examination of the three scenarios, which assume the use of present day tether materials such as Spectra™ 2000, with an ultimate tensile strength of 4.0 GPa and a specific density of 0.97, we found that the total mass ratio of the Boost Facility increased rapidly with decreasing initial payload velocity, becoming larger than 300 for Mach 12 and below, even with the assumption of a safety factor of 2.0 along most of the tether instead of a more conservative safety factor of 3.0. Increasing the initial payload altitude from 110 km to 185 km only decreased the total mass ratio numbers by about 10%. It is thus obvious that it is more important for the hypersonic vehicle to operate at higher speed than at higher altitude, provided it is outside the atmosphere (>80 km) so the tether doesn't overheat during the rendezvous and pickup.

**TABLE D-3. Tether Boost Facility Parameter Variations with Initial Payload Velocity Variation-185 km-F2.0**  
 Robert L. Forward, Tethers Unlimited, Inc. - 19 Oct 2000

**Fixed Parameters**

Tether length 600km  
 Rendezvous Altitude 185 km (100 n.mi.)  
 TCS Mass 150 Mg (10X payload mass)  
 Payload Mass 15 Mg  
 Tether Safety Factor 2.0 except 3.0 at tip  
 Minimum Tip Altitude 80 km

Run	Rendezvous					Facility			Mass Ratio			Tip Altitude			de GTO
	Velocity		Altitude		Accel	CM Peri	CM Apo	Tip Vel	TCS	Tether	Total	Perigee	Apogee	Apogee	
	(Mach)	(m/s)	(km)	(n.mi.)											
3610	19.0	5791	185	100	0.79	681	1665	1965	10	7	17	129	97	1.00	
3611	18.0	5486	185	100	1.10	654	1490	2251	10	11	21	143	80	1.62	
3612	17.0	5182	185	100	1.47	629	1282	2526	10	19	29	155	80	3.25	
3613	16.0	4877	185	100	1.88	608	1071	2797	10	31	41	165	80	21.56	
3614	15.0	4572	185	100	2.35	593	890	3068	10	52	62	172	80	-5.47	
3615	14.0	4267	185	100	2.86	584	752	3344	10	88	98	177	80	-2.58	
3616	13.0	3962	185	100	3.39	580	655	3627	10	150	160	180	80	-1.75	
3617	12.0	3658	185	100	3.95	581	592	3913	10	255	265	182	80	-1.36	
3618	11.0	3353	185	100	4.53	<b>585</b>	<b>585</b>	4213	10	447	457	183	112	-1.13	
3619	10.0	3048	185	100	5.13	<b>590</b>	<b>590</b>	4515	10	788	798	184	140	-0.98	

As better materials with greater ultimate tensile strength become available the total tether masses would drop dramatically. Even a factor of only 2 or 3 in tensile strength would make a major difference in the presently large mass ratios at the lower initial payload velocities. Considering the number of years that will be needed to develop a hypersonic vehicle to use with the HASTOL Architecture, it is highly likely that stronger materials will become available, so perhaps the present HASTOL Architecture study should assume the use of a future material rather than present-day materials.

We also found that the HASTOL system is "over-capable", in that it throws payloads to final velocities that are greater than is needed. We need to find methods of operating the Boost Facility so that it picks up the payload and tosses the payload at CM orbit positions that are not at perigee or apogee, and tether rotation angles that are not at zenith or nadir. We also need to find methods to change the tether length, rotation rate, and orbital parameters of the Boost Facility before, during, and after the payload interaction to achieve a desired final payload velocity at a minimum value of maximum tether stress, so as to minimize the tether mass and thus the total facility mass.

The major conclusion of this study, is that to end up with a HASTOL Architecture design with a reasonable total facility mass ratio (less than 100 times the payload mass), we will need to find:

- (1) Hypersonic vehicles with >Mach 12 velocity at >80 km altitude.
- (2) Tether materials with higher ultimate tensile strength.
- (3) Tether structure designs that allow the use of lower engineering safety factors.
- (4) Phased tether rotations and orbits to insure the tether tip altitude is always >80 km.
- (5) Methods of operating the Boost Facility to minimize tether stress.



## **Appendix E**

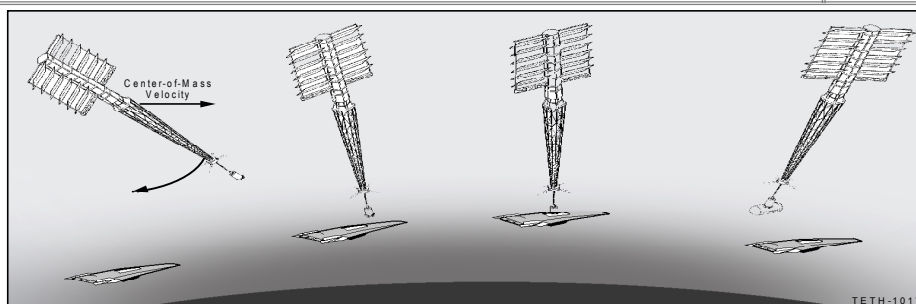
### **Hypersonic Airplane Space Tether Orbital Launch -- HASTOL**

### **Rendezvous and Capture Simulation Dan Nowlan, Karl Oittinen**

This presentation focuses on a discussion of the rendezvous and capture (R&C) simulation. This is a tool being used to design and analyze the critical R&C phase of the HASTOL system operations.

The discussion begins with a brief overview of the R&C scenario under investigation. Sensor, actuator and guidance software considerations are then presented. The R&C simulation is especially useful in identifying such hardware and software requirements. A specific R&C scenario simulation is then described in terms of a timeline/sequence of events, a block diagram and via a number of performance plots. An animation of this simulation is shown subsequently. The simulation discussion ends with the listing of a few specific tasks to be conducted in the near term.

# R&C Scenario Overview



## Space Tether (ST)

- 700km x 640 km orbit
- Main tether length = 600 km
- Grapple assembly tether length = 500 m
- CM perigee velocity = 7554 m/sec
- Main tether rotation rate = 0.33 deg/sec

## Hypersonic Airplane (HA)

- 200 feet long, 275,000 lb
- Main engine power off at rendezvous
- Apogee velocity = 4636 m/sec
- Due east trajectory
- Payload rotation & elevator mechanisms

## Rendezvous and Capture

- Altitude = 150 km
- ST at perigee, HA at apogee
- Velocity = Mach 17
- Equatorial plane

The picture characterizes the general R&C concept. The chart text provides specific details on the R&C scenario that is simulated.

The space tether (ST) is 600 km long and in an elliptical orbit. The nominal R&C point is at the ST perigee. There is also a 500 m grapple assembly tether. The grapple assembly is released just prior to the R&C point to allow the ST to free fall with the hypersonic airplane (HA). The ST center of mass (CM) velocity at perigee is ~ 7554 m/sec. The picture indicates that the ST rotation counters the CM velocity such that the tether tip net velocity equals that of the HA. A ST rotation rate of ~ 0.328 deg/sec produces a “countering” velocity of 2918 m/sec and a net tip velocity of 4636 m/sec.

The HA is assumed to be unpowered for the one minute prior to the nominal rendezvous point. It is flying a due east trajectory. It is assumed to have a mechanism which rotates the payload to the vertical position prior to capture. This puts the primary capture acceleration loads along the payload centerline axis which is similar to launch vehicle loads. A payload elevator mechanism is also modeled but not operative in this scenario simulation.

The overall R&C occurs at 150 km and Mach 17. The ST is at perigee while the HA is at apogee. The ST and HA trajectories are both in the equatorial plane.

# Rendezvous Sensor Considerations



<u>Concept</u>	<u>Considerations</u>
<b>HA - Active Ka band radar</b> <b>Grapple - Interactive radar beacon</b>	<ul style="list-style-type: none"> <li>• HA transmits interrogation waveforms</li> <li>• Grapple transmits response pulse train</li> <li>• Relative range/angles, range rates</li> <li>• Accuracy ~ 0.5 m</li> </ul>
<b>Grapple - Continuous radar beacon</b> <b>HA - Passive radar receiver</b>	<ul style="list-style-type: none"> <li>• Grapple transmits in R&amp;C timeframe</li> <li>• HA uses SBL/LBL interferometry</li> <li>• Derived relative position/rates</li> <li>• Angular accuracy ~ 0.05 deg</li> </ul>
<b>Grapple - GPS rcvr. comm. link</b> <b>HA - GPS rcvr. comm. link</b>	<ul style="list-style-type: none"> <li>• Grapple GPS P/V data sent to HA</li> <li>• HA GPS data provides its own P/V data</li> <li>• Satellite selection coordination possible</li> <li>• Can approach DGPS performance</li> <li>• Accuracy ~ 1.0 m</li> </ul>
<b>HA - P/L mechanism LRF</b>	<ul style="list-style-type: none"> <li>• Precise vertical separation</li> </ul>

Boeing personnel in St. Louis (John Castagno, Charlie Tolson, Pat McKillip) have identified several sensor configuration concepts to support the HASTOL rendezvous. These are listed in the table along with some corresponding operational and performance details.

The first concept has an active Ka band radar on the HA and interactive beacon on the ST grapple assembly. The HA transmits interrogation waveforms while the grapple beacon transmits a response pulse train after HA waveform detection. Relative range, angle and rate information is obtained with accuracies ~ 0.5 m.

A second concept has a ST grapple beacon providing a continuous signal during the R&C timeline. The HA has a passive radar receiver which performs short baseline (SBL) and long baseline (LBL) interferometry based on the received ST beacon signal. Relative range and rate information is derived with angular accuracies ~ 0,5 deg.

A GPS based concept is also identified. It includes GPS receivers and com links on both the ST grapple and HA. The ST grapple position and velocity (P/V) data is sent to the HA to perform the rendezvous guidance. The comm link also permits satellite selection coordination between ST and HA GPS receivers to enhance relative performance and approach differential GPS (DGPS) accuracies ~ 1.0 m.

A HA elevator mechanism is identified to provide vertical correction capability and permit vertical biasing of the ST and HA trajectories to enhance safety.

# GPS Performance Comparisons



<u>Error Source</u>	<u>PPS</u>	<u>DGPS (50km)</u>	
Ephemeris Data	2.1	0.0	} DGPS Gain
Satellite Clock	2.1	0.7	
Ionosphere	1.2	0.5	
Troposphere	0.7	0.5	
Multipath	1.4	1.4	
Receiver Measurement	0.5	0.2	} DGPS Loss
Reference Station Error	<u>N/A</u>	<u>0.4</u>	
UERE (rms)	3.6	1.8	
Filtered UERE (rms)	3.3	1.1	
Vertical (VDOP = 2.5)	8.3	2.8	
Horizontal (HDOP = 2.0)	6.6	2.2	

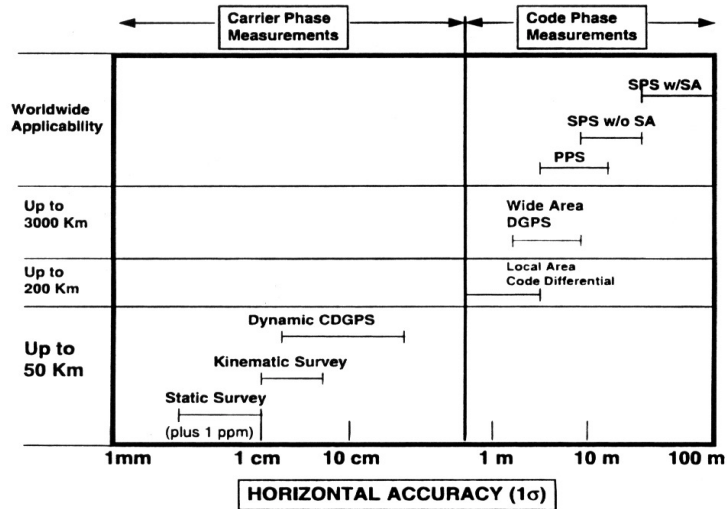
The radar based rendezvous sensor concepts typically have accuracies that improve with decreasing range. Divert requirements on the other hand become more demanding as maneuvers occur closer to rendezvous. A GPS based sensing concept offers the possibility of better performance at longer ranges and hence less demanding divert requirements.

This chart lists seven types of GPS errors along with their corresponding single receiver precise precision service (PPS) and differential GPS (DGPS) errors, in meters. Chart absolutes aren't as important here as the relative differences between PPS and DGPS performance.

DPGS provides a significant reduction in the first four error sources while adding an additional contributor (reference station error). It is felt that use of PPS receivers on the ST grapple assembly and HA with satellite selection coordination can approach DGPS performance. Additionally, the high altitude rendezvous may significantly reduce or eliminate the tropospheric error contributions and a portion of the ionospheric effects.



# DGPS Horizontal Accuracy



This figure illustrates the potential performance of various DGPS implementations. The ordinate describes GPS receiver separation from a ground reference station while the abscissa provides absolute horizontal accuracy information.

The HASTOL GPS sensor concept does not strictly involve a ground reference station. The HASTOL rendezvous focus is on accurate relative information. With this in mind, one can view the HA as the reference station. Referring to the figure, rendezvous accuracies of 1 m or less seem plausible.

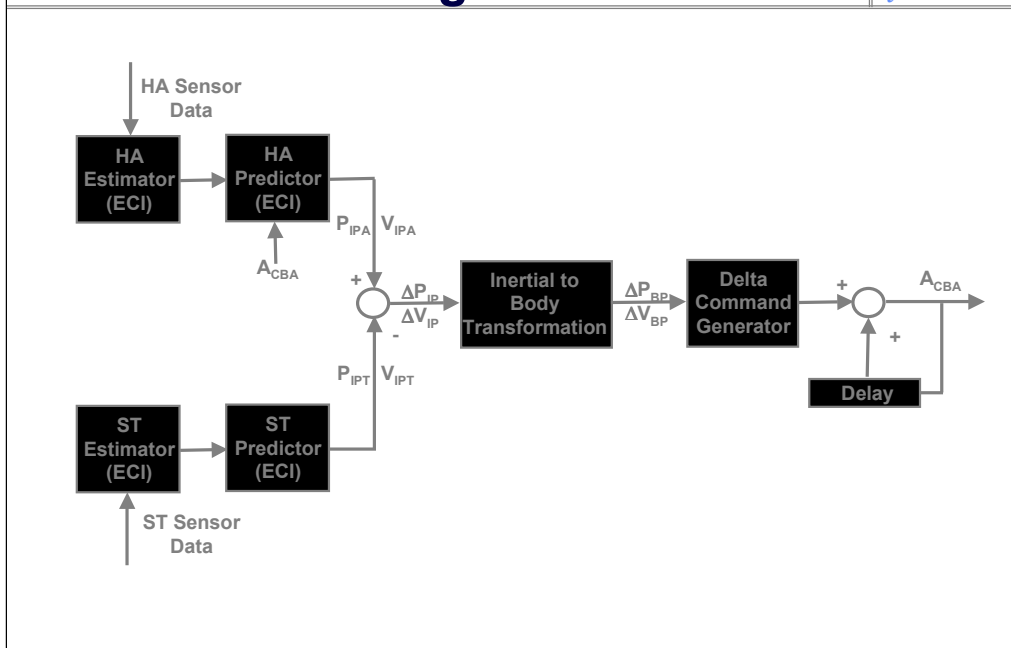
# Rendezvous Actuator Considerations



<u>Concept</u>	<u>Considerations</u>
<b>HA linear articulation</b> <ul style="list-style-type: none"><li>• Divert thrusters</li><li>• Rocket/TVC</li><li>• P/L rotation/elevation mechanism</li></ul>	<ul style="list-style-type: none"><li>• Relatively large (HA) mass to move</li><li>• Readily serviceable/replenishable</li></ul>
<b>Grapple linear articulation</b> <ul style="list-style-type: none"><li>• Divert thrusters</li><li>• Electric motor/plate</li></ul>	<ul style="list-style-type: none"><li>• Relatively small (grapple) mass to move</li><li>• Thrusters require replenishment</li></ul>

Rendezvous actuator concepts include equipment to move either the ST grapple assembly or the HA. Some options are identified in this figure. The HA is serviceable and expendables can be readily replenished. This is not the case with the grapple assembly. Therefore the approach is to first see if HA linear articulation schemes can accomplish the rendezvous without grapple articulation. From an actuator sizing viewpoint the HA is relatively large compared with the ST grapple assembly and will require larger control authority to produce similar relative motion.

# Rendezvous Guidance Block Diagram



This chart provides a block diagram of the rendezvous guidance algorithm. This is currently envisioned as a software package resident in the HA. The algorithm uses ST and HA sensor data to develop estimates of the current ST and HA positions and velocities in earth centered inertial (ECI) coordinates. An acceleration model then propagates the current states to the nominal rendezvous time. Position and velocity differences at rendezvous are then transformed to body coordinates and gained to produce the HA body linear articulation commands.

The HA predictor includes the previous acceleration commands ( $A_{CBA}$ ) in the prediction computations. These are assumed to decay as a function of guidance gains. This means that the command generator during any one cycle is producing a delta command. This is then added to the previous command to get a total command.

Earlier versions of the HA and ST predictors used curve fits for the three acceleration components. Sensitivity studies indicate that the HA acceleration model has to be quite accurate in order to minimize rendezvous state prediction errors. A dynamic HA acceleration model has been implemented and is in checkout.

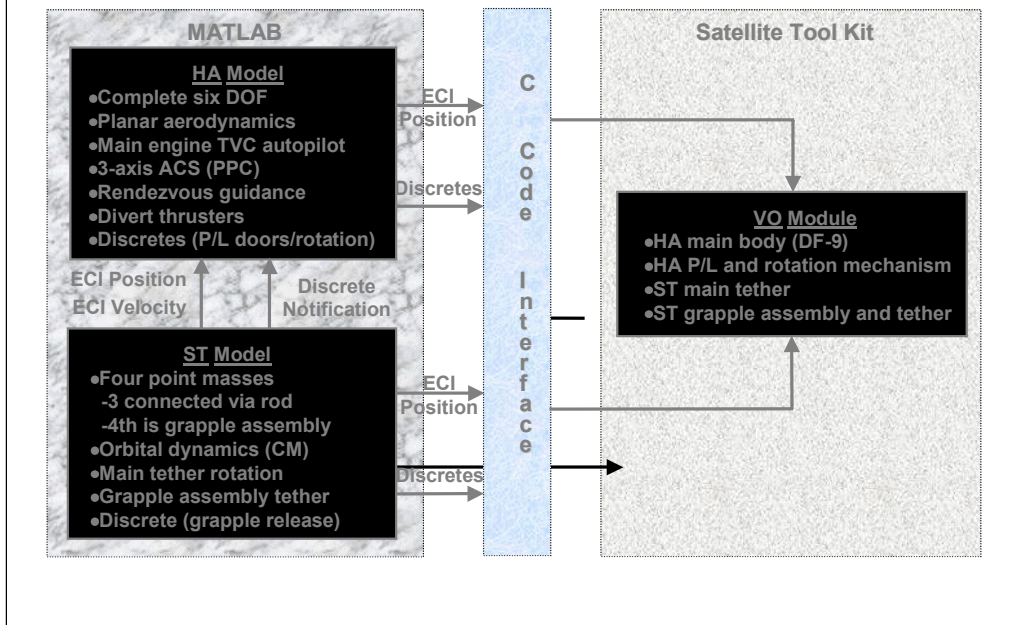
# R&C Scenario Timeline/Sequence of Events



<u>Time</u> (sec)	<u>Event</u>
0	Start R&C scenario
5	Initiate guidance predictions
15	Issue P/L bay door discrete
30	Issue P/L rotation mechanism commands
45	P/L rotation complete
58	Issue grapple assembly release discrete
60	Nominal capture point
65	End grapple assembly freefall
120	End R&C scenario

This table provides a timeline/sequence of events for the particular scenario simulated. The guidance predictor starts at 5 seconds. A HA payload bay door discrete is issued at 15 seconds by the HA rendezvous algorithm. Payload rotation mechanism commands are initiated at 30 seconds. Rotation rates are 6 deg/sec resulting in an upright payload position at 45 seconds. The grapple assembly is released at 58 seconds. The nominal capture point is 60 seconds. The grapple assembly continues in freefall until the grapple assembly tether reaches its maximum of 500 m at 65 seconds. The scenario concludes at 120 seconds.

# R&C Simulation Block Diagram



The R&C simulation block diagram is presented in this figure. The simulation is hosted on a Silicon Graphics workstation. It has detailed HA and ST dynamics and control models running in the MATLAB computer aided control system design environment. Position and discrete data is sent through a C-code interface to the Satellite Tool Kit (STK). The STK VO module is used to provide a visualization of the rendezvous and capture. Individually modeled bodies include the HA main body, HA payload (P/L) and rotation mechanism, ST main tether and ST grapple assembly and tether.

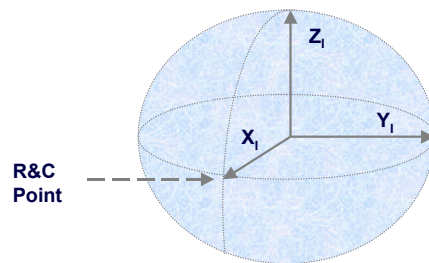
The HA model is a complete six degree-of-freedom model of the dynamics and control effects. It includes a thrust vector control (TVC) autopilot, a three-axis attitude control system (ACS) modeled after the Delta launch vehicle upper stage coast controller, the rendezvous guidance algorithm discussed previously, linear divert thrusters, and discrettes to initiate payload bay door opening and payload rotation.

The ST model consists of four point masses. Three masses model the two main tether body tips and the center of mass (CM). These are assumed to be connected via a rod which rotates around an imaginary pivot at the CM. The CM orbital dynamics parameters are initialized and then converted to ECI coordinates. The fourth mass models the grapple assembly. Prior to rendezvous this is allowed to freefall until its displacement from the third mass reaches 500 m. At this point it becomes dynamically constrained to the main body.

# R&C Scenario Simulation Plots



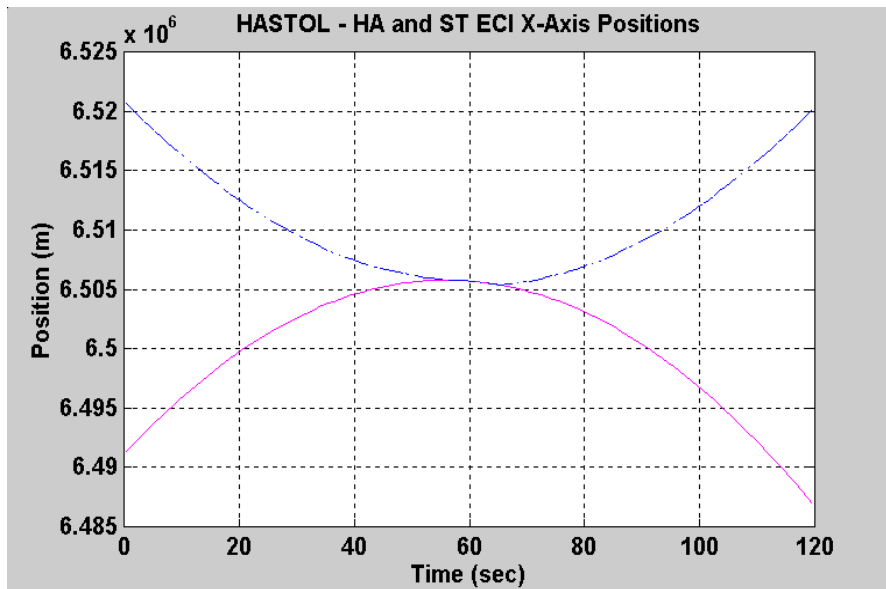
- Hypersonic airplane (HA) and space tether (ST) data
  - Absolute ECI positions, velocities, accelerations
  - Relative ECI positions, velocities, accelerations
  - ECI coordinates
- ECI coordinates
  - Selected time to align Earth fixed x-axis with vernal equinox
  - R&C essentially over the Greenwich meridian at the equator



This chart defines the types of plots to follow and the ECI coordinate system. The initial scenario time is selected to cause the nominal rendezvous point to occur over the Greenwich meridian at the equator.

The scenario essentially occurs in the x-y plane. There is very little out-of-plane (z-axis) motion.

# HA and ST ECI X-Axis Positions

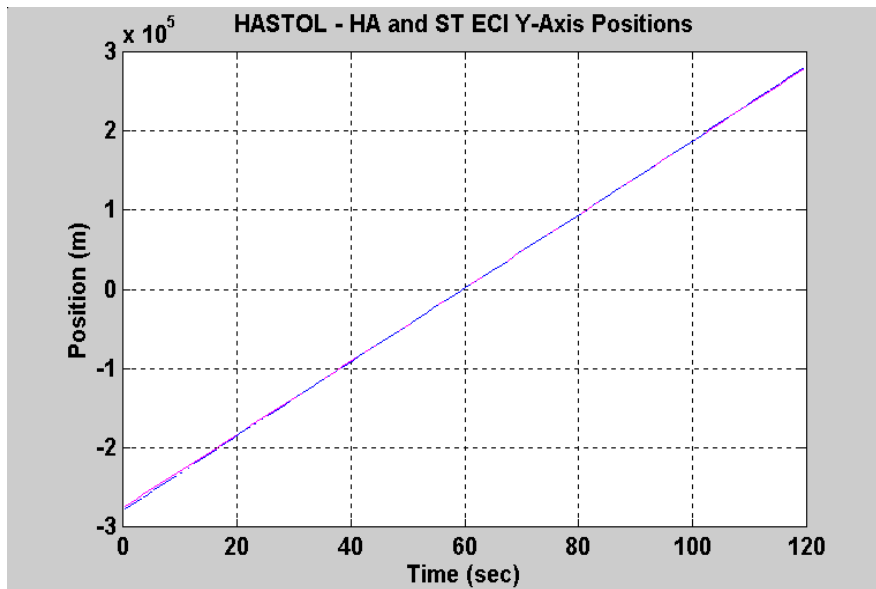


The charts with two curves all have the first identified parameter plotted as a solid magenta curve and the second plotted as a dashed blue curve.

The ST plots provide information for the ST grapple assembly.

The scale for these plots is about  $6 \times 10^6$  m. The curves indicate that at rendezvous the HA approaches apogee while the ST reaches perigee.

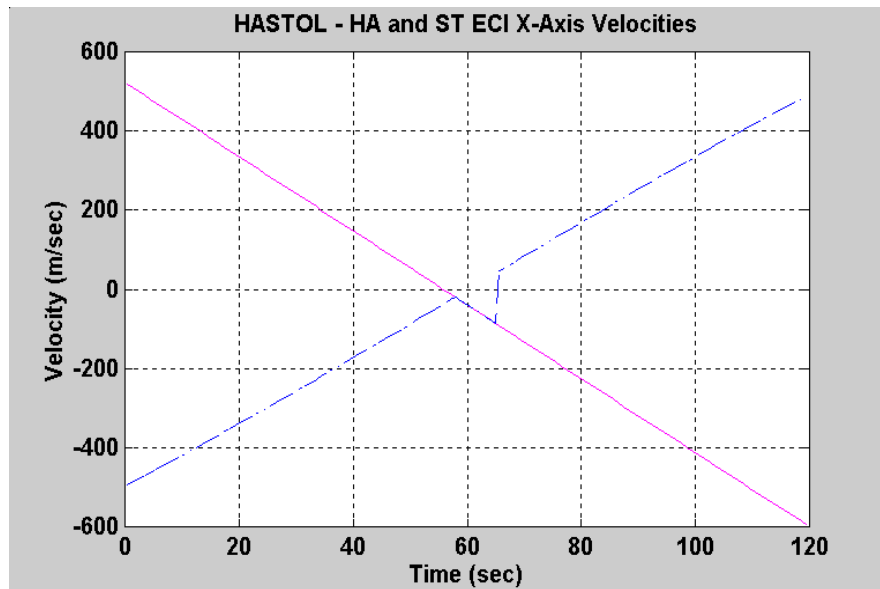
## HA and ST ECI Y-Axis Positions



The curves here show that the the ST grapple assembly and HA are reasonably close in the y-axis position for the entire R&C scenario duration.

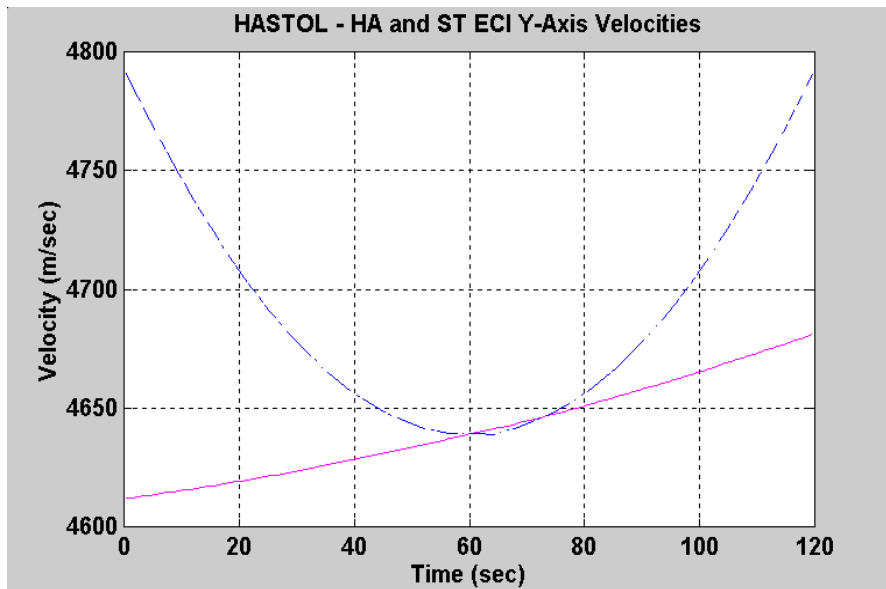


## HA and ST ECI X-Axis Velocities



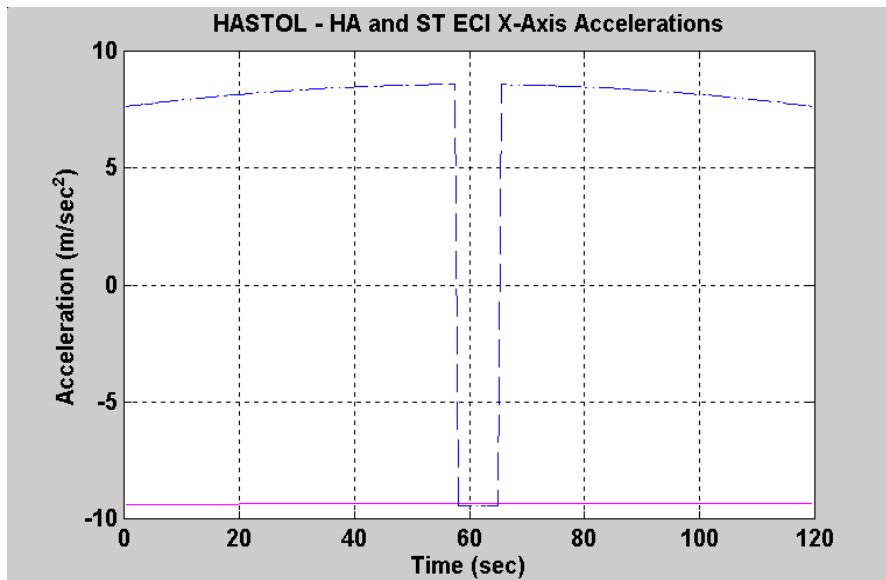
These curves provide some insight into the dynamics around rendezvous. Recall that the x-axis coordinate is essentially vertical at the rendezvous point. At 58 seconds the grapple assembly is released. The plots indicate that during the freefall period, the ST and HA vertical velocities are very close. Once the grapple assembly tether reaches its maximum length, its freefall ends. It is then effectively reattached to the ST main body.

# HA and ST ECI Y-Axis Velocities



These curves show that the nominal rendezvous velocity is 4636 m/sec or Mach 17. The flattened part of the ST curve around 60 seconds reflects the freefall dynamics.

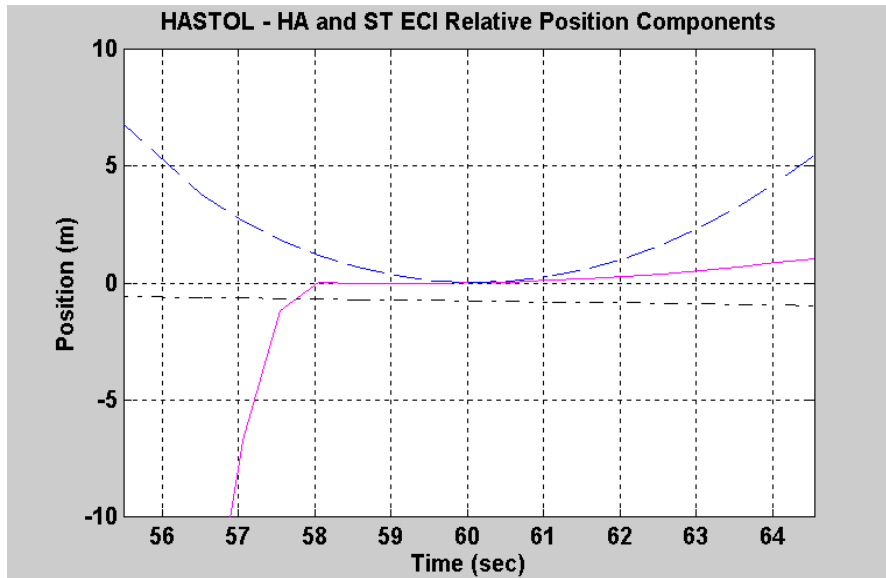
# HA and ST ECI X-Axis Accelerations



The x-axis acceleration plots are a direct indication of the freefall period. During the time period that the grapple assembly is allowed to drop from the ST main body, its accelerations are essentially the same as those for the HA. This provides more constant relative velocities and positions at rendezvous.

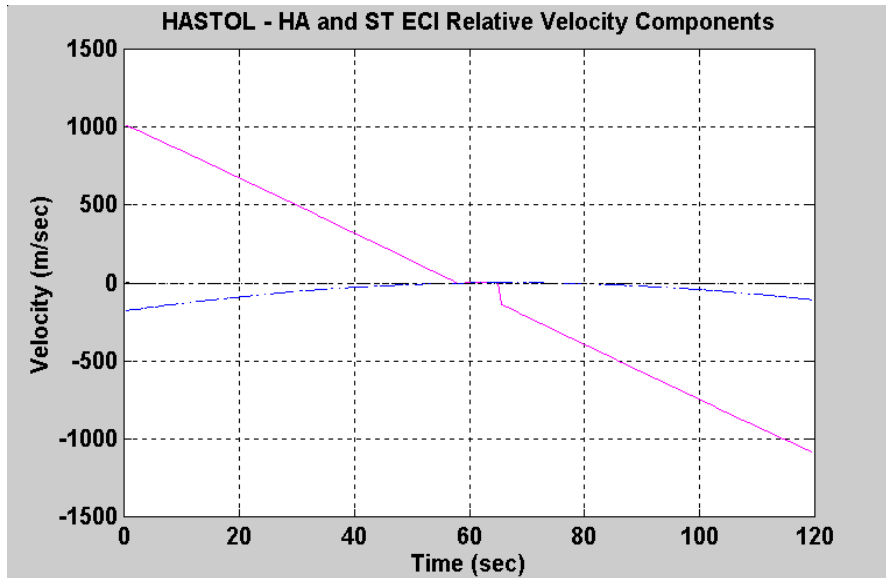
The stable freefall period in this scenario lasts about seven seconds. The interval can be made longer by using a longer grapple assembly tether. However this produces higher acceleration loads on the payload once the grapple assembly tether reaches its limit.

# HA and ST ECI Relative Positions



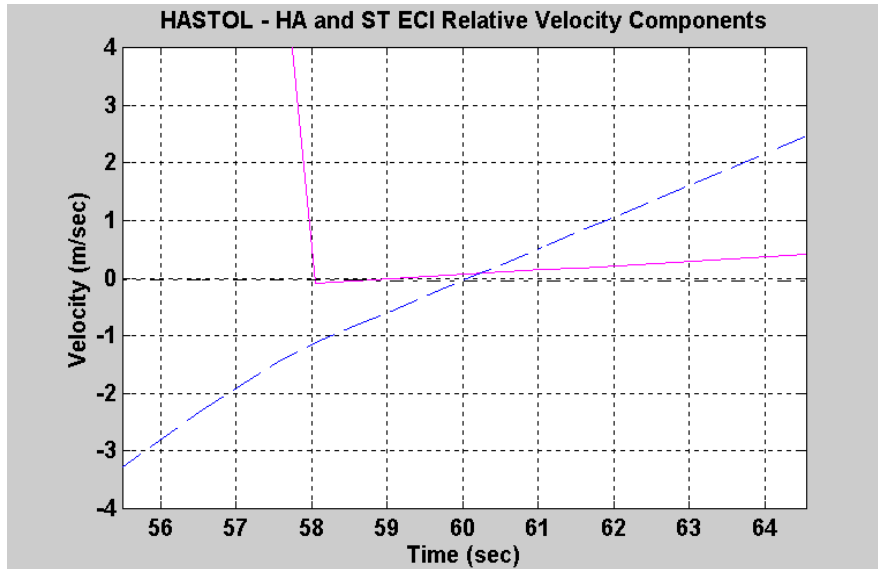
The data here represents an expansion of the previous plots around the rendezvous point. The x-axis and y-axis relative positions are essentially identical at 60 seconds. The z-axis relative position is under 1 m and can conceivably be reduced with a HA payload elevator.

# HA and ST ECI Relative Velocities



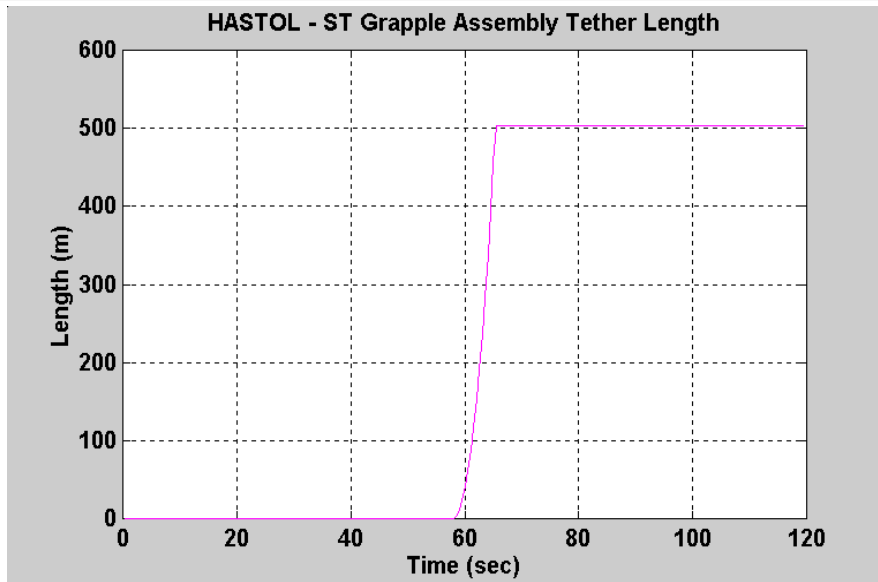
These plots show x-axis (solid magenta), y-axis (dashed blue), and z-axis (dashed black) relative velocities, computed as HA velocity - ST velocity. The x-axis relative velocities are ~ 1000 m/sec early on but are significantly reduced around the rendezvous point.

# HA and ST ECI Relative Velocities



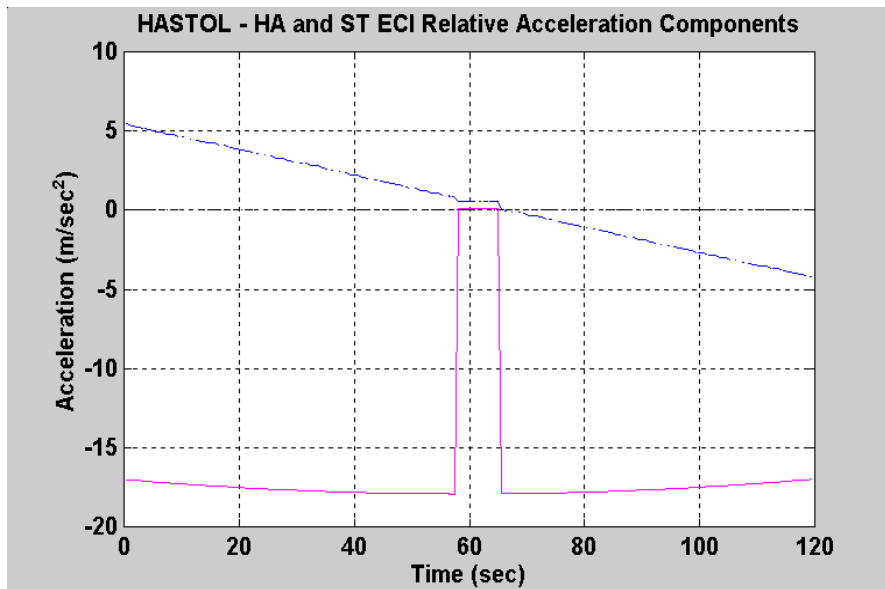
The data here represents an expansion of the previous plots around the rendezvous point. The x-axis and z-axis relative velocities are essentially identical at 60 seconds. The y-axis relative velocity is within  $\pm 0.6$  m/sec in the two second band around 60 seconds.

# ST Grapple Assembly Tether Length



This curve shows the grapple assembly tether length. It takes about seven seconds to reach its maximum of 500 m.

# HA and ST ECI Relative Accelerations



These plots show x-axis (solid magenta), y-axis (dashed blue), and z-axis (dashed black) relative accelerations, computed as HA acceleration - ST acceleration. The curves clearly show the freefall period and its influence on the relative dynamics. The x-axis and z-axis relative accelerations are extremely small around the nominal rendezvous point. The y-axis relative acceleration is about  $0.5 \text{ m/sec}^2$ .



## APPENDIX F

# HASTOL TETHER FACILITY DESIGN 2

Rob Hoyt

**Tethers Unlimited, Inc.**  
www.tethers.com

### System Design Requirements:

The requirements imposed upon the HASTOL tether facility design were:

- Capability to pick a payload up from a hypersonic airplane apogee of Mach 17 at 150 km altitude. Assuming the trajectories of the airplane and tether facility are in the Earth's equatorial plane, the velocity of the airplane at apogee, relative to the inertial frame, is 5,110 m/s.
- Payload capacity of 5,500 kg.
- Capability to toss payload to a Geostationary Transfer Orbit (GTO)
- Orbit of tether after payload toss shall be such that the tether tip cannot drop below 80 km altitude.
- Nominal acceleration level on payload while attached to tether is  $\leq 1.5$  gees.
- Peak acceleration level on payload is 3 gees.
- Capability to reboost facility to original orbit within 1 month.

### Design Method

The tether facility design was developed using the MX tether design Excel worksheet developed by TUI. This worksheet uses Keplerian orbital dynamics equations, a stepwise-tapered model of the tether mass, and an iterative solver to determine a tether facility design.

### System Design

The orbital parameters and mass sizing for the HASTOL Tether Facility are shown in Table 1. The tether masses just under 69 times the mass of the payload it is designed to boost. The tether itself masses 58.8 times the mass of the payload. The mass of the control facility was chosen to be 10 times the payload mass. More detailed data on the system design are given in Table 2. The tether tapering is shown in Figure 1; this tether taper was calculated using a safety factor of 3.0 for the entire tether.

The total mass of the facility is driven mainly by the need to keep the facility and tether above the Earth's atmosphere after the payload toss.

In order for the tether tip to be able to rendezvous with the hypersonic airplane, the tether must rotate with a tip velocity of 2.5 km/s. If the tether were to release the payload at the top of its rotation, it would give the payload an additional 2.5 km/s  $\Delta V$ , injecting it into a highly elliptical orbit with an apogee of 114,000 km. The system can, however, deliver the payload to other transfer orbits by releasing the payload before the tether reaches its vertical orientation. To deliver the payload into a GTO, the tether would release the payload when the tether is 38.63 from vertical. This will toss the payload into a 682x35,790 km transfer orbit. At its apogee, the payload would require a  $\Delta V$  of 1428 m/s to circularize into a GEO orbit.

### Reboost Power Requirements

When it captures and later tosses the payload, the tether facility transfers to the payload approximately 220 GJ of energy. In order to restore the facility orbit within one month using electro-

dynamic tether boosting, the tether facility must perform thrusting at an orbital average rate of 76 kW. Using the average thrust efficiency of 40  $\mu\text{N/W}$  calculated in previous simulations of the MMOSTT tether facility, and assuming that the tether facility is able to collect solar power during roughly 50% of its orbit, the tether facility will require a power supply capable of generating approximately 500 kW when illuminated.

**Table 1. Summary Data for HASTOL Tether Boost Facility Design**

<b>System Masses</b>		<b>Tether Characteristics</b>	
Tether mass	323,311 kg	Tether Length	636,300 m
CS Active Mass	51,510 kg	Tether mass ratio	58.78
<b>CS Ballast Mass</b>	<b>3490 kg</b>	Tether tip velocity at catch	2,517 m/s
Grapple mass	650 kg	Tether tip velocity at toss	2,481 m/s
<b>Total Facility Mass</b>	<b>378,961 kg</b>	Tether angular rate	0.00583 rad/s
		Gravity at Control Station	0.73 g
<b>Total Launch Mass</b>	<b>375,471 kg</b>	Gravity at payload	1.48 g
		Rendezvous acceleration	1.50 g
<b>Payload Mass</b>	<b>5,500 kg</b>		

<b>Positions &amp; Velocities</b>	<b>Pre-Catch</b>		<b>Joined System</b>	<b>Post-Toss</b>		
	<b>Payload</b>	<b>Tether</b>	<b>Post-catch</b>	<b>Tether</b>	<b>Payload</b>	
resonance	2.22	1	0	0	1	
perigee altitude	km	-4603	582	576	569	683
apogee altitude	km	150	805	650	512	35782
perigee radius	km	1775	6960	6954	6948	7061
apogee radius	km	6528	7183	7028	6890	42160
perigee velocity	m/s	18789	7627	7591	7559	9834
apogee velocity	m/s	5110	7390	7511	7622	1647
CM dist. From Station	m		204469	210647	204469	
CM dist. To Grapple	m		431831	425653	431831	
$\Delta V$ to Reboost	m/s				69	
$\Delta V$ to Correct Apogee	m/s					0
$\Delta V$ to Correct Precess.	m/s					58
$\Delta V$ To Circularize	m/s					1428

<b>Basic Orbital Parameters</b>							
semi-major axis	km	4152	7072	6991	6919	24610	
eccentricity		0.6	0.016	0.005	-0.004	0.713	
inclination	rad	0	0	0	0	0	
semi-latus rectum	km	2792	7070	6991	6919	12096	
sp. mech. energy	m <sup>2</sup> /s <sup>2</sup>	-4.80E+07	-2.82E+07	-2.85E+07	-2.88E+07	-8.10E+06	
vis-viva energy	m <sup>2</sup> /s <sup>2</sup>	-9.60E+07	-5.64E+07	-5.70E+07	-5.76E+07	-1.62E+07	
period	sec	2662	5918	5817	5727	38423	
period	min	44.4	98.6	97.0	95.5	640.4	
station rotation period	sec		1077.8	1077.8	1077.8		
rotation ratio			5.5	5.4	5.3		

**Table 2. HASTOL Tether Boost Station Orbital Parameters**

**HASTOL Tether Boost Station Orbital Parameters**

Nominal Tether Length: 630 km

**Rendezvous:**

Airplane Apogee Altitude 150 km  
 Airplane Apogee Mach# 17 mach  
 Airplane Vel. wrt Air 4635 m/s  
 Airplane Vel. wrt inertial 0 m/s

**Defined Constants**

GM Earth 3.986E+14 m<sup>3</sup>/s<sup>2</sup>  
 Earth radius 6378136.3000 m  
 Earth surface gravity 9.80655 m/s<sup>2</sup>  
 J2 1.08263E-03  
 J4 -1.61620E-06

desired payload final apogee 35786 km  
 total DV to payload 4998.9 m/s

**Tether Parameters**

system mass ratio 68.9  
 facility mass ratio 10.0  
 tether mass ratio 58.8  
 tether tip velocity at catch 2517 m/s  
 tether tip velocity at throw 2481 m/s  
 tether angular rate 0.00582973 rad/sec  
 gravity at endmass 0.73 g  
 gravity at payload 1.48 g  
 Rendezvous Acceleration 1.50 g

**System Masses**

tether mass	323,311 kg
CS Active Mass	51,510 kg
CS Ballast Mass	3,490 kg
CS Total Mass	55,000 kg
grapple mass	650 kg
<b>total mass</b>	<b>378,961 kg</b>
payload mass	5,500 kg

Positions / Velocities	pre-catch		joined system		post-throw			
	payload	tether CM	post-catch CM	pre-throw CM	tether CM	payload		
resonance ratio		2.223	1		1	6.71		
perigee altitude	ap	m	-4,602,810	581,831	575,653	575,653	569,475	682,603
apogee altitude	aa	m	150,000	805,000	649,985	649,985	511,737	35,782,107
perigee radius	rp	m	1,775,327	6,959,967	6,953,789	6,953,789	6,947,612	7,060,739
apogee radius	ra	m	6,528,136	7,183,136	7,028,121	7,028,121	6,889,873	42,160,243
perigee velocity	vp	m/s	18,789	7,627	7,591	7,591	7,559	9,834
apogee velocity	va	m/s	5,110	7,390	7,511	7,511	7,622	1,647
CM dist. From Station		m		204,469	210,647	210,647	204,469	
CM dist. To Grapple		m		431,831	425,653	425,653	431,831	
Reboost ΔV		m/s					69	
Perigee Tip Altitude		m		150,000	150,000	150,000	137,645	
Apogee Tip Altitude		m		373,169	224,332	224,332	79,906	
Tip Velocity wrt CM				2,517	2,481	2,481	2,517	
<b>Basic Orbital Parameters</b>								
semi-major axis	a	km	4151731	7071552	6990955	6990955	6918742	24610491
eccentricity	e		0.5724	0.0158	0.0053	0.0053	-0.0042	0.7131
inclination	i	rad	0	0	0	0	0	0
semi-latus rectum	p	km	2791504	7069791	6990758	6990758	6918622	12095756
sp. mech. energy	SME	m <sup>2</sup> /s <sup>2</sup>	-4.80E+07	-2.82E+07	-2.85E+07	-2.85E+07	-2.88E+07	-8.10E+06
vis-viva energy	C3	m <sup>2</sup> /s <sup>2</sup>	-9.60E+07	-5.64E+07	-5.70E+07	-5.70E+07	-5.76E+07	-1.62E+07
period	P	sec	2662.3	5918.1	5817.2	5817.2	5727.3	38423.0
period	P	min	44.4	98.6	97.0	97.0	95.5	640.4
period	P	hr	0.740	1.644	1.616	1.616	1.591	10.673
station rotation period		sec		1077.782	1077.782	1077.782	1077.782	
rotation ratio				5.491	5.397	5.397	5.314	

**Calculations for off-Vertical toss:**

Payload:

Tether angle at toss: -38.63 deg  
 -0.67422 radians  
 Tip Vel radial 1549.137 m/s  
 orbital 1938.488 m/s  
 Payload v radial 1549.137 m/s  
 orbital 9,530 m/s  
 Radius at toss 7286307 m

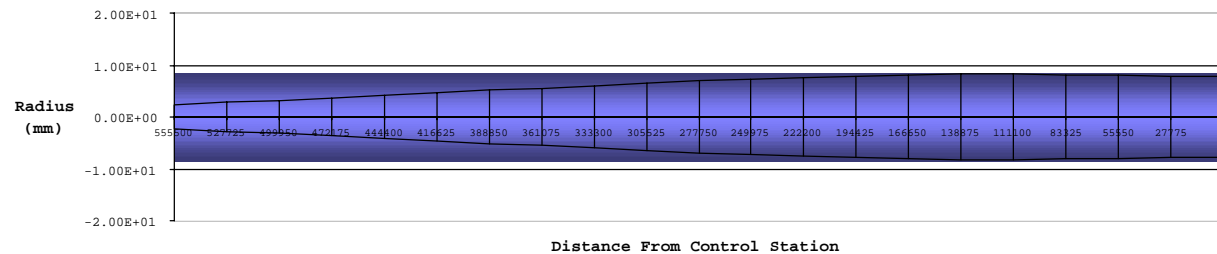


**Figure 1. Tether diameter (assuming tether were constructed as a single, solid cable).**

## Appendix G

### MODULAR DESIGN OF A TETHER BOOST FACILITY FOR EARTH-TO-ORBIT LAUNCH ASSIST

Robert P. Hoyt

**Tethers Unlimited, Inc.**

www.tethers.com

#### Introduction

The Hypersonic Airplane Space Tether Orbital Launch (HASTOL) System concept utilizes a reusable launch vehicle and a space tether in orbit around the Earth to launch payloads from the Earth's surface into orbit.<sup>1,2</sup> In order for the space tether component of such an ETO launch system to be capable of picking a payload up from a suborbital vehicle and boosting it into orbit, the tether system must have a mass many times that of the payload. This is due to the fact that orbital dynamics and momentum conservation require that the tether system have a mass significantly larger than the payload mass to keep the tether from dropping into the atmosphere after catching and tossing a payload. Current designs for a HASTOL tether facility mass between 60-70 times the mass of the payload it can transport. Such a tether system will have to be deployed in a modular fashion, with modules sized to fit within available launch vehicles. In this document we describe an evolved Tether Facility Concept which is designed to be built modularly. The first component deployed would be a 100 km long, fully operational Tether Facility capable of boosting 2,500 kg payloads from LEO to GTO. Subsequent modules would add tether length and power modules to increase the system capabilities so that it can boost 5,500 kg payloads from suborbital trajectories into orbit. A total of 20 launches would create a 636 km long Tether Boost Facility able to pick payloads up from an Reusable Launch Vehicle (RLV) flying at Mach 17 at 150 km altitude and either lift the payloads into LEO or boost them to GTO.

#### Modular Construction

To minimize the development and deployment costs of a HASTOL tether facility, the system should be designed so that it can be constructed of a number of essentially identical components. In this effort, we considered several approaches to modular construction of the tether system, including:

1. Deploying an initial full-length but "thin" tether facility with a low load capacity, then launching identical full-length thin tether facilities, which are ganged together in parallel with the initial facility to increase the total load capacity of the combined facility;
2. Deploying an initial launch facility, then attaching additional power modules to the control station and attaching additional lengths of tether in series and parallel;
3. Deploying an initial launch facility, then launching multiple nearly-identical tether facilities and combining them in series with the initial launch facility to create a longer, more capable tether with power/control stations spaced along the tether.

After evaluating these options, we concluded that the third method would likely provide the best solution because it will minimize the complexity of assembling the components and because spacing the power stations along the length of the tether will reduce the maximum voltages that must be applied to the tether.

A concept design for this modular tether architecture is illustrated in Figure G-1. The system sizing and orbital design is shown in Table G-1. The system sizing was calculated assuming that the tether is constructed primarily of Spectra 2000, which has a tensile strength of 4 GPa and a density of 0.97 g/cc.

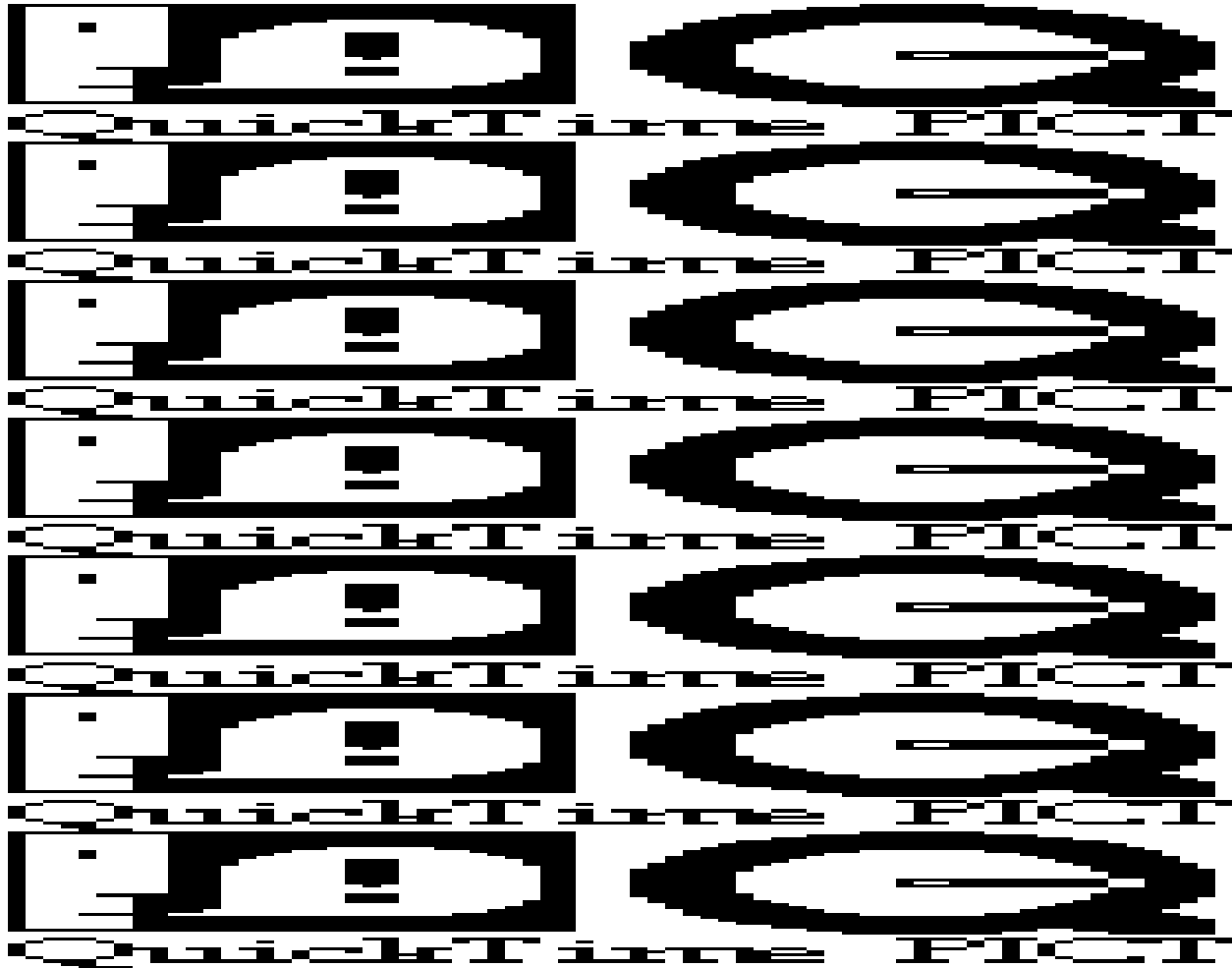


**Figure G-1.** Modular tether facility concept.

(The scale of the tether segments is greatly reduced in this image for illustrative purposes.)

The sizing was calculated with a safety factor of 3.0 for nominal loads. The calculation of the system sizing also took into account the mass of the expansion modules spaced along the tether.

The first components to be deployed would be a 13,750 kg control facility, a 650 kg grapple assembly, and a 8,000kg, 110 km long tether. This initial component would be sized to be launched into LEO on a Delta-IV-H vehicle. This first tether system will be capable of boosting 2,500 payloads from LEO holding orbits to geostationary transfer orbit.<sup>3</sup>

Once this initial tether facility has been deployed and its systems have been checked out by boosting several payloads to GTO, a second Delta-IV class launch vehicle would be used to bring an expansion module up to the tether facility. This expansion module would consist of a smaller power module and tether deployer massing 2,500 kg and an 81-km long tether massing approximately 13,000 kg. The expansion module would be attached to the existing facility in series, increasing the tether length. Additional launches of expansion modules would increase the tether length and facility power. Each expansion module would contain a tether deployer with a spool able to hold approximately 20 m<sup>3</sup> of tether (at a 75% packing efficiency).

#### *Tether Tapering*

To achieve the overall tapering of the tether necessary to minimize its total mass, each segment of tether would be constructed with a different total-line-area cross-section to cope with the stress in that segment,

while the length would be accordingly adjusted to fit within the deployer spool volume. The length of each segment is plotted in Figure G-2. In order for the tether to be capable of surviving the orbital debris and micrometeoroid environment for many years, the tether segments will be constructed in the Hoytether™ pattern, which spreads the tether material out in an open net configuration with multiple, interconnected lines, with the pairs of secondary lines interconnecting adjacent primary lines typically half the area (0.707 the diameter) of the primary lines. If these tether segments are constructed primary lines having diameters of 2 mm, the number of primary lines in the segments will vary between 24 at the grapple end of the tether to 206 at the center of mass of the system, as illustrated in Figure G-3.

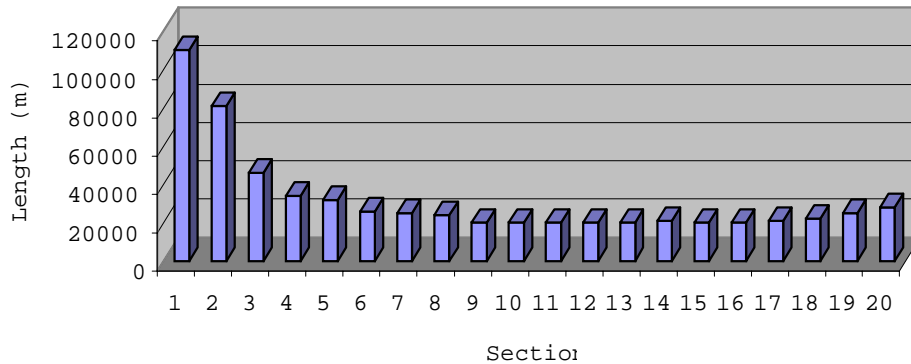


**Figure G-2.** Length of tether segments, chosen to fit within a 20 m<sup>3</sup> deployer volume.

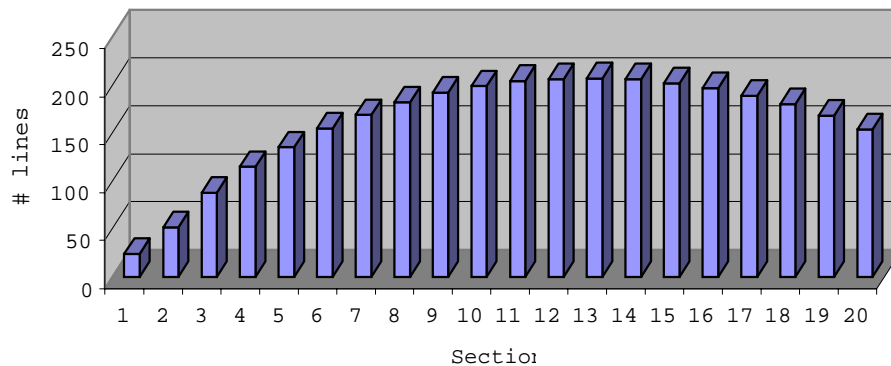


**Figure G-3.** Number of 2 mm diameter lines required to make up each segment of tether (includes both primary and secondary lines).

Alternatively, the number of primary lines could be held constant at 24, while the diameter of the primary lines would be made to vary from 2 mm in Segment 1, which is under the lowest stress, to 5.9 mm in Segment 13, which is under the highest stress.

*Catastrophic Damage Recovery Capability*

With this serial modular design, because the power and control stations are redundant and spread out along the length of the HASTOL facility, the facility is better able to cope with and recover from catastrophic damage or failure. If a power or control system module fails, the facility can still operate using the other 19 power/control modules. If the tether fails, the two parts of the facility on either side of the break still have the power and control capability to "fly" themselves using electrodynamic tether propulsion. Depending upon the orbits they are injected into at time of tether failure, the two segments should be able to establish safe orbits, then fly to and couple to the ends of to a replacement module.

**Table G-1. Summary of HASTOL Modular Tether Facility Design Concept**

<u>System Masses</u>		<u>Tether Characteristics</u>	
Tether mass	292,605 kg	Tether Length	636,300 m
Control Station Mass	17,240 kg	Tether mass ratio	53.20
<b>Total Expansion Module IV</b>	<b>47,500 kg</b>	Tether tip velocity at catch	2,522 m/s
Grapple mass	650 kg	Tether tip velocity at toss	2,478 m/s
<b>Total Facility Mass</b>	<b>357,995 kg</b>	Tether angular rate	0.005567 rad/s
<b># Delta-IVH Launches:</b>	<b>20</b>	Gravity at Control St	0.60 g
		Gravity at payload	1.41 g
<b>Payload Mass</b>	<b>5,500 kg</b>	Rendezvous acceleration	1.43 g

<u>Positions &amp; Velocities</u>		<u>Pre-Catch</u>		<u>Joined System</u>	<u>Post-Toss</u>	
		<u>Payload</u>	<u>Tether</u>	<u>Post-catch</u>	<u>Tether</u>	<u>Payload</u>
perigee altitude	km	-4603	603	595	549	700
apogee altitude	km	150	890	719	587	35744
perigee radius	km	1775	6981	6973	6927	7078
apogee radius	km	6528	7268	7097	6965	42122
perigee velocity	m/s	18789	7632	7594	7596	9820
apogee velocity	m/s	5110	7331	7461	7554	1650
CM dist. From Station	m		183241	191126	183241	
CM dist. To Grapple	m		453059	445174	453059	
<sup>2</sup> V to Reboost	m/s				78	
<sup>2</sup> V to Correct Apogee	m/s					1
<sup>2</sup> V to Correct Precess.	m/s					468
<sup>2</sup> V To Circularize	m/s					1426
Minimum Tip Altitude	km		150		134	
Maximum Tip Altitude	km		1343		1040	
<b>Basic Orbital Parameters</b>						
semi-major axis	km	4152	7125	7035	6946	24600
eccentricity		0.6	0.020	0.009	-0.003	0.712
inclination	rad	0	0	0	0	0
semi-latus rectum	km	2792	7122	7035	6946	12119
sp. mech. energy	m <sup>2</sup> /s <sup>2</sup>	-4.80E+07	-2.80E+07	-2.83E+07	-2.87E+07	-8.10E+06
vis-viva energy	m <sup>2</sup> /s <sup>2</sup>	-9.60E+07	-5.59E+07	-5.67E+07	-5.74E+07	-1.62E+07
period	sec	2662	5985	5873	5762	38398
period	min	44.4	99.7	97.9	96.0	640.0
station rotation period	sec		1128.7	1128.7	1128.7	
rotation ratio			5.3	5.2	5.1	

1. Grant, J., et al, "The HASTOL Tether System Applied to Commercial Launch", AIAA Paper 2001-3966, 37th Joint Propulsion Conference, Salt Lake City, UT, 8-11 July 2001.
2. Martin, J., Hollowell, S., "Vehicle Evaluations for Tether-Assisted Launch to Orbit", AIAA Paper 2001-1897, 10th International Space Planes and Hypersonic Systems and Technologies Conference, Kyoto, Japan, 24-27 April 2001.
3. Hoyt, R.P., "Design and Simulation of a Tether Boost Facility for LEO⇒GTO Payload Transport," AIAA paper 2000-3866, 36<sup>th</sup> Joint Propulsion Conference, Huntsville, AL, 17-19 July 2000.

## Appendix H

Submitted for publication in the Proceedings of STAIF 2002, Albuquerque, NM, 3-7 February 2002

### **Estimate of Avoidance Maneuver Rate for HASTOL Tether Boost Facility**

Robert L. Forward  
Tethers Unlimited, Inc.  
19011 36th Ave W, Suite F  
Lynnwood, WA 98236  
Phone: 425-744-0400; Fax: -0407; Cell: 206-391-4161  
Email: forward@tethers.com

#### **Abstract**

The Hypersonic Airplane Space Tether Orbital Launch (HASTOL) Tether Boost Facility will have a length of 636 km. Its center of mass will be in a 604 km by 890 km equatorial orbit. It is estimated that by the time of the start of operations of the HASTOL boost facility in the year 2020, there will be 500 operational spacecraft using the same volume of space as the HASTOL facility. These operational spacecraft would likely be made inoperative by an impact with one of the lines in the multiline HASTOL Hoytether™ and should be avoided. There will also be non-operational spacecraft and large pieces of orbital debris with effective size greater than five meters in diameter that could cut a number of lines in the HASTOL Hoytether™, and should also be avoided. It is estimated, using two different methods and combining them, that the HASTOL facility will need to make avoidance maneuvers about once every four days if the 500 operational spacecraft and large pieces of orbital debris greater than 5 m in diameter, were each protected by a 2 km diameter miss distance protection sphere. If by 2020, the ability to know the positions of operational spacecraft and large pieces of orbital debris improved to allow a 600 m diameter miss distance protection sphere around each object, then the number of HASTOL facility maneuvers needed drops to one every two weeks.

#### **Introduction**

The Hypersonic Airplane Space Tether Orbital Launch (HASTOL) Boost Facility<sup>1,2</sup> will have a very long, very wide rotating tether in a slightly elliptical orbit around the equator of the Earth. It is designed so that the tip of the tether can reach down to 150 km in altitude to pick up a payload from a hypersonic airplane or reusable rocket launch vehicle. As a result of its physical size and combined rotational and orbital motion, the tether facility will sweep out a large volume of space in the region between 150 km altitude and 1350 km altitude during its years of operation. There will also exist many large space objects in orbit between those same altitudes, some of them operational spacecraft. This analysis attempts to estimate the number of potential closest approaches per year between the tether facility and the operational spacecraft or large orbital debris objects that would require the HASTOL Tether Boost Facility to maneuver around the object by changes to its orbit, rotation, or shape to avoid a collision.

#### **HASTOL Tether Facility Interaction Area Parameters**

The HASTOL tether facility has a total length  $L=636$  km from the outer tip of the Tether Control Station (TCS) at one end of the tether to the grapple at the other end. During normal operation,



the HASTOL tether facility is rotating rapidly enough that the facility typically makes 5-6 rotations per orbit. The tether facility thus approximates a "randomly tumbling object". For a randomly tumbling object, the instructions<sup>3</sup> for the NASA/JSC ORDEM96.EXE program that generates an estimate of the orbital debris flux, recommends that the "effective" interaction area to be used with the flux estimate generated by the program should be the total surface area of the object divided by 4. For the diameter D of the tether, we can use either the physical diameter to calculate "collision" rates or a "stand-off" diameter to calculate "close approach" rates. For a tether of length L and diameter D, the surface area is  $A=\pi DL$ , and the "effective" interaction area is  $A/4$ . The flux F of objects generated by the NASA/JSC ORDEM96.EXE program for a given diameter of object, is given in units of "objects greater in diameter than the selected diameter per year per square meter of effective interaction area". Thus, the interaction rate C between the flux F of objects and the tether with given length L and diameter D is given by Equation (1):

$$C = \frac{AF}{4} = \frac{\pi}{4} DLF \quad . \quad (1)$$

The ORDEM96.EXE program produces estimates for all orbital debris objects in space, including very large spacecraft. It does NOT include any estimate for micrometeorites, which must be obtained from another NASA/JSC Technical Memorandum reference<sup>4</sup>. In the >1 m size range we are considering in this analysis, the number of orbital debris objects is much greater than the number of meteorites, so we can neglect the meteorite flux for this analysis.

#### **Selecting HASTOL Boost Facility Tether Diameter and Area**

As we shall see later, the major type of spacecraft that will require that the HASTOL Boost Facility undertake an avoidance maneuver, will be the numerous, very large Iridium spacecraft which operate at 776 km altitude, right in the middle of the operational altitude band of the HASTOL facility. The Iridium spacecraft body is 4.06 m long by 0.76 m wide along each of three sides of the triangular body. In a functioning spacecraft the body is aligned along the local vertical in a gravity gradient stabilized mode. At the upper end of the spacecraft are the two panels of the solar power array, which are 3.31 m long and 1.17 m wide. Including the structure holding the solar panels on the spacecraft body, on Iridium spacecraft has a "wingspan" of nearly 9 m. There are presently 87 Iridium spacecraft in 86.4 degree inclination circular orbits at an altitude of 776 km. Twelve of the spacecraft are not responding to ground commands and cannot be deorbited by the Iridium operators. By the time the HASTOL Boost Facility is operational in 2020, there will probably be 100 Iridium spacecraft in orbit, 66 operational, 6 spares, and the rest nonfunctional and unable to deorbit.

In order to insure tether survival if the avoidance maneuver fails and a collision occurs, we need to design the tether with a minimum diameter such that the tether can survive a passage of an Iridium spacecraft completely through the tether. By making the tether diameter a factor  $g>3$  times the 9 m wingspan of the Iridium spacecraft, we can limit the number of primary line cuts by the passage of the Iridium spacecraft to the point where the tether will not fail. The factor g will be determined by a number of parameters, primarily the nominal and peak stresses in the tether lines and the design of the Hoytether<sup>TM</sup>. For our initial selection, we will take  $g\sim 3$  and fix

the average working diameter of the tether as  $D=30$  m. If we select 24 primary lines for the Hoytether™, the spacing between the primary lines will be 3.9 m. If we select 18 primary lines, the spacing will be 5.2 m. The length of the Hoytether has been determined by the HASTOL design studies to be 636 km. Using this assumption, the total surface area of the HASTOL Boost Facility is  $A=\pi DL=6.0 \times 10^7 \text{ m}^2=60 \text{ km}^2=(7.75 \text{ km})^2!$

### **HASTOL Boost Facility Operational Parameters**

The HASTOL Boost Facility<sup>1,2,5-7</sup> will spend most of its time in a slightly elliptical equatorial orbit with an apogee of 890 km and a perigee of 604 km. The apogee velocity is 7331 m/s while the perigee velocity is 7631 m/s. The orbital period is 99.8 minutes and the rotation period is 18.8 minutes, or a ratio of 5.3 facility rotations per orbit of the facility center of mass. The center of mass of the facility will be 454 km from the grapple end and 182 km from the Tether Control Station end. Thus, the grapple end of the facility will scan over an altitude range that goes from a low of 150 km when the facility is at perigee and the grapple end is pointed toward the nadir, to a high of 1344 km when the facility is at apogee and the grapple end is pointed toward the zenith. The station end of the facility will scan the altitude range from 422 km to 1072 km. It should be noted that the rotation is not phased with the orbit, except at the time for payload pickup, so at perigee passage the grapple end of the tether would not necessarily be reaching down to 150 km (or up to 1344 km at apogee).

After the HASTOL Boost Facility has picked up a payload, but before it has tossed it, it will be in a 720 by 596 km orbit, with a period of 97.9 minutes. The rotation rate of the facility still remains at 18.8 minutes, since the payload had a velocity that matched the grapple velocity when it was picked up by the grapple. The center of mass of the HASTOL facility and the perigee drops 8 km during the pickup, and the apogee of the orbit drops 170 km, but the angular velocity does not change. For a half-rotation, lasting only 565 s or 9.4 minutes, the grapple end of the tether sweeps from 150 km to 1166 km, releasing the payload at the zenith angle for maximum boost to the payload, or earlier, if boost of the payload to a lower orbit is desired. It is only during this 9.4-minute period that the tether is under its maximum stress load.

After the payload has been released, the HASTOL Boost Facility drops into a circular orbit at 550 km altitude and a period of 96.0 min. With the release of the payload, the center of mass of the facility is now back at 454 km from the grapple end and 182 km from the TCS end. The rotational period of the tether has not changed from 18.8 min and is now at 5.1 rotations per orbit. The grapple end of the tether sweeps over the altitude range from 96 km to 1004 km, while the station end sweeps over the altitude range from 368 km to 732 km. The electrodynamic tether reboost system now starts operating to add energy and angular momentum to the facility orbit to raise the facility from a 550 km circular orbit to a 604 by 890 km elliptical orbit in preparation for the next payload boost operation. (Note that no energy or angular momentum needs to be added to the rotation of the tether as the boost operation does not change the tether rotation rate.) We thus see that the operators of the HASTOL Boost Facility need to identify and avoid large spacecraft or small operational spacecraft that orbit in the altitude range from 96 to 1344 km, with particular emphasis on the altitude range from 400 km to 1100 km.

### **Estimate Of The Number Of Spacecraft To Be Avoided**

The U.S. Space Command maintains a catalog<sup>8-10</sup> of all objects still in space that have been detected by their various radar and optical tracking systems. These objects range from ~10 cm diameter pieces of junk to the very large and growing International Space Station. To date, there have been 26,859 objects launched into space, of which 17,864 have deorbited, leaving 8995 objects in space. Of these 8995 objects, 6170 are pieces of space debris, 93 are space probes that have left Earth<sup>8</sup>, and 2732 are Earth orbiting satellites. Of these, 793 are in GEO<sup>9</sup>, leaving 1939 spacecraft below GEO. Of these 1939 spacecraft, it is estimated<sup>10</sup> that 546 are operational spacecraft. A list of the general spacecraft category types to be found in LEO, the 546 spacecraft that are operational, and the 385 spacecraft which pass through the altitude ranges scanned by the HASTOL tether, and which need to be avoided, is given in Table I. As can be seen, the 87 Iridium spacecraft represent over 20% of the objects to be avoided.

TABLE I - SPACECRAFT IN LEO

TYPE	TOTAL	ALIVE	AVOID	PERIGEE	APOGEE	INCLINATION
Iridium	87	73	87	779	776	86.4
Globalstar	52	52	0	1415	1412	52.0
GPS (NAVSTAR)	40	24	0	20200	20200	55.1
GLOSNAS	44	44	0	19125	19125	64.8
Cosmos	31	28	31	960	1010	83.0
Orbcomm	36	36	36	815	815	45.0
LEO Navigation	50	37	37	980	980	82.9
Molniya	27	27	0	S. Hem. 457	40860	62.8
Earth Resources	55	51	51	500	800	Mostly Pola
Space & Earth Science	50	47	42	500	800	Mostly Pola
LEO Weather	40	17	17	600	1200	Mostly Pola
Engineering	19	17	14	various	various	various
Radio Amateur	40	32	30	600	1000	Mostly Pola
Military	11	11	7	various	various	various
Classified (guess)	20	20	20	?	?	Mostly Pola
Other	42	30	30	various	various	various
TOTALS	644	546	402			

In evaluating the present-day population of LEO spacecraft, it is expected that some of the older spacecraft will fail or be turned off, while new spacecraft will be launched to replace them, resulting in a slow growth of the number of operational spacecraft. The probability of the launch of more constellations of LEO spacecraft does not look high, considering in the financial difficulties of Iridium, GlobalStar, Orbcomm, Teledesic, SkyBridge and others. It is therefore estimated that the population of operation spacecraft which will be operating in the altitude and inclination range swept out by the HASTOL Boost Facility in 2020 and beyond, will not grow significantly from the present 402 and will be about 500 spacecraft.

### Estimating Avoidance Maneuver Rate

The International Space Station, which operates at a nominal altitude of 400 km, is a special case that needs to be treated separately and given a wide margin. In addition, the ISS has the ability to maneuver itself out of the way if the tether facility somehow loses its ability to maneuver. The following analysis applies only to the remaining spacecraft in LEO. There are four ways one might go about estimating the avoidance maneuver rate.

### **Brute Force Direct Calculation Method**

As pointed out by Cooke, et al.<sup>11</sup>, probably the best way to estimate the rate at which the HASTOL Boost Facility will need to maneuver to avoid close encounters with operational LEO spacecraft would be the "Brute Force" approach. One obtains the orbital parameters of the 402 spacecraft in the "AVOID" column of Table I from the Space Command listing, generate similar orbital parameters for an additional 98 fictitious spacecraft, and "run" those 500 orbits against the orbital and rotational parameters for a HASTOL Boost Facility operating in an equatorial orbit with the orbital and rotational parameters mentioned earlier. This is time consuming to set up and run, but would give results that most people would "believe" in.

### **Intersecting Disk-Ring Method**

Cooke, et al.<sup>11</sup> also used the Matney, et al.<sup>12</sup> "Intersecting Disk-Ring" analytical method for calculating the close approach of a tether in a given orbit with a catalog of objects with different orbits that passed through the flat disk-ring region scanned by the tether, and got similar rates of close approach passes for both the "Brute Force" and the "Intersecting Disk-Ring" methods. Unfortunately, the Intersecting Disk-Ring method assumes that the tether is hanging vertically in a gravity gradient stabilized mode. In this constant vertical orientation of the tether, the tether is always moving at right angles to its length direction and scans out a flat, uniform width, disk-ring shape with a simple analytical description. A rapidly rotating tether, however, spends only a small part of its time moving at right angles to the tether length. For example, part of its time it is moving in "javelin" mode, with its velocity direction along its length, resulting in a very small interaction area. This complex mixture of tether motion and tether rotation results in a very complex shape for the swept area that would be difficult to handle analytically.

### **Swept Volume to Total Volume Ratio Method**

In this analysis, we will calculate the volume of space that is swept out by the tether over a year, and compare that with the total volume of space between the altitudes that the tether can visit. In that volume of space will be circulating the 500 spacecraft that need to be avoided. The number of avoidance maneuvers needed per year is then obtained by multiplying the ratio of the swept volume to the total volume times the number of spacecraft in the total volume.

The swept volume of the tether per unit of time will be calculated by multiplying the "effective" interaction area of the tumbling tether times its velocity. As shown by Cooke, et al.<sup>11</sup> in their Figure 3, and by Matney, et al.<sup>12</sup> in their Figure 5, the encounter rate can rise to very high levels when the tether is in an orbit that is the complement of the orbit of the spacecraft. Fortunately for ease of this analysis, that will not be the case for the HASTOL Boost Facility, which will be

in an equatorial orbit to service the GTO boost market, while nearly all LEO operational spacecraft are in orbits that are significantly inclined with respect to the equatorial orbit, so they can scan or service most of the Earth's surface. As we shall see later in Table II, the typical closing velocity estimated by the NASA/JSC ORDEM96.EXE program<sup>3</sup> between the HASTOL tether and the typical operational spacecraft ranges from 7.5 to 10 km/s and averages about 9 km/s. Since most of the interactions will take place at nearly the same velocity of 9 km/s, it is useful to switch to a different frame of reference, where the spacecraft to be avoided are assumed to be non-moving and scattered randomly around in the total volume reachable by the tether, while the tether moves through that space full of stationary objects at a fictitious "orbital" velocity equal to the closing velocity of  $v_C=9$  km/s.

The total volume  $V_T$  of the space around the Earth which the tether can interact with, ranges in altitude from a low of  $H_L=150$  km to a high of  $H_H=1344$  km, which are the highest and lowest point that the grapple end of the tether can reach under normal operation. After a toss, when the HASTOL Boost Facility center-of-mass is in a circular orbit at 550 km altitude, the grapple end of the tether will temporarily reach down to 96 km altitude, but the HASTOL Boost Facility will immediately initiate orbit reboost activities using its electrodynamic tether propulsion capability to raise the perigee to 604 km. From that point on, the lowest altitude the grapple can reach will be  $H_L=150$  km. With these assumptions, the total volume  $V_T$  where both the spacecraft and tether can interact, is given by Equation (2), with  $R_E=6371$  km as the mean radius of the Earth,  $H_L=150$  km, and  $H_H=1344$  km.

$$V_T = 4\pi \left[ (R_E + H_H)^3 - (R_E + H_L)^3 \right] = 2.3 \times 10^{21} \text{ m}^3 \quad (2)$$

One could argue that since most satellites are in orbits greater than 500 km in altitude, that the "total volume" where both spacecraft and the tether can interact, should be the volume of space between 500 and 1344 km. But then, we would have to calculate the time the two ends of the tether were not in the spacecraft-defined "total volume". By defining the total volume by the extent of the tether, we make the calculations easier and will probably get close to the same results.

The volume swept per unit time  $V_S(t)$  by the tether is the effective interaction area of the tumbling tether given by Equation (1) times the effective closing velocity  $v_C$  times the time  $t$  as shown in Equation (3):

$$V_S(t = 1 \text{ yr}) = \frac{\pi}{4} DLv_C t = 1.4 \times 10^{17} D \text{ m}^3 \quad , \quad (3)$$

where we have assumed that the length of the tether is  $L=636,000$  m, the closing velocity is  $v_C=9,000$  m/s, the time  $t=3.16 \times 10^7$  s is one year, and  $D$  is the effective diameter in meters of the avoidance region around tether.

The ratio of the two volumes gives the fraction of the total volume that the tether sweeps out in one year. The number of spacecraft  $n$  passing within a distance  $D/2$  of the tether during that year is the total number  $N=500$  of spacecraft to be avoided times the ratio of the two volumes, as given by Equation (4), where  $D$  is in meters:

$$n = N \frac{V_s}{V_T} = 0.030 D \quad , \quad (4)$$

If the minimum desired approach distance of the tether is taken as a kilometer or 1000 m, then D=2000 m. The HASTOL Boost Facility will need to make about 60 maneuvers a year, or an average of a little more than one a week.

If the avoidance distance is taken as 300 meters, ten times larger than the physical diameter of the tether, then D=600 m, and the HASTOL Boost Facility will need to make about 18 maneuvers per year or an average of one every 3 weeks.

We could consider NOT building an avoidance maneuver capability into the HASTOL Boost Facility, and just "take our chances" with hitting an existing space object. The physical collision radius is given by the physical radius of the tether plus the radius of the spacecraft. For a tether of diameter 30 m and a typical spacecraft with a nominal diameter of 5 m, the effective collision diameter is D=35 m. From Equation (4) it is seen that if the HASTOL facility does not engage in avoidance maneuvers, the tether will physically collide with one large operational spacecraft per year. Although the failsafe Hoytether™ design used in the HASTOL Boost Facility would allow the tether to survive most such impacts, the operational spacecraft would probably be rendered non-operational by an encounter with the "whiplash" of a low-mass but high-speed tether line hitting it at 9 km/s (Mach 34). If we assume that in addition to the 500 operational spacecraft, there are about 1000 upper stages, non-operational spacecraft, and other large pieces of orbital debris that are "wide" enough to be certain to cut one or more of the lines in the Hoytether™ as they pass through the tether, then the HASTOL facility tether will collide with about 3 large objects per year. This estimated significant potential collision rate indicates what we knew already - that the HASTOL Boost Facility MUST have a built-in capability to be aware of and avoid operational spacecraft plus large pieces of orbital debris.

#### **NASA/JSC ORDEM96.EXE Method**

Another method for obtaining an upper bound on the number of avoidance maneuvers that the HASTOL Boost Facility will need to make in a year, is to use the NASA computer program ORDEM96.EXE<sup>3</sup> to calculate the orbital debris flux for large diameter objects in space. The ORDEM96.EXE program does not distinguish between operational spacecraft and worthless orbital debris. Still, it would be wise for the operators of the HASTOL Boost Facility to avoid hitting any large objects, even if the failsafe Hoytether™ design will allow the tether to survive the resulting tether line cuts.

The ORDEM96.EXE program was activated and the orbital debris flux in number of objects per year per square meter of "interaction area" was obtained for objects larger in size than 1, 3 and 5 meters passing through the equatorial plane in the year 2020 over the altitude range from 1350 km to 200 km (the minimum altitude ORDEM96.EXE will accept). The results are tabulated in Table II.

TABLE II - FLUX OF LARGE SPACECRAFT FROM 200 TO 1350 KM ALTITUDE

ALTITUDE	FLUX (D>1m)	VELOCITY	FLUX (D>3m)	VELOCITY	FLUX (D>5m)	VELOCITY
(km)	( $10^{-7}/\text{m}^2\text{-yr}$ )	(km/s)	( $10^{-8}/\text{m}^2\text{-yr}$ )	(km/s)	( $10^{-9}/\text{m}^2\text{-yr}$ )	(km/s)
200	0.28	7.63	0.90	7.67	1.07	7.67
250	0.52	7.43	1.67	7.47	1.98	7.47
300	0.88	7.55	2.83	7.60	3.35	7.60
350	1.51	7.75	4.83	7.82	5.72	7.82
<b>400</b>	2.53	7.93	8.08	8.01	9.57	8.01
<b>450</b>	3.37	8.43	10.70	8.54	12.60	8.54
<b>500</b>	5.27	8.67	16.60	8.78	19.70	8.78
<b>550</b>	8.15	8.92	25.80	9.02	30.50	9.02
<b>600</b>	12.00	9.25	37.80	9.34	44.80	9.34
<b>650</b>	16.40	9.58	52.00	9.68	61.50	9.67
<b>700</b>	20.40	9.82	64.30	9.90	76.10	9.90
<b>750</b>	21.50	9.87	67.20	9.95	79.60	10.00
<b>800</b>	19.90	9.75	60.80	9.83	72.00	9.83
<b>850</b>	18.90	9.43	56.50	9.48	66.90	9.48
<b>900</b>	20.10	9.02	60.00	9.02	71.10	9.02
<b>950</b>	16.20	9.00	46.70	8.97	55.30	8.97
<b>1000</b>	11.10	9.04	31.60	9.01	37.40	9.01
<b>1050</b>	7.73	9.05	22.10	9.01	26.20	9.01
<b>1100</b>	5.60	9.07	16.00	9.04	19.00	9.04
1150	4.26	9.06	12.10	9.04	14.30	9.04
1200	3.36	9.02	9.49	9.00	11.20	9.00
1250	2.79	8.96	7.82	8.94	9.26	8.94
1300	2.65	8.95	7.49	8.92	8.87	8.92
1350	3.53	9.15	10.40	9.14	12.30	9.14
<b>CM-GRAPPLE</b>	8.71	8.85	26.40	8.88	31.26	8.88
<b>CM-STATION</b>	12.61	9.12	38.41	9.17	45.48	9.17

During most of its time in orbit, the center of mass of the HASTOL Boost Facility is in a 604 km by 890 km orbit (shown in bold italics in the ALTITUDE column). The Tether Control Station end of the tether, which is 182 km from the center of mass of the facility, scans through the altitudes from 422 km to 1072 km (shown in bold in the ALTITUDE column). The Grapple end of the tether, which is 454 km from the center of mass, scans through all the altitudes from 150 km to 1344 km.

Since we have the flux data information available by altitude, we have calculated separately the average flux seen by the two portions of the tether on either side of the center of mass. The average flux and velocity seen by the 454 km long portion of the tether from the center of mass to the grapple end of the tether is given in the row labeled "CM-GRAPPLE", while the average flux and velocity seen by the 182 km long portion of the tether from the center of mass to the Tether Control Station end of the tether is given in the row labeled "CM-STATION".

If we insert the flux  $F$  and the length  $L$  of each of the two portions of the tether into Equation (1) and sum them, we can get Equation (5) for the estimated "interaction rate"  $C$  for the whole tether as a function of the effective diameter or stand-off distance  $D$ .

$$C = \frac{\pi}{4} [F_G L_G + F_S L_S] D \quad , \quad (5)$$

where  $F_G$  and  $F_S$  are the flux levels seen by the grapple and station ends of the tether respectively, and  $L_G=454$  km and  $L_S=182$  km are the lengths of the two ends of the tether measured from the center of mass of the facility.

The effective closest approach distance  $D$  that signals the need for an avoidance maneuver, will be much larger than the physical diameter of the tether and can be assumed to be constant over the whole length of the facility. The effective diameter  $D$  for a "collision" will depend upon the physical diameter of the tether, which could vary along the tether if the tether is tapered. Since, however, we have decided to set the physical diameter of the tether at a minimum of 30 m so as to cope with strikes by very large spacecraft, we will assume the "taper" in the tether, needed to cope with the variation in stress in the tether, will be a variation in the thickness of the separate lines in the Hoytether™, and not a variation in the diameter of the Hoytether™ net itself.

For the case where it is desired to avoid coming near large spacecraft with effective widths greater than 5 m, the values of the flux parameters in Equation (5) are  $F_G=3.1 \times 10^{-8}$  objects/m<sup>2</sup>-yr and  $F_S=4.5 \times 10^{-8}$  objects/m<sup>2</sup>-yr. When these are inserted in Equation (5), along with the lengths  $L_G=454$  km and  $L_S=182$  km, we obtain Equation (6) for the yearly close approach rate  $C(>5m)$  at which spacecraft greater in diameter than 5 m have a close approach to within distance  $D/2$  of the tether, where  $D$  is in meters:

$$C(> 5m) = 0.017 D \text{ (close approaches/yr)} \quad . \quad (6)$$

If the closest approach distance is taken to be 1000 m, then  $D=2000$  m and Equation (6) estimates that the number of close approaches of spacecraft larger than 5 m in size will be 34 per year, which would require an avoidance maneuver about once every 10 days.

We can do a similar calculation for the close approaches of all objects greater than 3 m in size. For this case, the flux levels about an order of magnitude higher and are found from Table II to be  $F_G=2.6 \times 10^{-7}$  objects/m<sup>2</sup>-yr and  $F_S=3.8 \times 10^{-7}$  objects/m<sup>2</sup>-yr. When these are inserted in Equation (5), along with the lengths  $L_G=454$  km and  $L_S=182$  km, we obtain Equation (7) for the yearly close approach rate  $C(>3m)$  at which spacecraft greater in diameter than 3 m have a close approach within distance  $D/2$  of the tether:

$$C(> 3m) = 0.19 D \text{ (close approaches/yr)} \quad , \quad (7)$$

where again,  $D$  is in meters. If the closest approach distance is taken to be 10 times larger than the diameter of the tether, or 300 m, then  $D=600$  m and Equation (7) estimates that the number of close approaches per year of objects greater than 3 m in size will be 114, or about one every three days.

We can continue with a similar calculation for the close approaches of all objects greater than 1 m in size. For this case the flux levels are slightly higher and are found from Table II to be



$F_G=8.7 \times 10^{-7}$  objects/m<sup>2</sup>-yr and  $F_S=12.6 \times 10^{-7}$  objects/m<sup>2</sup>-yr. When these values are inserted in Equation (5), along with the lengths  $L_G=454$  km and  $L_S=182$  km, we obtain Equation (8) for the yearly close approach rate  $C(>1\text{m})$  at which spacecraft greater in diameter than 1 m have a close approach within distance  $D/2$  of the tether, where  $D$  again is in meters:

$$C(> 1\text{m}) = 0.49 D \text{ (objects/yr)} \quad , \quad (8)$$

If we subtract out the objects that are greater than 3 m in size, which we will be avoiding by maneuvering the HASTOL Boost Facility, that leaves a collision rate of objects larger than 1 m in size but smaller than 3 m in size, given by Equation (9), with  $D$  again in meters:

$$C(1-3\text{m}) = C(> 3\text{m}) - C(> 1\text{m}) = 0.30 D \text{ (objects/yr)} \quad . \quad (9)$$

If we assume that the physical diameter of the tether is 30 m and the physical diameter of the object is 3 m, then a collision will take place between the tether and the object when  $D=33$  m. We thus can expect a collision with an object bigger than 1 meter and less than 3 meters about 10 times a year, or a little less than once per month. These objects can cut only a few lines in the Hoytether, since we will have made the separation distance between the primary lines in the Hoytether™ about 4-5 m. As a result of this analysis, it looks like we do not need to track and avoid objects smaller than 3 meters in diameter unless we know they are operational spacecraft. [If the operational spacecraft are smaller than 1 meter in size, it is quite likely they will pass through the Hoytether™ net, with its 4-5 meter spacing between the primary lines, without striking any of the lines!]

### Combining Two Analyses

The two analyses calculate tether interactions between different classes of space objects. The Volume Ratio Method only deals with operational spacecraft and ignores very large pieces of "space junk" that could harm the HASTOL Hoytether™. The NASA/JSC method allows us to estimate the interaction of the tether with all types of large space objects, including large pieces of space junk. The large object estimates using the NASA/JSC method include most of the operational spacecraft, but not all of them, since many science, engineering, and amateur payloads (about 15% of the 402 in Table I) are smaller than 3 meters in diameter.

If we assume that an avoidance maneuver should be initiated if the tether will approach within 1 km of an operational spacecraft or piece of orbital debris greater than 5 km, then from the discussion after Equation (4) we find that there will need to be 60 maneuvers per year to avoid operational spacecraft, while from the discussion after Equation (6) there will need to be 34 maneuvers per year to avoid space objects greater than 5 m in diameter - some of which are operational spacecraft and some of which are dead spacecraft or large upper stages. Since, of the 1939 payloads in the present U.S. Space Command catalog, only 546 or 28% are listed as "alive" in Table I, and the remaining 72% are large pieces of space junk, and we apply that same percentage to the 34 maneuvers due to space objects greater than 5 m in diameter, we get an estimate of 25 maneuvers due to space objects larger than 5 m in diameter that are not operational spacecraft. Combining the two estimates produces an estimate of a total of 85 maneuvers of the HASTOL facility per year to avoid coming within a two kilometer diameter "protection sphere" around not only all operational spacecraft, but all space objects large enough

to endanger the HASTOL Hoytether™. This annual rate would require the HASTOL facility to initiate an avoidance maneuver on the average of once every 4 days.

By 2020 the U.S. Space Command should be able to predict the future position of operational spacecraft and large pieces of space junk to 300 m or better, especially considering that the large objects have a large radar signature and a low drag area to mass ratio. Also, most operators of operational spacecraft in LEO will be able to furnish an accurate position fix of their spacecraft by using the GPS constellation at 20,200 km altitude above them. If we assume a 300 m closest approach instead of a 1000 m closest approach, or a decrease in distance  $D$  by a factor of 3.33, the total number of maneuvers needed per year would drop from 85 per year to 25 per year. This would require the HASTOL facility to initiate an avoidance maneuver only about once every two weeks.

### Summary

We have estimated the interaction rate of the larger objects in Earth orbit with a very large diameter, very long HASTOL Boost Facility tether operating between 150-1350 km altitude in an equatorial Earth orbit by two different methods. One method considers only operational spacecraft and compares the scanned volume of the tether with the total volume in which the operational spacecraft orbit. The other method estimates the interaction rate of the total large space object flux in Earth orbit with the two ends of the tether. Both methods gave comparable results. The two results were then combined, taking into account the different space object populations they represented. It was estimated that the HASTOL facility will need to make avoidance maneuvers about once every four days, if the 500 operational spacecraft and the large pieces of orbital debris greater than 5 m in diameter were each protected by a 2 km diameter miss distance protection sphere. If by 2020, the ability to know the positions of operational spacecraft and large pieces of orbital debris has improved to allow a 600 m diameter miss distance protection sphere around each object, then the number of required HASTOL facility maneuvers drops to once every two weeks.

### Acknowledgements

This work was supported by a subcontract with The Boeing Company under the "Hypersonic Airplane Space Tether Orbital Launch Architecture Study" with the NASA Institute for Advanced Concepts, Bob Cassanova, Director.

### References

1. Robert L. Forward, Thomas J. Bogar, Michal E. Bangham and Mark J. Lewis, "Hypersonic Airplane Space Tether Orbital Launch (HASTOL) System: Initial Study Results", Paper IAF-99-S.6.05, 50th IAF Congress, Amsterdam, The Netherlands, 4-8 October 1999.
2. Thomas J. Bogar, Michal E. Bangham, Robert L. Forward, and Mark J. Lewis, "Hypersonic Airplane Space Tether Orbital Launch (HASTOL) System: Interim Study Results", Paper AIAA-99-4802, 9th Space Planes and Hypersonic Systems and Technologies Conference, Norfolk, VA, 1-5 November 1999.
3. D.J. Kessler, J. Zhang, M.J. Matney, P. Eichler, R.C. Reynolds, P.D. Anz-Meador, and E.G. Stansbery, A Computer-Based Orbital Debris Environment Model for Spacecraft Design and

- Observations in Low-Earth Orbit, NASA TM-104825, Johnson Space Center, Houston, TX, 1996. [See internet web site: <<http://www.orbitaldebris.jsc.nasa.gov/model/ordem96.html>> to download paper and the computer program ORDEM96.EXE that can be used to obtain an estimate of the orbital debris flux as a function of object size, altitude, orbit, and velocity.]
4. B. Jeffrey Anderson, Editor and Robert E. Smith, Compiler, Natural Orbital Environment Guidelines for Use in Aerospace Vehicle Development, Section 7 - "Meteoroids and Orbital Debris", Don Kessler and Herb Zook, NASA TM-4527, June 1994. [See specifically Fig. 7-2 "Comparative Debris and Meteoroid Fluxes" on page 7-4.]
  5. Robert P. Hoyt, "Design and Simulation of Tether Facilities for the HASTOL Architecture", AIAA Paper 2000-3615, 36th Joint Propulsion Conference, 17-19 July 2000.
  6. John Grant, John Martin, Dan Nowlan, Brian Tillotson, and Robert P. Hoyt, "The HASTOL Tether System Applied to Commercial Launch", AIAA Paper 2001-3966, 37th Joint Propulsion Conference, Salt Lake City, UT, 8-11 July 2001.
  7. Robert P. Hoyt, "Modular Design of a Tether Boost Facility for Earth-To-Orbit Launch Assist", Subcontract Report for Boeing HASTOL Contract with NIAC. (July 2001).
  8. U.S. Space Command, "Satellite Box Score", <<https://www.cheyennemountain.af.mil/cmoc/boxscore.htm/>>. [Note "s" after "http".]
  9. NASA Goddard Space Flight Center, "Orbital Data", <<http://oig1.gsfc.nasa.gov/>>.
  10. T.S. Kelso, "Celestrak", <<http://celestrak.com/>>
  11. William J. Cooke, David B. Spencer, B. Jeffrey Anderson, and Robert M. Suggs, "Tether Survivability and Collision Avoidance: Is LEO the Right Place for Tethered Systems?", Proceedings STAIF 2001 Forum, Albuquerque, NM, 11-15 February 2001.
  12. Mark Matney, Donald Kessler, and Nicholas Johnson, "Calculation of Collision Probabilities for Space Tethers", Paper IAA-00-IAA.6.5.02, 51st IAF Congress, Rio de Janeiro, Brazil, October 2000.

## Appendix I

Submitted to 38th AIAA/ASME/SAE/ASEE Joint Propulsion Conference, Indianapolis, Indiana, 7-10 July 2002

### **HASTOL Tether Boost Facility Module Replacement Rate Due to Space Impactor Cuts**

Dr. Robert L. Forward  
Tethers Unlimited, Inc., 19011 36th Avenue West, Suite F  
Lynnwood, WA 98036-5752  
Phone: 425-744-0400; Fax: -0407; Email: <Forward@tethers.com>

#### **Abstract**

This analysis calculates the long term effect of multiple cuts by small orbital debris and micrometeorite impactors of the line segments in the failsafe Hoytether™ structure presently planned as part of the Hypersonic Airplane Space Tether Orbital Launch (HASTOL) Tether Boost Facility. We find that with the present modular Hoytether™ design, using presently available tether materials, that of the 20 tether modules in the Hoytether™, 18 of them will never need replacement in the 30 year commercial operational lifetime of the facility. Of the two remaining portions, the longest, thinnest tether module at the grapple end of the facility will need replacement after 8.5 years, while the next longest, next thinnest tether module from the grapple end will need replacement after 15 years. These time-between-replacement rates could be increased to 100 years or more with improvements in the strength of tether materials or the use of a more complex "fractal" Hoytether™ design, where the lines in the main Hoytether™ are themselves mini-Hoytethers™.

#### **Introduction**

The Hypersonic Airplane Space Tether Orbital Launch (HASTOL) Architecture<sup>1-3</sup> utilizes the combination of a hypersonic airplane meeting up with an orbiting rotating tether boost facility to launch payloads from the Earth's surface and place them into orbit, as shown in Figure 1. The HASTOL Tether Boost Facility<sup>4,5</sup> will have a very long (636 km), very wide (>30 m diameter) rotating tether in a slightly elliptical 603 km by 890 km altitude orbit around the equator of the Earth. It is designed so that the tip of the tether can reach down to 150 km in altitude to pick up a payload from a Mach 17 hypersonic airplane (or a reusable sub-orbital launch vehicle). As a result of its large physical size and combined rotational and orbital motion, the tether will sweep out a large volume of space in the region between 150 and 1343 km altitude during its years of operation. The tether to be used in the HASTOL facility will be a long-life failsafe Hoytether™ structure<sup>6</sup> which can reliably survive multiple cuts of its tether line segments by small micrometeorite and orbital debris (M/OD) impactors<sup>7</sup>.

In order for the Tether Boost Facility of such an ETO launch system to be capable of picking a payload up from a suborbital vehicle and boosting it into orbit without the facility dropping down into the upper atmosphere in the process, the facility must have a mass many times that of the payload. Current designs for a HASTOL Tether Boost Facility<sup>5</sup> have a mass between 60-70 times the mass of the payload it is designed to boost. Such a tether system will have to be deployed in a modular fashion, with modules sized to fit within available launch vehicles.

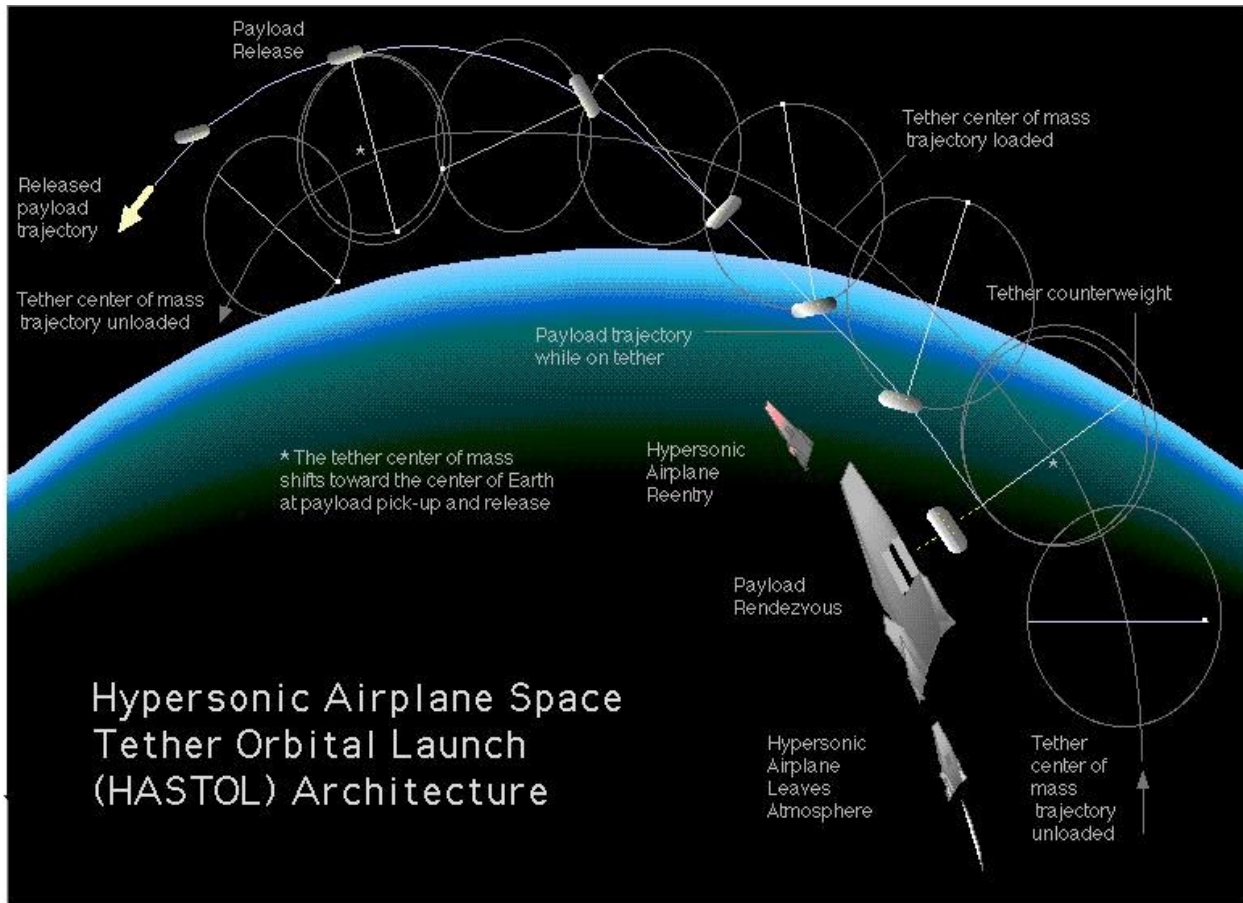


**Figure 1.** Hypersonic Airplane Space Tether Orbital Launch (HASTOL) Architecture

### Modular Construction

To minimize the development and deployment costs of a HASTOL Tether Boost Facility, the facility has been designed so that it can be constructed of a number of essentially identical components. The modular construction method selected consists of deploying an initial tether boost facility, small - but fully functional - then launching additional nearly-identical modules consisting of a power and tether deployer station with its tether. These modules would be combined in series with the initial tether boost facility to create a longer, more capable tether boost facility with power stations spaced along the tether, as illustrated in Figure 2. The tether boost facility size and mass was calculated assuming that the tether is constructed primarily of presently commercially available Spectra™ 2000, with a specific density of 0.97 g/cc and a breaking tensile strength of 4.0 GPa, with the tether operated with a safety factor of 3.0 for nominal loads. The calculations of the system mass also took into account the mass of the power and tether deployer station modules spaced along the tether.

The first module was sized so it could be launched into LEO on a single Delta-IV-Heavy launch vehicle. It consists of a 17,240 kg main Tether Control Station, a 650 kg grapple assembly, and a 110 km long, 8000 kg tether. This first module will be a completely functional Tether Boost Facility and would be capable of boosting 2,500 kg payloads, which have been placed into LEO holding orbits by expendable launch vehicles, into a geostationary transfer orbit (GTO).

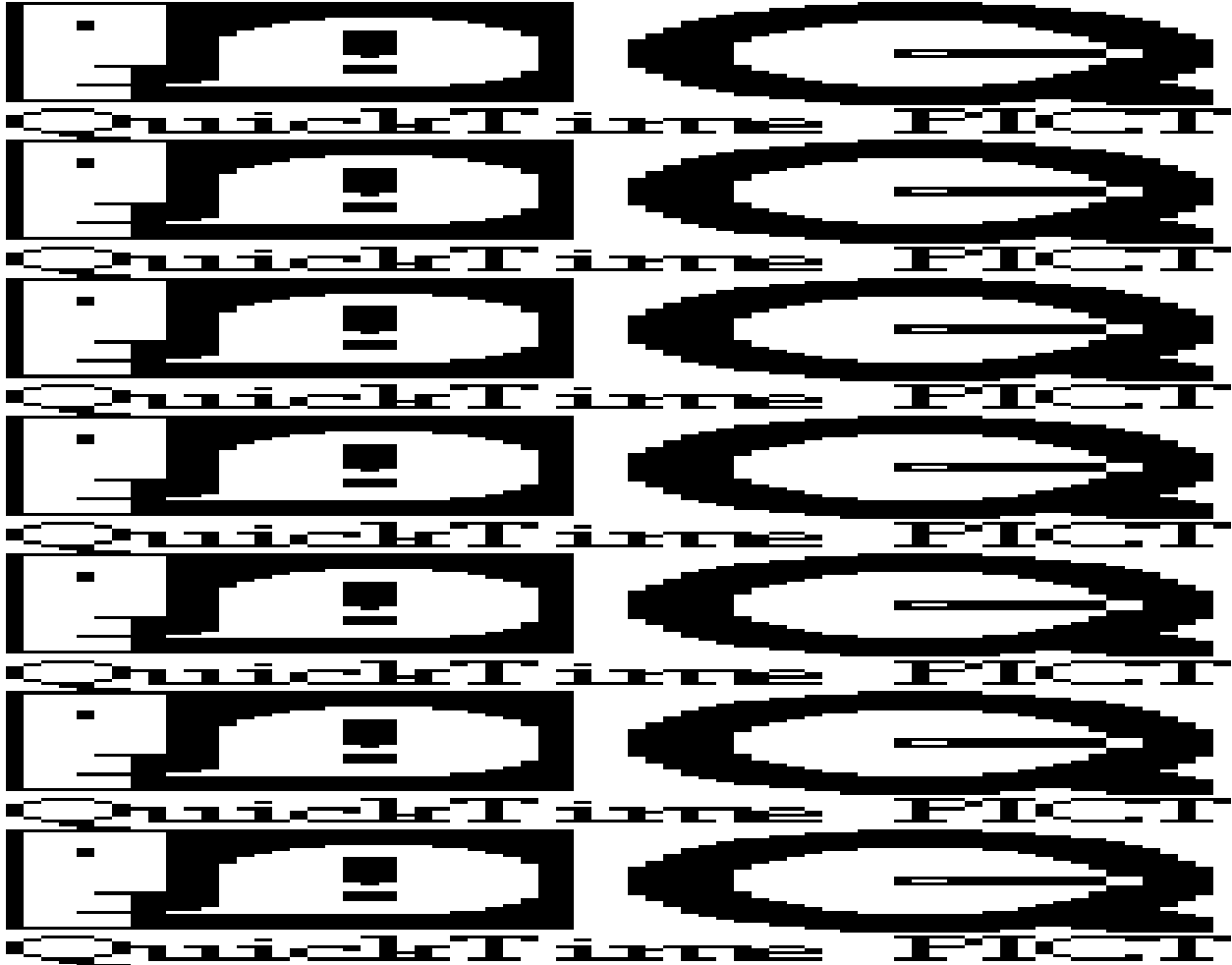


**Figure 2.** Modular tether facility concept.

(The scale of the tether segments is greatly reduced in this image for illustrative purposes.)

Once this initial Tether Boost Facility has been deployed, and its systems have been checked out by boosting several payloads from LEO to GTO, 19 additional Delta-IV class launch vehicles would be used to bring 19 additional expansion modules up to the tether facility. Each expansion module would consist of a small power and tether deployer station massing 2,500 kg containing a tether deployer with a spool able to hold approximately 20 m<sup>3</sup> of tether (at a 75% packing efficiency), massing approximately 13,000 kg. The length of the tether in each module would be determined by the thickness of tether lines needed for that module. Each expansion module would be attached to the existing facility in series, increasing the tether length. A total of 20 launches would create a 636 km long Tether Boost Facility able to pick up 5,500 kg payloads from a hypersonic airplane or a reusable sub-orbital launch vehicle flying at Mach 17 at 150 km altitude, and either lift the payloads into LEO or MEO, or boost them to GTO.

### Hoytether™

The tether structure which will be used in the HASTOL Tether Boost Facility will be a long-life, failsafe, interconnected multiline net structure called the Hoytether™. The Hoytether™ concept was invented by Robert P. Hoyt while he was a graduate student working for Dr. Robert L. Forward on a 1992 NASA study contract to design Failsafe Multiline Tether Structures for Space Propulsion<sup>6</sup>, and was given the now-trademarked name of Hoytether™ by Dr. Forward. The failsafe feature<sup>7</sup> of the Hoytether™ structure is illustrated in Figure 3. In Figure 3, the diameter of the Hoytether™ has been greatly expanded compared to the length, which allows the details of the Hoytether™ construction and operation to be seen, but badly distorts the angle between the secondary lines and primary lines at their interconnection points. The interconnection angles in the Figure 3 diagrams are 30-40 degrees, whereas in reality, the interconnection angle in a real Hoytether™ is typically less than 5 degrees. It is this narrow interconnection angle, which has the secondary lines running almost parallel to the primary lines, that allows the secondary lines to quickly pick up the load from a cut primary line segment and put it back on the uncut segments of the primary line, without passing the load on to the nearby primary lines.

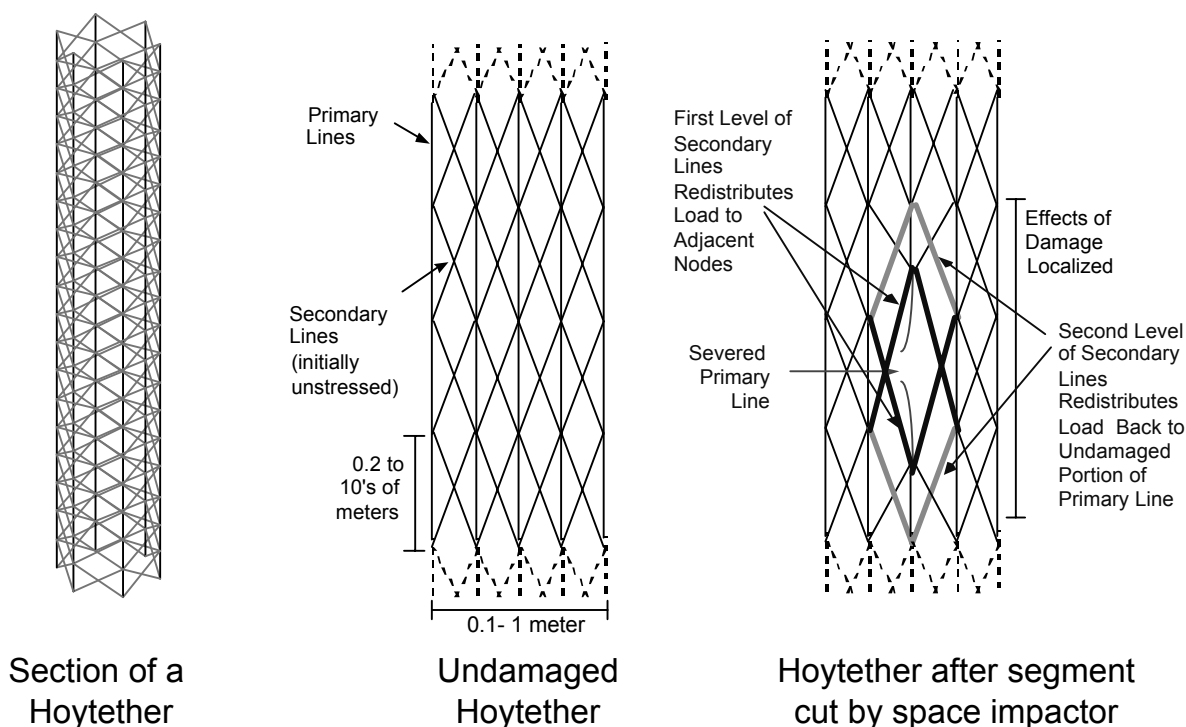


**Figure 3.** Interconnected multiline failsafe Hoytether™ structure

### Tether Tapering

To achieve the overall tapering of the HASTOL tether necessary to minimize its total mass, the tether in each module is constructed with a different total cross-sectional area to cope with the stress seen by the tether at that particular position in the array, with the length then adjusted to fit within the 20 m<sup>3</sup> deployer spool volume. The length of the tether in each module is plotted in Figure 4. (The center of mass of the tether boost facility is between module 12 and 13.) There are 24 primary lines in the Hoytether™ and 48 secondary lines, each half the area of a primary line. For a constant mass of tether in the 20 m<sup>3</sup> deployer module, the diameter of the primary lines in each module will vary inversely with the length of the tether as shown in Figure 5.

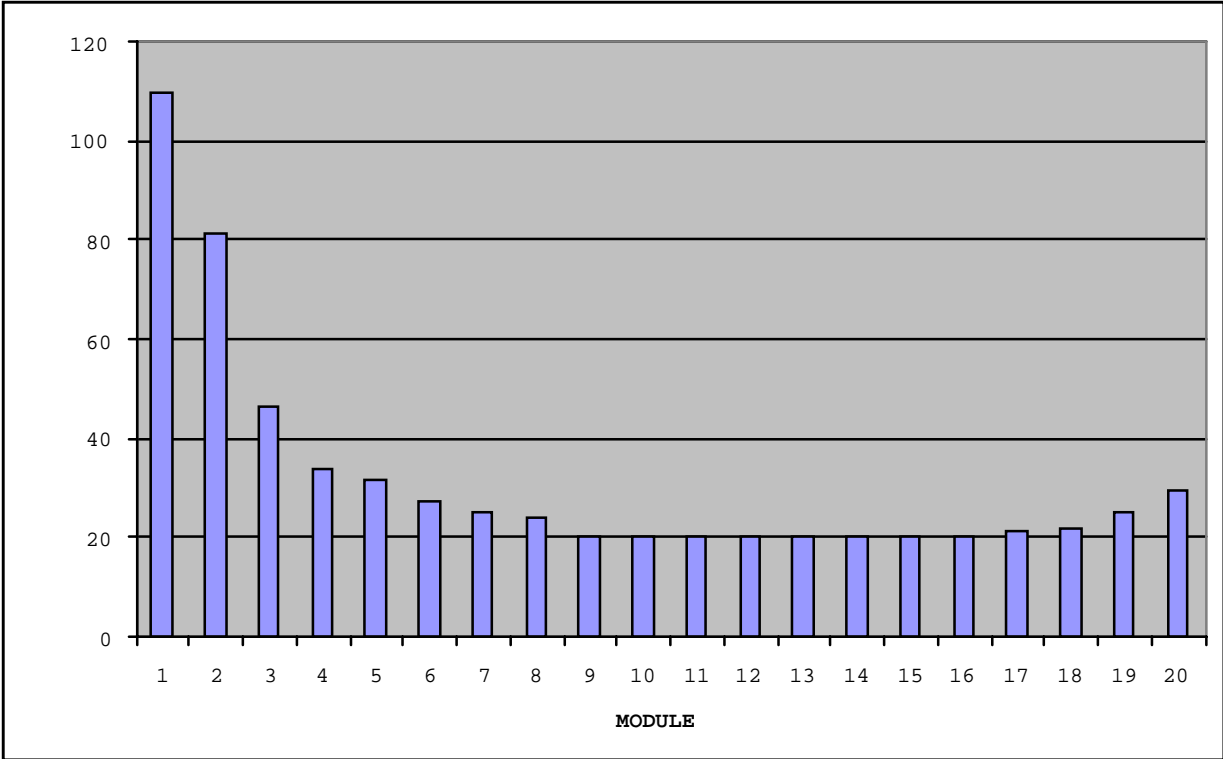


Figure 4. Length of tether in a module - adjusted to fit within a 20 m<sup>3</sup> deployer volume.

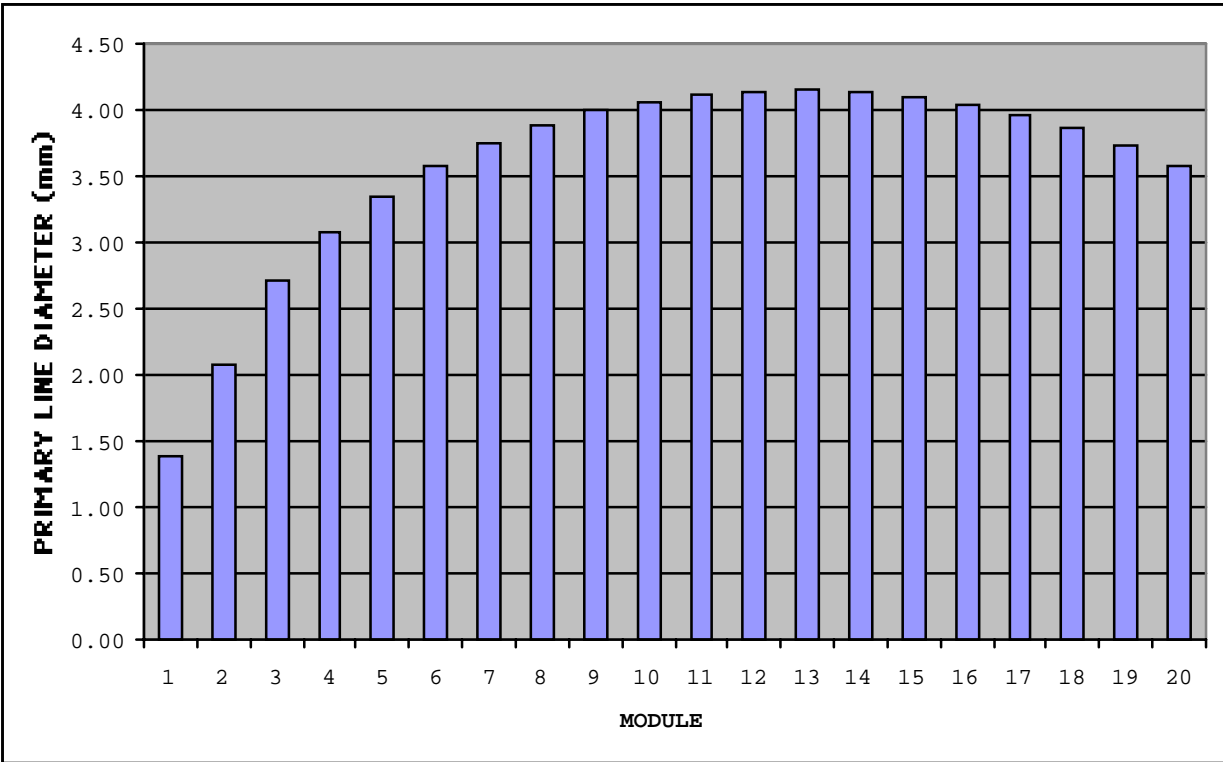


Figure 5. Diameter of each of the 24 primary lines in a given tether module.



### Selecting HASTOL Boost Facility Hoytether™ Diameter

As presently designed, the HASTOL Tether Boost Facility will be operating in the altitudes from 150 to 1343 km, which includes the 776 km operational altitude of the Iridium satellite constellation. The Iridium spacecraft body is 4.06 m long by 0.76 m wide along each of the three sides of the triangular body. In a functioning spacecraft the body is aligned along the local vertical in a gravity gradient stabilized mode. At the upper end of the spacecraft are the two panels of the solar power array, which are each 3.31 m long and 1.17 m wide. Including the structure holding the solar panels onto the spacecraft body, the Iridium spacecraft have a "wingspan" of nearly 9 m. There are presently 87 Iridium spacecraft in 86.4 degree inclination circular orbits at an altitude of 776 km. Twelve of the spacecraft are not responding to ground commands and cannot be deorbited by the Iridium operators. By the time the HASTOL Tether Boost Facility is operational in 2020, it is estimated there will probably be 100 Iridium spacecraft in orbit, 66 operational, 6 spares, and the rest nonfunctional and unable to deorbit.

The HASTOL Tether Boost Facility will be designed and operated so that the system has the capability of keeping track of operational spacecraft and large pieces of orbital junk, and will control the rotational phase and bending contour of the tether to avoid coming near those objects. In a previous study<sup>8</sup>, it was estimated that if each operational spacecraft and large piece of orbital debris were "protected" by a 600 m diameter "avoidance bubble", that the HASTOL facility would have to make an avoidance maneuver only about once every two weeks. In order to insure tether survival if the avoidance maneuver fails and a collision occurs, we need to design the tether with a minimum diameter such that the tether can survive a passage of an Iridium spacecraft completely through the tether. By making the tether diameter a factor  $g > 3$  times the 9 m wingspan of the Iridium spacecraft, we can limit the number of primary line cuts by the passage of the Iridium spacecraft to the point where the tether will not fail. The factor  $g$  will be determined by a number of parameters, primarily the nominal and peak stresses in the tether lines and the design of the Hoytether™. For this analysis, we will take  $g \sim 3$  and fix the average working diameter of the tether as  $D = 30$  m.

### HASTOL Tether Stress Levels

The modular HASTOL™ tether designed by Hoyt<sup>5</sup> has a stated "safety factor" of 3 when using Spectra™ 2000, a highly-oriented polyethylene polymer fiber produced by AlliedSignal which has been in multiton commercial production since 1997. AlliedSignal quotes a ultimate breaking stress for Spectra™ 2000 of 4.0 GPa and a specific density of 0.97 g/cc. If we assume that half of the tether mass is in slack secondary lines, which are carrying no load, then that means all the load is being carried by the primary lines operating at a "safety factor" of 1.5, or a stress of  $1/1.5 = 67\%$  of the breaking stress of Spectra™ 2000. This is indeed a very high stress level for an operational system.

It should be recognized, however, that the quoted percentage stress level only applies to Spectra™ 2000. AlliedSignal has in the laboratory improved versions of Spectra™ with higher ultimate breaking stress and the same density. There are also much stronger materials on the horizon, specifically carbon nanotubes, which have a still higher strength to density ratio. The use of these new materials to replace Spectra™ 2000 will mean that the operational stress level of the HASTOL tether that is 67% of the breaking stress of Spectra™ 2000, will be a lower percentage of the breaking stress of the stronger materials. It should also be noted that the mass

of the HASTOL Tether Boost Facility is NOT determined by the strength of the tether material. The HASTOL Tether Boost Facility MUST be heavier than 60 times the payload so that the orbit of the facility does not drop too far down toward the atmosphere after pickup and toss of a payload. Thus, newer, stronger, materials will be used to improve the operational safety margin, not reduce the facility mass.

### **Survival of HASTOL Tether Under Multiple Random Small Cuts**

In prior studies<sup>7</sup> of the lifetime of a Hoytether™, where the stress levels in the tether were low, it could be assumed that nearly all of the lines in the tether would have to be cut at the same "level" of the tether before the tether would fail. This allowed the use of a survival calculation method<sup>7</sup> that enumerated all the possible ways the tether could fail, and calculated the probability that one of those possible ways would indeed occur. This could then be used to estimate the tether "lifetime" or the rate at which repair or replacement of the tether would be needed. At high initial stress levels (>50%), this direct enumeration method is no longer easy to do. We therefore had to devise a new method to estimate the rate at which it would be desirable to replace or repair a damaged portion of the tether.

### **Random Cut Simulations of HASTOL Hoytether™ Structure**

To estimate how many cuts a highly stressed Hoytether™ could withstand without failing, we carried out some multiple random cut simulations using the proprietary Hoytether™ stress analysis program TetherSim™ developed by Robert P. Hoyt. A Hoytether™ was simulated with 24 primary lines in a circle 30 meters in diameter. With 24 primary lines, the spacing between the primary lines is  $\pi D/24=3.9$  m. The simulation had 40 interconnection nodes along the length of the structure, where the secondary lines are connected to the primary lines. More nodes would increase the simulation run time excessively. The secondary lines were not connected to each other where they crossed. The 40 nodes resulted in each primary line being divided into 39 segments or "levels". Five levels at each end of the 39 level section were protected from random cuts to avoid "end effects", leaving a 29 level center section which was subjected to random cuts. The total number of primary line segments subjected to cuts was 24 lines times 29 segments per line or 696 line segments. This relatively large sample size indicates that the simulation should be accurate to about  $(696)^{1/2}/696=26/696$  or about 4%. Since there are twice as many secondary lines as primary lines, the total number of secondary line segments subjected to random cuts was 1392 line segments.

The distance between interconnection nodes, and therefore the length of each primary line segment, was chosen as 50 m, so that the angle between the secondary lines and the primary lines would be a narrow angle for best operation of the "self-mending" feature of the Hoytether™ structure<sup>6,7</sup>. In this design, with the primary line spacing at 3.9 m, the angle was  $\arctan(3.9/50)=4.5$  degrees. With the distance between nodes set at 50 m, the total length of the 40 node segment being simulated was 39 levels times 50 m per level or about 2 km, which is a small fraction of the 636 km long HASTOL tether.

The secondary lines were selected to be half the area of the primary lines since prior studies have shown this is close to optimum. The secondary line area could have been selected to have less area. This would mean that for a fixed mass tether, there would be more area available for the

primary lines, lowering the initial stress on them. In this high stress simulation, a smaller secondary line area might have been more optimum, but that was not what was simulated.

The TetherSim™ program also allows for "excess slack" in the secondary lines, typically 1.005 (0.5% excess), since one of the major features that makes the Hoytether™ work so well, is that the secondary lines are deliberately kept initially unloaded, so that the Hoytether™ does not "neck in" under load. It is only when a primary line segment is cut that the secondary lines pick up some of the load and become stressed. As shown in Figure 3, for each primary line cut, **four** secondary lines (2 on each side) come in to replace the cut primary line. Since the total area of the four secondary lines is **twice** the area of the primary line they replace, the amount of tether area available for carrying the load **increases** in the cut area, and the average stress in that area is now **less** than the initial stress on the primary line in the uncut state. This "rip stop" activity of the secondary lines prevents the load from the cut primary line from being passed on to the nearest neighbor primary line segments in the radial and longitudinal directions, which are actually slightly **unloaded** after the cut. The next-nearest neighbor primary line segments, which are along the four diagonals from the cut primary line segment, do experience an increase in stress, but as we shall see later, it is very small. The selection of the proper amount of initial slack is presently an "art". In prior high stress simulations, Hoyt has found that an initial "slack" of less than 1.000 helped, since the secondary lines helped carry some of the load during the high stress portions of the operation between pickup and toss of the payload. This would cause the Hoytether™ to neck in during the 9.4 minutes the payload was attached, slightly increasing its vulnerability. To avoid this necking in, we selected for these simulations an excess length of zero percent, or an excess slack factor of 1.000.

Although the maximum stress on the Spectra™ 2000 primary lines of the HASTOL Tether Boost Facility can be as high as 67% during the 9.4 minute interval between payload pickup and toss, the stress level without a payload attached is 60%. Since the stress level is mostly due to the rotation of the HASTOL facility about its center-of-mass with an 18.8 minute period, and the rotation rate does not change before, during, or after payload pickup and toss (the orbit altitudes drop, but the tether rotation remains constant), then nearly all of the time, except for 9.4 minutes once every week or so, the tether is at a stress level of 60%. Therefore, for this simulation, we assumed a tether stress level in the primary lines of 60% of breaking stress.

### **Single Cut of Primary Line Segment in Middle of HASTOL Hoytether™**

To show how well the failsafe Hoytether™ design can cope with a cut, we used the TetherSim™ program to calculate the residual stresses in each of the primary line segments after a single cut of a single primary line segment in the exact middle of the 40 node tether structure. A "map" of the primary line stress levels are shown in Figure 6. The X-axis represents the segment level of the 39 segments along the length of the tether being simulated, the Y-axis indicates the stress level on the primary line segment at that point, while the Z-axis represents the 24 primary lines "unrolled" from a hollow tube into a plane. The point with a stress of 0% is the position of the cut primary line segment. The nearest neighbor points on either side of the cut segment are the primary line segments closest to the cut segment in the longitudinal and radial directions. Note that the stress levels on the segment of the primary line with the cut segment are less than 60%, but not zero, despite the cut in their line. This is because the stress released by the cut primary line segment is being carried around the cut segment by the secondary lines (which are not

represented in this primary line segment stress map) and nearly all of it is restored back onto the uncut segments of the primary line after about 3 levels in the longitudinal direction on either side of the cut segment. In the radial direction, the nearest neighbor primary line segment is **unloaded** by the action of the secondary lines around the cut, while the next nearest neighbor primary line in the radial direction is hardly "aware" that a cut has taken place. The four small blue pyramidal peaks in Figure 6 represent the four next-nearest neighbor line segments in the four diagonal directions from the cut primary line segment. The stress on these four segments rises due to the cut, but only from 60% to 62.9%. The flatness of the stress map in areas away from the cut region represents how minimal the effects of the cut are in regions far from the cut. The blue "X-shaped" region represents slightly increased stress levels from 60.0% to only 60.1%, while the orange color in the rest of the flat region represents slightly decreased stress levels from 59.9% down to 59.8%. In the following multiple random cut simulations, the stress patterns observed for a number of random cuts are just the "summations" of a number of these single cut stress patterns.

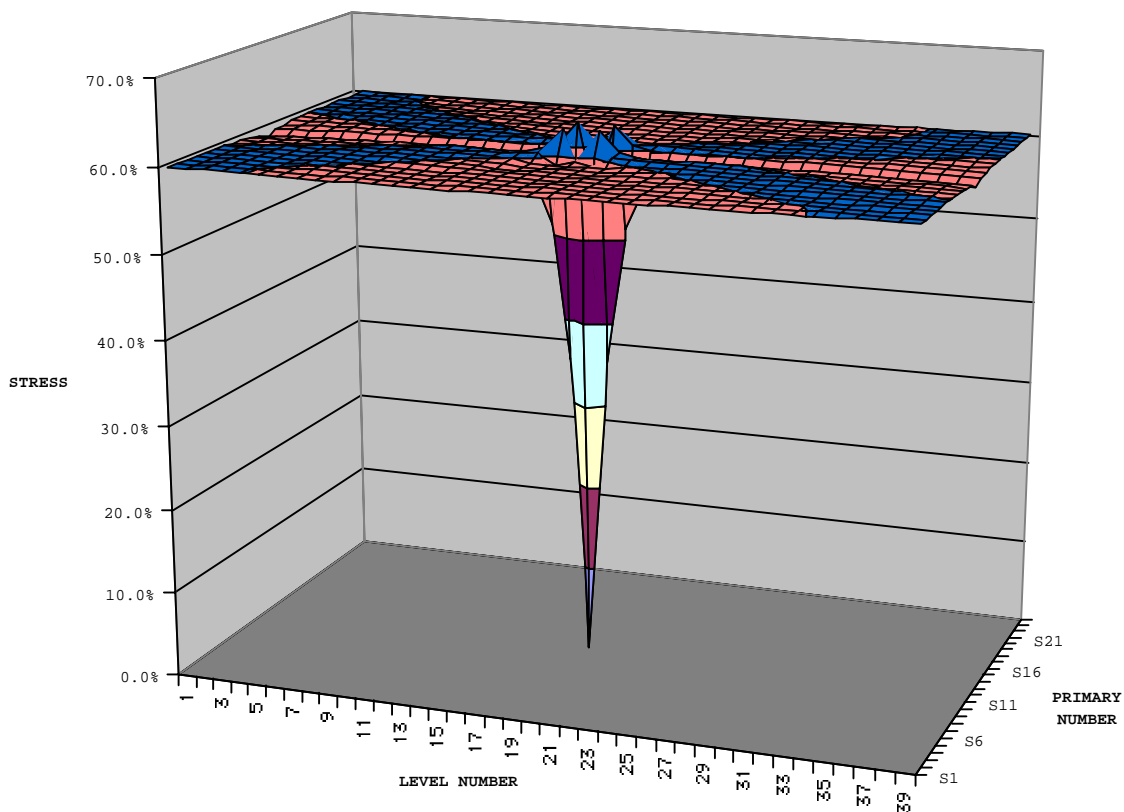


**Figure 6.** Single cut of primary line segment in a 24 primary line tubular Hoytether™ operating at a nominal 60% primary line stress level.

### Simulation of Random Cuts of 10% of Primary Line Segments

We then had the TetherSim™ program carry out a random cutting of the 29 middle "levels" of the 39 level tether. The program randomly cuts about 4 times as many secondary lines as primary lines. First, there are twice as many secondary lines as primary lines. Second, the secondary lines, being smaller in diameter, should be more susceptible to cuts by small space

impactors. Actually, a factor of 0.707 decrease in line diameter for lines with diameters in the millimeter range usually causes a factor of about 3 increase in cut rate, rather than the factor of 2 built into the program. This needs to be fixed in the next version of TetherSim™.

We first ran a number of simulations to the point where the build-up of stress, caused by multiple cuts randomly occurring close to each other, finally loaded a line segment to the point where it broke without being cut. The break could be either a primary or secondary line segment. The simulation stops at that point, allowing a "snapshot" to be saved. If directed, it continues the iteration, spreading out the stress due to the line segment break. Sometimes the line break does not cause further breaks (especially if it was a secondary line that broke). Usually, however, the stress released by a broken line causes further line segments to break and the tether starts to "rip" - and fails. There is good reason for this. A line segment is only stressed near breaking when it is surrounded by lots of random cuts. There is therefore very little "reserve" left in the number of still slack secondary lines to cope with the increased stress. After a large number of runs, we found that for a Hoytether™ with an initial stress of 60%, the tether will start failing when about 10% of the primary lines segments have been damaged by random cuts. An example is shown in Figure 7.

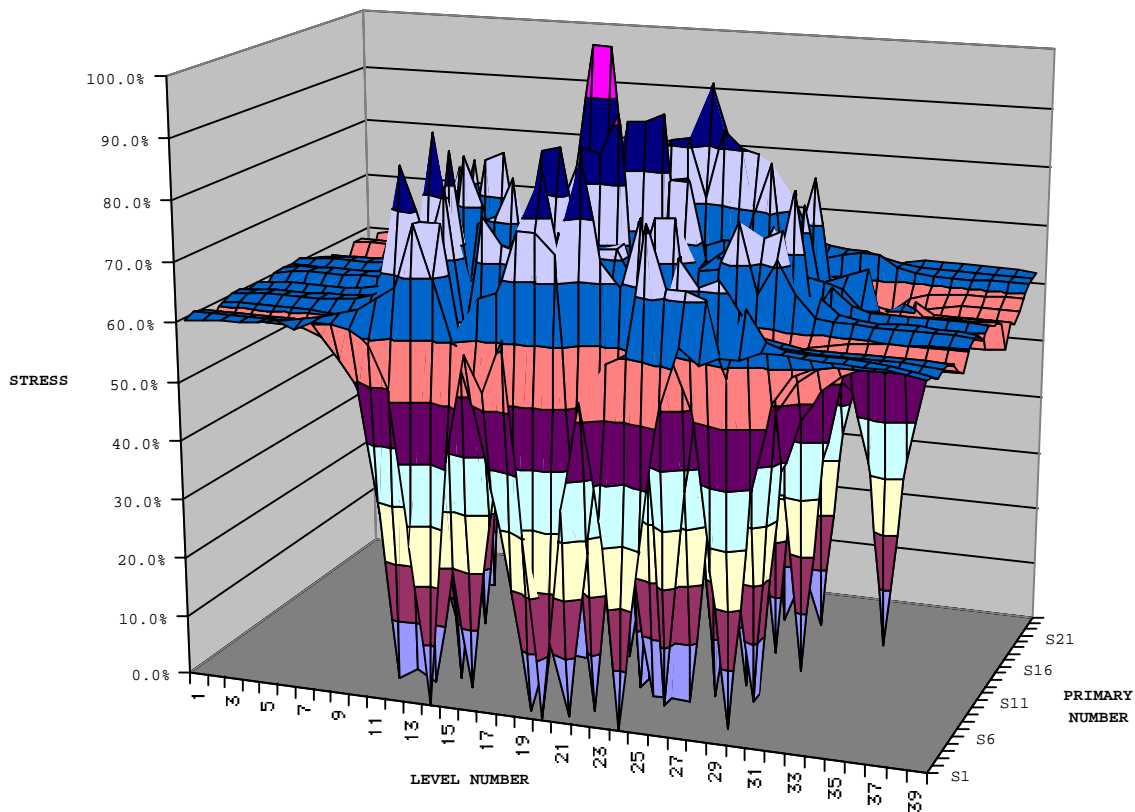


**Figure 7.** Random cuts of  $75/696=10.8\%$  of primary line segments and  $237/1392=17.0\%$  of secondary line segments - 60% initial stress. 98.9% maximum stress buildup after cuts - Hoytether™ about to fail.

### Simulation of Random Cuts of 5% of Primary Line Segments

We then did a number of runs where we attempted to stop the random cutting process at about 5% of the total number of primary line segments or about 35 primary line segment cuts and 140 secondary line segment cuts. Since there are only 24 primary lines, this means that nearly 80% of the primary lines in this short section of tether being simulated has been cut at least once, about 48% of them have been cut two or more times, and 20% of them have been cut three or more times. A typical result is shown in Figure 8. Usually the maximum stress levels rose to about 80% on a few of the primary line segments which happened to be surrounded by a number of cuts, but very seldom did those stress levels rise to 90%.

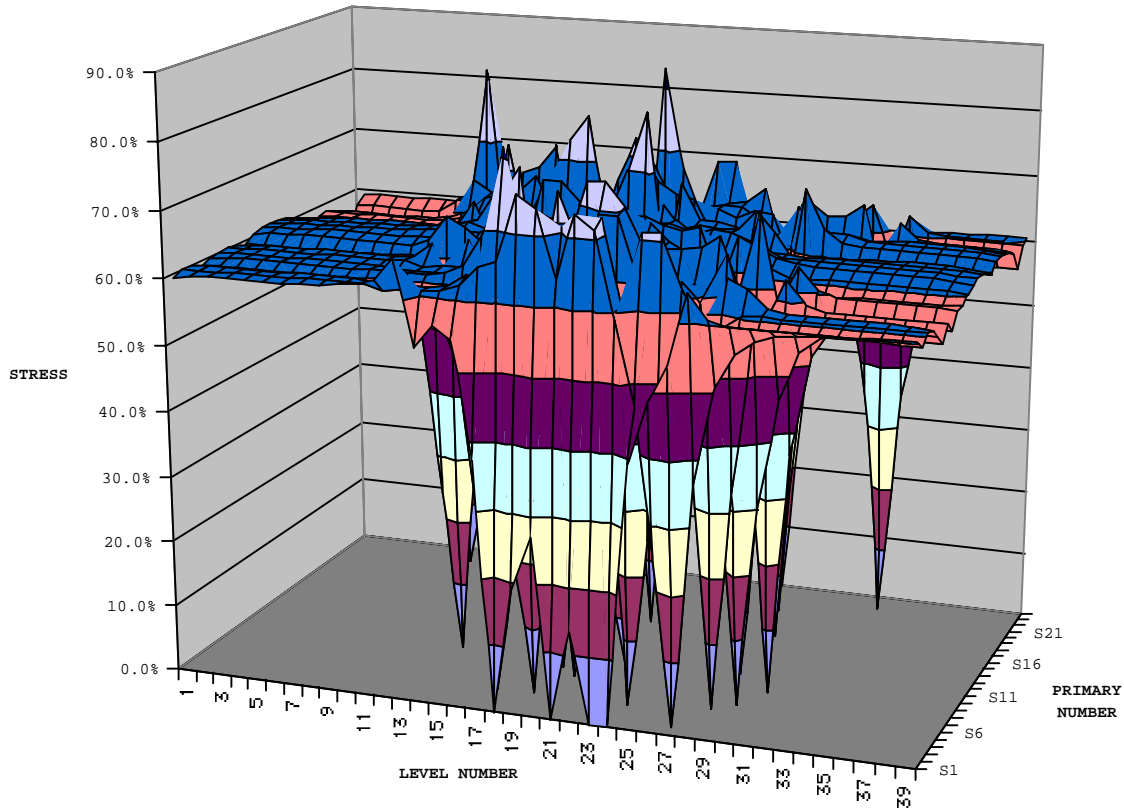


**Figure 8.** Random cuts of  $39/696=5.6\%$  of primary line segments and  $160/1392=11.5\%$  of secondary line segments - 60% initial stress. 82% maximum stress buildup after cuts. Hoytether™ surviving nicely.

From these simulations we estimate that a random cut percentage of 5% seems to be a "safe" level that will insure high probability of survival of the Hoytether™ when the primary lines of the Hoytether™ are operated at 60% of their breaking stress. Of course, being random, there is always the possibility that a number of the random cuts will hit the same portion of the tether early in its exposure life and cause an early failure. The operators of the HASTOL Tether Boost Facility, however, can be made aware of the positions of each break by measurements made of the shock vibrations traveling up and down the cut primary line. The time difference between the arrival of the up and down pulses can pinpoint the position of the break along the tether. If the number of cuts reach a significant level in a particular region of the tether before the normal replacement time, the operators can arrange for a replacement or repair of the tether.

### **HASTOL Tether Boost Facility Operational Parameters**

The HASTOL Tether Boost Facility<sup>1-5</sup> will spend most of its time in a slightly elliptical equatorial orbit with a perigee altitude of 603 km and an apogee altitude of 890 km. The perigee velocity is 7632 m/s while the apogee velocity is 7331 m/s. The orbital period of the facility is 99.7 minutes and the rotation period is 18.8 minutes, or a ratio of 5.3 facility rotations per orbit of the facility center of mass. The center of mass of the facility will be 453 km from the grapple end and 183 km from the Tether Control Station end. Thus, the grapple end of the facility will scan over an altitude range that goes from a low of 150 km when the facility is at perigee and the grapple end is pointed toward the nadir, to a high of 1343 km when the facility is at apogee and the grapple end is pointed toward the zenith. The Tether Control Station end of the facility will scan the altitude range from 420 km to 1073 km. It should be noted that the rotation is not phased with the orbit, except near the time for payload pickup, so at perigee passage the grapple end of the tether would not necessarily be reaching down to 150 km (or up to 1343 km at apogee).

After the HASTOL Tether Boost Facility has picked up a payload, but before it has tossed it, it will be in a 719 by 595 km orbit, with a period of 97.9 minutes. The rotation rate of the facility still remains at 18.8 minutes, since the payload had a velocity that matched the grapple velocity when it was picked up by the grapple. The center of mass of the HASTOL facility and the perigee drops 8 km during the pickup, and the apogee of the orbit drops 171 km, but the angular velocity does not change. For a half-rotation, lasting only 565 s or 9.4 minutes, the grapple end of the tether sweeps from 150 km to 1164 km, releasing the payload at apogee for maximum boost to the payload, or earlier, if boost of the payload to a lower orbit is desired. It is only during this 9.4-minute period that the tether is under its maximum stress load.

After the payload has been released, the HASTOL Boost Facility drops into a nearly circular 549 by 587 km altitude orbit with a period of 96.0 min. With the release of the payload, the center of mass of the facility is now back at 453 km from the grapple end and 183 km from the Tether Control Station end. The rotational period of the tether has not changed from 18.8 min and is now at 5.1 rotations per orbit. The grapple end of the tether sweeps over the altitude range from 96 km to 1040 km, while the station end sweeps over the altitude range from 366 km to 770 km. The electrodynamic tether reboost systems on each power module now start operating to add energy and angular momentum to the facility orbit to raise the facility back to a 603 by 890 km elliptical orbit in preparation for the next payload boost operation. (Note that no energy or angular momentum needs to be added to the rotation of the tether as the boost operation does not change the tether rotation rate.)

### **Estimate of Small Impactor Flux Rates**

Now that we have an estimate of the percentage of primary line segment cuts that the HASTOL Hoytether™ can cope with, without coming close to a failure condition, we can estimate the total number of cuts that percentage represents in a given tether module. We next need to calculate the rate at which the primary line segments in each tether module will be cut by small space impactors. With that, we can calculate the rate at which a tether module will need to be replaced. There are two sources of small impactors in space in the 150 to 1343 km altitude range where the HASTOL Tether Boost Facility will operate - orbital debris and micrometeorites.

**Orbital Debris**

The flux of small orbital debris impactors varies considerably with altitude and inclination, and even with time. For this analysis we used the NASA computer program ORDEM96.EXE and the NASA Technical Memorandum TM-104825<sup>9</sup> to calculate the orbital debris flux for an object in equatorial orbit (inclination 0 degrees) for different size impactors at different altitudes. The ORDEM96.EXE program produces estimates for all orbital debris objects in space, including very large spacecraft. It does NOT include any estimate for the micrometeorite flux, which must be obtained from another NASA/JSC Technical Memorandum<sup>10</sup>, and this micrometeorite impactor flux added to the orbital debris impactor flux. The flux estimate obtained from the NASA ORDEM96.EXE program includes the (small) probability that a primary line segment will be cut by a large spacecraft or other large impactor. A large impactor, however, will cut many primary line segments all at once at the same "level" of the Hoytether™, and needs to be treated differently. This has been done in an earlier paper<sup>8</sup>, which should be consulted and used along with this paper to understand all the hazards of the interaction of the HASTOL Hoytether™ with objects in the space environment and how to mitigate them.

**Micrometeorites**

The micrometeorite flux comes in from outside the Earth, largely from the asteroid belt, and is roughly constant with altitude. At the lower altitudes there is a partial shielding by the Earth blocking part of the incoming flux, but this is partially compensated by a "focusing" of the incoming flux due to the gravity field of the Earth. For this analysis we will use the graph in Figure 7-2 on page 7-4 the NASA Technical Memorandum TM-4527<sup>10</sup> to obtain an estimate of the micrometeorite flux. The graph is specifically for the micrometeorite flux at the International Space Station at 400-km altitude in a 51.6 degrees inclination orbit during the year 2000. We will assume it applies to all altitudes from 400 km on up, and all inclinations and all time, which is not an unreasonable assumption considering the interplanetary source of the flux.

**Estimate of Cutting Impactor Size for a Given Diameter Line**

The small impactors striking the line segments in a Hoytether™ have a very high impact velocity. The micrometeorites drop in at Earth escape velocity or higher, and when this is combined with the orbital velocity of the tether, results in impact velocities with respect to the tether of the order of 15 km/s. The small orbital debris objects have Earth orbital velocities of 7.5 km/s, similar to that of the orbital velocity of the tether. They are usually in inclined orbits and will have impact velocities with respect to the tether in its equatorial orbit of the order of 8 to 10 km/s. Both of these impact velocities are high enough that the impactor and the portion of the tether that they collide with, are heated into an incandescent plasma that "melts" the nearby tether that isn't physically struck. After studying the nearly perfect hemisphere craters caused by both micrometeorite and orbital debris impactors striking the solid aluminum plates on the Long Duration Experiment Facility (LDEF), debris experts estimated that the ball of plasma "melted" a hole in the solid plates that was three times the diameter of the impactor. This led to the use of a "rule of thumb" of assuming a "lethality factor" of  $k=1/3=0.33$  when estimating the size of an impactor needed to cut (melt) a tether line - any impactor larger in diameter than one-third the diameter of the tether would cut the tether.

However, multistrand tether lines are not solid plates. There is now experimental evidence that tether lines made of multiple strands of fiber are much less susceptible to cuts by impactors. The



Tethered Physics Experiment (TiPS)<sup>11</sup> was deployed in space on 20 June 1996 into a circular orbit of 1022 km altitude and 63.4 degrees inclination, and was still uncut as of 20 June 2001 - five years later. The tether was 4 km long and consisted of eight multifilament Spectra™ 1000 high-strength oriented polyethylene strands braided into a hollow braid around ordinary acrylic household yarn to keep the braid "fluffed out". The initial diameter was about 2.5 mm. Under high load the diameter could shrink to 2.0 mm, but there is almost no gravity gradient load on the TiPS tether. If we use the old "lethality factor" of  $k=1/3$ , then the diameter of the space impactor capable of cutting the tether would be  $i=2.5 \text{ mm}/3=0.83 \text{ mm}$ . At 1022 km altitude, the flux of cutting micrometeorite impactors with diameters greater than 0.83 mm is about 0.02 cuts/m<sup>2</sup>-yr, while the flux of cutting orbital debris impactors is about 0.06 cuts/m<sup>2</sup>-yr, for a total of  $F=0.08 \text{ cuts/m}^2\text{-yr}$ . The broadside area of the non-tumbling  $d=2.5 \text{ mm}$  diameter by  $L=4 \text{ km}$  long tether is  $B=dL=10 \text{ m}^2$ , which gives a cut rate of the non-tumbling tether of  $C=BF=0.8 \text{ cuts/yr}$  or 1 cut every 1.25 years. If this  $k=1/3$  lethality factor is correct, the probability that the TiPS tether survived 5 years is an "unlikely"  $\exp(-5/1.24)=2\%$ . If we use a "lethality factor" of  $k=1/2$ , or  $i>1.25 \text{ mm}$ , then the flux of cutting micrometeorite impactors is found to be 0.002 cuts/m<sup>2</sup>-yr, while the flux of cutting orbital debris impactors is 0.0165 cuts/m<sup>2</sup>-yr, for a total flux of 0.0185 cuts/m<sup>2</sup>-yr or a cut rate of 0.185 cuts/yr or 1 cut every 5.4 years, which is close to the demonstrated lifetime of the tether. We will thus use a "lethality factor" of  $k=1/2$  in this analysis.

#### **Calculation of Small Cutting Impactor Total Flux Variation With Altitude**

The ORDEM96.EXE program was activated and the orbital debris flux in number of cutting impactors per year per square meter of tether "interaction area" was obtained for space impactors larger in size than 0.7, 1.0, 1.5 and 2.0 mm passing through the equatorial plane in the year 2020 at 50 km altitude intervals over the altitude range from 1350 km to 200 km (the minimum altitude ORDEM96.EXE will accept). The results are tabulated in the "Debris Flux" columns in Table I. To these we added the micrometeorite flux for those same size impactors, when the altitude was greater than 400 km. Interestingly, the micrometeorite flux and the orbital debris flux are almost equal in amplitude and slope at 400 km. The orbital debris flux below 400 km drops rapidly with altitude because of air drag. For this analysis, we assumed air drag would affect the micrometeorite flux also, and that the total flux below 400 km was twice the orbital debris flux. For 150 km we just extrapolated the data from the ORDEM96 200 km altitude data point. Errors in the flux numbers below 400 km will have little effect on the results, as most of the impactor flux comes from orbital debris impactors in the altitude range from 650 to 1100 km.

During most of its time in orbit, the center of mass of the HASTOL Boost Facility is in a 603 km by 890 km orbit. The Tether Control Station end of the tether, which is 183 km from the center of mass of the facility, scans through the altitudes from 420 km to 1073 km. The Grapple end of the tether, which is 453 km from the center of mass, scans through all the altitudes from 150 km to 1343 km.

TABLE I - SMALL METEOROID AND ORBITAL DEBRIS FLUX FROM 150 TO 1350 KM ALTITUDE

LINE DIAMETER	D = 0.14 cm		D = 0.20 cm		D = 0.30 cm		D = 0.40 cm	
IMPACTOR SIZE	I > 0.07 cm		I > 0.10 cm		I > 0.15 cm		I > 0.20 cm	
METEOR FLUX	$F_M = 0.0250/m^2-yr$		$F_M = 0.0060/m^2-yr$		$F_M = 0.0025/m^2-yr$		$F_M = 0.0005/m^2-yr$	
ALTITUDE (km)	DEBRIS FLUX TOTAL FLUX (#/m <sup>2</sup> -yr) (#/m <sup>2</sup> -yr)		DEBRIS FLUX TOTAL FLUX (#/m <sup>2</sup> -yr) (#/m <sup>2</sup> -yr)		DEBRIS FLUX TOTAL FLUX (#/m <sup>2</sup> -yr) (#/m <sup>2</sup> -yr)		DEBRIS FLUX TOTAL FLUX (#/m <sup>2</sup> -yr) (#/m <sup>2</sup> -yr)	
150	0.0005	0.0010						
200	0.0017	0.0034						
250	0.0039	0.0078	0.0012	0.0024				
300	0.0086	0.0172	0.0029	0.0058				
350	0.0154	0.0308	0.0052	0.0104	0.0016	0.0032		
400	0.0211	0.0461	0.0072	0.0132	0.0022	0.0047	0.0009	0.0014
450	0.0250	0.0500	0.0085	0.0145	0.0025	0.0050	0.0011	0.0016
500	0.0285	0.0535	0.0097	0.0157	0.0029	0.0054	0.0012	0.0017
550	0.0335	0.0585	0.0114	0.0174	0.0034	0.0059	0.0015	0.0020
600	0.0416	0.0666	0.0143	0.0203	0.0043	0.0068	0.0019	0.0024
650	0.0549	0.0799	0.0191	0.0251	0.0059	0.0084	0.0026	0.0031
700	0.0759	0.1009	0.0268	0.0328	0.0082	0.0107	0.0036	0.0041
750	0.1070	0.1320	0.0383	0.0443	0.0118	0.0143	0.0051	0.0056
800	0.1560	0.1810	0.0558	0.0618	0.0172	0.0197	0.0074	0.0079
850	0.2400	0.2650	0.0861	0.0921	0.0265	0.0290	0.0114	0.0119
900	0.3910	0.4160	0.1410	0.1470	0.0431	0.0456	0.0186	0.0191
950	0.4360	0.4610	0.1570	0.1630	0.0481	0.0506	0.0207	0.0212
1000	0.1780	0.2030	0.0641	0.0701	0.0197	0.0222	0.0085	0.0090
1050	0.0771	0.1021	0.0277	0.0337	0.0089	0.0114	0.0037	0.0042
1100	0.0505	0.0755	0.0182	0.0242	0.0056	0.0081	0.0025	0.0030
1150	0.0399	0.0649	0.0144	0.0204	0.0045	0.0070		
1200	0.0338	0.0588	0.0122	0.0182				
1250	0.0297	0.0547	0.0107	0.0167				
1300	0.0278	0.0528						
1350	0.0292	0.0542						
<b>AVE. FLUX</b>	<b>0.1055</b>		<b>0.0404</b>		<b>0.0152</b>		<b>0.0065</b>	

**HASTOL Tether Effective Interaction Area**

During normal operation, the HASTOL tether facility is rotating rapidly enough that the facility typically makes 5-6 rotations per orbit. The tether facility thus approximates a "randomly tumbling object". For a randomly tumbling object, the instructions<sup>9</sup> for the NASA/JSC ORDEM96.EXE program recommends that the "effective" interaction area to be used with the flux estimate should be the total surface area of the target divided by 4. For a single tether line segment of diameter d and length s, the surface area is  $A=\pi ds$ , and the "effective" interaction area of the randomly tumbling line segment is  $A/4$ . The flux F is given in units of "objects greater in diameter than the selected diameter per year per square meter of effective interaction area". Thus, the interaction rate C between the flux F of "cutting" impactors and the tether line segment is given by Equation (1):

$$C = \frac{AF}{4} = \frac{\pi}{4} dsF \quad . \quad (1)$$

**Replacement Rate of HASTOL Hoytether™ Modules**

Now that we have the diameters of the primary lines on the 20 modules that make up the HASTOL Hoytether™, the small space impactor flux that can cut those line diameters, and the percentage number of cuts in a module which will call for a replacement of the module, we can calculate the replacement rates for the individual modules.

### Replacement Rate For Grapple End Module of HASTOL Hoytether™

The "first" or outermost module of the tether is the end near the grapple. Because it has to support only the mass of the payload and its own mass, it has the finest diameter lines with a primary line diameter of  $d=1.38$  mm and a secondary line diameter of  $d/1.414=0.98$  mm. Because of the fine lines, the length of this tether module can be longer for a given total tether mass launch limit, and is  $L=110$  km in length. This end of the tether also scans all the altitudes from 150 km to 1343 km as the tether rotates and orbits about the Earth. Using the "lethality factor" of  $k=1/2$ , the minimum diameter of an impactor that will cut one of the primary lines is  $i>kd=d/2=0.7$  mm. The ORDEM96.EXE program was used to obtain an estimate for the orbital debris flux of cutting impactors at 50 km intervals between 150 km and 1350 km. These are tabulated in the first column of data in Table I. The flux for micrometeorite impactors greater than  $i=0.7$  mm at 400 km altitude was obtained from Figure 7-2 of NASA TM-4527 and was found to be  $F_M=0.0250$  cuts/m<sup>2</sup>-yr. At 400 km altitude and above, the micrometeorite flux was added to the orbital debris flux to obtain the total flux of cutting impactors in the second column. Below 400 km altitude, the debris flux was multiplied by 2 to obtain an estimate of the total flux. The Average Total Flux was then obtained by averaging all the flux estimates in the Total Flux column, and was found to be  $F=0.106$  cuts/m<sup>2</sup>-yr for the primary lines of diameter  $d=1.4$  mm.

The total surface area of one of the primary line segments on this first module of the HASTOL Hoytether™, with a diameter  $d=1.4$  mm and segment length  $s=50$  m, is  $A=\pi ds=0.22$  m<sup>2</sup>. Since the tether is "tumbling", the effective collision area is 1/4th the physical area of the tether, or  $A/4=0.055$  m<sup>2</sup>. Using Equation 1, the cut rate for that primary line segment is therefore  $C=FA/4=0.0058$  cuts/yr or 1 cut every 172 years. There are  $n=24$  primary lines in the Hoytether™, and there are  $m=110$  km/50 m=2200 connection intervals along this first module of the HASTOL tether, so there are a total of  $nm=52,800$  primary line segments. At a cut rate of 0.0058 cuts/yr for each primary line segment, the average number of cuts per year of the 52,800 primary line segments will be 306 cuts per year or about one cut per day. If we assume that it is time to replace the first section of the HASTOL Hoytether when the number of primary line segments cut has reached 5% of the total number of primary line segments, then that time arrives when an average of 2,640 primary line segments have been cut. At a rate of 306 cuts per year, those number of cuts will be reached in 8.6 years. This estimated time of 8.6 years can be more easily calculated by taking 5% of the 172 year lifetime for a single primary line segment. The number of primary line segments being cut is large enough that the time at which replacement is needed can be treated statistically, since the cuts are random in time and space. The random variations about the average will be small, typically  $(2640)^{1/2}/2640=51/2640$  or a one sigma error of 2%. Because the error in the probable number of cuts is small, this means that the time at which the number of cuts will reach the replacement level of 5% will be close to the average predicted time, or  $8.6\pm 0.2$  years, so the replacement can be on a scheduled basis rather than the operators having to be concerned with "counting" all the cuts as they come.

### Replacement Rate For Next Module of HASTOL Hoytether™

We then repeated the analysis for the next module of the tether, which is  $L=81$  km long and has a primary line diameter  $d=2.1$  mm and a secondary line diameter of  $d/1.414=1.45$  mm. This portion of the tether scans the altitudes from 250 km to 1250 km as the tether rotates and orbits about the Earth. Using the "lethality factor" of  $k=1/2$ , the minimum diameter of an impactor that will cut one of the primary lines is  $i>kd=d/2=1$  mm. The ORDEM96.EXE program was used to

obtain an estimate for the orbital debris flux for objects 1 mm in diameter or greater at 50 km intervals between 250 km and 1250 km. These are tabulated in the second set of data in Table I. The flux for micrometeorite impactors greater than  $i=1$  mm at 400 km altitude was obtained from Figure 7-2 of NASA TM-4527 and found to be  $0.006 \text{ cuts/m}^2\text{-yr}$ . At 400 km altitude and above, the micrometeorite flux was added to the orbital debris flux to obtain the total flux in the second column. Below 400 km altitude, the debris flux was multiplied by 2 to estimate the total flux. The Average Total Flux was then obtained by averaging all the flux estimates in the Total Flux column, and was found to be  $F=0.04 \text{ cuts/m}^2\text{-yr}$  for the primary lines of diameter  $d=2.1$  mm.

The total surface area of one of the primary line segments on this next module of the HASTOL Hoytether™, with a diameter  $d=2.1$  mm and segment length  $s=50$  m, is  $A=\pi ds=0.33 \text{ m}^2$ . Since the tether is "tumbling", the effective collision area is 1/4th the physical area of the tether, or  $A/4=0.082 \text{ m}^2$ . The cut rate is therefore  $C=FA/4=0.0033 \text{ cuts/yr}$  or 1 cut every 303 years. Using the same arguments as before, with  $n=24$  and  $m=81 \text{ km}/50 \text{ m}=1620$ , and  $0.05mn=1944\pm 44$  or 2% error, the estimated replacement time for this tether module is  $15.2\pm 0.3$  years.

### **Replacement Rate For Next Two Modules of HASTOL Hoytether™**

We then repeated the analysis for the combined replacement lifetime of the next two modules of the tether, since they have similar diameters of 2.7 mm and 3.1 mm, or an average diameter of about 3 mm, and similar lengths of 46 km and 34 km, which total  $L=80$  km. These modules of the tether scan the altitudes from 350 km to 1150 km. Using the "lethality factor" of  $k=1/2$ , the minimum diameter of an impactor that will cut one of the primary lines is  $i>kd=d/2=1.5$  mm. The ORDEM96.EXE program was used to obtain an estimate for the orbital debris flux at 50 km intervals between 350 km and 1150 km. These are tabulated in the third set of data in Table I. The flux for micrometeorite impactors greater than  $i=1.5$  mm at 400 km altitude was obtained from Figure 7-2 of NASA TM-4527 and found to be  $0.0025 \text{ cuts/m}^2\text{-yr}$ . At 400 km altitude and above, the micrometeorite flux was added to the orbital debris flux to obtain the total flux. Below 400 km altitude, the debris flux was multiplied by 2 to obtain an estimate of the total flux. The Average Total Flux was then obtained by averaging all the flux estimates in the Total Flux column, and was found to be  $F=0.015 \text{ cuts/m}^2\text{-yr}$  for primary line segments of diameter  $d\sim 3$  mm.

The total surface area of one of the primary line segments on these modules of the HASTOL Hoytether™, with a diameter  $d\sim 3$  mm and segment length  $s=50$  m, is  $A=\pi ds=0.47 \text{ m}^2$ . Since the tether is "tumbling", the effective collision area is 1/4th the physical area of the tether, or  $A/4=0.118 \text{ m}^2$ . The cut rate for that primary line segment is therefore  $C=FA/4=0.0018 \text{ cuts/yr}$  or 1 cut every 566 years. Using the same arguments as before, with  $n=24$ ,  $m=80 \text{ km}/50 \text{ m}=1600$ , and  $0.05mn=1920\pm 44$  or 2% error, the estimated replacement time for these modules of the tether is  $28.3\pm 0.6$  years, which means that these two modules will not need replacement unless it is desired to operate the HASTOL facility longer than the nominal 30 year commercial operational lifetime.

### **Replacement Rate For Remaining 16 Modules of HASTOL Hoytether™**

We then repeated the analysis for the remaining 16 modules of the tether which average 23 km in length and have primary line segment diameters of about  $d\sim 4$  mm. These portions of the HASTOL Hoytether™ scan the altitudes from 400 km to 1100 km as the tether facility orbits between 604 km and 890 km altitude. Using the "lethality factor" of  $k=1/2$ , the minimum

diameter of an impactor that will cut one of the primary lines is  $i > kd = d/2 = 2.0$  mm. The ORDEM96.EXE program was used to obtain an estimate for the orbital debris flux at 50 km intervals between 400 km and 1100 km. These are tabulated in the fourth set of data in Table I. The flux for micrometeorite impactors greater than  $i = 2.0$  mm at 400 km altitude was obtained from Figure 7-2 of NASA TM-4527 and found to be  $0.0005$  cuts/m<sup>2</sup>-yr. The micrometeorite flux was added to the orbital debris flux to obtain the total flux in the next column. The Average Total Flux was then obtained by averaging all the flux estimates in the Total Flux column, and was found to be  $F = 0.0065$  cuts/m<sup>2</sup>-yr for the primary line segments of diameter  $d \sim 4$  mm.

The total surface area of one of the primary line segments on one of these portions of the HASTOL Hoytether™, with a diameter  $d \sim 4$  mm and segment length  $s = 50$  m, is  $A = \pi ds = 0.63$  m<sup>2</sup>. Since the tether is "tumbling", the effective collision area is 1/4th the physical area of the tether, or  $A/4 = 0.16$  m<sup>2</sup>. The cut rate is therefore  $C = FA/4 = 0.00102$  cuts/yr or 1 cut every 979 years. Using the same arguments as before, with  $n = 24$ ,  $m = 23$  km/50 m = 460, and  $0.05mn = 552 \pm 23$  or 4% error, the estimated replacement time for any one section of this center portion of the tether is  $49 \pm 2$  years. This is longer than the useful 30 year commercial operational lifetime of the facility, so these modules will never need replacement or repair during their operational lifetime due to cuts by small impactors.

#### **Future Improvements in HASTOL Hoytether™ Module Replacement Lifetimes**

The replacement lifetimes of the modules in the HASTOL Hoytether™ can be increased to 100 years or more by two relatively simple methods - use of stronger tether material and more complex Hoytether™ designs. The HASTOL Tether Boost Facility will not be operational in space any time soon, probably not until 2020. By that time, stronger tether materials will become available than the Spectra™ 2000 assumed in the present design. Since the HASTOL facility must have a minimum mass in order to be able to lift and toss large payloads without being deorbited, the tether mass will not be decreased when the stronger material is used, instead the same mass of tether will be used to carry the same stress load. An increase in the breaking stress tension of the tether material, however, means that the stress as a percentage of breaking stress of the tether material will drop. This will mean that the Hoytether™ can survive having a larger percentage of its primary strands being cut before coming close enough to the failure point that module replacement is needed. Even without an increase in tether material strength, the replacement lifetime can be increased to over 100 years by making each line in the HASTOL Hoytether™ a 6 primary line mini-Hoytether™ structure which is 2 cm or more in diameter. It would now take a space impactor 1 cm across to cut 2 or more of the lines in this mini-Hoytether™, and the flux of small impactors 1 cm in size is down by a factor of 670 from the 1 mm impactors that would cut the line if it were a compact braid instead of a mini-Hoytether™.

#### **Conclusions**

We have analyzed that the present modular Hoytether™ design for the HASTOL system which assumes the use of presently available tether materials operating at high stress levels. We find that of the 20 modules making up the HASTOL Hoytether™, 18 of them will never need replacement in the estimated 30 year commercial operational lifetime of the facility. Of the two remaining two modules, the longest, thinnest module at the grapple end of the facility will need replacement after 8.5 years, while the next longest, next thinnest module from to the grapple end will need replacement in 15 years.

### Acknowledgements

This work was supported by a subcontract with The Boeing Company under the "Hypersonic Airplane Space Tether Orbital Launch Architecture Study" with the NASA Institute for Advanced Concepts, Bob Cassanova, Director.

### References

1. Robert L. Forward, Thomas J. Bogar, Michal E. Bangham and Mark J. Lewis, "Hypersonic Airplane Space Tether Orbital Launch (HASTOL) System: Initial Study Results", Paper IAF-99-S.6.05, 50th IAF Congress, Amsterdam, The Netherlands, 4-8 October 1999.
2. Thomas J. Bogar, Michal E. Bangham, Robert L. Forward, and Mark J. Lewis, "Hypersonic Airplane Space Tether Orbital Launch (HASTOL) System: Interim Study Results", Paper AIAA-99-4802, 9th Space Planes and Hypersonic Systems and Technologies Conference, Norfolk, VA, 1-5 November 1999.
3. John Grant, John Martin, Dan Nowlan, Brian Tillotson, and Robert P. Hoyt, "The HASTOL Tether System Applied to Commercial Launch", AIAA Paper 2001-3966, 37th Joint Propulsion Conference, Salt Lake City, UT, 8-11 July 2001.
4. Robert P. Hoyt, "Design and Simulation of Tether Facilities for the HASTOL Architecture", AIAA Paper 2000-3615, 36th Joint Propulsion Conference, 17-19 July 2000.
5. Robert P. Hoyt, "Modular Design of a Tether Boost Facility for Earth-To-Orbit Launch Assist", Ninth Monthly Subcontract Report for Boeing HASTOL Contract with NIAC. (June 2001); submitted to Proceedings of STAIF 2002 Forum, Albuquerque, NM, 3-7 Feb 2002.
6. Robert L. Forward, "Failsafe Multistrand Tether Structures for Space Propulsion", AIAA Paper 92-3214, 28th AIAA/ASME/SAE/ASEE Joint Propulsion Conference, Nashville, TN, 6-8 July 1992.
7. Robert L. Forward and Robert P. Hoyt, "Failsafe Multiline Hoytether Lifetimes", Paper AIAA 95-2890, 31st AIAA/ASME/SAE/ASEE Joint Propulsion Conference, San Diego, CA, 10-12 July 1995.
8. Robert L. Forward, "Estimate of Avoidance Maneuver Rate for HASTOL Tether Boost Facility", Tenth Monthly Subcontract Report for Boeing HASTOL Contract with NIAC (July 2001); submitted to Proceedings of STAIF 2002 Forum, Albuquerque, NM, 3-7 Feb 2002.
9. D.J. Kessler, J. Zhang, M.J. Matney, P. Eichler, R.C. Reynolds, P.D. Anz-Meador, and E.G. Stansbery, A Computer-Based Orbital Debris Environment Model for Spacecraft Design and Observations in Low-Earth Orbit, NASA TM-104825, Johnson Space Center, Houston, TX, 1996. [See internet web site: <<http://www.orbitaldebris.jsc.nasa.gov/model/ordem96.html>> to download paper and the computer program ORDEM96.EXE that can be used to obtain an estimate of the orbital debris flux as a function of object size, altitude, orbit, and velocity.]
10. B. Jeffrey Anderson, Editor and Robert E. Smith, Compiler, Natural Orbital Environment Guidelines for Use in Aerospace Vehicle Development, Section 7 - "Meteoroids and Orbital Debris", Don Kessler and Herb Zook, NASA TM-4527, June 1994. [See specifically Fig. 7-2 "Comparative Debris and Meteoroid Fluxes" on page 7-4.]
11. TiPS URL: <<http://code8200.nrl.navy.mil/tips.html>>.